Characterising the cleaning behaviour of brewery foulants.

To minimise the Cost of Cleaning In Place Operations.

by

Kylee Rebecca Goode

A thesis submitted in partial fulfilment for the

degree of Doctor of Engineering

in the college of Engineering and Physical Sciences

School of Chemical Engineering

August 2012

UNIVERSITYOF
BIRMINGHAM

University of Birmingham Research Archive

e-theses repository

ABSTRACT

Industry operations require a clean plant to make safe, quality products consistently. As well as product quality, the environmental impact of processes has become increasingly important to industry and consumers. Cleaning In Place (CIP) is the ubiquitous method used to ensure plant cleanliness and hygiene. It is therefore vital the system is optimal and efficient. I.e. the correct cleaning agent is delivered to the fouled surface at the right time, temperature, flow rate and concentration. This cannot be assured without effective online measurement technologies.

Fryer and Asteriadou (2009) describe how the nature of a fouling deposit can be related to the cost of cleaning. The evolution of three key deposit types has also enabled current fouling and cleaning literature to be easily classified. In the brewery there are many types of soil that need to be cleaned of which the cost of cleaning was unknown. The cost of fermenter CIP in one brewery was found to be £106 k per year. Effective fouling methods for yeast and caramel; and the relationship between flow, temperature, and caustic concentration in the removal of yeast and caramel soils seen in industry has been done. This work has helped determine effective cleaning methods for these soils from stainless steel coupons and pipes.

Fermentation vessels have been found by Goode et al., (2010) to have two types of soil: A – fouling above the beer resulting from the act of fermentation, and B – fouling below the beer resulting from emptying the fermenter. The type B fouling below the beer was found to be a type 1 soil that could be removed with water. An increase in flow velocity and Reynolds number decreased cleaning time. An increase in temperature did not decrease cleaning time significantly at higher flow velocities, 0.5 m s^{-1}. Fouling above the beer occurs when material is transported to and stick on to the wall during fermentation foaming. This happens initially and as a result the fouling has a long aging time. This yeast film represents a type 2 deposit, removed in part by water and in part by chemical. Most of the deposit could be removed by rinsing with warm water. At 50°C the greatest amount of deposit was removed in the shortest time. A visually clean surface could be achieved at all temperatures, 20, 30, 50 and 70°C, using both 2 and 0.2 wt % Advantis 210 (1 and 0.1 wt % NaOH respectively). A visually clean surface was achieved quicker at higher detergent temperatures rather than rinsing at higher flow velocity or concentration. This finding suggests most deposit can be removed with warm water and cleaned with lower detergent concentrations. Currently in the brewery 2 % NaOH is used at 70°C.

Caramel represents a type 3 soil. When heated it sticks to stainless steel and requires chemical action for removal. Confectionary caramel was cooked onto pipes and coupons and the effect of flow velocity, temperature and concentration on removal determined. At high flow velocity most of the deposit could be removed from the pipe using water. There was no significant difference in the mass of caramel removed by the water however. A visually clean surface was achieved by rinsing at 80°C with 2.5% Advantis. A visually clean surface could not be achieved at lower temperatures at higher concentration, 5% Advantis, or at higher flow velocity.

The measurement of online conductivity and flow rate values was invaluable during each experiment. Turbidity values did indicate the removal of yeast and caramel from pipes however offline measurements were required to confirm removal. Caramel removal could be wholly quantified by mass when cleaning pipes. The integration of the turbidity values measured during each rinse correlated well with the mass of deposit removed in most cases. Coupon cleaning was wholly quantified by area . A cost saving of £69 k can be made by optimising fermenter CIP to warm pre-rinsing followed by ambient caustic circulation. An £8 k saving can be made by optimising yeast tank CIP to pre-rinsing only and acid sanitisation. Industry must ensure effective online CIP measurements are made throughout cleaning to describe the process effectively and enable optimisation. It is crucial to have cleaning measurement information to hand because that is how we ensure our customers they are buying a quality product. Also you cannot optimise what you do not measure effectively.

ACKNOWLEDGEMENTS

TABLE OF CONTENTS

LIST OF FIGURES

LIST OF TABLES

NOMENCLATURE

Abbreviations

AFM	atomic force microscopy
ATP	adenosine triphosphate
β-Lg	beta lactoglobulin
BSA	bovine serum albumin
CAM	cellulose acetate membrane
CFD	computational fluid dynamics
CFU	colony forming unit
CFV	cross-flow velocity
CIP	Cleaning In Place
CO_2	Carbon dioxide
DAL	De-aerated liquor
DVLO	Derjaguin, Landau, Verwey and Overbeek theory
ED	equivalent diameter,
EHEDG	European Hygienic Engineering & Design Group
EP	electropolished
ERT	electrical resistance tomography
FDG	fluid dynamic gauging
FTU	Formazin turbidity unit
FV	Fermentation Vessel
GSK	GlaxoSmithKline
Hl	hectolitres
HNO_3	nitric acid
ID	inner diameter
IMECA®	interactive membrane controlled electrochemical activation
KOH	potassium hydroxide
KPI	Key Performance Indicator
kWh	Kilowatt hour
L	length
LVR	Linear viscoelastic region
MF	microfiltration
MHFS	Microfoil heat flux sensor.
MSS	mechatronic surface sensor,
MV	Maturation vessel
NaClO	sodium hypochlorite
NaOH	sodium hydroxide
NF	nanofiltration
OD	outer diameter
PFA	Perfluoroalkyoxy
PHE	plate heat exchanger
Ppm	parts per million
PT	pressure transmitter
PTFE	Polytetrafluoroethylene
Re	Reynolds number
RJH	rotating jet head
RO	reverse osmosis
RSH	rotating spray head
SB	spray ball
SCM	sweet condensed milk
SD	standard deviation
SG	specific gravity
SOP	standard operating procedure

SP	Set Point
ss	stainless steel
Tc	thermocouple
TP	temperature probe
TPA	top plate assembly
UF	Ultrafiltration
UHT	ultra high temperature
V	valve
w/v	weight per volume
w/w	weight per weight
WPC	whey protein concentrate
Wt	weight
YST	yeast storage tank
ZEAL	Zero Emissions by Advanced cLeaning

Symbols

R_a	Surface roughness parameter	μm
τ	Shear stress	kg m^{-1} s^{-2} (Pa)
Re	Reynolds number	
θ_c,	Dimensionless cleaning time	
t	Time	s
R_d	Resistance	m^2 K kW^{-1}
w	Fluid velocity	m s^{-1}
W	Waviness	
ω	Angular frequency,	rad s^{-1}
G'	Elastic modulus	kg m^{-1} s^{-1} (Pas)
G''	Viscous modulus	kg m^{-1} s^{-1} (Pas)
Δ	Difference	
P	Pressure	kg·m^{-1}·s^{-2}
U	Heat transfer coefficient	kW m^{-2} K^{-1}
x	Thickness	m
λ	Thermal conductivity	W m^{-1} K^{-1}
D	Diameter	
q	Heat flux	kW m^{-2}
φ	MHFS constant	V^{-1}
$\kappa(T_B)$	Dimensionless temperature factor	
V	Voltage output	μV
n	Rheological constant	
My	Mass yeast slurry	g
L_w	Volume of wort	L
u_y	Yeast slurry addition rate	g L^{-1}
C	Consistency	%
V	Viability	%
FTU_p	Cleaning time of the Kemtrak probe	s
FTU_{pr}	Integration of FTU values during the pre-rinse	FTU
$FTU_{tcirc-to}$	Integration of FTU values during chemical circulation	FTU

Subscripts

w	Wall
50%	50% cells removed
HFS	Heat flux sensor
c	Clean
os	Oscillating
stat	Stationary
max	Maximum
A	Angular
I	Inlet
O	Outlet
d	Deposit
f	Fouling
e	Equivalent
av	Average
s	Sensor
y	Yield
x	No further deposit removed
circ	Circulation

CHAPTER 1: INTRODUCTION

1.1 Chapter Introduction

In the brewing industry, productivity and consumer safety is fundamental to the success of a branded business. This is achieved by the consistent manufacture of a good quality safe product. As such, product quality and safety must conform to the required level. Non-conformance can be a result of fouling layers building up in a plant or other problems. In beer brewing and other food and beverage manufacturing operations, Cleaning In Place (CIP) is used to remove residual product, fouling and microbes that are remaining in the process line from production. The act of cleaning therefore maintains product quality, safety, and production efficiency. Scottish and Newcastle CIP philosophy is detailed below which remains valid to the nature of this work:

1) To ensure all production, processing and packaging plant is cleaned by a regime and to a schedule which ensures cleanliness and microbiological integrity at all times.

2) To achieve the above with minimum cost, energy and delay to production in a manner which ensures human, plant, product and environmental safety.

3) To target effective soil removal with physical and detergency efficiency, this precludes the need for chemical sterilants (sanitisers).

During CIP water and/or chemical is circulated around plant process equipment. The process is generally now fully automated with cleaning following a series of steps of prescribed time, flow rate, temperature and chemical concentration. However, cleaning efficiency is not quantified. The purpose of this introduction is to present:

(1.2)   An outline of brewery operations;

(1.3)   the fouling problem identified in the brewery;

(1.4)   the drivers for change that have brought CIP processes under scrutiny,

(1.5)   the technical challenges that need to be overcome to achieve CIP operations of optimum efficiency;

(1.6)   the aim of project ZEAL;

(1.7)   the business case put forward to support the work done in project ZEAL and in this thesis; and

(1.8)   thesis structure and Chapter 1 summary.

1.2 Brewery operations

Beer is a complex mixture with over 450 constituents and macromolecules including proteins, nucleic acids, polysaccharides and lipids (Briggs et al., 2004). It can be defined as fermented cereal grain extract, typically malted barley, with hop bittering and aromas. Beer can be subdivided into ale or lager depending on the processing conditions and yeast strain used in the fermentation step. Generally the raw materials for beer brewing are the same: malt, water, hops, and yeast, but the amounts and type of each are specific to a brewery. Green beer (unfiltered) is

dispensed into cask and filtered beer (bright beer) is packaged into bottles, cans, or kegs. An overview of the brewing process is illustrated in Figure 1.1.
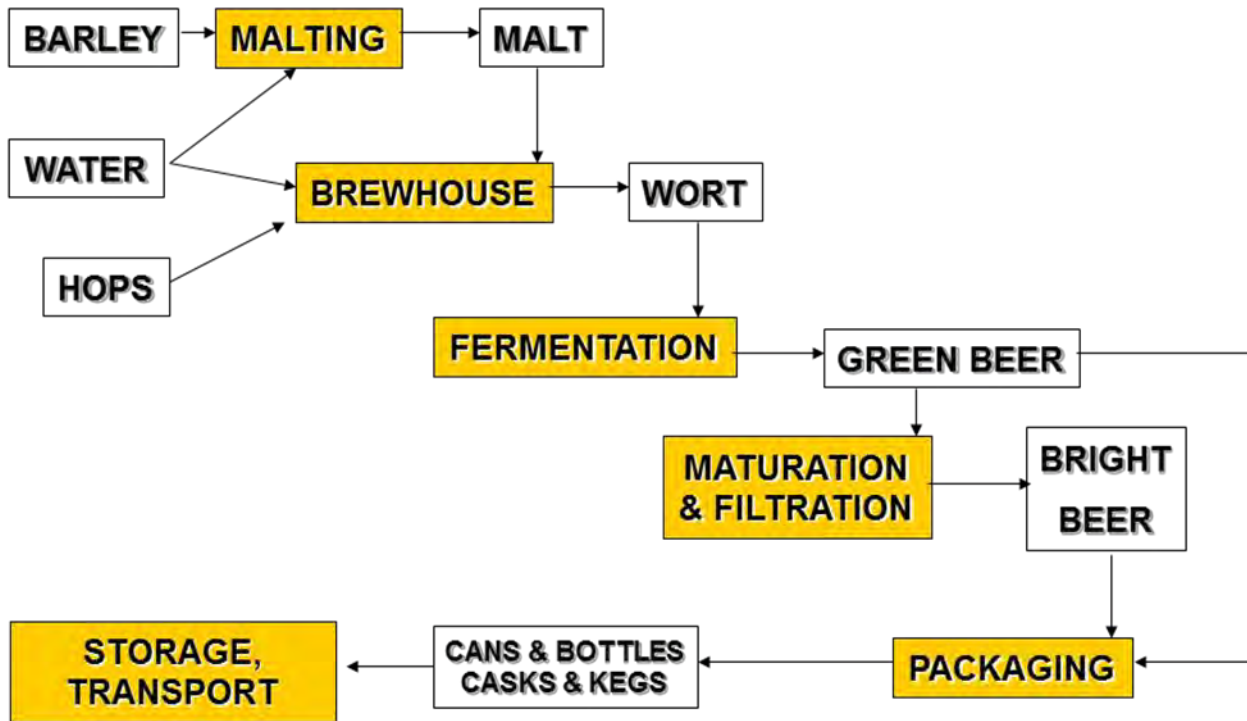
Figure 1.1: Schematic of brewery operations. The general process stages are in yellow and products in and out of the system are in white.

Malting is now typically an independent process separate from the brewery. Within each process stage highlighted in yellow in Figure 1.1 there is a series of sub steps required to make and package beer;

(i)   *Brewhouse* - to convert starches to sugar the malt is milled, hydrated and heated through a series of steps. The liquid sugar, wort, is then cooled for fermentation.

(ii) *Fermentation and maturation* - to convert sugar to alcohol the wort is added to yeast and left for a number of days. The immature beer is separated from the yeast and left for another number of days to mature in flavour.

(iii) *Filtration* - To separate all the yeast from the mature beer, the beer is filtered and called bright beer.

(iv) *Packaging* – The bright beer is dispensed into kegs, cans and bottles. The beer is pasteurised in line before the keg is filled and in the final pack; cans and glass bottles.

Brewing process plant and brewery operations have been defined and understood throughout history. As such there is always scope to optimise the process equipment and operations to increase productivity and decrease cost and environmental impact. A large scale brewery can produce 4 000 000 hectolitres (hl) (400 000 m^3) annually.

1.3 The fouling problem

During fermentation material sticks to the walls of the vessel which needs to be removed before the next fermentation can take place. This is typically done by cleaning with water and chemicals. In beer fermentation vessels there are two distinct deposit types to be cleaned classified as type A and type B foulants (Goode et al., 2010) and discussed in Chapters 4 and 5, defined as:

(i) *Type A* – deposit formed above the beer in the head space of the vessel during fermentation, discussed in Chapter 5,

(ii) *Type B* - Residual yeast attached to the vessel wall and cone during emptying, discussed in Chapter 4.

Figure 1.2 illustrates these deposits. Type A deposit forms during fermentation above the beer in the head space of the vessel; type B deposit forms at the wall and the cone during emptying before cleaning.

Figure 1.2: View into the top of a fermenter (through man way door) after fermentation prior to cleaning.

To have a zero emissions process there should be no waste being produced. To make processes more sustainable a value added use for the waste, in this case the fouling, should be determined. Figure 1.3 illustrates a process to determine the value of waste, also called by product. The material should be defined in the first instance so that potential use and value can be defined. To do this a series of processes should be determined, as indicated in the flow diagram in Figure 1.3:

(i)   *What is the by product (or fouling)?* - This is unknown for fermenter type A material. The composition of the material should be defined so that potential value (and use) can be defined.

(ii) *Product value* - If the material has value it should be collected and sold if feasible.

(iii) *Prevention of fouling* - If the material does not have significant value it should be prevented from occurring. This however is not easy and as of yet an effective prevention strategy for fouling material has not been demonstrated in industry.

(iv) *Removal by cleaning* - If the material cannot be prevented it should be removed. Typically by cleaning. Currently in the brewery this fouling is cleaned without specific knowledge of the material composition. This is illustrated by the dashed red line in Figure 1.3.
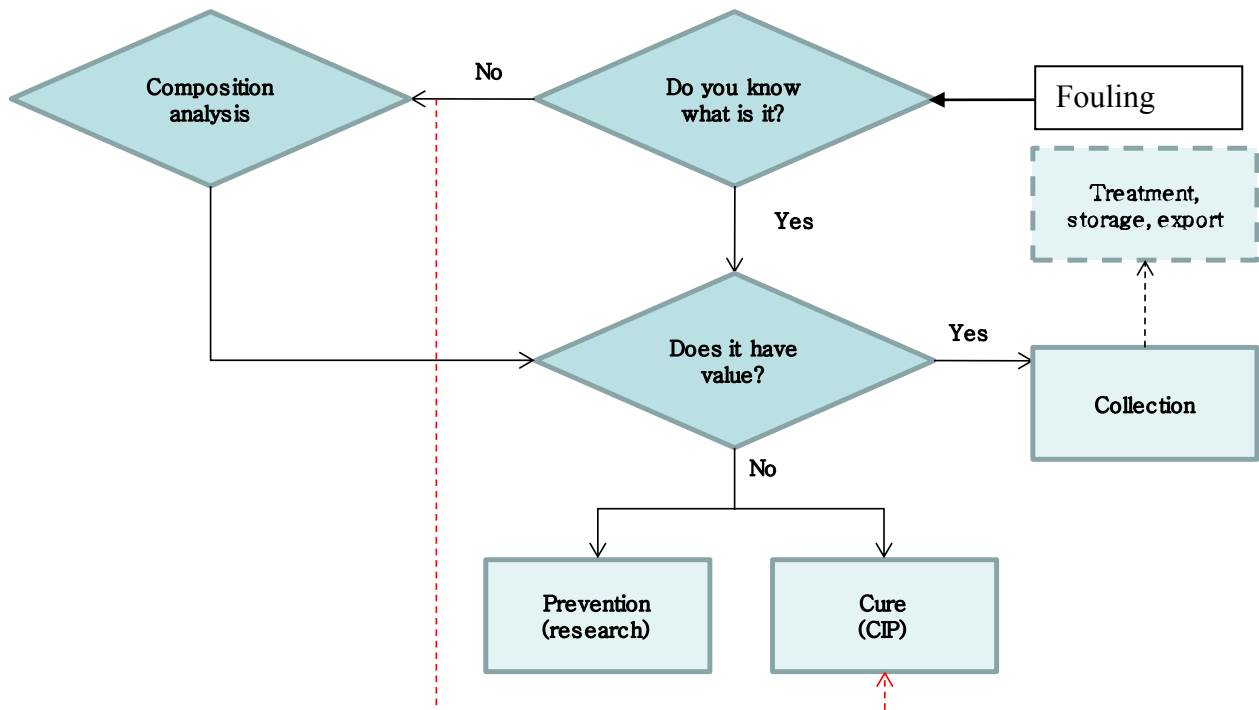
Figure 1.3: Flow diagram for deciding how to tackle fouling.

1.4 The drivers for change

One of the challenges for industry is to minimise its impact on the environment, with particular emphasis at the current time on reducing climate change. Improvement in cleaning processes can play a small but relevant part in reducing the environmental footprint of a plant, in particular in the reduction in greenhouse gas emissions. Brewers are under considerable pressure to reduce the carbon footprint of their products and to minimise energy and water use. This has seen brewers set challenging targets for energy and water reduction. Currently across the Heineken group it takes 4.35 hl (0.435 m^3) of water, 8.9 kWh of electricity and 81.6 MJ of thermal energy to make 1 hl of beer. The target for 2010 was to reduce water consumption by 17%, electricity use by 18% and thermal energy use by 6%. 9.6 kg CO_2/hl beer in 2009 was to be reduced by 12% in 2010 (Heineken Sustainability report, 2009).

CIP operations use considerable amounts of water, energy and chemicals producing large amounts of effluent. This effluent needs to be processed or treated before reuse or disposal. A brewery discharging direct to a water company has very high charges, often based on a variation of the Mogden formula (Briggs et al., 2004). This is due to the very high solids content, BOD and COD of the effluent along with potential extremes of temperature and pH. The cost of external effluent treatment has made the substantial investment required for on-site effluent treatment plants (ETP) more attractive. Energy generation from by-products generated in the effluent treatment plant is considered 'green' energy and so government grants can be accessed. These help to push a plant towards a zero emissions operation.

The economic and ecological footprint of cleaning operations has been overlooked in the past for a number of reasons;

(i)   The potential cost of brand damage from product failure may be of the order of many million pounds. This has resulted in little incentive to change CIP operations that are known to result in efficacious plant, and

(ii)   CIP is a "non-added value" process often considered separate to production efficiency and so the cost of CIP is often not known.

CIP is required to regain operational efficiency. The build-up of fouling layers in the plant increases the thickness of heat transfer surfaces and therefore the thermal resistance of the surface. This reduces heat transfer efficiency in heat exchangers, increasing the energy load required to heat the surface to the required temperature. In a brewery 42 % of the total energy requirement is used to boil wort (Felgantraeger and Ricketts, 2003). As wort is boiled, a number of physical-chemical changes occur, some of which result in fouling deposits. Initially, the wort passes over the heated surface as a single phase liquid at a turbulent flow rate. As the liquid gains more heat, bubbles form creating a vapour phase. The bubbles initially form at the heated surface giving saturated nucleate boiling. It is believed that as the temperature of the surface is increased the wort may be separated from the surface by a layer of steam, and solids can precipitate and bake onto the surface (Briggs et al., 2004). Figure 1.4 illustrates the fouling layers present in an external wort boiler at the brewery opened for maintenance. Wort is passed through the tubes.
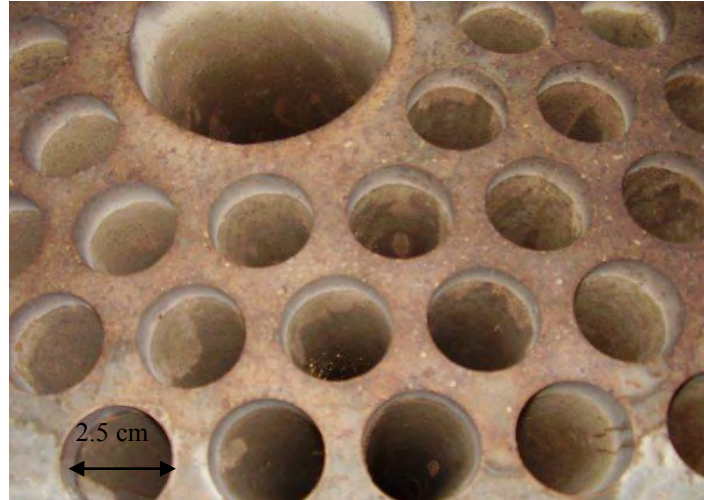
Figure 1.4: Birds eye view into a wort boiler opened for maintenance. The fouling layers are present on the interior of the tubes. Small tubes have a diameter of 2.5 cm.

As deposit layers increase, at some critical point wort processing must stop and the plant is cleaned. The fouled plant has a higher running cost than when the plant is clean. A balance needs to be found between production time lost to cleaning, with the risk to product safety and the higher processing costs. This raises a series of questions:

(i) what is the optimum method of cleaning the plant?

(ii) when is the optimum time after which the plant should be cleaned? What factors dictate this?

CIP operations are an area of production not yet fully optimised. This is an area in many plants where the benefit of optimisation has not been fully realised. Understanding the nature of the foulant during cleaning can lead to a more targeted cleaning operation to reduce cost and emissions.

1.5 Challenges to CIP optimisation

Within individual manufacturers, chemical companies and organisations such as the European Hygienic Engineering & Design Group (EHEDG), a significant body of cleaning knowledge exists. The EHEDG has produced extensive guidelines on the types of surface and equipment that is easy to clean such as in the EHEDG Yearbook (2009). Cleaning regimes determined by industrialists and suppliers have often been kept confidential and plant specific. This has resulted in the independent development of cleaning regimes. The best way to clean a product has often been determined for a specific deposit on a specific piece of equipment. This is because it is not possible to predict in advance how a given piece of equipment can be cleaned. As a result the direct implementation of cleaning findings throughout an industry is not always possible and can only be applied semi-empirically. A questionnaire completed by industrial partners in the ZEAL consortium, listed in Table 1.4, revealed that the industry knows a repeatable level of cleanliness is required and achieved currently, but not how to optimise CIP without compromising current cleanliness. The function and aim of project ZEAL is detailed in Section 1.6.

1.5.1 CIP best practice in a brewery

As a rule of thumb water rinsing is used first to remove loosely bound soil, alkali chemicals are used to remove organic soils and acids are used remove inorganic soils and mineral scales such as beerstone (O'Rourke, 2003). This is due to the different solubilities of different foulants. The solubility of typical food components; sugar, fat, protein and mineral salts are listed in Table 1.1. The manufacture of beer is complex and involves the stages illustrated in Figure 1.5. All stages of the process encounter fouling problems.

Table 1.1: The solubility of food deposit types before and after thermal treatment (adapted from Grasshoff, 1997).

Component deposited	Solubility	Ease of Removal	Fouling mechanism	Change upon heating	Ease of removal
Sugar (organic)	Water soluble	Easy	Crystallisation	Charamelisation	More difficult
Fat (organic)	Water and alkali soluble	Difficult	Crystallisation	Polymerisation	More difficult
Protein (organic)	Water soluble, alkali soluble, slightly acidic soluble	Very difficult	Chemical reaction	Denaturation	More difficult
Mineral salts (inorganic)	Water solubility variable, most are acid soluble	Easy to difficult	Crystallisation	Interactions with other constituents	Generally easier

CIP regimes used by Heineken UK for wort boilers, fermenters, yeast storage vessels and beer storage tanks are detailed in Table 1.2. The classification of fouling type in the Table has been done using the criteria set out by Fryer and Asteriadou (2009), discussed in the following paragraphs. A flow velocity of at least 1.5 m s^{-1} is used in pipe lines as a rule of thumb. Best practice CIP regimes proposed by Heineken NV suggest that lower CIP temperatures and chemical concentrations can be used in the UK to achieve the same level of cleanliness. The current CIP regime of vertical FVs (fermentation vessels) and MVs (maturation vessels) includes an ambient pre-rinse, hot caustic rinse (2 w/v %) at 65 - 70°C, intermediate water and disinfection. Specific stage times are detailed in Appendix A, Table A.2. In industry, it recommended that the first rinse in cleaning (called the pre-rinse) uses water. There are various reasons for this;

(i)   *The product is protected* – diluted product rather than chemical contaminated product would be wasted if cleaning started while product remained in the line or the tank.

(ii)   *Safety* – there is less risk to employees in proximity of CIP at the onset.

(iii) *Cost and environmental impact* – disposal and treatment cost of fouled water is significantly less than that of fouled chemical.

Brewing stages	Fouling	CIP Requirements
MALTING	**PARTICULATES**	*Physical/visual*
BREWHOUSE	**PROTEINS AND MINERALS**	*Visual and Chemical*
WORT COOLING		
FERMENTATION	**YEAST FILMS, PROTEINS**	*Chemical and microbiological*
CONDITIONING		
BRIGHT BEER TANK	**BEER AND MINERALS**	
PACKAGING		
DRAUGHT DISPENSE	**BIOFILM**	
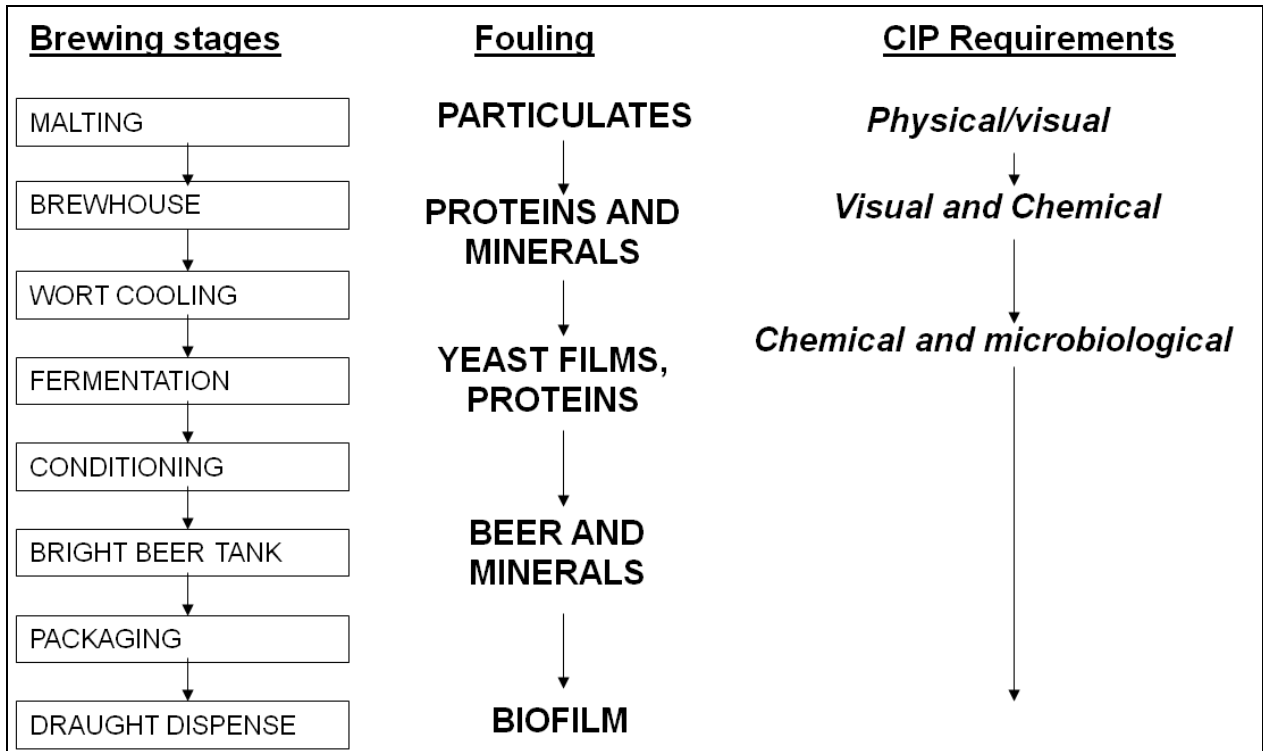
Figure 1.5: Schematic of brewery operations (left) and the fouling deposit encountered (middle). The cleaning requirements at each stage are indicated (right).

Currently the time to clean a plant is dictated by customer practice rather than by online data measured at the plant. Cleaning is done when operational efficiency reaches a low level or there is a gap in production. The optimum time to clean may be when the deposit has the weakest attachment to the surface. This might increase CIP frequency, but give a shorter run time and/or less chemical severity, and so the overall process may be more efficient than if the process were run for longer. Lower temperatures and concentrations might be used to remove the deposit producing smaller volumes of effluent with a lower environmental impact. Understanding the effect of cleaning parameters on the removal behaviour of deposits is critical in prescribing the most efficient CIP regime.

Table 1.2: Recommended CIP regimes for different deposit types in breweries.

Plant Geometry	Fouling Encountered	Fouling Type	Heineken NV CIP Best Practice Regime
Brewhouse wort boiler	Protein, beer stone	Type 3	1. Hot water pre-rinse (80°C) 2. 80°C caustic solution 2-3% (w/v) for 20-45 minutes 3. Hot water final rinse (80°C)
Vertical Fermentation vessels (FVs) and maturation vessels (MVs)	Yeast, protein, slight beer stone	Type 2	1. Caustic pulses 1% (w/v) at ambient 2. Intermediate water (ambient) 3. Acid circulation (30 min) at ambient 4. Intermediate water (ambient) 5. Disinfectant circulation (30 min) at ambient 6. Final cold sterile water rinse
Yeast storage vessels	Yeast, protein, slight beer stone	Type 1	1. Cold water pre-rinse 2. Caustic pulses 1% (w/v) at ambient 3. Acid circulation (30 min) at ambient 4. Intermediate water (ambient) 5. Disinfectant circulation (30 min) at ambient 6. Final cold sterile water rinse 7. Cold sterile water final rinse
Bright beer storage tanks	Traces of beer and foam	Type 1	1. Cold water pre-rinse 2. Cold acid solution (30 min) at ambient 3. Intermediate water (ambient) 4. Disinfectant circulation (30 min, ambient) 5. Sterile water

Fryer and Asteriadou (2009) suggest a classification of cleaning problems in terms of cleaning cost and soil complexity. A diagrammatic representation of this relationship from the published paper is presented in Figure 1.6. This classification enables the nature of a foulant to be related to the type of cleaning employed and the cost. This classification also indicates the environmental impact of the type of cleaning employed. For example the complex soils require chemical and thermal treatment. The generation of energy and the use and disposal of cleaning chemicals is costly. The environmental impact will also be larger than water rinsing. A range of cleaning protocols is likely to exist for a given material i.e. a 'cleaning index'. For example a clean surface could be achieved using a high flow rate and cool cleaning fluid or using warm cleaning fluid at lower flow rate. Ideally CIP systems would be flexible so any cleaning protocol from the 'index' could be selected to satisfy the production constraints at the time of CIP. For example fast

cleaning to maximise production capacity and ambient cleaning to achieve environmental targets (Fryer et al., 2011). Three deposit types were classified by Fryer and Asteriadou (2009) representing a broad range of cleaning problems experienced in food, beverage and person care product production:

  (i) type 1 deposit: viscoelastic or viscoplastic fluids such as toothpaste and yoghurt that can be rinsed with water,

 (ii) type 2 deposit: microbial and gel-like films such as biofilm, polymers, and Turkish delight, removed in part by water and in part by chemical, and

(iii) type 3 deposit: solid-like cohesive foulants formed during thermal processing of a product such as milk pasteurisation and wort evaporation. These products require chemical action for removal.
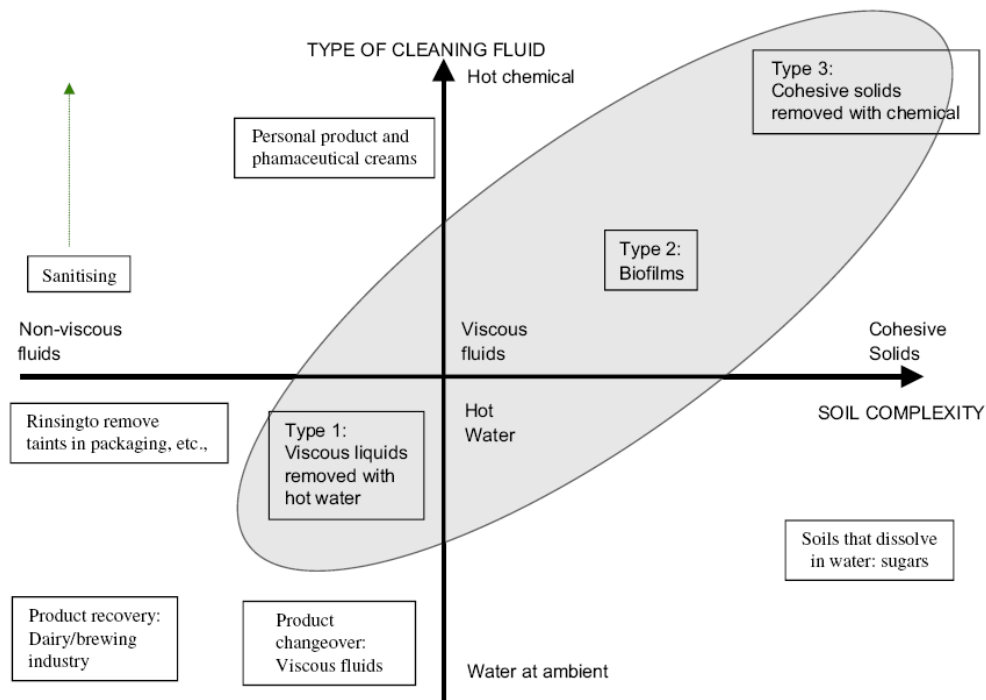
Figure 1.6: Cleaning map; a classification of cleaning problems based on soil type and cleaning chemical use, from Fryer and Asteriadou (2009).

Brewery operations encounter all three types of fouling, illustrated in Table 1.2 and Figure 1.5. Fryer and Asteriadou (2009) have classified cleaning types based on fouling types. However in industry, CIP regimes tend to be longer than strictly necessary and include several cleaning phases. The cleaning of packaging process lines also uses harsh chemical cleaners irrespective of whether there is fouling present. This is for peace of mind of the manufacturer. After CIP the product is deemed to be safe and ready for consumption by the consumer.

1.5.2 Process design

Supplier companies (such as Alfa Laval and GEA) design and manufacture state of the art equipment that is designed to be cleaned efficiently. From working with suppliers to design the best possible cleaning regime on site, Heineken UK has determined best practice design for efficient CIP. These include;

(i)   avoid geometric designs where low flows or stagnant flow can occur; and plant surfaces should have a surface roughness (R_a) no greater than 0.8 μm,

(ii)   all tanks should have a means of visual inspection and be cleaned using cleaning heads according to supplier specifications which are suitable for the tank and the soil,

(iii)   sample taps must be designed to be hygienic and cleaned by CIP where feasible.

Geometric designs where poor flow can occur include T-pieces with dead legs larger than half the diameter of the main pipe, in systems with expansion sections or where the flow is split between two pipes, and in vessels with corners or horizontal outlets.

Advances in computational fluid dynamics (CFD) have meant it is now possible to model flow and heat transfer in new and existing equipment to a good degree of accuracy. This helps to reduce money and time required to optimise equipment design. For example various investigators have used CFD to model velocity profiles during removal of type 1 deposit in T-pieces (Asteriadou et al., 2006; Jensen et al., 2007), valves (Friis and Jensen, 2002) and pipes (Sahu et al., 2007). Real plant however is made up of many pieces of equipment and a number of soil types. This complexity means that CFD modelling is still not viable for complete plant testing and experimentation is still required. Hence designing a whole process plant is a semi-empirical process, and will rely on final testing during commissioning. Modelling of areas of plant known to be difficult to clean may well help in de-bottlenecking these areas of the process and so significantly improve overall cleaning efficiencies.

1.5.3 How clean is clean?

The severity (chemical requirement) of cleaning needed can be determined by the ability to manufacture product to the same quality and safety after each clean. The severity or cleaning required depends on the industry. Pharmaceutical operations cannot tolerate the presence of even one contaminating microbe as it would be detrimental to drug function and safety, whereas a greater microbial load can be tolerated in food and beverage processing as long as growth is stopped. The cleaning requirement of a process can be subdivided into levels of cleanliness (Christian, 2004);

    (i)   *physically clean* - no physical detection of the deposit by eye,

    (ii)   *chemically clean* - absence of non-inherent substances like cleaning chemical,

(iii)   *biologically clean* - free of viable microorganisms typically termed sterile,

(iv)   *atomically* clean - clean at the nano-meter length scale.

The function and aim of project ZEAL, is described in Section 1.6. A questionnaire was answered by the industrialists involved in the project: Heineken UK, Unilever, GSK, and Cadburys; to understand the level of clean required for products in production plants and how cleaning was monitored. The findings of this questionnaire are presented in Table 1.3. It was revealed that in most instances 'clean' was determined by eye and validated using microbial enumeration techniques. Enumeration techniques often take 2 – 7 days to obtain results because microbial growth (or lack of growth) is the time limiting step. This often means that microbial enumeration is a retrospective tool used to validate CIP. However microbial enumeration techniques are used extensively to minimise the risk of product recall. Faster methods of identification are required. The questionnaire also revealed that the companies involved in the project use similar CIP monitors: temperature, flow, pressure, conductivity and pH. These monitoring techniques can also be used to give an indication of what is removed from a surface. The difference in pressure drop can indicate fouling build up (Robbins et al., 1999) and fouling removal during cleaning (Fryer et al., 2006) of a plate heat exchanger.

Table 1.3: ZEAL industrialist definitions of clean and measurement.

Company	Cadbury	GlaxoSmithKline	Heineken UK	Unilever
Product/ Equipment	Sugar, chocolate and caramel in heat exchangers	Toothpaste in pipe work	Fermenters and wort in heat exchangers	Home and personal care products in pipe work
Definition of clean	Visually and microbiologically	Fluoride concentration	Visually and microbiologically	Visually
Validation method	Experience and visually	HPLC or rinse water and swabs	Visually, ATP counts and rinse water microbe concentration	Visually with endoscope
Methods tried	-	Conductivity of final rinse	UV, pH, and final rinse conductivity	Conductivity, turbidity rinse water, Heat flux sensor
Methods for the future	COD monitoring and ATP of final rinses	NMR, T-rays	Particle size and count of rinse water	Impedance spectroscopy, Electrical resistance tomography

1.6 The aim of project ZEAL

Project ZEAL was co-funded by the Technology Strategy Board's Collaborative Research and Development programme, following open competition it involved a number of academic institutions, industrial and supplier partners: Alfa Laval, Cadbury Ltd., Ecolab Ltd., Newcastle University, Heineken UK Ltd., GEA Process Engineering Ltd., Unilever UK Central Resources Ltd., Imperial College of Science Technology and Medicine, GlaxoSmithKline, Bruker Optics Ltd. and the University of Birmingham. The role and expertise of each partner in the project is detailed in Table 1.4.

Table 1.4: Project ZEAL partners and their roles.

Company	Role and expertise
University of Birmingham	Experimentalists
Newcastle University	Develop predictive mathematics for clean
Imperial College of Science Technology and Medicine	CFD of cleaning processes
Heineken UK Ltd	Provide the research problem, industrial expertise and plant facilities
GlaxoSmithKline	Provide the research problem, industrial expertise, plant facilities and project management
Unilever	Provide the research problem, industrial expertise and plant facilities
Cadbury Ltd	Provide the research problem, industrial expertise and plant facilities
Alfa Laval	Provide industrial CIP equipment and expertise
GEA Process Engineering Ltd	Design industrial CIP circuits and expertise
Ecolab Ltd	Provide industrial CIP chemicals and expertise
Bruker Optics	Provide Infrared spectroscopy probes and expertise

Project ZEAL shared a vision: to develop new technological approaches to the measurement, modelling, monitoring and control of cleaning to reduce environmental footprint of plants and processes. If accurate measurement and modelling of cleaning phenomena can be made then cleaning times can be reduced and energy and water can be saved. A future possibility is that an intelligent cleaning system may be possible. The vision for such a system is that an operator inputs a few parameters such as geometry, system volume/length and soil type and then online measurements are used to control the process and end cleaning at the appropriate time. If cleaning phenomena could be accurately modelled, future plant and products could also be modelled. This would enable CIP efficiency to be quantified before the plant was built. This approach would minimise the economic and ecological footprint of new process plants.

The collaborative approach to cleaning research undertaken by this project enabled critical cleaning problems to be identified and investigated. The project identified three critical soil types presented in Section 1.5.1. The cleaning behaviour of yeast aged for different lengths of time in

brewing (a problem already discussed in Section 1.3), and cooked caramel (a problem in confectionary processing), represent type 1, 2 and 3 soils. The cleaning of these deposits is presented in this thesis. By investigating shared cleaning problems a wider approach directly applicable to industrial CIP optimisation could be adopted. The aim of the work undertaken and presented in this thesis is:

(i)   to provide insight into the removal behaviour of type 1, 2 and 3 soils largely relevant to breweries,

(ii)   to describe approaches to measuring cleaning phenomena – does one size fit all? And,

(iii)   to demonstrate the benefits that can be delivered to production sites from investigating and improving CIP efficiency.

It is impossible however to quantify benefits without knowing the specifics of current CIP processes. For example; how long is a cleaning cycle? - how much water, energy, and chemical is used and how much effluent is produced? CIP cost can be quantified from this and future reductions can be measured. It is not possible to quantify improvements if they cannot be measured.

1.7 Quantifying CIP performance of fermenters and areas of improvement

A benchmark study to quantify CIP time, water, effluent, chemicals, electricity, energy, cost of fermentation vessel CIP was done in a Heineken UK brewery. This data was previously unknown to the plant and to the industry. The study was based on a questionnaire designed by Prof. Roger Benson based on his manufacturing benchmark tools (Benson and McCabe, 2004). The

questionnaire was modified so that CIP key performance indicators (KPIs) could be quantified. The methods used to obtain and analyse the data are detailed in Appendix A. The KPIs quantified are presented in Table 1.5. The proposed KPIs suggest that electricity, energy, water and CIP time are measured as a function of the amount of product made; and that the usage of chemicals are measured as a function of the product cost. Cost per clean, cleaning cost as a percentage of manufacturing cost, production capacity used for cleaning, and yield loss due to cleaning were also quantified as indicators of CIP performance. From Table 1.5 it can be seen Fermenter CIP was comparable to the current best in class CIP. Best in class figures were provided by Roger Benson during the ZEAL project from benchmarking CIP in six independent plants. Figures presented in the following section are accurate for 2010.

Table 1.5: ZEAL CIP KPIs, fermenter CIP and best in class in 2010 (provided by Roger Benson).

CIP KPIs proposed	Unit	Fermenter CIP	Best in Class CIP
KWh used in cleaning/m^3 unit product	kWh/m^3	0.0070	0.0033
Ratio water used in cleaning/unit of product	tonne/tonne	0.04	0.0007
Cleaning time/m^3 product	minutes/m^3	0.4838	0.0009
Cleaning chemical cost/product cost	%	0.0014	0.0014
Cost/clean	£	40.03	40.03
Cleaning cost as % manufactured cost	%	0.0034	0.0034
Capacity used for cleaning	%	0.006	0.004
Yield loss due to cleaning	%	0.0083	0.0083

1.7.1 Fermenter cleaning time

Total fermenter CIP time was calculated as the total time of the automated CIP stage times (53 minutes) listed in the Appendix, Table A.2, plus manual routing carried out by the operators (10 minutes), also detailed in Appendix A. The total downtime from this cleaning operation per year is around 111 days. Cleaning time could be separated into value added time and non-value added time. Value added time included stages of the CIP operation that were actually cleaning or

sanitising the surface. Non-value added time included operations that did not specifically clean the surface for example filling, emptying and scavenging and heating. Just over half, 57%, of the time was found to be value added time and so 43% was not value added time which gives a target for reduction.

Portions of the plant are often modified or upgraded and the associated CIP system is assumed to remain fit for purpose, i.e. the CIP set is able to deliver adequate flow rate, temperature and chemical concentration to the plant for the contact time required. To minimise non-value added CIP time, the CIP unit setup, volume, and operation should be reassessed at least annually to ensure it is fit for purpose and operating correctly. There are also a number of other approached to reduce time:

(i) To reduce filling and emptying time the CIP pumping capacity should be increased so larger volumes can be removed or added in less time.

(ii) There may now be better methods to heat detergent faster than steam injected heat exchangers.

(iii) Manual routing sections of the CIP operation could be re-made as automated. Having manual routing of some fermentation block operations provides flexibility; but the set up and deconstruction of flow plates is time consuming, unsafe and less hygienic than enclosed stainless steel routing.

(iv) The detergent and final disinfection step could be combined. The combination of the two cleaning phases into one would save time, chemical and water by removing the intermediate rinse. The effectiveness of one stage chemical cleaners has not been adopted

in industry because of high cost and reduced cleaning flexibility (Heineken UK personal communication, 2007).

To further reduce fermenter CIP time, value added CIP stage times need to be optimised. To achieve this, comprehensive studies are required to demonstrate the effectiveness of water and chemical at removing deposit at different temperatures and flow rates. Work carried out in Chapters 4, 5 and 6 aims to demonstrate this for yeast and caramel deposits and relate the findings to cleaning real plant geometries.

1.7.2 Cost of fermenter CIP

The sequence of events during fermentation vessel CIP is given in Table 1.6. Manually positioning pipe work takes 5 – 10 minutes prior to and after this sequence of events. Carbonation of the caustic recovered from fermentation CIP results in two detergent tank dumps per week. Fresh caustic is then added to the tank and heated to 65°C which takes approximately one hour. Figure 1.7 indicates the cost of each CIP resource in both fermentation vessel CIP and detergent tank dumping. There is no cost for sanitiser, waste yeast or manual routing because these factors are not part of the detergent tank recharge operation.

Table 1.6: FV CIP stages and individual stage times.

CIP sequence	Time (s)
1. Fill the system	60
2. Pre-rinse	480
3. Pre-rinse scavenge	45
4. Pre-rinse purge	300
5. Detergent circulation	840
6. Detergent scavenge	45
7. Intermediate rinse	360
8. Intermediate rinse scavenge	45
9. Sanitizer fill	60
10. Sanitizer injection	54
11. Sanitizer circulation	780
12. Final rinse	0
13. Final scavenge	60
14. Final drain down	0

Factors contributing to the cost of fermentation vessel CIP at the brewery were waste yeast, thermal energy (steam), electricity (for pumping), reverse osmosis water, manual involvement (manual routing) and chemicals (caustic, additive (Stabilon WT), and sanitiser (P3 Oxysan ZS)). Figure 1.7 indicates the cost of each CIP factor in this CIP operation.
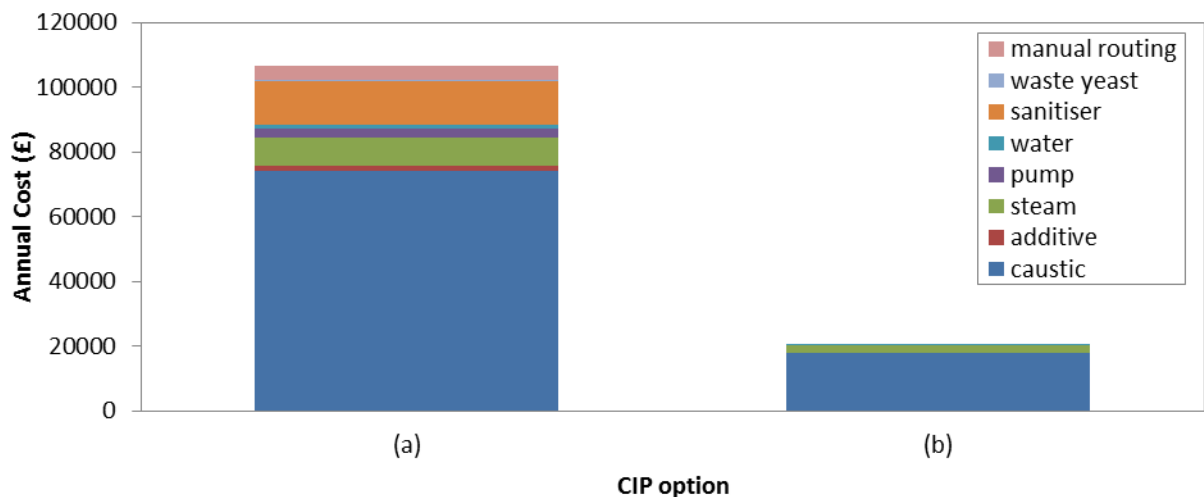
Figure 1.7: Factors contributing to the annual cost of (a) fermentation vessel CIP and (b) CIP caustic tank refills and recharges at the Brewery (2010).

Fermentation vessel CIP:

The cost per clean was £40.03 as indicated in Table 1.5. The annual cost of fermentation vessel CIP was approximately £107 k. Chemical use represents 84 % of the total cost of fermentation vessel CIP: 70 % caustic use, 13 % sanitiser use and 1 % additive use. The cost of thermal energy represents 8 % of the cost.

CIP tank refills and recharges:

The cost of a caustic tank refill and recharges was £197. The annual cost of CIP detergent tank refill and recharge was £20 k. Caustic use represents 87 % of the annual cost and steam represents 11 % of the cost.

Concentrated caustic (48 w/v %) is typically generated by one of three methods: the mercury cell, the diaphragm cell, or the membrane cell. All three methods are energy intensive. The range of energy required by each process is listed in Table 1.7. Around 300 tonnes of 47 % caustic are used in FV CIP and tank recharges per year. The energy requirement for this amount would be approximately 750 – 960 MWh per year depending on the generation method used (see Table 1.7). ZEIMANN have a technology called the ZIEMANN IMECA® (interactive membrane controlled electrochemical activation) system that enables a brewery to generate a sodium hydroxide cleaning detergent (Katholyte) and a sanitiser (Annolyte) on site. The products are made from an electrochemical reaction between a salt solution (NaCl) and salt free drinking water. The ZEIMANN group stated (in their 2007 annual report) that after use of these chemicals since April 2006 cleaning was 99.99% sterile and operation and maintenance costs were

substantially reduced from the previous year. The system also removed the risk involved in handling hazardous CIP chemicals. IMECA. (ZEIMANN, 2007).

Table 1.7: Energy requirement for 1 ton of caustic (48% (w/v)) by Electrolytic processes (from India Infoline Ltd, 2002).

Energy kWh/ton	Mercury	Diaphragm	Membrane
Electricity	2800-3200	2500-2600	2300-2500
Steam (equivalent)	0	700-900	90-180

1.8 Summary, thesis aims and direction

This introduction has illustrated the range of fouling problems and cleaning requirements in the brewing industry, with specific focus on fermenter fouling and cleaning. The cost and downtime of fermenter CIP has been demonstrated and the importance of optimising CIP in breweries and other food and beverage manufacturers to minimise energy, water and effluent from CIP highlighted. Optimisation of CIP can be achieved by understanding the relationships between the different phases involved in fouling and cleaning: the deposit, the surface, cleaning time, temperature, mechanical action, and detergent concentration. The challenges to optimising current CIP practice include: the lack of experimental data that has been demonstrated to be directly applicable to industrial systems; and the lack of suitable on line measurement technologies that indicate a microbiologically clean surface. These challenges need to be overcome to apply bench and pilot scale findings in industry.

There are savings to be made by measuring the energy, water, chemicals and waste from CIP. The quantification of time, energy, water and chemicals used in one CIP regime revealed potential CIP improvements. The use of hot caustic was the biggest contributor to CIP cost and

environmental impact. Various routes to optimisation have been suggested in the business case, Section 1.7.

The objective of the work undertaken in this thesis is to shed light on the fundamental relationship between the phases involved in cleaning a range of deposit types relevant to brewing operations. In this work yeast slurry was used to represent type 1 and type 2 deposits and cooked caramel was used to represent a type 3 deposit.

An account of the current knowledge and studies relevant to brewery fouling and cleaning is documented in Chapter 2. The methods and materials used to generate and analyse deposits, cleaning regimes and data is presented in Chapter 3. The removal behaviour of yeast slurry from stainless steel surfaces is presented and discussed in Chapter 4. The cleaning behaviour of aged yeast slurry and cooked caramel is reported in Chapters 5 and 6 respectively. The implications of cleaning findings in the brewing industry are reported in the discussion section of each Chapter. The conclusion of this work and some proposed future work is presented in Chapter 7.

CHAPTER 2: REVIEW OF CURRENT FOULING AND CLEANING STUDIES

2.1 Chapter Introduction

The purpose of this Chapter is to place the work contained in this thesis in context, and with reference to other studies. The introduction highlighted the aim of the work: to investigate and describe some of the routes to optimising Cleaning In Place (CIP) in the brewing industry. To achieve this, the survey of the literature in this Chapter considers:

(i) Fouling and potential routes to its prevention in industry,

(ii) Deposit cleaning behaviours types and determining the effect of CIP parameters: time, temperature, mechanical and chemical action on cleaning,

(iii) Novel methods of cleaning, and

(iv) Measurement technologies for CIP.

Research into efficient cleaning will hopefully reduce the running cost and the environmental footprint of the plant. Scope for reduction has been demonstrated by the business case presented in Chapter 1, Section 1.7. These findings are important to the industry because their

implementation can be done relatively quickly and at low cost. However, the long term solution to fouling is yet to be determined. The causes of fouling and some prevention strategies are discussed briefly. The majority of this literature review focuses on cleaning innovations that could be used to improve CIP performance; and solve the immediate problem in the industry.

2.2 Fouling studies

Fouling is defined as the unwanted build-up of material on a surface. The fouling process generally involves a number of steps (Epstein, 1983);

(i)   surface conditioning,

(ii)   mass transfer of species to the surface,

(iii)   surface deposition, and

(iv)   deposit aging.

There is also a classification of fouling mechanisms demonstrated by Bott (1990) detailed in Table 2.1. Problems from fouling have been reported in the food and beverage industry, illustrated in Table 2.2.

Table 2.1: Fouling mechanisms adapted from Bott (1990) and Sharma et al., (1982).

Fouling Mechanism	Underlying Process
Crystallisation	Formation of crystals on the surface formed from solutions of dissolved substances when the solubility limit is changed. Cooled surfaces are subject to fouling from normally soluble salts, fats and waxes. Inversely soluble salts, *e.g.* calcium carbonate deposits onto heated surfaces. Where the fluid or components of the fluid solidify onto the surface this is called *solidification fouling* (Sharma (1982)).
Particulate deposition	Small suspended particles such as clay, silt or iron oxide deposit onto heat transfer surfaces. Where settling by gravity is the determining factor this is then called *sedimentation fouling*.
Biological growth (biofouling)	The deposition and growth of organic films consisting of microorganisms and their products, called biofilm. Macrobial fouling attachment and growth of macroorganisms, such as barnacles or mussels can proceed.
Chemical reaction at fluid/surface interface	The deposit formed on the surface (particularly heat transfer surfaces) is not the initial reactant (*e.g.* in petroleum refining, polymer production, dairy plants).
Corrosion	The material of the heat transfer surface is involved in reactions with components of the fluid to form corrosion products on the surface, i.e. a specific type of chemical reaction fouling.
Freezing	Deposit formed from a frozen layer of the process fluid, for example ice.

Table 2.2: Reported fouling problems in the Food and Beverage Industry (ZEAL consortium personal communication, 2007).

Fouling process example	Induced by temperature?
Protein deposition in heat exchangers	Yes
Mineral deposition in heat exchangers	Yes
Ice build up in freezers	Yes
Scale build up in cooling water systems	Yes
Fat burn on in ovens	Yes
Product solidification	Yes
Growth of biofilm	No
Accumulation of material in low flow areas of equipment	No
Fouling of membranes	No

2.2.1 A specific case: beer fermentation and fouling

In the UK, beer fermentation and maturation (secondary fermentation) tends to be a batch process in stainless steel vessels which can be cooled. Figure 2.1 (a) illustrates a schematic of a typical dual purpose fermenter with the recommended filling level (working volume) and the total

volume including CO_2 atmosphere (gross volume). Figure 2.1 (b) illustrates a dual purpose fermenter with the convection pattern of beer, identified by the arrows, under different cooling regimes: 1 – high level cooling and 2 – low level cooling. The * indicates that the cooling jacket is on. Secondary fermentation is slower and at lower temperature with lesser amounts of yeast (Lewis and Young, 2002). During both processes, a foam forms above the beer. This is called kräusen by microbrewers meaning "frizzy" in German. This foaming leads to the deposition of material on the wall of the vessel within the head space. This foam has been commented on by microbrewers and seen by other authors including Cluett (2001). Photographic documentation of the material is presented in Figure 2.2.

The amount and severity of the foam is dependent on carbon dioxide evolution during fermentation, which is dependent on

(i) the metabolic activity of the yeast.

(ii) the size and shape of the vessel.

Rapid production of carbon dioxide bubbles is believed to enhance convection currents in fermenters which results in a large volume of foam above the beer (Briggs et al., 2004). Cylindroconical fermentation vessels are normally 3 – 4 times taller than their diameter, which could be up to 4 m in large scale breweries. Larger height to diameter ratio tends to produce carbon dioxide bubbles more quickly generating a larger volume of foam.

(a)

(b)
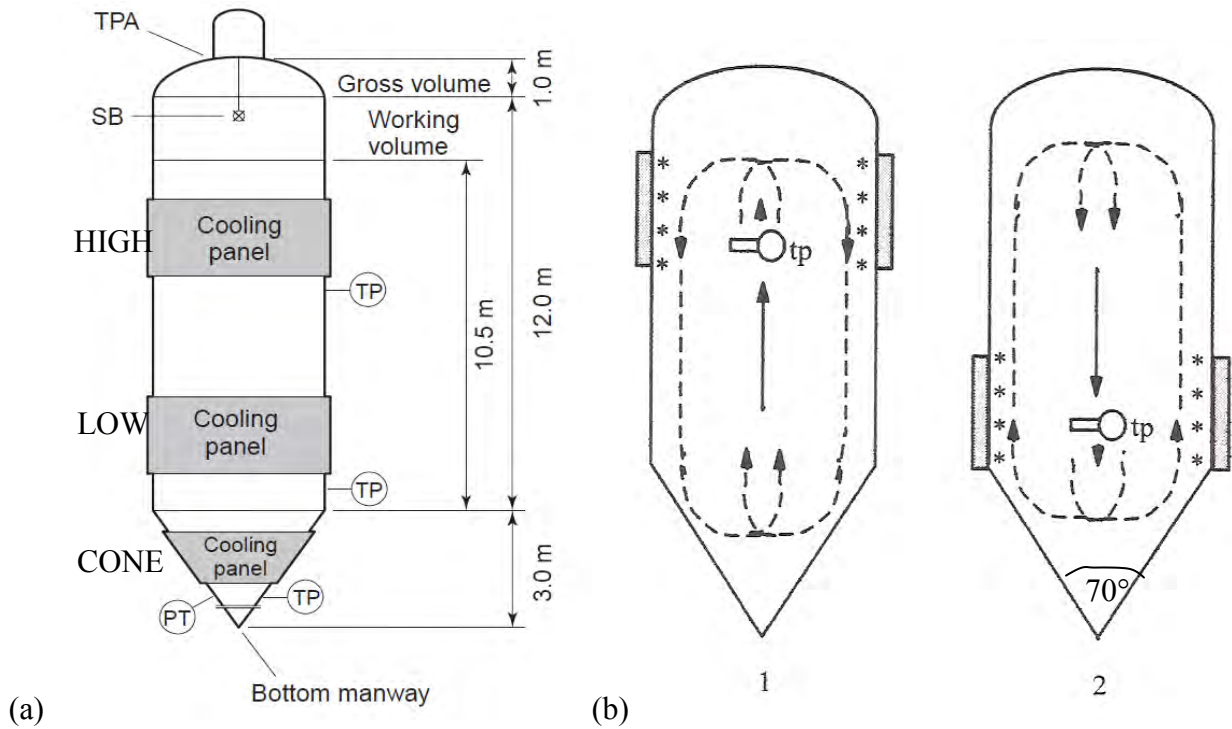
Figure 2.1: (a) Schematic of a dual purpose cylindroconical fermenter (Briggs et al., 2004). SB – spray ball, TPA – top plate assembly, TP – temperature probe, PT – pressure transmitter. (b) Schematic of beer movement in tall cylindroconical fermenters (Lewis and Young, 2002), 1 – high level cooling when the beer is above the temperature of maximum density, 2 – low level cooling when the beer is below the temperature of maximum density. The cooling panels are labelled in (a).

(a)

(b)
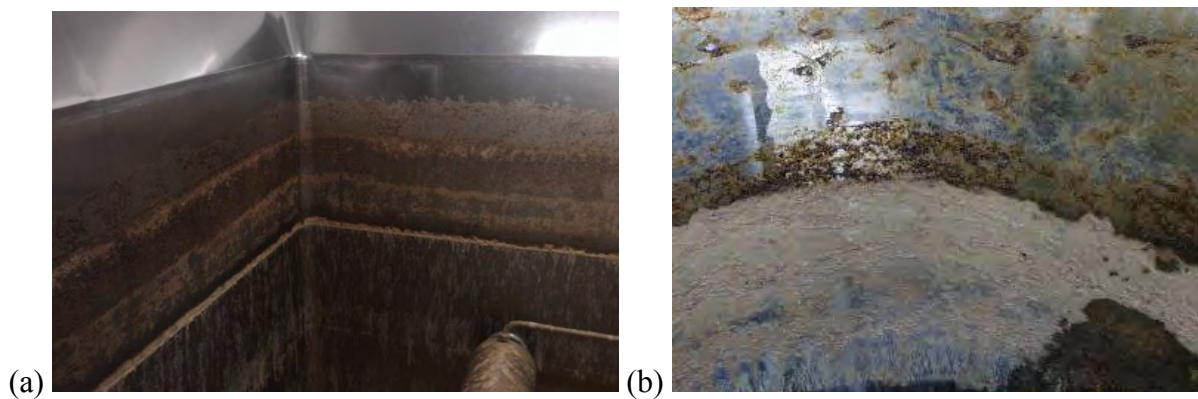
Figure 2.2: Kräusen remaining of the walls of (a) the Caledonian Brewery open square fermenter and (b) the top interior of a 500 l working capacity cylindroconical fermenter (from Cluett, 2001).

Figure 2.3 (a) indicates the rate of CO_2 evolution during batch fermentation. An initial lag in CO_2 production is followed by accelerated evolution reaching a maximum. There is a linear deceleration phase after this. Fermentation is exothermic due to yeast metabolism, thus the rate of CO_2 evolution can be related to the increase and decrease in temperature seen during typical ale fermentation. An example of ale fermentation is given in Figure 2.3 (b). The temperature can in turn be related to the foaming action during fermentation. Figure 2.3 (c) illustrates typical lager fermentation. The time frame to attain the desired gravity is longer for lagers than ales. This is because lager fermentations are done at lower temperatures than ale fermentations. Lower temperatures will reduce yeast metabolism and the rate of CO_2 production which will in turn reduce the foam produced. This also suggests that foaming produced during secondary fermentation will also be less due to lower temperatures used and yeast contained in the beer.

(a)

(b)

(c)
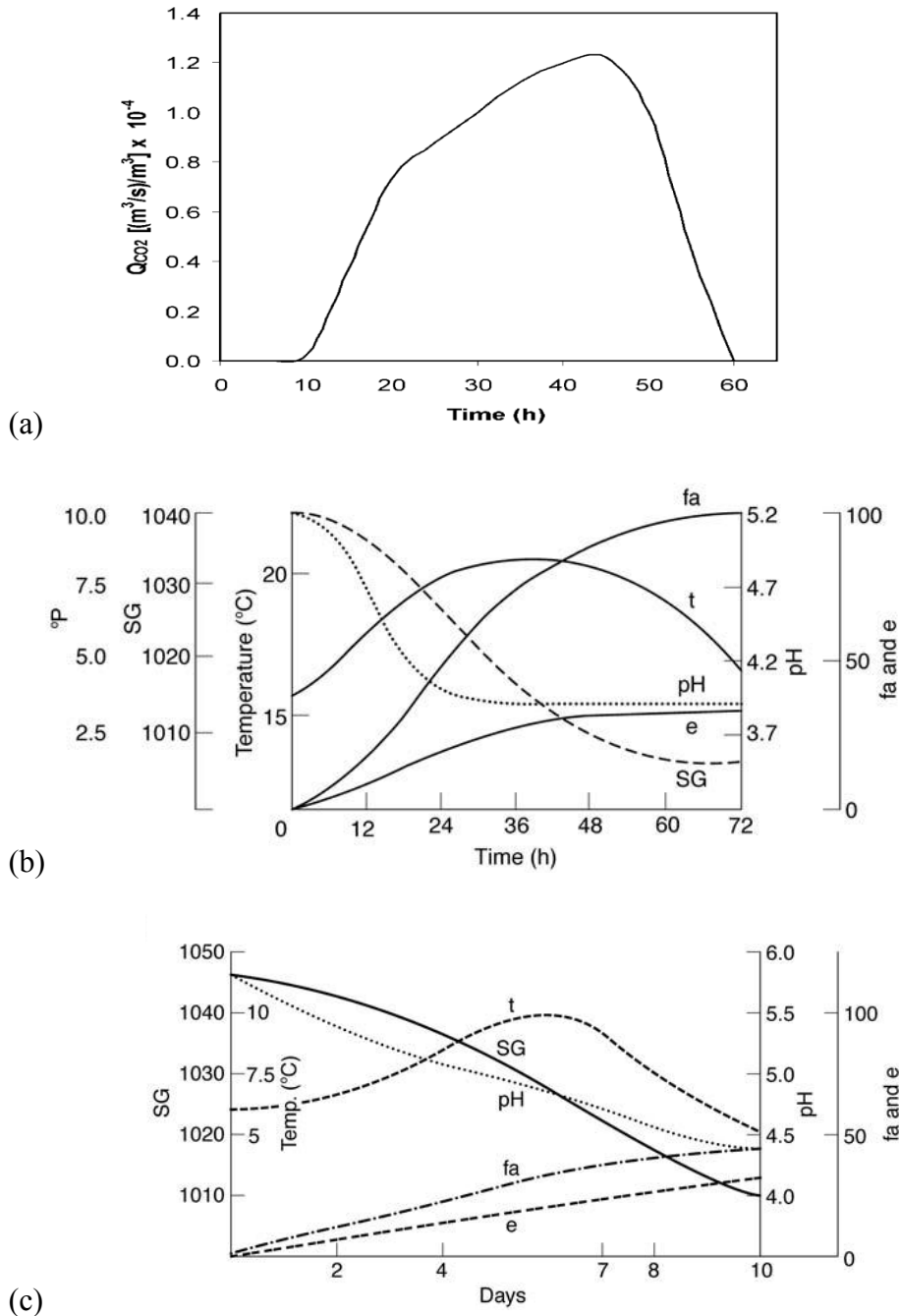
Figure 2.3: (a) CO_2 evolution (from Boswell et al., 2003), (b) the fermentation profile typically of ale and (c) the fermentation profile typically of lager (from Briggs et al., 2004). SG – specific gravity, T – temperature, fa – fusel alcohols (mg l^{-1}), e – esters (mg l^{-1}). The pH tends to fall as amino acids and ammonium ions are taken up by the yeast, and organic acids are secreted.

The heat given out during fermentation will peak at the maximum fermentation rate, typically within the first 40 - 60 h for ale fermentation (Lewis and Young, 2002). At maximum fermentation rate foaming is most vigorous and material from the foam attaches to the vessel wall in the head space. The foam collapses when the temperature and thus yeast activity decreases. During the remaining fermentation time may be changing the adhesion of the material on the surface. The duration of lager fermentation and maturation is longer than for ale. This may mean that even though less foam and less deposit are produced, the deposit formed may be harder to remove due to the longer aging time. The head space will also be at a higher temperature than the beer due because it is located above the level of the high cooling jacket. The heated head space could be further baking the material onto the wall of the vessel, especially in summer.

When fermentation vessels are emptied residual material that looks like yeast slurry sticks to the vessel wall. This creamy deposit is illustrated in Figure 2.4. Salo et al., (2008) added riboflavin which is fluorescent under a UV lamp to the beer before emptying the vessel. Upon emptying the vessel the walls were not fluorescent; as yeast is not naturally fluorescent the wall material is most likely yeast. Yeast cells were cultured from contact agars of the vessel in the study. In a large scale vessel the emptying time is minimised but can be anywhere from 3 – 12 h (Briggs et al., 2004). If the duration of emptying is increased the yeast can age on the surface for longer.

Salo et al., (2006) used fermentation cone deposit to create fouling on stainless steel plates. The cone deposit was aged on surfaces for 2 weeks; much longer than in normal beer fermentation operation. The plates were held at different cone angles during rinsing: 15, 35 and 55° (from the horizontal), which gave a flow velocity of $0.23 – 1.13$ m s^{-1}, $0.34 – 1.68$ m s^{-1} and $0.4 – 2.01$ m s^{-1}

from the top to the bottom of the plate. The authors found that this deposit could not be wholly removed using ambient water at 648 l h^{-1} (Re 1760) in any case. In fact only 20 - 30% of the soil was removed in all cases. No significant effect of cone angle was found. The cone angle of fermentation vessels tends to be 70° (see Figure 2.1) to enable efficient separation of yeast from beer (Briggs et al., 2004). This angle would enable higher flow velocities at the cone.

Figure 2.4: 80 l stainless steel tank (0.8 m by 0.4 mm) with residual yeast fouling attached to the wall and the cone. The wall was also sampled by contact agar (from Salo et al., 2008).

2.2.2 Adhesion of microbes to surfaces

If fouling did not occur there would be little need for cleaning. The principal factors responsible for adhesion between surface and foulant include: (i) van der Waals forces, (ii) electrostatic forces, (iii) and contact area effects; the greater the area the greater the total attractive force (Bott, 1995). Microbes are unlikely to attach to a surface if they are not in close proximity to it; in the range of van der Waals and ionic forces. Therefore microbes have to be in close proximity to each other and/or the surface to stick to it. Microbes have a natural affinity to surfaces. Yeast readily attaches to stainless steel and plastics, elastomers (Guillemot et al., 2006) and glass

(Mercier-Bonin et al., 2004) all of which are used extensively in the beer brewing and dispense industries. Mozes et al., (1987) found that yeast could attach and form a dense layer of cells on stainless steel and aluminium at pH 3 and 5 - 6. This group also determined a dense layer of yeast cells would attach to glass and plastics if the negative charge was reduced by treatment with ferric ions.

A minimum adhesion energy exists between the deposit and the surface over the surface free energy range 20–40 (mN m^{-1}); the following equation relates free energies from DVLO theory:

$$\sqrt{\gamma_S^{LW}} = \frac{1}{2}\left(\sqrt{\gamma_D^{LW}} + \sqrt{\gamma_F^{LW}}\right)$$

[2.1]

Where γ_S^{LW}, γ_D^{LW}, and γ_F^{LW} are the Lifshitz–van der Waals (LW) surface free energy of the surface, deposit and fluid respectively they can be quantified from contact angle measurements (Zhao et al., 2004). Liu et al., (2006) studied the interactions of 316 L stainless steel and baked and unbaked tomato deposit. A minimum removal energy range of 20 – 25 mN m^{-1} was found in both cases. Either side of this surface energy range the adhesive strength of the deposit on the surface increased. The influence of surface energy on adhesion is well known in marine and medical biofouling characterised by the 'Baier curve' (Baier, 1980). This curve demonstrates the weakest adhesive strength of bacteria to be at surface energies in the region of 25 mN m^{-1}.

Surface roughness and topography has been shown by various authors to affect the retention of microbes on the surface. Surface roughness exists in two principal planes, one perpendicular to the surface described as height deviation and one in the plane of the surface described by spatial

parameters. The effect of the average surface roughness height, R_a, on microbial retention has been investigated most thoroughly. Product contact surface finishes with a R_a value of up to 0.8µm are recommended (Lelieveld et al., 2005), which is often called 2B finish stainless steel. Akhtar (2010) characterized the average roughness of 316 L stainless steel, ceramic, PTFE coated steel and glass all with a R_a less than 0.8 µm as literature recommends. Experiments used atomic force microscopy (AFM) to measure the interaction between different fouling deposits and surfaces. At the nanometer length scale she found that:

(i)   Silica particles had a significant attraction of 1.70 mNm^{-1}, to stainless steel both in water and sorbitol; this is of relevance to toothpaste adhesion,

(ii)   Glass particles had a significant interaction to caramel and SCM, more so than stainless steel (as shown in Figure 2.5),

(iii)   The interaction force of PTFE particles and Turkish delight (agar based), was greater than that of stainless steel particles to Turkish delight (as shown in Figure 2.5),

(iv)   Toothpaste interacted with glass and stainless steel similarly and found to be less adhesive than the other food products mentioned.
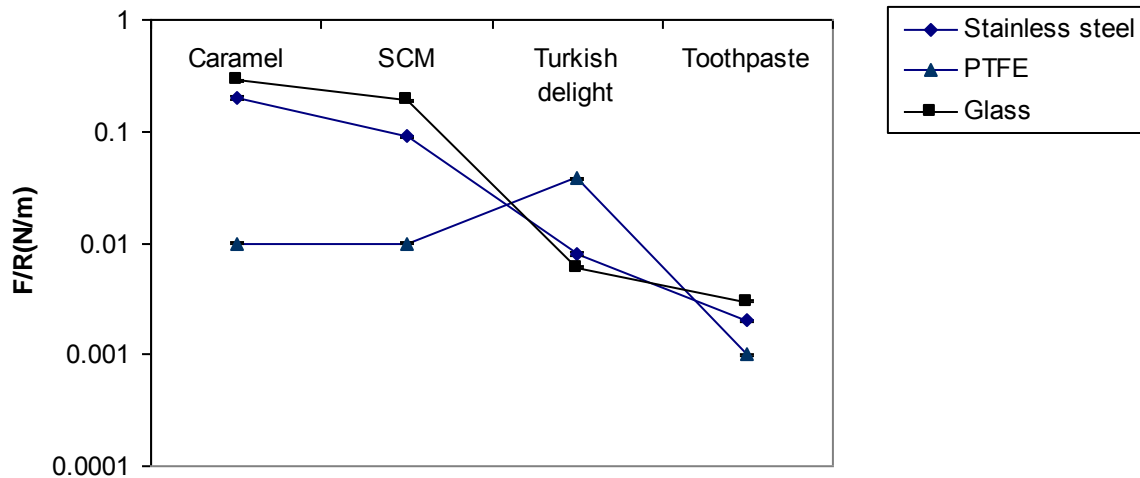
Figure 2.5: Force of attraction between stainless steel, PTFE and Glass particles and different food materials (From Akhtar, 2010). F/R is Force/radius in Nm[-1].

At the micrometer length scale, using micromanipulation probes, Akhtar (2010) found that the adhesion behaviour for Turkish delight was the same as at the nanoscale. I.e. the force to remove Turkish delight from PTFE surfaces is higher than for steel and glass. However caramel, SCM and toothpaste adhered more strongly to stainless steel at the microscale. Turkish delight, SCM and toothpaste appeared adhesive whereas caramel appeared cohesive; the forces binding caramel together were greater than those binding it to the surface, so it tended to be removed in one chunk rather than in layers. When the temperature of the caramel and whey protein was increased from 30 to 90°C, the adhesion to steel reduced significantly. Increasing the pulling speed of the AFM probe and contact time did not affect the adhesion caramel and but a variable result was found for whey. At low and high temperature, 30 and 90°C, caramel and SCM had a lower adhesion to PTFE than stainless steel and whey protein had a comparable adhesion to stainless steel and PTFE.

Whitehead and Verran (2006) reviewed the effect of R_a and topography on microbial retention. Research suggests that a surface with a R_a value close to the cell size increases retention on the surface. Smoother or rougher surfaces could result in lower retention. Rod shaped cells seemed to orient themselves in grains and grooves of similar size. Yeasts were found to require larger defects (5 µm) for retention however smaller daughter cells were retained in smaller defects (2 µm).

Cluett (2001) investigated the effect of stainless steel surface finish on the fouling and cleaning of a beer fermenter. Surface finishes investigated included 2B milled stainless steel, mechanically polished 120 grit and 240 grit and electropolished (EP) stainless steel. The top surface of the fermenter was half EP, half 240 grit, and the cone was EP. The cylinder of the vessel had all finishes, one quarter of the vessel from top to bottom represented by each surface finish. After lager fermentation lasting 12 days Cluett found that all surfaces fouled similarly and the level of deposition was heavy. He also found that all the surfaces cleaned similarly using a similar CIP regime with a spray ball (pre-rinse, caustic, water, acid, water, and sanitiser). However number of viable microbes was found to decrease in the cone at the bottom of the vessel.

2.2.3 Preventing fouling

Methods of preventing fouling that have been discussed in the literature include:

(i) "Non-stick surfaces" and design achieved by altering the surface material energy, finish and topography permanently or transiently

(ii) Altering product flow streams and operational parameters to minimise fouling mechanisms

(i) Non-stick design

Zhao et al., (2005a) found that stainless steel surfaces coated with Ag-PTFE reduced *E. coli* attachment by 94–98%, compared with silver coating, stainless steel or titanium surfaces. A surface with an energy (24.5 mN m^{-1}) roughly matching the theoretical minimum adhesion energy of the *E. coli*, 28.3 mN m^{-1}, was achieved. Composite coatings using nickel, phosphorus, copper and PTFE were also used by Zhao et al., (2005b) to create surfaces with specific energies shown to reduce biofouling. Later work by Pereni et al., (2006) confirmed the effect of surface free energy in minimising *P. aeruginosa* adhesion over a range of coatings including silicone, polished and non-polished stainless steel, PFA and PTFE nickel, phosphorus, aluminium composite coatings. Minimum retention of the bacteria was found at 20–27 mN m^{-1}. Silicone had a surface free energy of around 20 mN m^{-1} and the lowest CFU count. Biofilms are known to readily foul plastic pipes used in beer dispense. Beer is an electrolyte and can strip electrons from the plastic tubes leaving the pipe surface δ^+. It is believed proteins and microbes can then deposit on the plastic. It is also believed this effect occurs more readily at higher flow rates (Godfray, 2005). The company Beertech have a commercially available system that applies an alternating electromagnetic field to the beer flowing in a plastic pipe to reduce adhesion (Godfray, 2005).

Parbhu et al., (2006) used a transient treatment to modify the metal oxide surface. The treatment was present during the processing cycle and removed at high pH during alkaline cleaning. The treatment was shown to reduce the interaction potential between stainless steel and phosphate

anions resulting in significant reductions in fouling rates. Danfoss Bauer electronic motors in the food and drink industry have been coated with a time-release silver containing paint found to kill 99.9% of microbes (in dpa Electrical and Electronic, 2007).

(ii) Product and flow alterations

Dror-Ehre et al., (2010) tested the effect of biofilm development of *P. aeruginosa* when pre-treated in an aqueous solution of molecularly capped silver nanoparticles (MCNPs). Under specific conditions, cells and surfaces incubated for 39 h at 37°C, Ag-MCNPs retarded biofilm formation even when high percentage of planktonic *P. aeruginosa* cells survived pre-treatment with Ag-MCNPs. At the various incubation times a stable, low value of biomass was formed that could be easily removed. The authors found from micrographs of pre-treated cells that the intra cellular material was pushed towards the peripheral parts of the cell; a potential survival strategy.

Xiaokai et al., (2005) investigated the effect of electromagnetic treatment on water to minimise scale formation in the tubes of a plate heat exchanger. The technology is termed electromagnetic antifouling (EAF). The treatment was shown to aggregate particles in the flow which reduced precipitation at the wall. Liu et al., (2004) compared fouling of two phase flow (liquid-vapour) and three phase flow (liquid-vapour-solid) during the evaporation of Gengnian'an extract. The solid phase was added as inert solid particles. The two phase flow system generated fouling in 15 hours whereas the three phase flow system generated fouling after 60 h. Tse et al., (2003) found that in a two phase (liquid-vapour) wort boiling system that the wall temperature did not significantly affect the rate of fouling. Under conditions where vapour was condensed at lower

flow velocities (0.07 and 0.14 m s^{-1}) the initial fouling phase was more rapid than at the higher flow velocity. The authors found that the initial fouling rate halved as the flow velocity was doubled. These findings suggest that circulating fluid at a fast flow rate and adding a third phase would reduce fouling.

Pursuit Dynamics (Cambridge, UK) have a technology they propose heats wort more efficiently than current external wort boilers used in Heineken UK breweries. The PDX reactor is illustrated in Figure 2.6. In the PDX system steam is injected directly into the product stream rather than to the wall of the in external wort boilers. Flow is created through momentum transfer between the steam and the wort and the pressure drop generates suction pressure which pulls the fluid through the PDX reactor. A controllable supersonic shock wave is created which can dramatically increase flow rates or to aid homogenisation, mixing, heating or entraining without physical pumping. Heat transfer to the product is quoted as 95% efficient. An array of 8 PDX reactors has a wort processing capacity of 2450 – 4400 hl h^{-1}. Food grade steam and filtration is however required requiring capital expenditure and space on plant (PDX, personal communication (2007)).

The PDX reactor is of 3A hygienic design and the company claim no fouling occurs within the PDX reducing the frequency of CIP. Campden BRI also tested the efficiency of the PDX reactor when heating a 100 hl tank of detergent for CIP vs. a pump and plate heat exchanger (1000 kg h^{-1} and steam at 1.5 bar). The reactor, using 5 bar steam at 600 kg h^{-1}, was found to heat the tank volume to 70°C in a similar amount of time, and maintain the temperature. The PDX reactor was

also found to use 66 % less steam than the conventional heat exchanger loop (BRI, personal communication (2007).
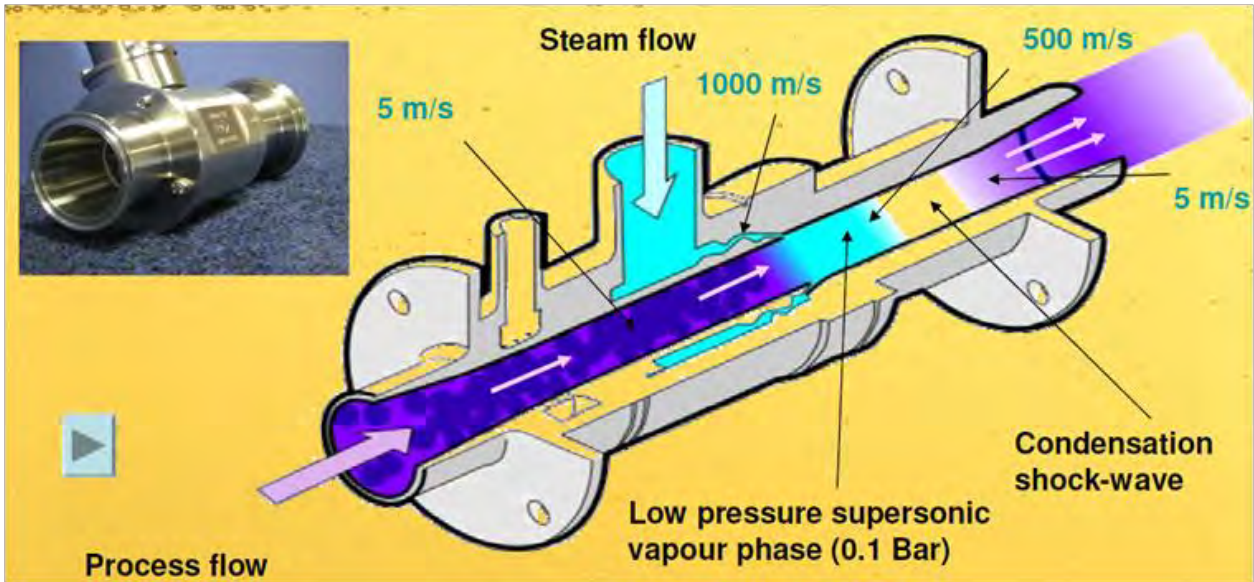
Figure 2.6: The PDX reactor (from PDX personal communication, 2007).

In dairy processing, Christian et al., (2002) found that increasing the mineral content of whey protein concentrate (WPC) during fouling on a plate heat exchanger, decreased the extent of fouling and altered the deposit composition closer to that of milk. Fickak et al., (2011) found that increasing the protein concentration of whey protein both increased the amount of the fouling on the pilot-scale heat exchanger and the time required to clean the fouling deposit by 0.5% NaOH.

Unfortunately an economically viable fouling prevention method is yet to be demonstrated in industry. Further research discussed in this Chapter considers the findings of studies relevant to optimising cleaning. Heineken CIP standard states that a pipe or vessel should be cleaned

immediately after a production cycle (HMESC: 02.32.04.001; 2009). An aged deposit is more difficult to remove than fresh and a type 1 soil could become a type 2 soil when aged.

2.3 Cleaning

Automated Cleaning In Place has been widely applied in dairy, brewing, food and wine processing for the last 50 years to return the plant to a clean state (Stewart and Seiberling, 1996). During CIP water and chemicals are circulated around the plant for a prescribed time (Tamime 2008). Cleaning is required to avoid microbial contamination and maintain process efficiency in food and beverage manufacturing. The presence of fouling on heat transfer surfaces reduces heat transfer efficiency and can promote microbial growth and survival (Bott 1995, Fryer et al., 2006). The CIP factors found to determine cleaning are described by Sinner's circle: a circle of the cleaning parameters, mechanical action, chemical action, time and temperature (Lelieveld et al., 2005). Cleaning can be dependent on the geometry. In a pipe the contribution of the cleaning factors are equal. In a pipe dead leg, time determines cleaning (Lelieveld et al., 2005).

Work done by Fryer and Asteriadou (2009) has proposed the classification of cleaning behaviours into three types on a 'cleaning map' presented previously in Chapter 1, Figure 1.6. The cleaning map is an important problem classification tool. This classification of soil types into cleaning behaviours enables studies to be compared across these groups. The cleaning behaviour of soils is closely correlated to cost with water at ambient condition at the least costly end and hot chemical at the most costly end. Work done by Yang et al., (2008) helped to classify cleaning optimisation into two types of investigation:

(i)   Engineering investigations: reducing energy, time, and cost in established cleaning regimes.

(ii)   Scientific investigations: achieving cleanliness or a cleaning time as a function of influencing factors; wall shear stress, temperature, surface type and finish etc...

Research relevant to this study that has considered the influence of cleaning parameters in flowing systems on the removal behaviour of deposits is listed in Tables 2.3 – 2.5. Table 2.3 details type 1 deposit removal studies, Table 2.4 details type 2 deposit removal studies and Table 2.5 details type 3 deposit removal studies. The geometry cleaned, effect of CIP parameters, and the method of determining cleaning efficiency is listed in each Table. Examples of each deposit type include:

(i)   Type 1: toothpaste, tomato paste, yoghurt, shampoo, beer, wine, milk and yeast.

(ii)   Type 2: microbes and microbial films of bacteria, spores and yeast species.

(iii) Type 3: WPC, cooked SCM, starch, boiled wort and egg albumin.

Table 2.3: Type 1 deposit CIP studies.

Deposit	Geometry	Effect of flow or τ_w	Effect of temperature	Effect Re	Cleaning Determinant	Reference
toothpaste	1 m L, 2" OD 316 L ss pipe (horizontal)	Increase flow velocity (1 to 3 m s^{-1}, decrease cleaning time.	Increase temperature (from 20°C), decrease cleaning time (to a point ~ 40°C).	Increase Re (4000 – 250,000, decrease cleaning time.	Turbidity reaches 4 ppm.	*Cole et al., (2010)*
shampoo	316 ss plate (350mm L, 30mm ID, 18.3mm ED) (vertical flow cell)	(0.14 - 0.47 m s^{-1}) higher flow velocity, more efficient removal at the start of cleaning.	(31 - 51°C), removal of shampoo layers faster at higher temperatures as cleaning proceeds.	-	Visual, MSS and Spectro-photometry	*Pereira et al., (2009)*
mustard	glass T-piece (variable depth T, 4 and 6 cm)	Increase flow velocity (1 to 1.88 m s^{-1}) increase removal rate.	-	Above a certain Reynolds number the recirculation zone length becomes constant.	visual	*Jensen et al., (2007)*
yeast cells re-hydrated (aged 1 h at ambient)	glass, polypropylene and polystyrene surfaces (210 × 90mm L) in horizontal flow cell	increase τ_w, decrease number of cells (i) linearly for plastics (ii) as a curve for glass	-	-	visual	*Guillemot et al., (2006)*
tomato paste	316L ss coupons (circular: 26 mm D) horizontal flow cell	(0.7, 1.5, 2.3 l min^{-1}) increase flow rate, the effect of temperature on cleaning time decreases	(30 , 50, 70°C) increase temperature, decrease the time to remove deposit	(850 - 4800 Re) increase Re, decrease cleaning time	visual, image analysis and MHFS	*Christian (2004)*

L = length, OD = outer diameter, ID = inner diameter, ED = equivalent diameter, ss = stainless steel, MSS = mechatronic surface sensor, MHFS = Microfoil heat flux sensor.

Table 2.4: Type 2 deposit CIP studies.

Deposit	Geometry	Effect of flow or τ_w	Effect of temperature	Effect of chemical/pH	Cleaning Determinant	Reference
yeast slurry (aged at 30°C, 5 days)	316 ss coupons (square: 30 x 30 mm L) in horizontal flow cell	Increase in flow velocity (0.26 to 0.5 m s^{-1}) decrease cleaning time at 50 and 70°C. Limited effect beyond 0.4 m s^{-1} at 20 and 30°C.	Increase temperature, decrease cleaning time.	1% NaOH	visual, image analysis and MHFS	*Goode et al., (2010)*
B.cereus spores	316L ss pipe (20 cm L, 2.37 cm ID) and 2 way valve (entry to exist 18 cm L, 3.5 cm ID)	-	-	NaOH 0.5% (w/w) at 60°C, 2200 l h^{-1}, up to 30 min. The % residual spores decreased as cleaning time increased.	Agar overlay technique using TTC (spores appear red)	*Le Gentil et al., (2010)*
yeast cells re-hydrated (aged 1 h at ambient)	316 L ss, (210 × 90mm L) in horizontal flow cell	increase τ_w, decrease number of cells barely for stainless steel (10 %).	-	-	Visual	*Guillemot et al., (2006)*
B.cereus spores (in milk)	304 L ss pipes (15 x 10^{-2} m L, 2.3 x 10^{-2} m ID) (horizontal)	Increase τ_w, (17.45 - 68.95 Pa i.e. 1.61 - 3.29 m s^{-1}) decrease number of spores (after 5 min). Contact time was more important in reducing spores	Rinsing at 60°C revealed less spores compared to 20°C at the same soaking times.	0.5% w/w of NaOH at 60°C	Agar overlay technique using TTC (spores appear red)	*Lelièvre et al., (2002)*
B.cereus spores (in custard)	Progressive-cavity pump (with axial or tangential exit pipe). Tangential was best. In the axial setup the number of CFU was > 10 CFU/cm in the pump body and gaskets.	-	-	pre-rinse 0.5m/s (6 min); 0.2% NaOH at 1.5m/s, 60°C (10 min); intermediate rinse 0.5m/s (6 min); 0.2% HNO$_3$ at 1.5 m/s, 60°C (10 min); final rinse 0.5m/s (6 min).	Agar overlay technique using TTC (spores appear red)	*Bénézech et al., (2002)*

L = length, OD = outer diameter, ID = inner diameter, ED = equivalent diameter, ss = stainless steel, MSS = mechatronic surface sensor, MHFS = Microfoil heat flux sensor.

Table 2.5: Type 3 deposit CIP studies.

Soil	Geometry	Effect of flow or τ_w	Effect of temperature	Effect Re	Effect of chemical/pH	Cleaning Determinant	Reference
Starch (with phosphorescent tracer molecules)	Continuous and abrupt expansions (ID 26mm, expanding from 26 to 38 mm)	Local cleaning time has a minimum where the τ_w shows a maximum and vice versa	N/A, constant	Re > 25 000 investigated.	N/A. Constant 0.5%.	Visual, image analysis	*Augustin et al., (2010)*
Cooked SCM (sweet condensed milk)	316 L ss coupons (square: 30 x 30 mm L)	Increase flow velocity from 0.25 - 0.5 m s^{-1}, decrease cleaning time at all temperatures	An increase in temperature (40, 60, 80°C) revealed a linear decrease in cleaning time	An increase in Re (6500 to 27,500) revealed a decrease in cleaning time according to Power law.	an increase from 0.5 to 1.5% NaOH did not significantly affect cleaning time at higher flow velocities	visual, image analysis and MHFS	*Othman et al., (2010)*
Egg Albumin	316L ss coupons (circular: 26 mm D)	Increase flow less significant at higher chemical concentrations.	30°C did not clean. Increase temperature, decrease in cleaning time. However 50°C removed more deposit at 1% NaOH than 70°C.	Increase Re (1090 - 4840) decreases cleaning time (at 50°C, 0.1 - 1% NaOH). At 70°C 0.1%, increase Re, increase cleaning time.	no cleaning at 0.1 wt% NaOH. Concentration 0.25 - 3% (at 50°C, 2.3 l min^{-1}) decreases cleaning time. Most significant at low flow (0.7 l min^{-1})	visual, image analysis and MHFS	*Aziz (2008)*
Whey protein concentrate (WPC)	316L ss coupons (circular: 26 mm D) horizontal flow cell	Limited benefit to increase flow velocity at 70°C and 1% NaOH. Benefit if increase flow at low concentration.	Increase temperature (30 - 70°C) decrease cleaning time at all flow rates and chemical concentrations (0.7, 1.5, 2.3 l min^{-1}, 0.1, 0.5, 1% NaOH)	Increasing Re (1090 - 4840) only beneficial at 0.1% NaOH.	limited benefit to increase concentration above 0.5%.	visual, image analysis and MHFS	*Christian (2004)*

L = length, OD = outer diameter, ID = inner diameter, ED = equivalent diameter, ss = stainless steel, MSS = mechatronic surface sensor, MHFS = Microfoil heat flux sensor,

Table 2.5 continued: Type 3 deposit CIP studies.

Soil	Geometry	Effect of flow or τ_w	Effect of temperature	Effect Re	Effect of chemical/pH	Cleaning Determinant	Reference
WPC	10 cm sections of ss tubes (6mm ID 0.15mm thickness) fouled in counter current heat exchanger	Increasing flow rate does not necessarily decrease cleaning time. It is important to decay phase time	Wall temperature did not affect the plateau. Increasing the bulk temperature decreases cleaning time.	Re 500 – 6500 investigated. As Re increases cleaning time decreases generally	N/A. Constant 0.5%.	Thermal resistance using MHFS and mass	*Gillham et al., (1999)*

L = length, OD = outer diameter, ID = inner diameter, ED = equivalent diameter, ss = stainless steel, MSS = mechatronic surface sensor, MHFS = Microfoil heat flux sensor.

WPC is often used in research studies to represent milk fouling deposit, because it is easier to handle and store, and the fouling composition easier to control and replicate. Robbins et al., (1999) compared the cleaning of milk and WPC from a plate heat exchanger (PHE). They found that in the pasteurisation and UHT sections of the PHE that both materials fouled heavily. However in the intermediate section WPC also fouled excessively whereas milk did not. Compositional analysis revealed protein fouling from both materials in the pasteuriser section. Increasing to UHT temperatures revealed milk fouling to become more mineral based whereas the WPC fouling remained predominantly protein based, suggesting comparison of milk and WPC fouling is not wise at UHT temperatures.

Yeast can exhibit type 1 (if in contact with glass) and type 2 (if in contact with stainless steel) cleaning behaviour. Guillemot et al., (2006) found that yeast cells could be wholly removed from glass using water but that yeast cells had a strong adhesion to stainless steel. The wall shear stress required to remove 50 % of the attached cells from stainless steel, denoted $\tau_{w50\%}$ was 30 Pa,

whilst for plastics $\tau_{w50\%}$ ranged from 1 to 2 Pa. The effect of surface type and fouling prevention methods are discussed in Section 2.7. The effect of CIP parameters on the removal of different deposit types is discussed in the following sections. Even though there is clear evidence deposit types are removed from surfaces differently the approach to cleaning is typically the same:

 (i)   Pre-rinse (or product recovery stage); to remove loosely bound soil,

 (ii)   Detergent phase (alkali or acid); to remove deposit,

 (iii) Intermediate rinse,

 (iv)   Sanitisation/disinfection step (chemical or thermal),

 (v)   Final water rinse.

Although disinfection is done after the deposit has been removed, this stage is often included as part of the CIP regime in industry. The purpose of this stage is to make the surface free of beer spoilage microbes, rather than to remove the foulant. In a brewery, yeast storage tanks are washed by a similar CIP regime as fermentation vessels (see Table 1.6). If this deposit could be removed from the vessel using water alone, the system could be sanitised after the water rinse negating the detergent phase. This CIP regime would save time, money and have a lower environmental impact than the current regime.

2.3.1 Product recovery

At the end of a process there can be a significant amount of material left in pipe work and in tanks. This product may be saleable, in which case it should be recovered, or it may be considered waste. In both cases the bulk of this material should be removed (generally in the first

rinse phase) prior to the "cleaning" phase. Type 1 deposits will generally be saleable product like toothpaste or shampoo, whose recovery should be maximised. Type 2 and type 3 deposits will generally be thin layers at the wall and so need to be removed to return the plant to a clean state. As such type 2 and type 3 deposits need not be recovered at the end of a process.

Product recovery can be done by pigging; driving an object through a pipeline by a fluid. The pig could be solid, liquid or gas. Solid pigs tend to be used in long sections of straight pipe work where complex geometries do not need to be navigated; for example in crude oil pipelines to remove paraffin was (Guo et al., 2005). The use of crushed ice (with a freezing point depressant) in pigging systems has been developed and researched at the University of Bristol to remove starch-water mixes (Quarini 2002). The void fraction of the ice is controlled so the pig can navigate bends and T-pieces as well as straight pipe work. Application of this technology in the food and beverage industry appears limited. The ice system is expensive to make and store. A company called Aeolus owns a "Whirlwind" technology that uses compressed air to remove soft deposits such as fruit juice from pipe work with bends (see www.aeolustech.co.uk). Application of this technology in the food and beverage industry is also limited, as the cost of compressed air is considerable.

2.4 The effect of CIP parameters on type 1 removal

Schlüßer (1976) compared cleaning behaviour of three type 1 soils; beer, wine and milk, illustrated in Figure 2.7. The products themselves were not heated. The cleaning profiles of each product were different. Research on type 1 product types suggest they are often shear thinning i.e. have an effective viscosity that is a function of shear rate, and exhibit viscoelastic properties. The

shear thinning rheology of yoghurt was determined by Henningsson et al., (2006) who also used cross-correlation of dual-plane electrical resistance tomography (ERT) to determine the velocity profile of yoghurt in a pipe. For flow velocities 0.05 to 0.25 m s^{-1}, yoghurt was observed and predicted to flow as a plug. If the process was set up so that yoghurt flows as a plug, at changeover the mixing zone between the two yoghurts would be smaller and yield losses reduced. Prediction of the mixing zone of a Hershel-Bulkley material with and without wall slip at 0.19 m s^{-1} was also done by Henningsson et al., (2006). With wall slip, it was predicted the material would have a larger plug flow region. Relating the rheology of a material to its flow behaviour in a pipe in the turbulent regime is however very complex.
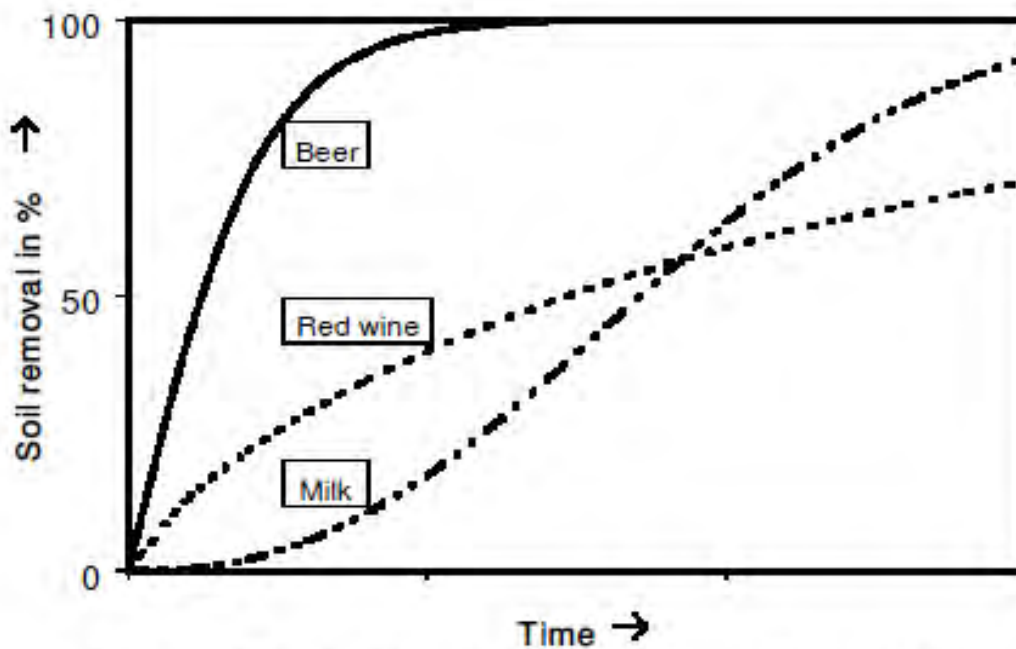
Figure 2.7: Cleaning characteristics of three type 1 products, beer, red wine and milk with water (Schlüßer, 1976).

2.4.1 Flow and wall shear stress

The flow rate has an effect on the removal rate of type 1 materials. The rheology of tomato paste has been represented by the Carreau model (Bayod et al., 2008), and the cleaning behaviour of

tomato paste in a flow cell has been investigated by Christian (2004). At 30°C it was found that by increasing the flow rate from 0.7 to 1.5 to 2.3 l min^{-1} (Re 750 and 4840) the cleaning time decreased. The relationship appears linear. This was also true at 50 and 70°C.

Shampoo (SUNSILK® (colour radiant)) was rinsed from a stainless steel plate in a vertical flow cell by Pereira et al., (2009), and they found that the faster the initial flow rate (in the range 0.14 - 0.47 m s^{-1}), the more shampoo was removed from a duct. The same effect was found for removing toothpaste from a pipe (Cole et al., 2010). The effect of wall shear stress (τ_w) in the range 0.5 to 10 Pa on toothpaste removal was studied. Shear stress accounts for fluid density and Re which are both affected by temperature. Toothpaste cleaning time is governed by two removal phases (Cole et al., 2010):

 (i)   Core removal – where most of the product is removed.
 (ii)   Thin film removal – where the remaining wall film of toothpaste is removed.

It was found that the time to remove the remaining film had by far the biggest impact on the cleaning time. For shampoo Pereira et al., (2009) found that flow velocity had the biggest impact on shampoo removal from the flow cell at the start of cleaning, less so as cleaning progressed.

2.4.2 Temperature

For cleaning of tomato paste in the flow cell, Christian (2004) found that an increase in temperature decreased the cleaning time by a linear relationship. Both an increase in temperature from 30 to 70°C and in flow velocity from 0.7 to 2.3 l min^{-1} decreased cleaning time. Cleaning

time reduced by a factor of 6 from the lowest flow rate and temperature to the highest flow rate and temperature.

Shampoo was rinsed at 0.14 m s^{-1} at 31 and 51°C by Pereira et al., (2009). After the initial bulk of shampoo was removed from the flow cell, it was found that the removal of shampoo layers occurred faster at higher temperatures. For toothpaste Cole et al., (2010) found an increase in the water temperature from 20 to 40°C decreased the cleaning time; however increasing the temperature above 40°C did not decrease cleaning time any further. The same effect may occur when rinsing shampoo however the investigators did not exceed a water temperature of 51°C in their experiments.

The effect of flow can be studied in terms of Reynolds number ($\frac{\rho v d}{\mu}$), or Re, and may provide further insight into removal behaviour and flow velocity; Re incorporates the fluid density and viscosity which change with temperature. For tomato paste cleaning it was found that cleaning time was correlated with Re (Christian, 2003). As the Re was increased from 800 to 4800 the cleaning time decreased according to a power law: $t_{c,HFS} = 2 \times 10^6 \, (Re)^{-0.97}$. $R^2 = 0.81$. Jackson and Low (1982) found a critical Re of 6300 for cleaning of dried tomato juice from a plate heat exchanger, below which little deposit was removed. Cole et al., (2010) found that for toothpaste cleaning (from various length scales and diameters) a dimensionless cleaning time, θ_c, could be plotted as a function of Re. $\theta_c = t_c \frac{v}{d}$ (where t_c is the cleaning time and d is length). A power law model was also defined: $\theta_c = 9 \times 10^7 \, (Re)^{-0.78}$; with a similar fit, $R^2 = 0.84$.

2.5 Design

1.5 m s^{-1} is the flow velocity most often reported by industrialists as that required to clean pipe lines effectively (ZEAL consortium, personal communication). This is however anecdotal with no theoretical justification (Changani et al., 1997). In industrial pipe systems there are however more complicated geometries such as bends, valves and T-pieces. This raises the question: does increasing the flow velocity decrease the cleaning time of other geometries? This gives a better indication of the effect of flow on the cleaning time of a whole system.

Jensen et al., (2007) filled a variable depth "upstand" (also called a T-piece) made from glass with commercially available mustard and rinsed with ambient water. The upstand depth was tested at 4 and 6 cm. The flow velocity was increased from 1 to 1.88 m s^{-1} to define the effect on cleaning the T-piece. The upstand used in the study is shown in Figure 2.8. Jensen et al., (2007) found that:

(i)   Increasing the flow velocity increased removal rate. However the authors suggested this was more likely due to greater acceleration of the water at 1.88 m s^{-1} into the T-piece. At the lower flow velocities flow had not fully developed before entering the T-piece.

(ii) Some areas of the T-piece were harder to clean than others. The position in the upstand most difficult to clean was always located in the same position (see Figure 2.9).
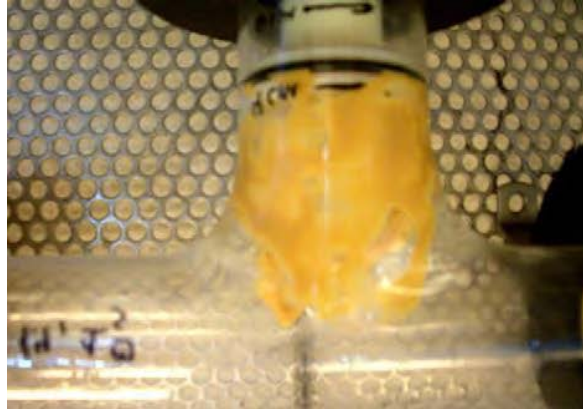
Figure 2.8: Upstand geometry used for investigating the influence of different flow rates during CIP (flow was from left to right) from Jensen et al., (2007).

As expected, the top of the upstand was difficult to clean. However an additional area located on the upstand pipe was always the last part to be cleaned in all the experiments, regardless of velocity. Jensen et al., (2007) used CFD simulations to predict the wall shear stress in the 4 cm upstand (illustrated as a downstand in Figure 2.9). Their CFD findings are illustrated in Figure 2.9 (a) – (c) where blue is low wall shear stress (0 Pa) and red is high wall shear stress (5 Pa). As the flow velocity was increased the blue area decreased in size. Within these simulations the area most difficult to clean, the centre of the upstand, is identified. Increasing the flow rate does not improve cleaning of this area. The wall shear stress achieved at this position is low at all three flow velocities. Other areas hardest to clean are circled.

(a) (b) (c)
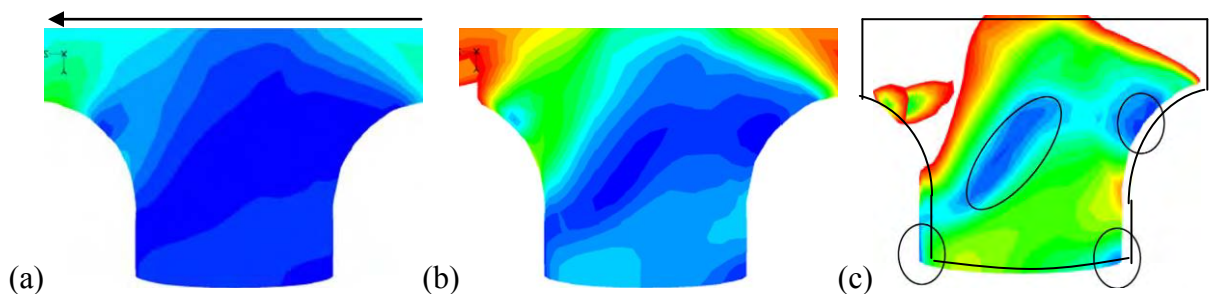
Figure 2.9: CFD simulations of the flow field in 4 cm upstand T piece at (a) 0.5 m s^{-1}, (b) 1 m s^{-1} and (c) 2 m s^{-1}. Blue is low wall shear stress (0 Pa) and red is high wall shear stress (5 Pa). White represents wall shear stress in excess of 5 Pa. Water enters the section from the right and exits the T section on the left represented by the arrow in (a). Jensen et al., (2007).

Jensen et al., (2007) examined the effect of pulsed flow in the upstand. They found that pulsing flow only affected the cleaning time of the 4 cm depth T piece, not the 6 cm depth T piece. They compared cleaning at 1 m s^{-1} (v$_1$), 2 m s^{-1} (v$_2$) and pulsing at 15 s (p$_1$) and 30 s (p$_2$). The cleaning time of the 4 cm upstand was longer when rinsed at 1 m s^{-1} than when the flow was pulsed. However rinsing the upstand at 2 m s^{-1} gave the quickest cleaning time. The authors concluded that at turbulent Re the area of the recirculation zone in the T-piece did not change. A recirculation zone is typically located after a pipe expansion and depends on Re and the expansion ratio. At lower Re (< 10 000 in this case) the length of the recirculation zone may change, hence faster cleaning times for pulsed flow at 1 m $^{-1}$ than using constant at 1 m s^{-1}.

Jensen and Friis (2005) used CFD simulations to predict the cleanability of a mix proof valve fouled with *B. Stearothermophilus* spores in accordance with the EHEDG standard cleanability test (EHEDG 1992; Timperley et al., 2000). In the EHEDG test the apparatus is filled with custard and/or spores. An area "difficult to clean" is defined as an area that produces yellow agar in three consecutive tests (EHEDG 1992). Yellow agar shows the presence of spores. The study revealed that the valve was easier to clean than the radial flow cell (detailed in Jensen and Friis (2004)). The study predicted that a critical wall shear stress of 3 Pa was necessary in both systems to ensure cleaning; however, areas of extremely low wall shear stress and some areas of wall shear stress higher than 3 Pa had spores remaining. The authors concluded that wall shear stress was not the only factor governing cleaning in this case. As spores are more likely a type 2 soil, this conclusion seems logical.

Bénézech et al., (2002) rinsed spores in custard from a progressive cavity pump (a type of positive displacement pump) using a standard CIP regime in two configurations (i) with an axial exit pipe i.e. custard was pumped out of the top of the pump body on the same axis as entry, and (ii) with a tangential exit pipe i.e. custard was pumped out of the body at the side off the axis of entry. The CIP consisted of a pre-rinse at 0.5 m s^{-1} for 6 minutes; 0.2 % NaOH rinse at 1.5 m s^{-1} 60°C for 10 minutes; intermediate rinse at 0.5 m s^{-1} for 6 minutes; 0.2 % HNO$_3$ rinse at 1.5 m s^{-1} 60°C for 10 minutes; final rinse at 0.5 m s^{-1} for 6 minutes. The group found that in the tangential set up all parts of the pump were cleaned to the same number of colony forming units per cm (CFU cm^{-1}), approximately 10 CFU cm^{-2}. The authors defined a high level of hygiene as counts < 18 CFU cm^{-2}. In the axial set up not all components were cleaned to the same level. There was an increased number of CFU cm^{-2} in the pump body and gaskets (> 18 CFU cm^{-2}).

To clean tanks spray devices, typically called cleaning heads are used. The design of cleaning head is of paramount importance to be effective. There are two main choices when cleaning vertical vessels such as fermenters: (i) static cleaning heads for example a spray ball (SB) and (ii) dynamic cleaning heads, for example rotary spray heads (RSH) or rotary jet heads (RJH). Examples of both are given in Figure 2.10. Typically spray balls operate at lower pressures and use water at a higher rate than rotating cleaning heads, which operate at higher pressures (around 5 bar). Heineken CIP best practice states to achieve good soaking and mechanical effect 1.5 l cleaning agent m^{-2} min^{-1} must be delivered to a surface. The standard also suggests the connecting pipe work should be cleaned at Re > 3000 to ensure turbulent flow and good cleaning (HMESC: 02.32.04.001; 2009). Morrison and Thorpe (2002) defined the wetting rate at the mass

flow rate (kg s^{-1}) required to completely wet a surface of width W (m). Wetting rates achieved by single jets from a sprayball was found to be $0.1 - 0.3$ kg m^{-1} s^{-1}.

The act of removing deposit from a vessel involves initial wetting and subsequent softening (or dissolution) of the deposit, followed by complete removal by further impingement. Morrison and Thorpe (2002) measured the dimensions of the area wet by the impaction of single water jets onto a sheet of painted acrylic for a range of pressures and distances from spray balls of different sized holes. They found that if the jet directly impacted the area to be cleaned, this area was clean within 60 s. The point of impact was smaller than the total area being wetted however certain areas were not cleaned by the spray ball. The width of the falling film from the point of impact remained the same size throughout rinsing. Jet break up was observed at 45°C which increased the distribution of the jet and cleaned a larger area. The authors recommended spray balls only be used to clean soiling that only required irrigation as impaction is not guaranteed. The efficiency of a spray ball and a RJH in cleaning a fermentation vessel was compared by Alfa Laval using a standard CIP regime: pre-rinse 7 – 10 minutes, caustic at 85°C for 5 minutes, and final rinse for 5 minutes (ZEAL consortium communication, 2010). This was achieved in 20 minutes by the RJH compared to 120 minutes for the spray ball. The wall shear stress and the wetting rate achieved by the falling film in a tank is decreased when the temperature is increased from 20 to 70°C suggesting cleaning fluid viscosity is an important factor in the formation of a liquid film on a surface.

(a)   (b)   (c)

Figure 2.10: Commercially available (a) spray ball (SB), (b) rotary jet head (RJH) and (c) rotary jet head (RJH) (from Alfa Laval personal communication, 2010).

The effectiveness of a spray cleaning a surface depends on the impact force of the jet and the wetting area around the point of impingement. In RJH cleaning the impact of the cleaning fluid on the wall is much larger than in SB cleaning due to higher delivery pressures achieved in the system. This delivers a larger wall shear stress to the deposit to be removed. Increasing the force of the jet can overcome large deposit hydration times and reduce removal times. The proportion of time, physical action, temperature and time delivered to the tank by a spray ball and a RJH are given in Figure 2.11. For spray ball cleaning, time is required to achieve deposit removal. For a RJH, mechanical action is required to achieve deposit removal so cleaning times are less reliant on contact time with chemical at high temperature.
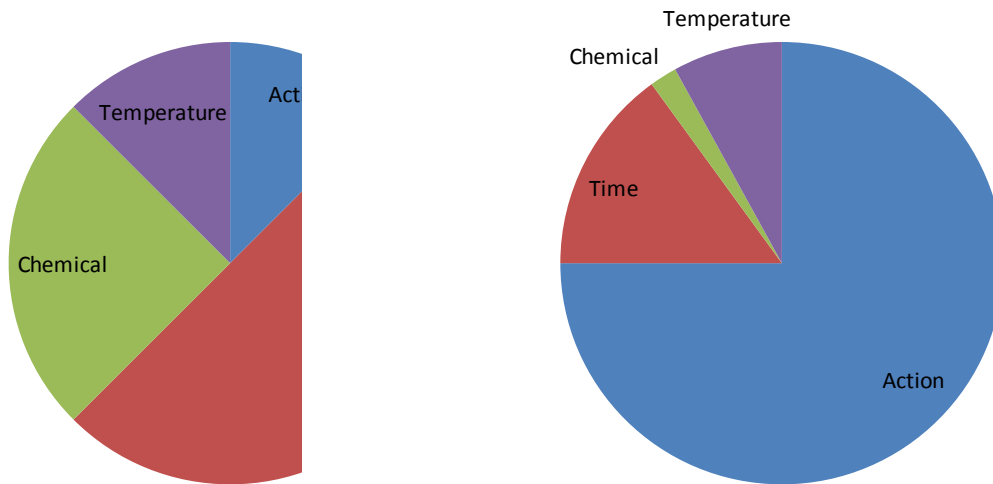
Figure 2.11: The time, physical action, temperature and time required for effective spray cleaning by (a) a spray ball and (b) a RJH (Jensen, 2010 personal communication).

Goode et al., (2010) found that in beer fermentation vessels there were two distinct deposit types to be cleaned, classified as type A and type B foulants:

(iii)   Type A - Formed during fermentation above the beer level at the top of the vessel,

(iv)   Type B - Residual yeast attached to the vessel wall and cone below the beer level during emptying.

Type B fouling was shown by Salo et al., (2008) in Figure 2.4. An example of the type A fouling viewed from a fermenter man way door at the top of the vessel is given in Figure 2.12.

Gasket

Type A fouling on
the vessel and the
gasket (samples had
been scraped from
the vessel)
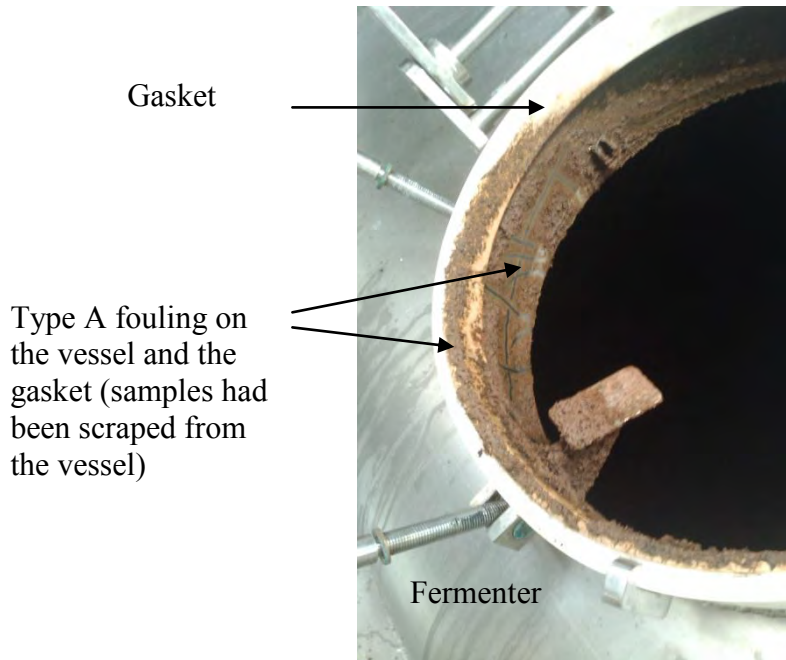
Fermenter

Figure 2.12: Type A deposit seen at the top of a fermenter around the man way door and the gasket.

Type B fouling has a shorter aging time than type A fouling. As such type B fouling can be removed by the falling film in a tank whereas type A fouling may require a larger impact force for removal or a combination of water and chemical rinses for complete removal. An important function of the cleaning head is it to ensure the interior of the vessel is contacted by the cleaning fluid. This is easier to achieve and guarantee using a RJH.

2.6 The effect of CIP parameters on type 2 and type 3 removal

Type 2 deposits tend to be viscoelastic, temperature dependent and/or time dependent (Rao 1999). Type 3 deposits tend to be thermally induced deposits which precipitate from the process stream onto the heat exchanger surface over time. Wort is a complex pseudo Newtonian fluid with several components that change structure and solubility upon heating, including carbohydrates, proteins, vitamins, minerals, and lipids. The effect of heat on these components is

detailed in Table 1.1, Chapter 1. The deposits formed during wort boiling are solid and dissimilar to the process stream (Tse et al., 2003). This deposit is shown in Figure 1.4, Chapter 1. Tse et al., (2003) found that the heaviest deposition was at the bottom of the test section obtained at the inlet of the tube. This deposit appeared dark brown and multi layered. At the lowest flow rate, 0.07 m s^{-1} the fouling appeared the most severe. The lightest deposition was at the top of the test section and at the highest wall temperature, 170°C. This deposit appeared smooth, patchy and lighter in colour. Increasing the tube wall temperature also increased the amount of this lighter deposit down the tube. These deposits were found to be chemically different. The authors suggested two fouling mechanisms: chemical reaction of species in the wort forming polymers and crystallisation of species from the wort due to evaporation at bubble nucleation sites in nucleate boiling regions.

2.6.1 Membrane cleaning

There are many types of filtration process in food and beverage manufacturing operations. The fouling of membranes alters permeability and selectivity and can be characterised by increased pressure differential and decreased membrane flux. Membranes used in the food and bioprocess industry include reverse osmosis (RO), nanofiltration (NF), ultrafiltration (UF), and microfiltration (MF) (Cui and Muralidhara, 2010). In the brewing industry beer is clarified using MF in which yeast readily fouls the membranes.

Güell et al. (1999) found that when yeast cells were present on cellulose acetate membrane (CAM) as a layer (yeast cake) the yeast was believed to have formed a secondary membrane. Increasing the thickness of the yeast cake reduced permeate flux and protein transmission through

the membrane. Increasing the yeast concentration in the feed solution resulted in lower fluxes and protein transmission through the CAM. Hughes and Field (2006) discuss the fouling of MF and UF membranes with yeast at sub critical fluxes where fouling is negligible. For the MF membrane the rate of fouling increased with increasing feed concentration, increasing membrane pore size and decreasing shear stress. The UF membrane could not be cleaned effectively.

Mores and Davis (2002) examined the effect of pulsing flow through a CAM to clean it. They found that the flux increased with increasing shear rate, back pulse pressure and back pulse duration. At higher shear rate and back pulse pressure multiple short back pulses were more effective in cleaning the membrane. At low shear rate and back pulse pressure, fewer longer back pulses were more effective. Longer weaker back pulses led to the highest recovered fluxes.

Shorrock and Bird (1998) fouled a MF membrane (hydrophilic polyethersulphone, 0.1 μm pore diameter) with yeast cake. Water rinsing was found to remove most of the deposit and an increase in temperature from 30 to 60°C was found to decrease fouling resistance (at 0.74 m s^{-1} cross-flow velocity (CFV)). At 40°C using NaOH an optimum concentration was found to give optimum flux through the membrane, 0.01 to 0.025 %. Formulated sodium hydroxide solution was found to restore membrane flux completely.

Cleaning of MF membranes with WPC was considered by Bird and Bartlett (2002) using a flat plate stainless steel membrane and by Blanpain-Avet et al., (2009) using a tubular ceramic membrane. An optimum alkaline detergent concentration 0.02 % NaOH found to give maximum flux after cleaning of the stainless steel membrane at 50°C, 1.67 m s^{-1}. Increasing the CFV from 1

to 6 m s^{-1} decreased fouling resistance of the ceramic membrane and gave the least amount of fouling present on the membrane after 20 minutes.

2.6.2 Flow and Temperature effect of water

For the type 3 deposits whey protein concentrate (WPC) and egg albumin Christian (2003) and Aziz (2008) found that neither deposit was removed with water rinsing at the temperatures and flow velocities investigated; 30 - 70°C and 0.7 – 2.3 l min^{-1}. The authors determined chemical action was required for their removal.

Guillemot et al., (2006) rinsed re-hydrated *S. cerevisae* cells from stainless steel in a flow cell over a wall shear stress range of 0 – 80 Pa. They found that as the wall shear stress was increased the number of cells remaining on the steel decreased. However, only a 10 % reduction in the number of yeast cells was achieved in this range of wall stress. Goode et al., (2010) rinsed aged yeast slurry from stainless steel coupons using water in a flow cell, and they found that increasing the flow velocity did not significantly affect the amount of deposit removed from the surface at ambient temperature; this was over a wall shear stress range of 0 – 1.24 Pa. Rinsing removed around 50 % of the deposit area. Goode et al., (2010) also found that increasing the temperature of the water rinse removed more deposit up to 50°C with flow rate having a negligible effect. However at 70°C decreased removal efficiency was observed, particularly at the highest flow velocity, 0.5 m s^{-1}.

The yeast was aged at different temperatures and for different times in the work by Guillemot et al., (2006) and Goode et al., (2010); 20 and 30°C and 1 h and 5 days respectively. The cell

concentration was also different at 0.0065 g ml^{-1} for Guillemot et al., (2006) and 1 g ml^{-1} for Goode et al., (2010). These findings suggest fouling conditions dictate cleaning behaviour. An example of this can be found from milk fouling. Robbins et al., (1999) found significant differences in WPC and milk fouling in a pilot plate heat exchanger at UHT temperatures. WPC fouling remained predominantly protein and milk fouling became predominantly mineral. Changani et al., (1997) mention that from cleaning observations protein is found to swell upon contact with sodium hydroxide and that minerals are left on the surface during NaOH cleaning. This suggests that the milk fouling formed at UHT temperatures would require an extra acid cleaning step to remove the minerals whereas WPC fouling would not.

2.6.2 Chemical effect on type 2 deposits

Various authors have investigated the removal behaviour of bacterial spores from stainless steel. Le Gentil et al., (2010) cleaned *B. cereus* spores from 316 L stainless steel pipes using 0.5 (w/w) % NaOH at 60°C at 2.2 l min^{-1}. The test was carried out over 30 minutes. As the cleaning time increased, the number of spores decreased as expected. In the first 10 minutes, up to 70 % of the spores were removed, less so in the remaining 20 minutes. Lelièvre et al., (2002) investigated the removal of *B. cereus* spores from 304 L stainless steel pipes, similar in length and diameter to the pipes used in the study by Le Gentil et al., (2010). 0.5 (w/w) % of NaOH was used at 60°C to rinse the pipe. In this study the effect of flow velocity and temperature was investigated over a 30 minute clean. The researchers found cleaning at 60°C removed more spores than rinsing at 20°C at each 5 minute time interval, at the same flow velocity, 1.97 m s^{-1}. They found that increasing the flow velocity from 1.61 to 3.29 m s^{-1} (τ_w = 17.45 to 68.95 Pa) at 60°C decreased the number of attached spores in the first 5 minutes. However after this time the contact time was more

important in removing the spores. The increased acceleration at higher flow rates may be controlling the number of spores removed in the first 5 minutes of cleaning, as found by Jensen et al., (2007).

Bremer et al., (2006) investigated the effect of alkali rinses and acid rinses (formulated and non-formulated) on removing a biofilm generated by re-circulating skimmed milk powder in a CIP skid for 18 h in 15 mm stainless steel tubes. There were a number of conclusions:

(i)   Rinsing with 1% NaOH (for 10 minutes, 65°C, 1.5 m s^{-1}) followed by 1% Nitric acid (for 10 minutes, 65°C, 1.5 m s^{-1}) reduced the number of cells to a similar level than that found after rinsing with only NaOH (at the same conditions);

(ii)   Formulated detergents (with surfactants, chelating agents, sequesterants) decreased cell numbers to the same level as rinsing with NaOH (at the same conditions);

(iii)   Addition of a surface active agent to the caustic significantly reduced the number of cells compared to standard CIP (NaOH and nitric acid in (i));

(iv)   Nitric acid with surfactants removed significantly more cells than just nitric acid;

(v)   Addition of a sanitizer step after CIP did not significantly reduce viable bacteria numbers.

The findings of this study suggest that caustic had the biggest impact on removing the biofilm. This suggests that the concentration of the alkali, the flow velocity and the temperature can be optimised to give the most efficient cleaning regime where all cells can be removed. The findings of this study suggest that caustic had the biggest impact on removing the biofilm. This suggests that the concentration of the alkali, the flow velocity and the temperature can be optimised to give

the most efficient cleaning regime where all cells can be removed. Additives have been developed containing surfactants which are designed to enhance NaOH cleaning effectiveness. Surfactants act to lower the surface tension of a liquid reducing its tendency to form droplets on a surface. As a result the liquid readily spreads over a surface to wet it. Surfactant-caustic blends are designed to wet a foulant is the shortest period of time to give a wetted foulant that becomes easier to remove by shear forces. Surfactants are widely used in biocides and sanitiers to kill microbes or biofilm. The surfactant can be positively charged and the microbe tends to be negatively charged creating an electrostatic bond. This causes stress on the microbe cell wall and eventual lysis. Simões et al., (2005) investigated the effect of a cationic surfactant QAC (quarternary ammonium compound) on biofilm removal from a surface. They found a maximum of 25% of the biofilm removed under both laminar and turbulent conditions. This occurred at a lower surfactant concentration (0.25 mM) under laminar condition than under a turbulent regime (0.5 mM).

Goode et al., (2010) investigated the effect of chemical on yeast removal from stainless steel coupons in a flow cell using 2% Advantis 210 (1% NaOH equivalent). They found that increasing the temperature from 20 to 70°C decreased the cleaning time. An increase in flow velocity at 50 and 70°C from 0.26 to 0.5 m s^{-1} also decreased the cleaning time however at 20 and 30°C, an increase in flow velocity from 0.4 to 0.5 m s^{-1} did not significantly decrease cleaning time.

2.6.3 Chemical effect on type 3 deposits

The effect of chemical cleaning of WPC from milk has been largely characterised in the literature as uneven. The cleaning process has three distinct phases seen by many independent researchers (For example Bird (1992), Gillham (1997), Grasshoff (1997), Tuladhar (2001) and Christian (2004)):

(i) *Swelling* — alkali solution contacts the deposit and causes swelling, forming a protein matrix of high void fraction.

(ii) *Erosion* — uniform removal of deposit by shear stress forces and diffusion. There may be a *plateau region* of constant cleaning rate, but this depends on the balance between swelling and removal.

(iii) *Decay* — the swollen deposit is thin and no longer uniform, so that removal of isolated islands occurs by shear stress and mass transport.

Many authors quote 0.5% NaOH to be optimal for WPC removal from stainless steel although the existence of cleaning optima has not been categorically proved. Bird and Fryer (1991) found that increasing the NaOH concentration to 2% can produce a deposit with a less open (dissolved) structure than at 0.5% lengthening the swelling phase. Plett (1985) reported that a maximum cleaning rate occurs when cleaning with detergent. The contribution of flow rate is hard to determine in chemical cleaning because both shear stress imposed on the deposit and mass flow to the deposit are dependent on the flow rate. In general the higher the flow rate, the shorter the cleaning time. Timperley and Smeulders (1988) found that the cleaning time of a PHE decreased with increasing flow velocity from 0.2 to 0.5 m s^{-1}. There are arguments supporting higher flow

rates which create turbulent conditions. This is because turbulent conditions are known to disrupt the boundary layer in cleaning. However Bird and Fryer (1991) found there was no significant change in cleaning rate when moving from laminar to turbulent flow. Disruption of the boundary layer is further discussed in Section 2.7. Generally increasing the temperature decreases the cleaning time. Gillham et al., (1999) found that removal of whey protein deposits from stainless steel pipes was strongly dependent on temperature (less so the swelling phase).

Sweet condensed milk (SCM) is an intermediate in the manufacture of some confectionary products, made by evaporating water from milk and adding sugar to lower the water activity of the product. SCM has 70 – 74% total solids of which 40 - 45% is sucrose (Fisher and Rice, 1924) leaving 29 - 30 % milk solids. In the study of Othman et al., (2010) SCM was cooked for 4 h at 85-90°C on stainless steel coupons and removed by chemical cleaning in a flow cell. It was found that increasing the flow velocity from 0.25 to 0.5 m s^{-1} decreased the cleaning time at all temperatures. An increase in temperature from 40 to 60 to 80°C decreased the cleaning time linearly. Interestingly, the authors found that increasing the NaOH concentration from 0.5 to 1.5 % did not significantly affect the cleaning time at each temperature. This agrees with findings for WPC cleaning that quote 0.5 % NaOH as the optimum concentration. It was the increase in temperature rather than the increase in chemical concentration that decreased cleaning time.

Cleaning time vs. Re was plotted for SCM at 1 % NaOH (40, 60 and 80°C) by Othman et al., (2010) and at 0.1, 0.5 and 1% NaOH (at 30, 50, 70°C) for WPC by Christian et al., (2004) given in Figure 2.13 (a) and (b). For WPC the range of Re investigated was around 800 to 4840. There were separate groups of data at each temperature that could not be plotted on one master curve.

This suggests temperature was the dominant parameter in controlling cleaning time. Christian (2004) concluded an increase in Re was only beneficial to cleaning time at low concentration. Jennings et al., (1957) suggested the existence of a threshold Re of 25,000 for cleaning a pipe surface of dry milk deposit before an increase in Re resulted in increased cleaning rate. For SCM the Re range investigated was much higher, from 6500 to 27,000. All the data collapsed onto one curve. As the Re increased the cleaning time decreased, suggesting Re was the dominant parameter controlling cleaning time. Othman et al., (2010) did find however that the effect of Re on cleaning time became less significant as the temperature was increased. Gillham et al., (1999) found that $\tau_w = Re^{-n}$ where n was in the range 0.2 - 0.35 for 0.5% NaOH, where τ_w is the wall shear stress. For SCM at 1% NaOH $\tau_w = Re^{-n}$ where n = -1.28 (R^2 = 0.92).
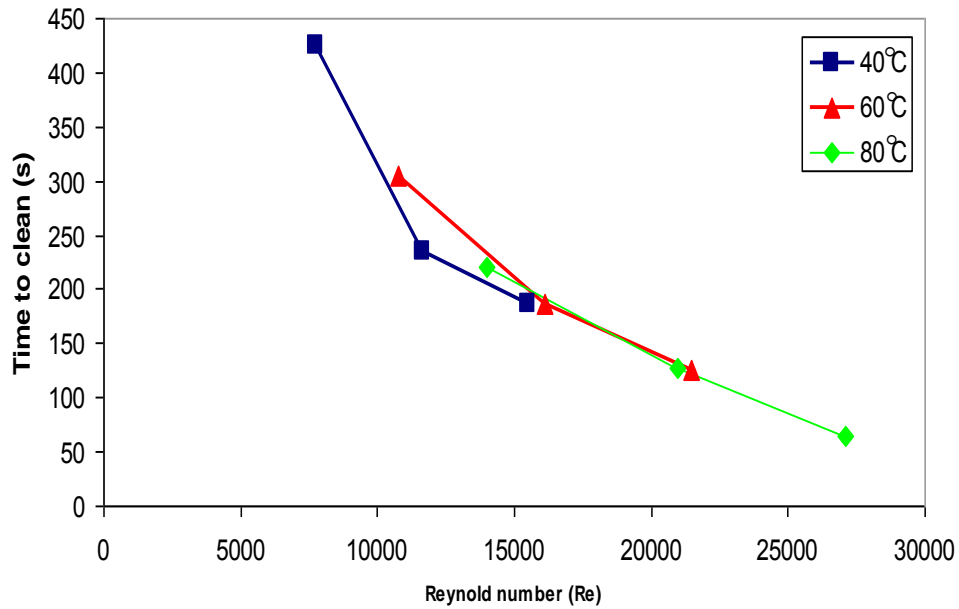
(a)
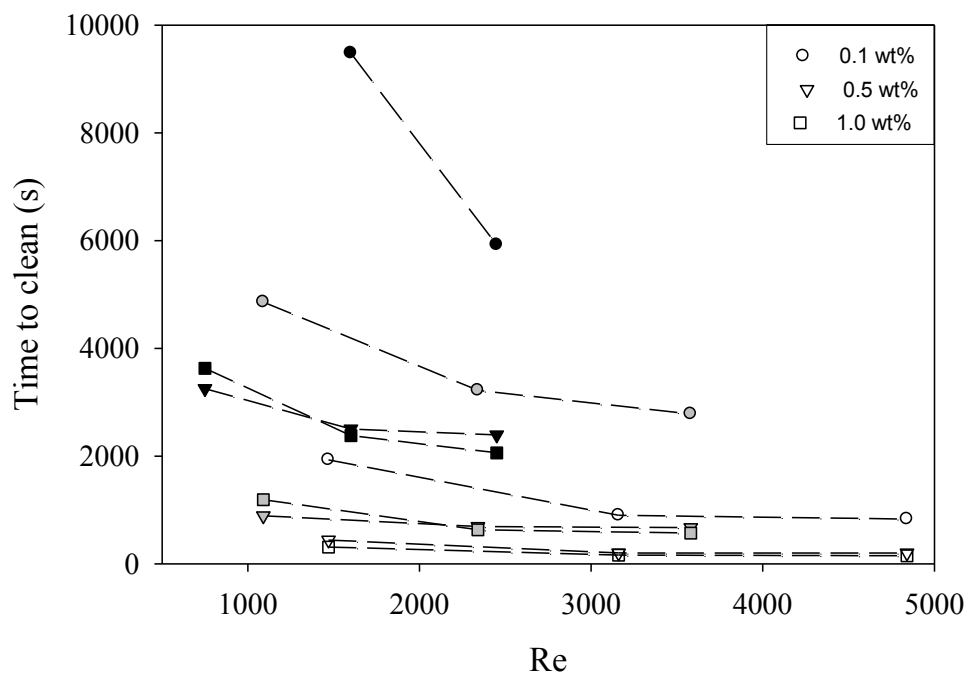
(b)

Figure 2.13: Re vs. visual cleaning time of (a) SCM at 40, 60 and 80°C using 1% NaOH (from Othman et al., 2010) and (b) WPC at 30, 50, 70°C, using 0.1, 0.5 and 1% NaOH (from Christian, 2003).

The cleaning of egg albumin was characterised by Aziz (2008). Generally an increase in temperature decreased the cleaning time. However at 1% NaOH, cleaning time was faster at 50°C than at 70°C. Deposit was not removed at 30°C at any flow velocity or NaOH concentration investigated. An increase in NaOH concentration from 0.25 to 3% NaOH decreased the cleaning time (at 50°C, 2.3 l min^{-1}); however increasing the flow rate had a less significant impact on cleaning time at higher chemical concentration. The author concluded a high temperature, mid to high flow velocity and mid-range chemical concentration appeared to be the optimum, similarly to WPC cleaning optima. For egg albumin the range of Re investigated was 1090 to 4840. There were separate groups of data at 50 and 70°C that could not be plotted on one master curve. This suggests temperature was the dominant parameter in controlling cleaning time similarly to WPC.

In Christian (2003) R_d profiles were measured in WPC cleaning experiments. These were conducted using 0.5% NaOH at 30, 50, 70°C and 0.7, 1.5, 2.3 l min^{-1}. R_d (the fouling resistance) is a measure of resistance to the flow of heat to the sensor. R_d measured at the same flow rate reduced R_d more rapidly as the temperature was increased from 30 – 70°C. An increase in flow rate from 1.5 to 2.3 l min^{-1} revealed similar R_d profiles, suggesting temperature dictated the cleaning time in this case.

For all type 3 deposits detailed here, temperature seems to be the dominant contributor to cleaning time at both low and high flow velocity and low and high concentration. This perhaps indicates a reaction rate event being the rate limiting step.

2.7 Novel approaches to decreasing cleaning time

There have been various methods trialled to improve cleaning effects which are discussed in this Section.

2.7.1 Boundary layer disruption

Various authors have considered pulsing flow in pipes to enhance wall shear stress at lower average flow velocities to enhance cleaning. Gillham et al., (2000) showed that pulsing flow at a relatively low frequency (2 Hz) enhanced cleaning of a tubular heat exchanger compared to the same steady flow velocity. A pulsed flow creates high periodic accelerations of the liquid flow. The directional change in the flow can increase mass transfer of the cleaning fluid to the surface decreasing cleaning times. A pulsed flow is characterized by a stationary base flow on which an oscillating fluid movement w_{os} is superimposed illustrated in Figure 2.14.
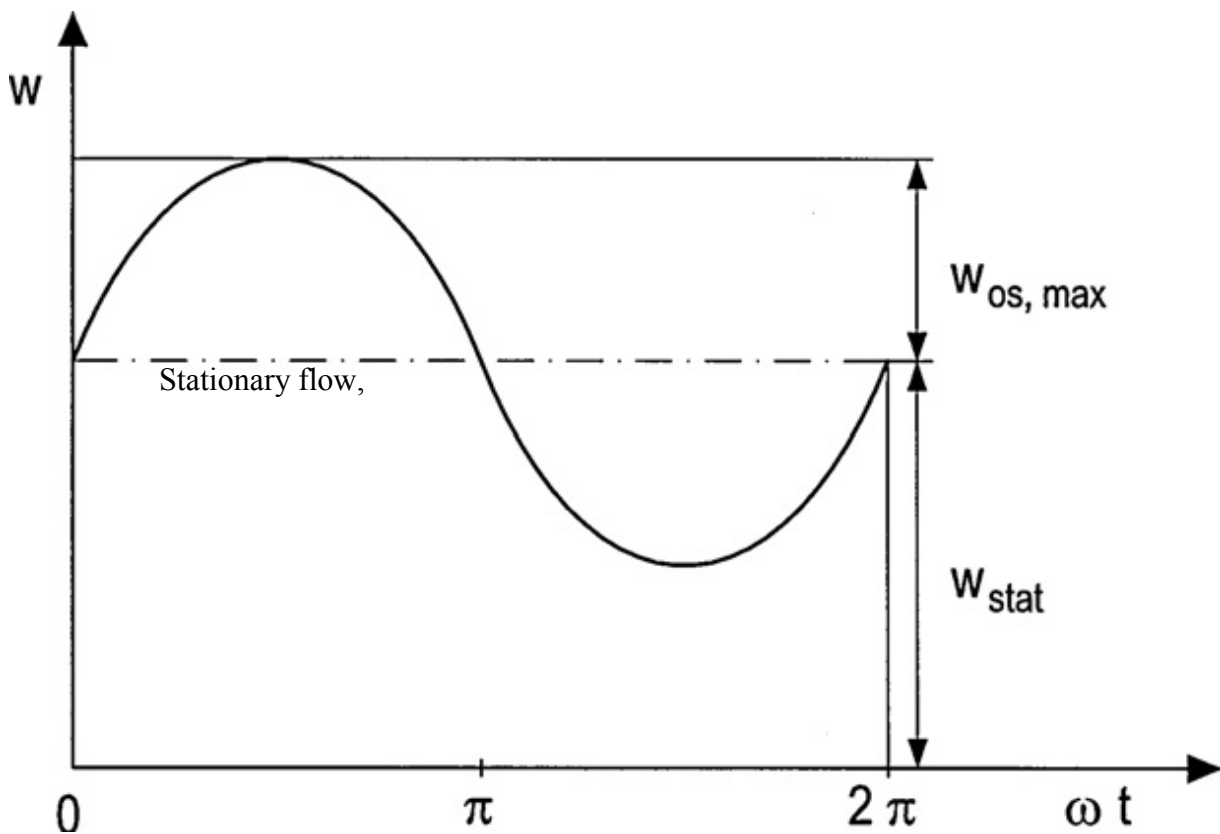
Figure 2.14: Stationary flow and oscillating components of flow, wos symbolises an oscillating fluid movement, wos,max is maximum oscillating fluid velocity, wstat is stationary fluid velocity and ωt is (Augustin et al., 2010).

The intensity of a superimposed pulsation ($w_{os,max}$ + w_{stat}) can be quantified using waviness, W, the ratio of the maximum oscillating ($w_{os,max}$) and the stationary or mean flow velocities, $\bar{w}$.

$$W = \frac{w_{os,max}}{\bar{w}}$$ [2.2]

$\bar{w}$ for an oscillation interval is defined by Augustin et al., 2010 as:

$$\bar{w} = \frac{1}{t_{os}} \int_0^{t_{os}} w(t) dt \text{ with } w(t) = w_{stat} + w_{os} = w_{stat} + w_{os,max}.\sin(\omega_t)$$ [2.3]

A higher value of waviness is believed to result in a separation of the viscous sublayer and the formation of eddy currents; flow reversal is critical. This effect can decrease the thickness of the laminar sublayer at the pipe surface when applying a turbulent flow. The temporary maximum velocity, $w_{os,max}$ can occur near the pipe wall resulting in large shear rates and high wall shear stresses. Bode et al., (2007) characterised a linear decrease of cleaning time with increasing waviness from 1 to 5. Below a waviness of 1 there is limited flow reversal in the pipe and the cleaning time increases. Augustin et al., (2010) compared the cleaning rate of deposit at a flow velocity of 1 m s^{-1} (Re 25 000) where waviness was 0, and pulsing the flow, where waviness was 1. They found that the amount of deposit in the pipe became asymptotic at 4 minutes using the pulsed flow regime and 6 minutes using the stationary flow regime. Augustin et al., (2010) have validated CFD models accompanying their cleaning data. Phosphorescent zinc sulphide crystals were used as an optical tracer enabling accurate characterisation of flow patterns.

2.7.2 Alternative cleaners

The efficacy of enzymes in cleaning has been investigated over the last decade. Graßhoff (2002) investigated the efficacy of Savinase, a protease (optimum temperature 50°C, pH 9.5), in cleaning a milk pasteuriser following a 15 minute acid wash. Increasing the concentration of the enzyme from 0.0025 to 0.05% at 60°C showed residual soil was removed faster. On plant the heat exchanger was opened and inspected after 45 minutes of enzyme cleaning and 6 minutes water rinsing (30 l min^{-1}). The interior surfaces were clean. Microbiological product samples collected showed no indication of microbial or enzyme contamination after CIP.

The use of commercial enzymes to clean UF membranes has been discussed by Petrus et al., (2008) and Allie et al., (2003). Petrus et al., (2008) used proteases to clean proteins (BSA and β-Lg) and defined an optimum concentration of 0.1% for 60 minutes. The enzyme deposited on the membrane when rinsed for longer than 60 minutes. Allie et al., (2003) used proteases and lipases to clean abattoir effluent. Up to 55% of fouling was removed with lipases and up to 70% using lipases and proteases and a flux recovery of up to 100%. However to apply enzyme cleaning in industry enzyme dosage, process control and economics need to be overcome.

2.7.3 Surface chemistry

A hygienic surface needs to be smooth, easy to clean, able to resist wear and retain its hygienic qualities. Stainless steel is the most common food contact material used in industry, being stable at a variety of temperatures, inert, relatively resistant to corrosion, and it may be treated mechanically or electrolytically to obtain surfaces which are easy to clean (Akhtar, 2010).

The wettability of a surface is dependent on its surface energy. A surface with a high surface energy is hydrophilic and a drop of cleaning fluid will spread over the surface. A low energy surface is hydrophobic and a drop of water-based cleaning fluid will not spread. Water partially wets glass and acrylic and does not wet Teflon (PTFE) surfaces. Wetting is determined by the nature of both the liquid and the solid substrate. The cleanability (and disinfectability) of stainless steel has been compared with those of other materials. It is said to be comparable to glass when cleaning microbes, and significantly better than polymers, aluminium or copper (Akhtar, 2010).

2.8 Alternative parameters relating to cleaning behaviour

Various authors have quantified parameters related to cleaning behaviour by other methods rather than in a flow cell or pilot plant. Some techniques used to infer cleaning data are discussed here.

2.8.1 Deposit shear

Simões et al., (2005) fouled stainless steel cylinders with *P. fluorescens* biofilm in a bioreactor. Three cylinders were rotated at 500, 1000, 1500, and 2000 min^{-1} sequentially (Re$_A$ 2400 to 16100) for 30 s each in phosphate buffer to assess the effect of rotation speed on biofilm removal. There was an optimum Re$_A$ of 8100 where 45 % of biofilm was removed. Either side of this Re$_A$ removal was less and similar at around 15 %. Cylinders were also submerged in different chemical solutions and rotated at 300 min^{-1} for 30 minutes and then were rotated at 500, 1000, 1500, and 2000 min^{-1} sequentially in phosphate buffer to test cleaning effectiveness. NaOH and sodium hypochlorite (NaClO) representing a CIP detergent and CIP sterilant were investigated. Irrespective of Re$_A$, NaOH and NaClO removed a similar percentage of biofilm at the same

concentrations (50, 200, and 300 mg L^{-1}); however at the highest concentration, 500 mg L^{-1}, NaOH removed approximately 5% more biofilm.

Demilly et al., (2006) characterised the removal of yeast cells as a function of wall stress from different stainless steel surfaces using a radial flow chamber, in which flow trajectory was from the centre of the plate outwards towards the edges of the plate. This is similar to the impingement of a water jet on a surface. Radial flow investigations may relate to the action of a cleaning head in a tank, to provide a microscale method of investigating water jets and deposit removal. The steel surfaces were micro-polished and electro-chemically etched with different grain sized and depths. The number of cells remaining vs. the original number of cells was defined. Interestingly the authors found a threshold shear stress about which cells were removed regardless of topography; that detachment of yeast cells was faster from etched steel than mirror polished steel.

Rheological tests have been used to study how materials respond to an applied stress or strain. In modern rheometers the deposit is sheared between two plates by a controlled stress or stain. Viscoelastic properties can be defined such as the elastic modulus (G') and the viscous modulus (G"). Vinogradov et al., (2004) characterised the rheology of a dental plaque biofilm. Biofilm rheology was found to be similar to organic polymers which tend to be viscoelastic, temperature dependent and/or time dependent (Rao, 1999). Characklis (1980) compared the elastic and viscous modules obtained for a biofilm and a cross-linked protein gel, fibrinogen. The elastic modulus was found to be the same order of magnitude for the protein gel and the biofilm.

2.8.2 Deposit deformation and strength

Two methods have been independently developed at Birmingham and Cambridge to determine the strength and deformation behaviour of soft-solid fouling layers on hard surfaces immersed in liquid; the micromanipulation technique and the Fluid Dynamic Gauging (FDG) technique respectively. The micromanipulation technique employs controlled strain parallel to the deposit, where a T-shaped probe is pulled across a horizontal circular plate at a constant height, removing the fouling deposit by a shovelling action. The FDG was developed to measure the thickness of soft-solid meso- and macro-layers on surfaces. The surface is immersed in a Newtonian liquid and a nozzle is brought close to the surface. A suction pressure differential is applied so that liquid is drawn into the nozzle. The gauging suction is increased until deformation is observed. Deformation of the deposit results in changes in h, the distance between the deposit and the gauge tip, which can be readily detected. The two techniques showed similar trends and complementary phenomenological detail when removing tomato paste in parallel studies (Hooper et al., (2006)). As the baking time increased the adhesive strength increased, as the hydration time increased the adhesive strength decreased.

The FDG technique has been used to study the effect of alkaline cleaning chemical concentration (0.3 - 2%), temperature (20 - 50°C) and velocity (0.03 - 0.3 m s^{-1}, Re: 500 – 10000) on whey protein (Tuladhar et al., 2002), the effect of drying time on tomato paste (Chew et al., 2004), and the effect of temperature and pH on gelatine film swelling (Gorden et al., 2010). The micromanipulation technique has been used to study the strength of *P. fluorescens* biofilm with growth medium velocity (Chen et al., 1998), the effect of baking, hydration time and temperature on tomato paste (Liu et al., 2002) and surface energy and cut height on tomato paste (Liu et al.,

2006). The same study considered the effect of drying/aging and cut height on bread dough, egg albumin and whey protein. The effect of ovalbumin concentration, temperature and NaOH concentration on egg albumin adhesion is presented by Liu et al., (2007). Tomato paste, bread dough and egg albumin deposits have been found to have a lower adhesive than cohesive strength, whilst whey protein has been found to have lower cohesive than adhesive strength.

Atomic force microscopy (AFM) has also been used to study deposit-surface interactions. In this technique a cantilever contacts the deposit and the force of detaching the cantilever is determined. Bowen et al., (2001) used AFM to study yeast cell detachment from hydrophobic and hydrophilic silicate surfaces with and without protein. The authors found that as yeast cells aged adhesion force changed. Also cells in the stationary phase adhered most strongly to the surface. Surface contact was demonstrated to be important where after 5 minutes adhesion force increased.

Whitehead et al., (2006) used AFM to assess the ease of removing *P. aeruginosa* (rods 1 μm width by 3 μm in length) and *S. aureus* (1 μm sphere) from a titanium dioxide surface; smooth and with defined surface features of 0.5 μm. To determine the ease of bacterial removal scans were carried out with increasing perpendicular force to the cantilever tip. Following each scan the number of remaining bacteria was counted. The perpendicular force had to be increased to remove any bacteria from the surfaces. *S. aureus* cells were found to be removed more easily from smooth surfaces at 30 mN, whereas *P. aeruginosa* cells were removed more easily from the defected surfaces. These finding suggest that cell orientation and thus contact surface area is important in determining the force of surface attachment and detachment.

Akhtar et al., (2010) used particle tips of different materials attached to the cantilever to study the detachment from toothpaste and some of its components, Turkish delight, caramel and SCM. The study did reveal significantly different detachment forces for different surfaces for the same deposit. Caramel and SCM seemed to be more difficult to detach from glass than stainless steel.

2.9 Measuring cleaning

It is essential to ensure the good performance of the cleaning process in order to maintain commercial stability and desired shelf life and quality of the products. The process of assessment requires:

 (i)   setting of standards;

 (ii)   reliable methods of performance measurement;

 (iii)   recording and reporting of results;

 (iv)   interpretation of results.

Assessment should always lead to appropriate action when defects in the system have been identified. An algorithmic sequence for an optimal cleaning method should be as demonstrated in Figure 2.15.
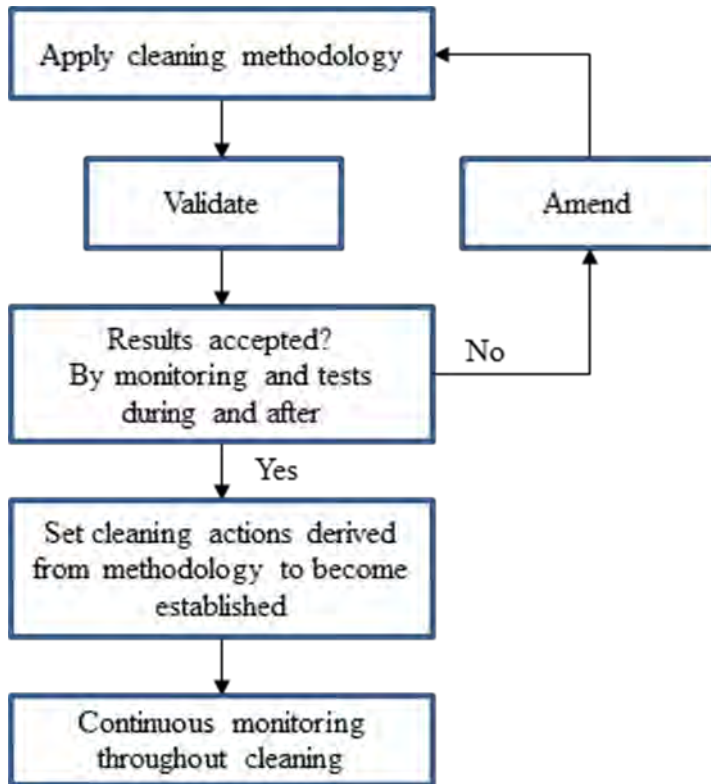
Figure 2.15: Algorithmic representation for an optimal cleaning method.

Processes used to establish and run operations include, validation, verification and monitoring. The definitions of these processes are:

(i)   *Validation* – determining which is the right method of cleaning; it is done before implementation of a new method and after alterations in an existing operation. It should always be up to date.

(ii)   *Verification* – are the results correct and accepted? Checks the system behaves in the pre-determined and expected way; after validation.

(iii)   *Monitoring* – continuous monitoring of specific points of a process determining if the process is under control; after verification.

Typical CIP validation, verification and monitoring tools include visual detection methods; microbial enumeration of CIP rinse water and in line probes that measure temperature, the proportion of hydrogen ions (pH) or electrolytes (conductivity) in the cleaning fluid. Ensuring the monitoring techniques used in CIP are giving reliable data is the first step to optimising CIP. Cleaning processes tend to be over conservative from fear of a product recall, which is costly. Yang et al., (2008) described the importance of forecasting models in the approach to optimise cleaning. Data that is measured at the beginning of CIP (where the confidence limit of variation is high) is used to predict the end point of cleaning (where the confidence limit of variation is low). Online application of such a tool would be valuable in optimising CIP. A range of measurement devices have been considered in the literature and have been used to assess either the cleaning fluid (bulk measurements) or the surface. Temperature and conductivity probes are typically used on line to monitor CIP. Conductivity is the measurement of electrolytes in a solution, defined as conductance in a given volume. The conductivity of acid and alkali is different to water so the chemical phases of cleaning can be clearly identified and the chemical recovered. Figure 2.16 illustrates where in a process line bulk and surface measurements may be taken. Green represents bulk measurements and red represents surface measures.
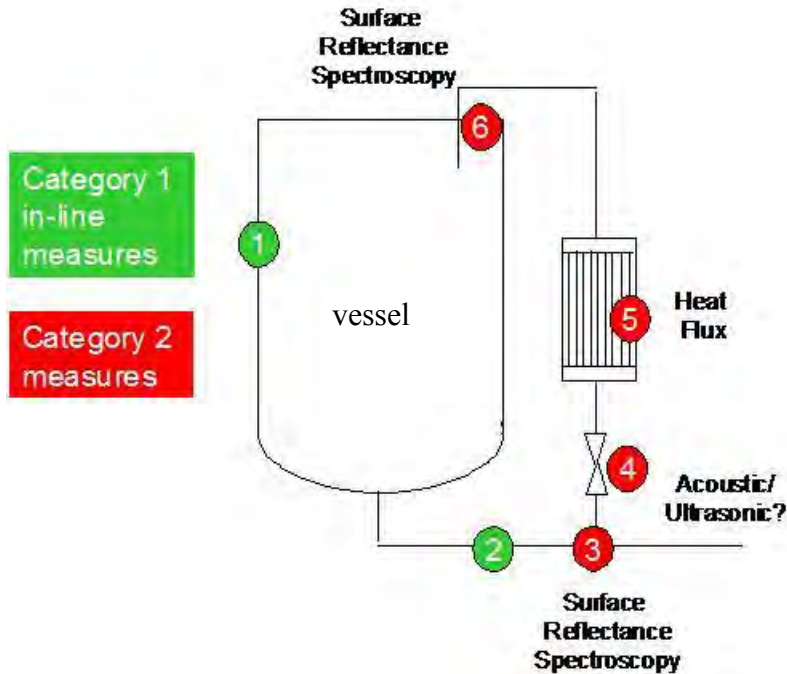
Figure 2.16: Potential locations of measurement techniques in a process line.

2.9.1 Bulk measurements

Online bulk measures monitor the fluid during cleaning. Typically temperature, flow, pressure, conductivity, and pH are monitored during CIP to ensure the process is under control. Pressure drop across a system (ΔP) is defined as: $\Delta P = P_I - P_O$ where P_I and P_O are the inlet and outlet pressure. P_O increases with time during fouling and decreases during cleaning generally. The rate of change of pressure can be used as a measure of cleaning. Fryer et al., (2006) illustrated that pressure drop initially increased across a plate heat exchanger during cleaning. When the cleaning chemical came into contact with the deposit, the deposit swelled and further increased the pressure drop through the processing plant before cleaning commenced. This effect has been well characterised in pulse flow cleaning by Christian and Fryer (2006). Robbins et al., (1999)

also used pressure drop across a plate heat exchanger to characterise the fouling nature of milk and whey protein fouling.

Van Asselt et al., (2002) demonstrated online monitoring of a dairy evaporator CIP by conductivity and pH. The chemical and water interfaces were clear. Conductivity can also be used to indicate product-water interfaces in non-chemical cleaning (Ecolab personal communication, 2009). Van Asselt et al., (2002) also demonstrated that measuring turbidity and calcium in the bulk liquid during chemical cleaning gave information on deposit removal. Turbidity is a measure of the light absorbed or scattered by a liquid from a known light source.

Van Asselt et al., (2002) found that turbidity determined in line and off-line gave different deposit removal profiles. The off-line turbidity samples taken during CIP were analysed at a later stage which the authors think altered the particle size of the samples, thus the turbidity measurement. Particles of different sizes scatter light differently. An angle of 11° is recommended for particles like yeast and 90° for colloidal solutions with a smaller particle size (Clauberg and Marciniak, 2009). However, non-product substances (such as air bubbles and detergent) can also absorb light giving misleading data (Ecolab personal communication, 2009).

CellFacts (Coventry, UK) have a patented off-line sampling technology which they have demonstrated determines particle size and density in rinse water samples, this was demonstrated in case studies on their website (http://www.cellfacts.com/Cleaning-In-Place.php). The company used this technology to determine particle size and density during CIP of a beer maturation vessel (Heineken UK personal communication, 2007). Figure 2.17 illustrates the number of particles in

the size range (i) 0 to 0.235 µm (represented by black diamonds) and (ii) 3.5 to 6 µm (represented by pink squares) deemed to be the size range of bacteria and/or proteins, and yeast cells respectively; although was not specification of bacteria or yeast type was done. The CIP regime was:

(i)   Pre-rinse using recovered water; (see stages 1, 2 and 3 in Figure 2.17)

(ii) Alkaline detergent phase using recovered caustic; (see stages 4 and 5 in Figure 2.17)

(iii) Intermediate rinse using fresh water; (see stages 6 in Figure 2.17)

(iv) Disinfection stage; (see stages 7 and 8 in Figure 2.17)

(v)   Final water rinse using fresh water; (see stage 9 in Figure 2.17)
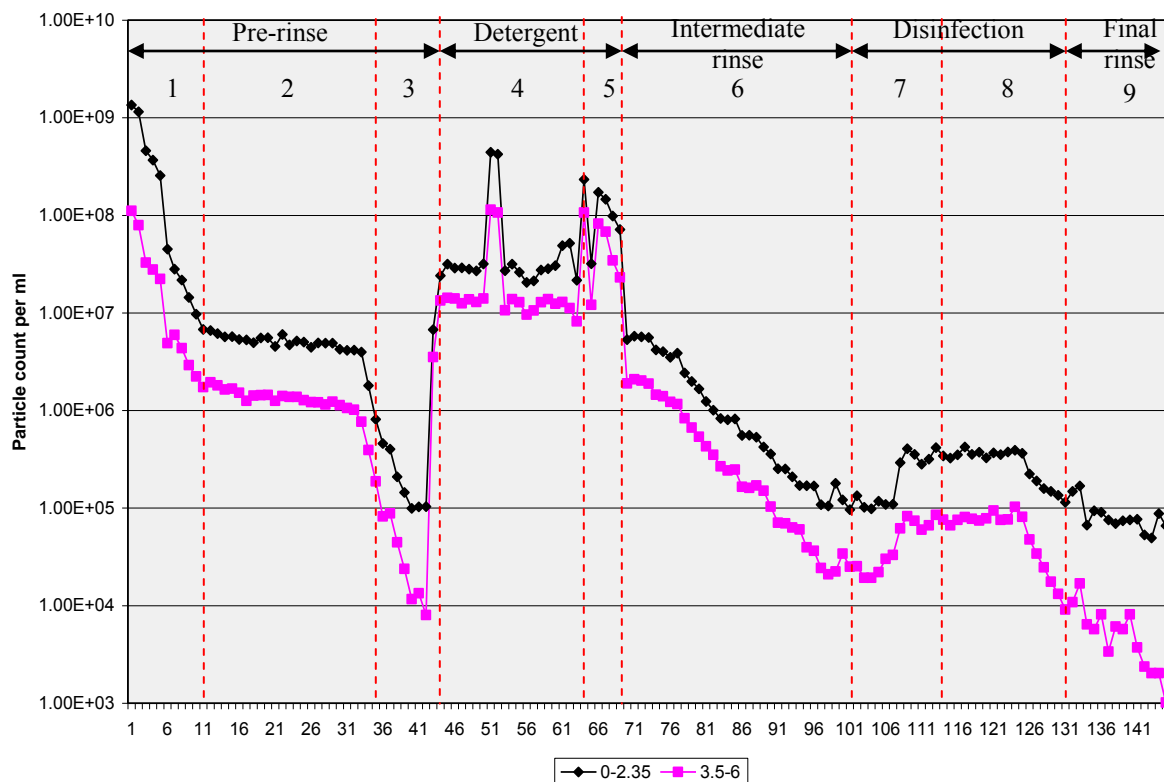
Figure 2.17: Particle density and size measured by the CellFacts equipment during CIP of a horizontal beer conditioning tank. Black diamonds represent small particles 0 - 2.35µm (bacteria and proteins), pink squares represent larger particles 3.5 – 6 µm (yeast cells).

During the pre-rinse illustrated in Figure 2.17, the particle density decreases rapidly in phase 1, less rapidly in phase 2, and decreases rapidly again in phase 3. Phase 1 indicated rapid removal of deposit and phase 2 indicated slower removal of deposit. Phase 3 was attributed to fresh water being used for the final part of the rinse (Heineken UK personal communication, 2007). The particle count almost becomes constant during phase 2 suggesting the pre-rinse had removed the majority of deposit during phase 1. The nature of a pre-rinse is to use water recovered from the intermediate and final rinse of a previous clean to save water. If the volume of recovered water in the pre-rinse tank runs out during the pre-rinse stage, fresh water is used for the remaining cleaning time. Fresh water had a lower particle count than the recovered water, indicated in phase 3 in Figure 2.17. These findings suggest the pre-rinse removes most fouling in phase 1 so the pre-rinse time can be reduced to that of phase 1 to minimise water use.

During the detergent phase illustrated in Figure 2.17, the particle density remained constant until approximately 5 minutes into phase 4. The particle count returned to a constant level for around 8 minutes, and increased during the last 5 minutes indicated by phase 5 in Figure 2.17. The data suggests fouling may have occurred and thus be removed from one particular are in the tank. The cleaning fluid from the RJH (rotating jet head, see Section 2.5) would have only contacted this section of the tank at certain times during the detergent phase due to the cleaning pattern of the RJH. As a result the intermediate rinse (phase 6) may have also removed deposit from the surface. The particle density reduced gradually in this phase. The purpose of the intermediate rinse is to rinse the caustic prior to acid sanitisation. This may also mean the detergent phase was not long enough as it did not remove all the deposit.

During the detergent phase, a portion of fresh water was added to the vessel creating a "pond" in the base of the vessel (phase 7 in Figure 2.17). The required volume of disinfectant was then dosed into this volume of water which is then circulated around the tank (phase 8 in Figure 2.17). The increase in particle density during disinfection suggests deposit was removed during this phase. The nature of the disinfection stage is to sanitise the surface. For disinfection to be effective the surface must be visually clean. After the disinfection step fresh water was used to rinse the vessel of sanitiser (phase 9). The final water rinse had a reduced particle density, and the number of smaller particles (0 - 2.35 μm) decreased more slowly than larger particles (3.5 – 6 μm); however the removal profiles of both particle sizes are similar during this CIP procedure.

Malvern Instruments (Malvern, UK) have commercially available technologies that could be used in a process line to monitor particle size during CIP. In their product catalogue these instruments are the Insitec L and SX. An on-line electrical resistance method has also been developed in the University of Auckland to monitor the fouling build-up and removal by measuring changes across a flow channel (Chen et al, 2004).

2.9.2 Surface measures

The measurement of heat transfer in fouling and cleaning is widely recorded: the change in heat transfer during fouling is accounted for by including a fouling resistance, R_f, in the equation relating the initial clean heat transfer coefficient, (U_0) to that at time t, (U_t):

(i) $\frac{1}{U_f} = \frac{1}{U_0} + R_f$. The extent of fouling may be expressed by a Biot number (Bi), which accounts for deposit thickness (x) and thermal conductivity (λ):

(ii) $Bi = R_f . U_0$ where $R_f = x/\lambda$ for the deposit. Deposit resistance during cleaning can be described (Tuladhar 2001):

(iii) $R_d = \dfrac{1}{U_c} - \dfrac{1}{U_t}$ where U_t and U_c are the heat transfer coefficient at time t and the heat transfer coefficient of the final clean system, so the rate of change of this is a measure of cleaning.

Various authors have reported heat transfer measurements during cleaning to assess the effect of cleaning parameters on the heat transfer coefficient and on fouling resistance, R_d, including Gillham et al., (1999, 2000), Christian (2004) and Aziz (2008). An example of R_d measured during the cleaning of (a) egg albumin and (b) whey protein using 0.5% NaOH at 1.5 l min^{-1} is illustrated in Figure 2.18. Rinsing egg albumin at 30°C revealed an unclean surface even after 3 hours.

(a)

(b)
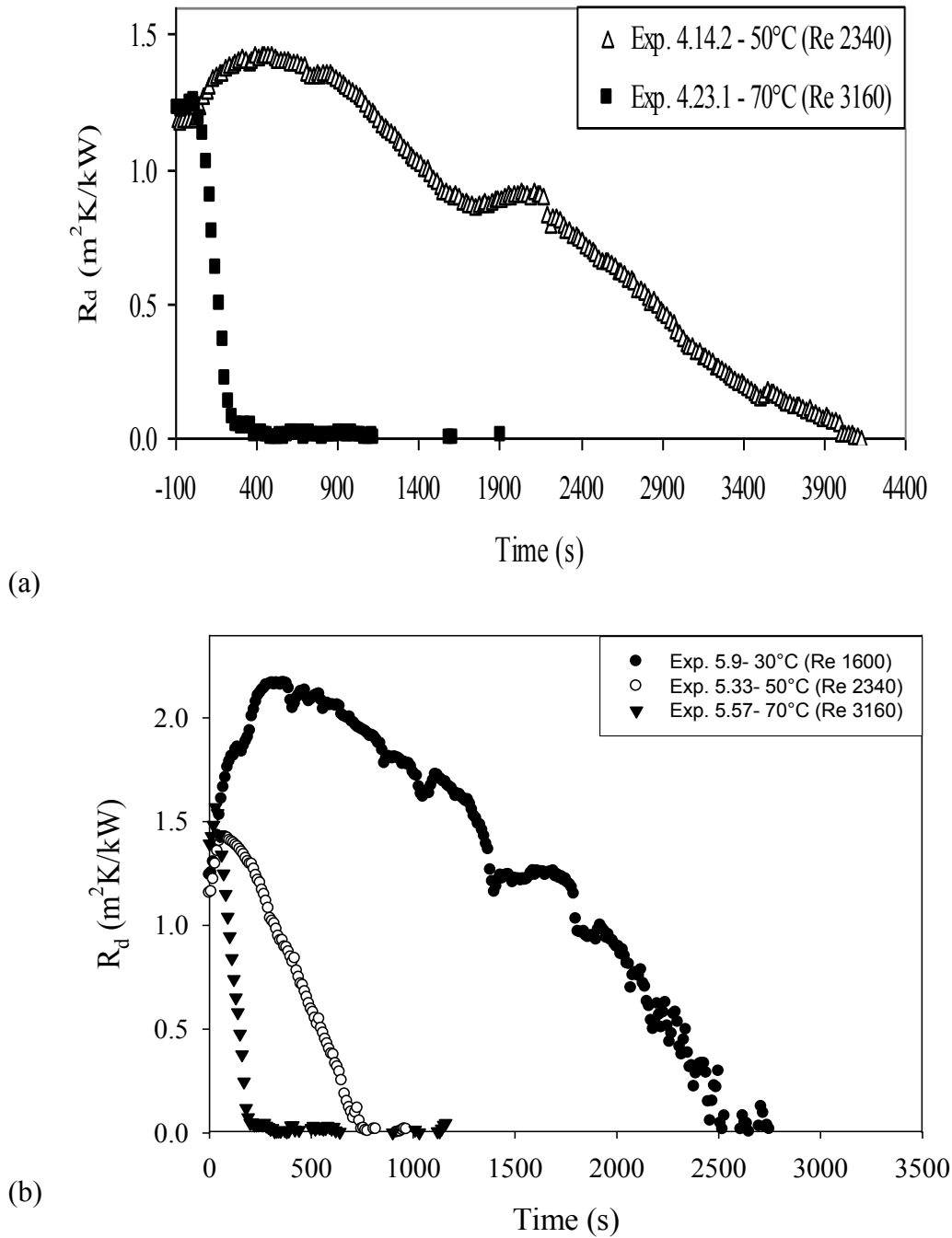
Figure 2.18: R_d profiles for (a) Egg albumen gel (from Aziz, 2008) and (b) whey protein (from Christian, 2003) with different flow temperatures: 30, 50 and 70°C using 0.5 wt% NaOH and a flow rate of 1.5 l min^{-1}.

Klahre et al., (2000) used differential turbidity to monitor biofouling on the pipe walls of water systems. The technique could be considered to study biofouling removal during cleaning. The use of a Mechatronic Surface Sensor (MSS) was being tested to monitor milk components such as calcium phosphate and whey proteins (Pereira et al, 2006) and shampoo (Pereira et al, 2009). The sensor measures changes in the vibration properties of surfaces due to the build-up or removal of fouling layers.

2.9.3 Measuring microbial cleanliness

There are many microbes known to contaminate beer and cause spoilage problems, see Table 2.6. Microbiological enumeration techniques are off-line retrospective techniques. Rinse water and surface swabs are plated on selective agar and viable microbes will present themselves within 3 to 7 days, depending on the microbe. Most informative swab and plate methods include contact agar method where the agar plate is pressed directly onto the surface and microbes enumerated directly (Salo et al., 2008). The cleanliness of a surface can be verified more quickly using ATP bioluminescence which indicates the presence (or absence) of microbes that are alive however the measure of ATP does not indicate microbe specificity. Microbes have been identified on surfaces using Infrared spectroscopy (Fornalik, 2008) and Raman spectroscopy (Rösch et al., 2003). Visual assessment, image analysis and measuring mass are also methods of determining the amount of deposit removed or remaining on a surface after cleaning, however most are off-line measures.

Table 2.6: The effect of contaminants during fermentation and in beer (from Storgårds, 2000).

Group or genera	Effects on fermentation	Turbidity	Ropiness	Off-flavours in final beer
Wild yeasts	Super-attenuation	+	−	Esters, fusel alcohols, diacetyl, phenolic compounds, H_2S
Lactobacillus, Pediococcus		+	+	Lactic and acetic acids, diacetyl, acetoin
Acetobacter, Gluconobacter		$+^{1)}$	$+^{1)}$	Acetic acid
Enterobacteria	Decreased fermentation rate, formation of ATNC	−	−	DMS, acetaldehyde, fusel alcohols, VDK, acetic acid, phenolic compounds
Zymomonas		$+^{2)}$	−	H_2S, acetaldehyde
Pectinatus		+	−	H_2S, methyl mercaptane, propionic, acetic, lactic and succinic acids, acetoin
Megasphaera		+	−	H_2S, butyric, valeric, caproic and acetic acids, acetoin
Selenomonas		+	−	Acetic, lactic and propionic acids
Zymophilus		$+^{3)}$	−	Acetic and propionic acids
Brevibacillus		−	+	−
Clostridium		−	−	Butyric, caproic, propionic, and valeric acids

ATNC; apparent total n-nitroso compounds, DMS; dimethyl sulphide, VDK; vicinal diketones, Fusel alcohols; n-propanol, iso-butanol, iso-pentanol, iso-amylalcohol
1) in the presence of oxygen, 2) in primed beer, 3) at elevated pH (5–6)

2.10 Conclusion

A fouling problem known to exist in the brewery has been presented clearly, and the current knowledge of fouling mechanisms has been discussed. Literature describing the adhesion of microbes to a range of surfaces used throughout the food and beverage industry has also been presented in the literature and discussed. Current fouling prevention methods are to modify the surface or to modify the process parameters. It has been mentioned that PDX have a novel reactor used to heat wort which claims to produce no fouling, but this has not been adopted within Heineken breweries and does not totally remove the need to clean.

Cleaning operations such as CIP are ubiquitously applied to remove unwanted fouling layers from process plant to maintain product safety and process efficiency. However, cost benefit analysis of CIP is not often done; as a result the route of optimisation in unclear. The grouping of deposits into three types has enabled easy presentation of recent studies that have investigated the effect of CIP parameters. This has enabled parallels in the literature to be drawn.

(i)   For type 1 deposits, cleaning time seems to be related to Re. An increase in Re seems to decrease cleaning time according to the Power Law model. It was also seen that increasing the flow rate or wall shear stress and cleaning temperature to a mid range temperature (up to 50°C) decreases cleaning time.

(ii)   For type 2 deposits, water rinsing parameters, temperature and wall shear stress, seemed to have a varied effects on removal. Removal behaviour seemed to be dependent on the microbial aging time on the surface. Using NaOH removed type 2 deposits in flowing systems. When considering one chemical concentration, flow and temperature were seen

to have the biggest effect at the start of cleaning but it was clear that contact time was an important factor as cleaning progressed.

(iii)   For type 3 deposits, specifically protein, an optimum NaOH concentration has been found to occur in numerous studies where excessive chemical causes formation of a deposit difficult to remove. However increasing wall shear stress and temperature were most beneficial to cleaning.

Novel surface coatings for stainless steel and alternative low environmental impact chemicals for cleaning are researched thoroughly at an academic scale. However application of these findings has not been adopted in industry. The factors affecting the application of research in industry include cost, maintenance, product safety and product quality. The longevity of surface coatings and the traceability of enzymes out of a test system have not been fully demonstrated; as such industry cannot justify changing its current CIP operation. Pulsing flow to achieve higher wall shear stress within a system looks like a promising route to improve cleanability of process lines. This could be achieved at very low cost because the equipment required is already used in CIP.

Numerous methods at varied stages of commercialisation have been demonstrated capable of monitoring cleaning in the bulk and at the surface. Turbidity and conductivity seem promising when measuring bulk flow. These probes tend to already exist in process lines to monitor products during production. The application in cleaning too is obvious and would be of low cost to investigate because the technology is already in place and in use. Emerging technologies that measure cleaning of the bulk and at the wall have also been presented. However the robustness and applicability of such systems in an industrial plant need to be determined. The measuring

point would have to indicate the cleanliness of the system effectively. There is the hope that forecasting cleaning will pave the way for the future of smart cleaning, where the end point of cleaning is indicated during cleaning on line rather than once at commissioning where cleaning times set in stone. This approach can be successful if measurements are robust and taken at the dirtiest point of a system.

CHAPTER 3: EQUIPMENT AND PROCEDURES

3.1 Chapter Introduction

The aim of this Chapter is to give details of the apparatus and procedures used to gain data and analyse the data presented throughout the remainder of this thesis. Chapter 1 has highlighted the importance of optimising CIP to the manufacturer. In a brewery various fouling deposits are found; ensuring CIP is optimum in all cases will undoubtedly reduce the cost and environmental impact of any process. Chapter 2 has presented broad knowledge of fouling mechanisms with focus on a specific fouling problem in the brewing industry, fermenter fouling. Strategies for the prevention of fouling have been discussed briefly in Chapter 2 with emphasis placed on current understanding of cleaning mechanisms. Understanding the factors that affect CIP effectiveness and efficiency can reduce the cost and effluent from the short term problem, cleaning.

This relationship between flow, temperature, concentration and time on deposit removal can be effectively studied on the cleaning rig (Christian, 2004, Aziz, 2008). Characterising the removal of different types of deposit on various length scales relevant to industry is important in

optimising CIP (Fryer and Asteriadou, 2009). Deposit behaviour, viscosity and adhesive/cohesive properties can be used to indicate cleaning behaviour (Akhtar, 2010). As such this Chapter contains the following Sections to give background understanding to the reader of experimental setups used to obtain the results presented in Chapter 4, 5 and 6:

(i)   the cleaning rig, operation, chemical use and cleaning measurements,

(ii)   the pilot plant, operation, chemical use and cleaning measurements,

(iii)   rheology procedures,

(iv)   micromanipulation procedures,

(v)   caramel fouling apparatus and procedure, and

(vi)   preliminary fermenter fouling and cleaning characterisation study.

The conclusions of this Chapter are presented in Section 3.8. The fouling method described in 3.6.1 to obtain type 3 soils was attempted with wort, and a thin layer of deposit was achieved. However the amount of deposit was not easily distinguished from the weight of the pipe; and the removal of the deposit was not evident using the pilot plant measurement techniques listed in Section 3.3.2. An image of this fouling on the inside of the 0.5 m pipe is given in Figure 3.1. The cleaning behaviour of an alternate type 3 soil was studied: caramel, a common fouling problem in confectionary processing (see Table 1.3).
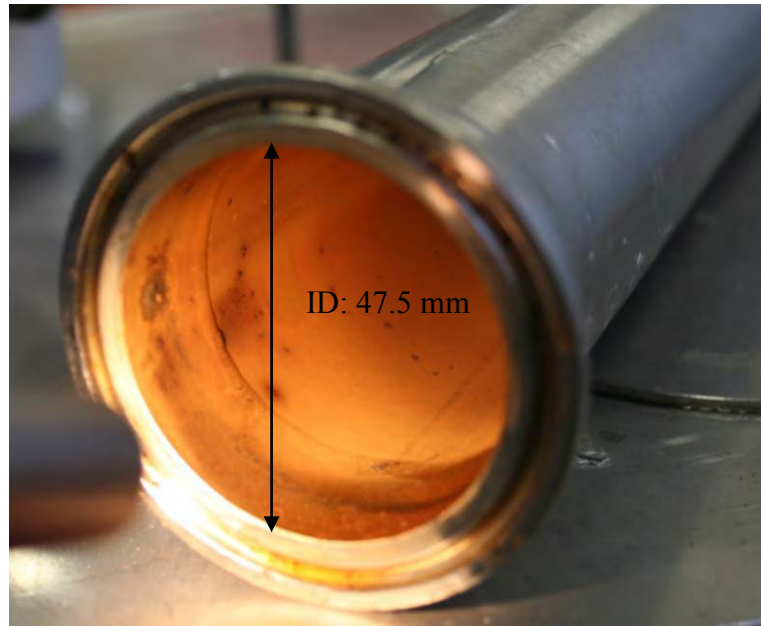
Figure 3.1: pipe fouled with wort after 24 h.

3.2 Cleaning Rig

The cleaning rig was used to study deposit cleaning on the centimetre scale. This is a flow cell which houses a fouled section which can be viewed during cleaning. The flow rate, temperature and chemical concentration can be set and then monitored. This rig has the same function as previous rigs (used by Aziz 2008 and Christian 2004): to quantify deposit removal visually and by monitoring heat flux, but the rig operates at higher flow rates. The schematic and photograph of the cleaning rig is presented in Figure 3.2 (a) and (b) respectfully. The direction of flow is from right to left (see Figure 3.2 (a)).

The test section is a square duct that was built to have an equivalent diameter, D_e, of 25 mm. The D_e is calculated from equation [3.1] where a and b are the horizontal and vertical wall lengths respectively.

$$D_e = \frac{(a.b)^{0.625}}{(a+b)^{0.25}} \qquad\qquad [3.1]$$

The duct test section was substituted by a 1 m stainless steel pipe with the same diameter for yeast slurry cleaning experiments presented in Chapter 4.
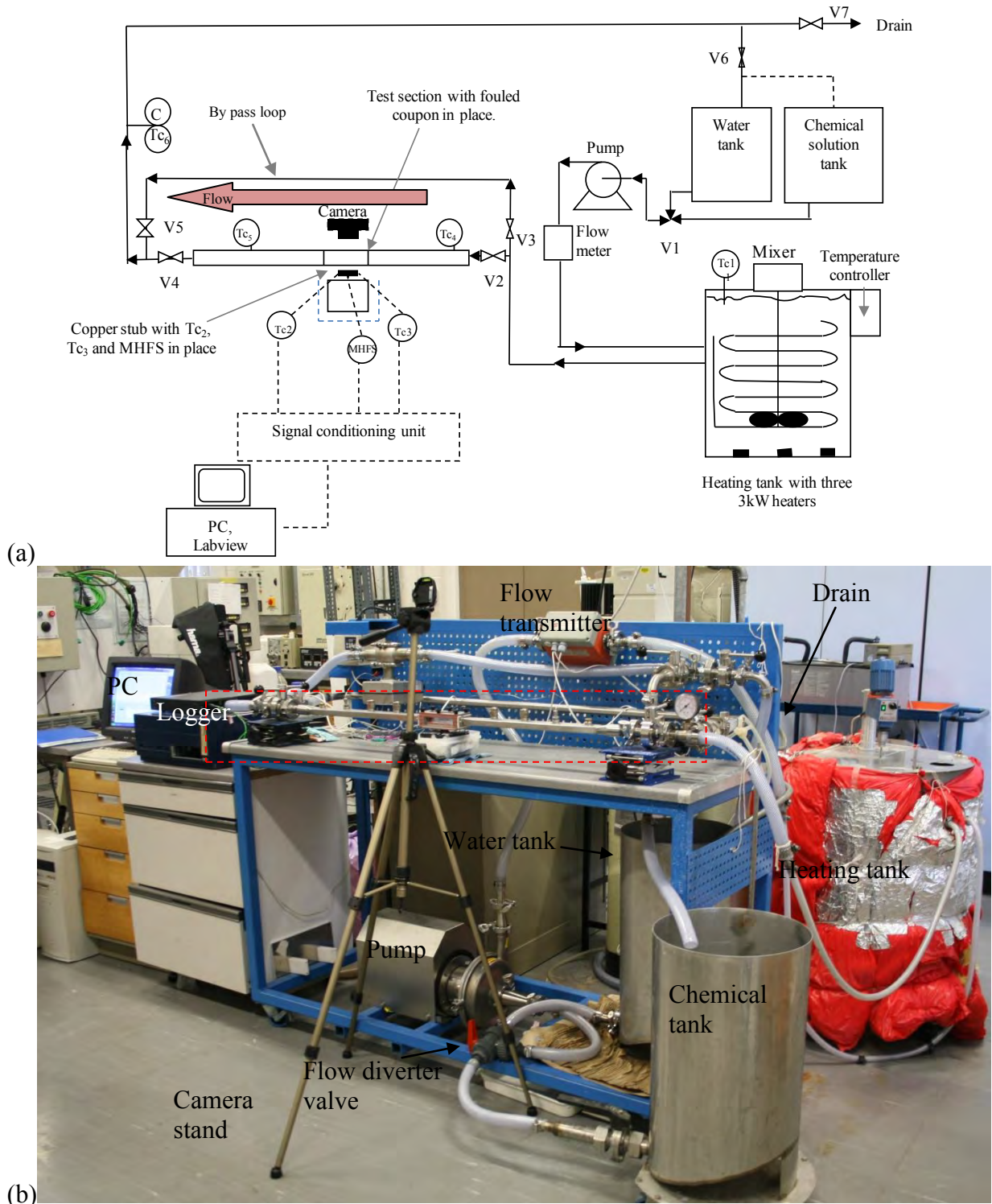
Figure 3.2: Cleaning rig (a) schematic, not to scale (to give an indication of scale, the test section is 1 m in length) and (b) digital image. The test section is mounted onto two jacks and is outlined by the dashed box. Tc – thermocouple, C – conductivity, V – valve, MHFS – microfoil heat flux sensor.

The part of the test section which houses the fouled coupon is illustrated in Figure 3.3 from (a) the top and (b) the side. This part of the test section is presented in Figure 3.4 as the modular design, where the base and top can be removed. The coupon fitted easily into the test section base minimising setup time between experiments. A thin layer of silicone grease was added to the rim of the coupon to hold it in place.

(a) (b)
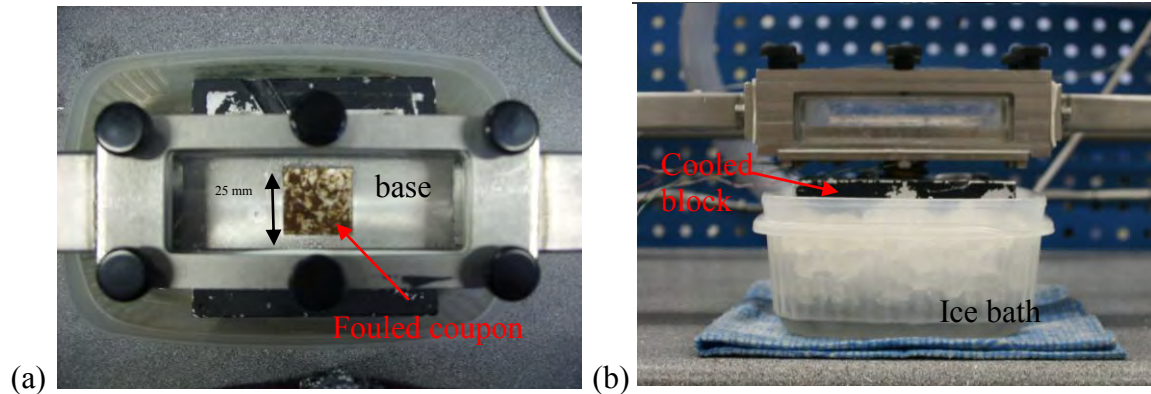
Figure 3.3: Test section (a) view from the top and (b) view from the side. Direction of flow is from right to left.
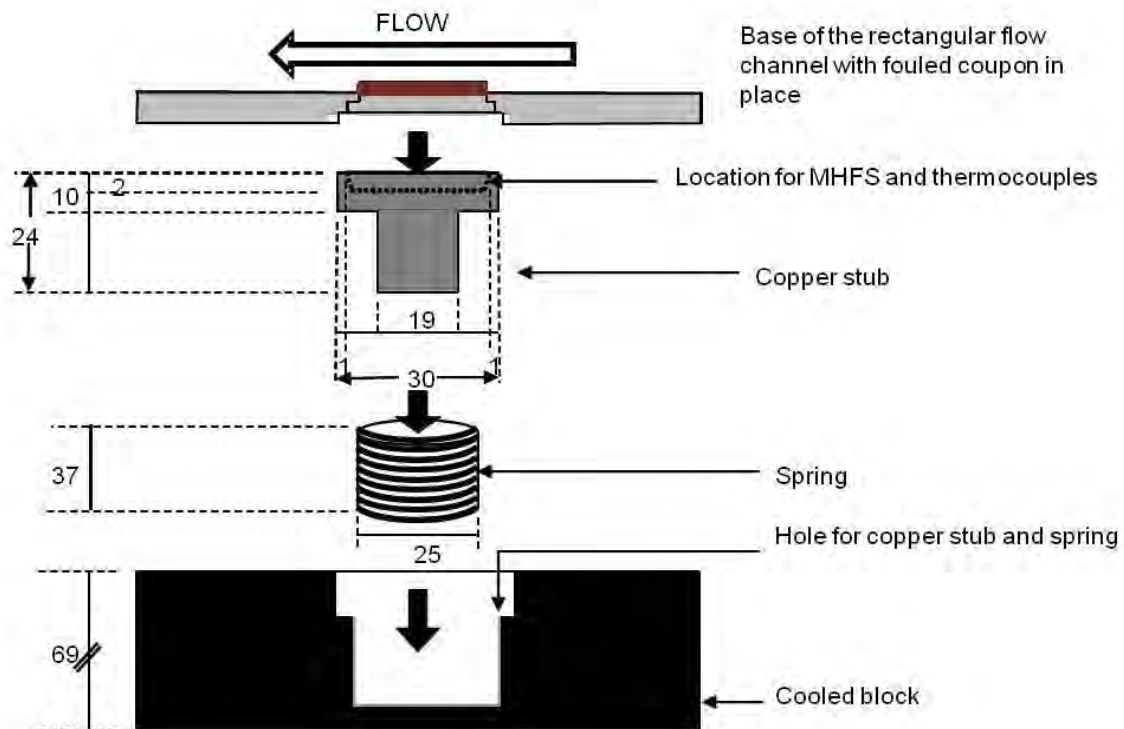
Figure 3.4: Assembly of the test section base and positioning of the copper stub and cooling block. All dimensions are in mm.

Two parameters were evaluated to monitor deposit removal;

(i)   The area of deposit removed (mm^2), quantified by image analysis described in Section 3.2.4, and

(ii)   Heat transfer coefficient (U in kW m^{-2} K^{-1}) calculated from the measured heat flux (q in kW m^{-2}), the average temperature of the test section cleaning fluid (T_{av}), and the temperature of Tc_2, the insulated thermocouple positioned below the coupon. This calculation is described in Section 3.2.5.

The flow rates achieved through the test section were in the range of 3.6 to 17.0 L min^{-1} (0.2 to 1.0 m^3 h^{-1}) giving flow velocities in the range of 0.12 to 0.6 m s^{-1}. The flow velocities were used to calculate Reynolds Numbers (Re) and wall shear stresses according to equation [3.2] and [3.3] respectively where $2\,500 < Re < 10^5$;

$$Re = \frac{\rho v d_e}{\eta_a}$$
[3.2]

$$\frac{\tau_w}{\rho v^2} = c_f = 0.079 Re^{-0.25}$$
[3.3]

The flow velocities used in experiments presented in this thesis were 0.13, 0.26, 0.4, and 0.5 m s^{-1}, at 20, 30, 50, 70 and 80°C, giving Re in the range 2 860 - 35 800 and surface shear stresses of 0.06 to 1.24 N m^{-2}. The wetting rate of the coupon was 0.02 – 0.47 kg s^{-1} m^{-1} (0.69 – 10.8 L min^{-1} m^{-2}). The wetting rate is within and above the range measured by Morrison and Thorpe (2002) during spray ball cleaning (see Chapter 2 Section 2.5). The flow velocities, Reynolds numbers,

and wall shear stresses achieved in the cleaning rig are smaller than those generated in industrial CIP. Survey of the literature presented in Chapter 2 describes film cleaning as the rate limiting step in tanks and pipes. This rig can study film cleaning albeit at lower Re and wall shear stresses than achieved in industry. The pressure at the point of impact from a rotating jet head used in tank cleaning can be up to 3000 Pa at 20°C, with the wall shear stress of the falling film is around 3.7 Pa (Alfa Laval personal communication, 2007).

3.2.1 Chemical concentration

The chemical used in experiments presented in this thesis was Advantis 210, a formulated alkaline detergent for beverage applications, recommended and provided by Ecolab, a partner in the project. Advantis 210 comprised 30 - 50 % NaOH and 10 - 20% KOH. 1 wt% NaOH and 2 wt% Advantis 210 was used at 30°C, 0.4 m s^{-1} to determine the cleaning effect on yeast slurry. Three repeats were done and the average area vs. cleaning time was plotted. This is illustrated in Figure 3.5. The Figure reveals:

 (i)   The removal profiles are similar and within the error of the experiment.

 (ii)   Rinsing using NaOH gave more variable removal profiles, seen here as a bigger error.

 (iii)   The removal profiles are most similar at the beginning and the end of cleaning. This is evident from the same average cleaning time and similar removal shape up to 60 s.
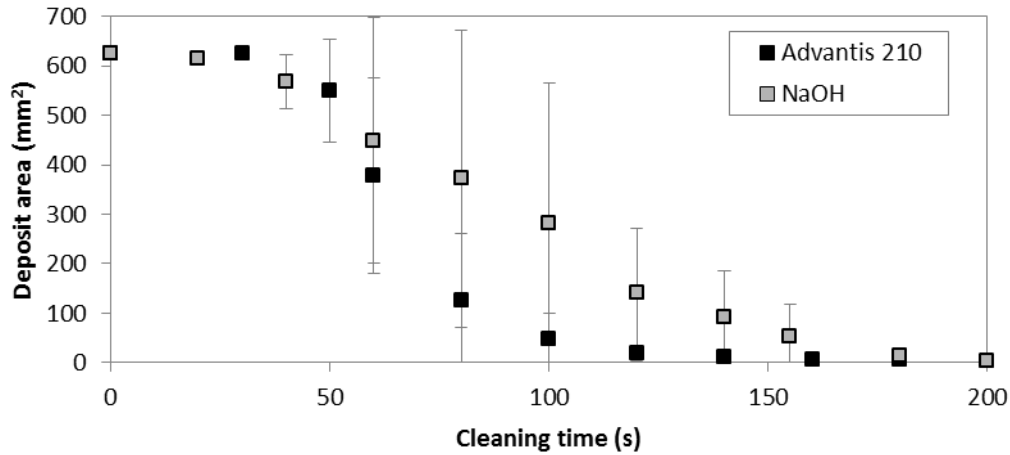
Figure 3.5: Removal behaviour of yeast at 0.4 m s^{-1} rinsed with 2 wt% Advantis 210 and 1 wt% NaOH. Data are of four repeats.

It was concluded that Advantis 210 was suitable for use in this project. Figure 3.6 illustrates the relationship between the concentration of Advantis 210 and the measurable conductivity. Conductivity is the measurement of electrolytes in a solution, defined as conductance in a given volume measured in mS cm^{-1}. The conductivity of acid and alkali is different to water so the chemical phases of cleaning can be clearly identified. The conductance of Advantis 210 was calibrated to a known concentration by Ecolab. The volume of Advantis 210 required per 40 L water to achieve a specific conductivity and concentration is also presented in Figure 3.6. The concentrations of Advantis 210 used in this thesis are 5 %, 2.5 %, 2 %, and 0.2 %, which contained 3 %, 1.5 %, 1 % and 0.1 % NaOH (wt %).
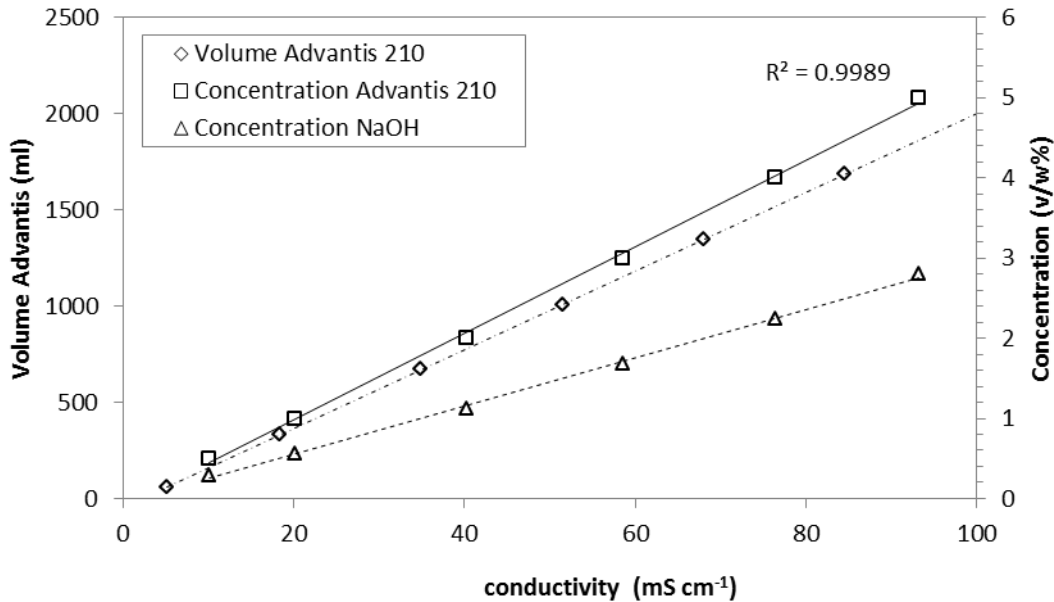
Figure 3.6: Concentration of Advantis 210 and weight percentage of NaOH in Advantis 210.

To obtain the required concentration in the cleaning rig system for circulation, water with the defined volume of Advantis 210 was pumped (centrifugal pump, Alfa Laval) from the chemical tank through the bypass loop, and back to the detergent tank. The highest flow rate was used, 1.04 m^3 h^{-1} (0.59 m s^{-1}), to achieve turbulent flow to ensure effective mixing. Once the conductivity was stable (usually within 2 minutes) a top up volume of Advantis 210 was added to achieve the required concentration, because of the additional volume of water retained within the cleaning rig system after each experiment. Figure 3.7 illustrates the conductivity and flow rate measured for one chemical concentration setup in the cleaning rig. In this case the target conductivity was 5 mS cm^{-1}. In the 2nd phase the flow rate was increased from 0.8 to 1 m^3 h^{-1}. The conductivity also increased indicating the flow rate needed to be high to ensure effective mixing of the chemical quickly.
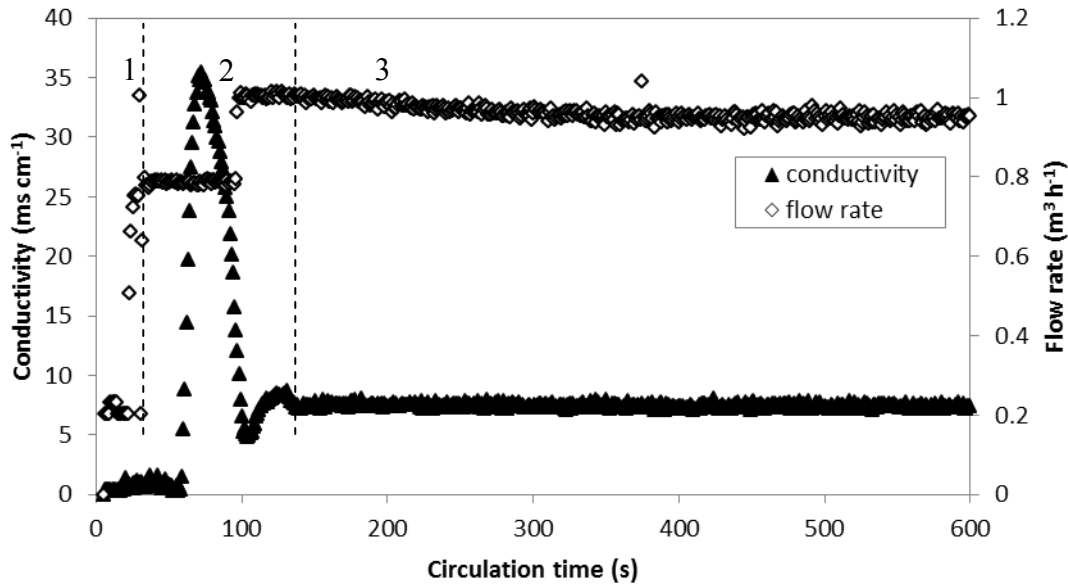
Figure 3.7: Addition and circulation of Advantis 210 to make a conductivity of 5 mS cm^{-1} where 1: addition of chemical, 2: chemical circulated and conductivity measured by the conductivity meter. Flow rate was increased to the maximum possible value, 3: Total mixing of the chemical.

3.2.2 Cleaning rig operation

A detailed SOP for the cleaning rig was developed and is presented in Appendix B. All experiments started and ended with water rinsing for safe handling of the test section. For both water and chemical rinsing experiments the flow continued for a further 300 to 500 s to assess U after deposit was removed.

3.2.3 Cleaning rig coupons

The surfaces used in cleaning rig experiments were milled from a sheet of 2 mm thick AISI 316 stainless steel. The coupons used in the cleaning rig were square: 30 by 30 mm, with a milled ridge 2.5 mm x 1 mm at the outer edge to allow the coupons to slot into the cleaning rig. The fouled surface area of each coupon was 625 mm^2. Each coupon was finished using p1000 grit sand paper which gave an average surface roughness of 0.25 – 0.3 μm for each coupon (Talysurf

120L, Rank Taylor Hobson). The roughness was measured as a 5 mm in three random locations on 5 of the coupons on the newly finished surfaces. 2D and 3D schematics of one of these surface measurements is illustrated in Figure 3.8 and 3.9 respectfully. The 3D surface measurement was a 1 x 1 mm square. Before experiments coupons were rinsed in distilled water to remove visible deposit and soaked in 2% (v/v) NaOH solution at 50°C for 15 to 20 minutes. The coupons were then rinsed in distilled water three times to remove the chemical and left face up on Kim paper towels to dry. The clean coupons were stored in Petri dishes.
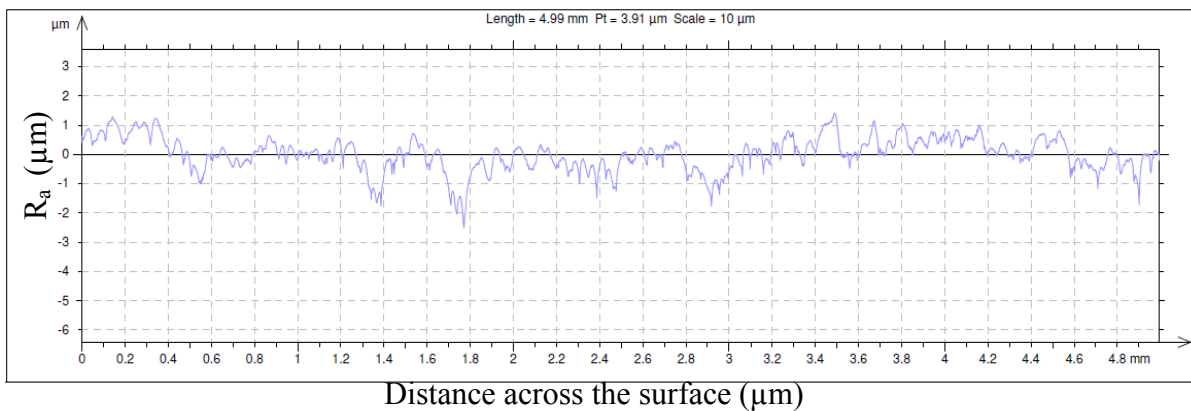
Figure 3.8: 2D measurement of coupon surface finish. For this coupon the Ra was 0.293 µm measured on a 1 mm x 1mm square.
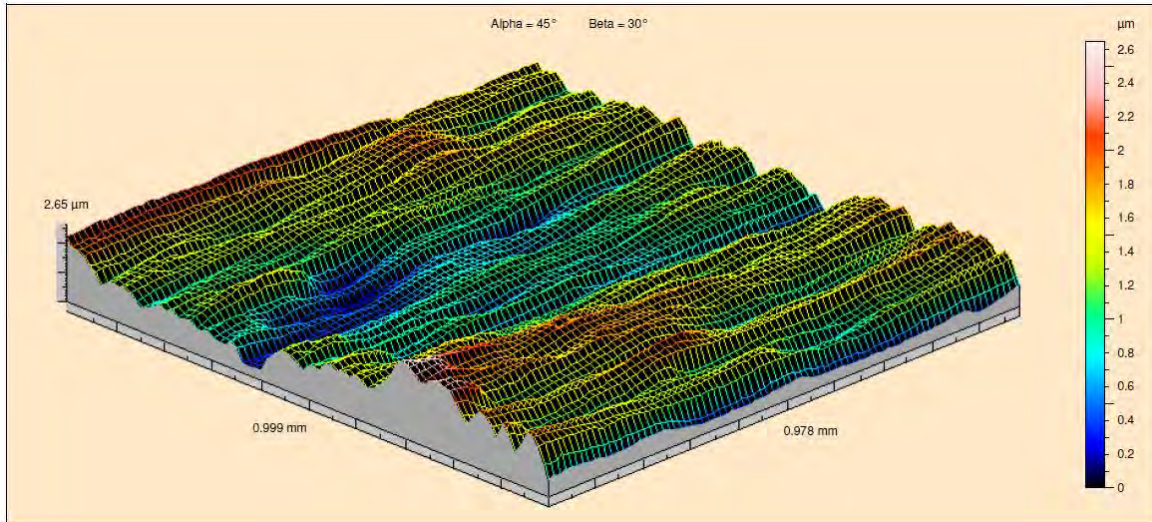
Figure 3.9: 3D measurement of coupon surface finish. For this coupon the Sa was 0.328 μm measured as a 5 mm line.

3.2.4 Calculating the area of deposit removed during cleaning

Deposit area (mm^2) was determined from images taken using a Canon EOS 30D digital camera (Canon, Japan). The area was determined for each image using software (Image J). 8-bit stacks of each series of images were created of a calibrated size. This was done by drawing a line the length of the coupon face on the top image and setting the length to 25 mm; the length of the coupon face. In grey scale the deposit and surface were indistinguishable. The images were modified in Photoshop CS2. The series of images were cropped to select only the coupon area. Deposit was selected using the magic wand tool and coloured black. Figure 3.10 illustrates (a) an image cropped in Photoshop and (b) the deposit selected black. The area calculated in Image J was 446 mm^2 i.e. 71 % of the deposit was present on the coupon.
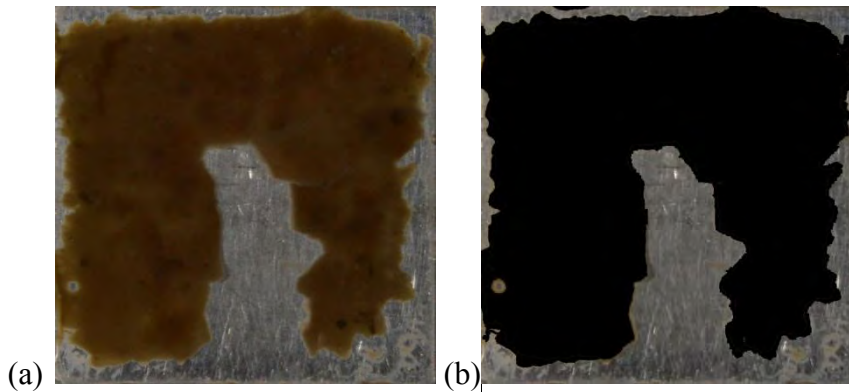
Figure 3.10: Aged yeast slurry on a coupon during cleaning at 20°C, 2% Advantis 210. (a) Original image (b) deposit selected using magic wand tool in Photoshop CS2.

3.2.5 Microfoil heat flow sensor (MHFS) theory

Measuring heat transfer across a rigid material such as stainless steel used to be done by measuring the temperature on both sides of the material; the inner and outer surfaces. Since the development of heat flux sensors, the heat transfer across a surface can be determined from measurement of temperature at the outer surface alone. The opposite sides of the stainless steel coupon will be at different temperatures creating a differential that can be measured. The MHFS (Model 20456-3, Rhopoint) was embedded into the copper stub along with Tc_2 and Tc_3 as illustrated in Figure 3.11. The block sits in an ice bath maintained at 0°C. The MHFS has been described in detail previously by Aziz (2010) and Christian (2004). In this case, approximately 80 % of the fouled area was covered by the MHFS (the area of the sensor, 500 mm^2, divided by the fouling area of the coupon, 625 mm^2). The construction of the MHFS is shown in Figure 3.11 (right).

The heat flux sensor is constructed with two temperature measuring elements, in this case chromel and alumel, physically separated by a thermal insulator. When the heat begins to

'transfer' through thermoelectric material A, the thermal energy at J_1 generates a small voltage. Heat passes through the insulating material (thermal barrier) and a differential temperature is generated. Since the temperature differential is proportional to the voltage differential, the heat transfer rate can be directly read out as a function of voltage. Direct measurement of the heat flux through the coupon can thus be made.
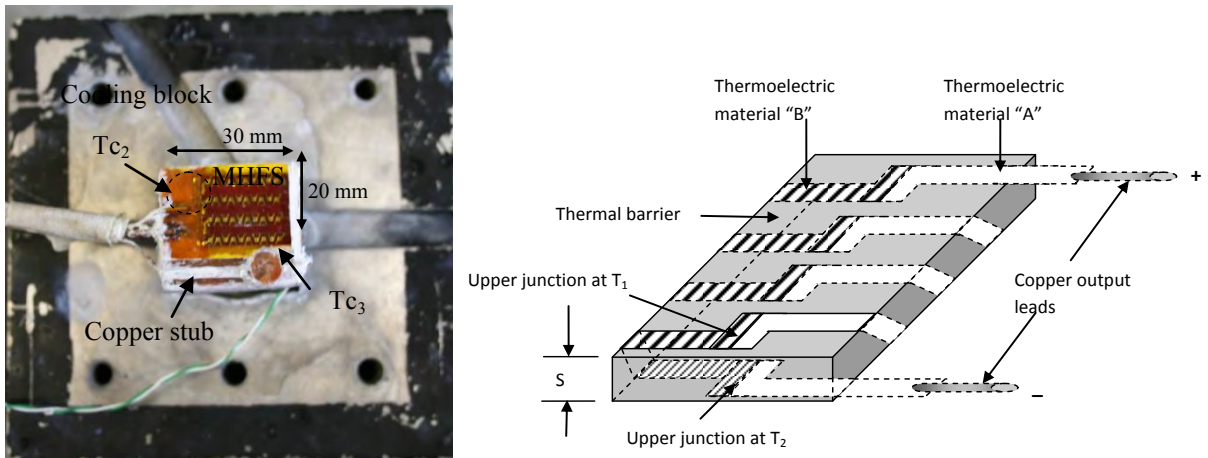
Figure 3.11: The copper stub positioned in the spring in the cooling block. The position of the MHFS, Tc_2 and Tc_3 are indicated (left). Schematic of the MHFS construction (Aziz 2008) (right).

To calculate the overall heat transfer coefficient (U) from the measured temperature and heat flow, kT_B was calculated to find heat flux (q) according to Equation [3.4];

$$q = \frac{\lambda_s}{x_s} \varphi . \kappa T_B . V \qquad [3.4]$$

Where q = heat flux (in kW m^{-2}), λ_s = sensor thermal conductivity (in kW m^{-1} K^{-1}), x_s = thickness of the sensor (in m), φ = a constant (in V^{-1}), $\kappa(T_B)$ = a dimensionless temperature factor and V = voltage output (in μV). RdF supplied a calibration chart of the MHFS for $\kappa.T_B$ as a function of

temperature. A linear relationship between $\kappa.T_B$ and temperature was found over the temperature range investigated $(20 - 80°C)$ The equation of this relationship was $\kappa = -0.001T_B + 1.0274$. T_B was approximated as Tc_2. RdF gave the value of;

$11.9 \ \mu V \ Btu^{-1} \ ft^{-2} \ hr^{-1}$ for the factor $\dfrac{\lambda_s}{x_s}\varphi$. Thus, $\dfrac{\lambda_s}{x_s}\varphi = \dfrac{1}{11.9} \dfrac{Btu \ ft^2 .hr}{\mu V}$.

Conversion of $Btu \ ft^2.h.\mu V^{-1}$ to SI units can be done by multiplying 11.9 by $3.154591 \ x \ 10^{-3}$ which gives $0.000265 \ kW \ m^{-2} \ \mu V^{-1}$. U was calculated from the recorded temperatures and the calculated heat flux according to:

$$U = \frac{q}{T_{av} - Tc_2}$$

[3.5]

Where q is the heat flux, Tc_2 is the temperature of the insulated thermocouple and T_{av} is the average of Tc_4 and Tc_5 (see Figure 3.2). Figure 3.12 (a) shows U_c, the heat transfer coefficient of a clean coupon, determined when the flow was increased and decreased at 70°C.The error associated with calculating U_c is in Table B.2 in the Appendix. As the flow rate is increased the boundary layer thickness decreases and a higher heat flux should be measured. The MHFS detects a change in voltage thus the heat transfer coefficient can be seen to change with flow rate. There is an increase in U_c with the onset of flow. Figure 3.12 (b) illustrates the effect of the flowing system on Tc_2, T_{av}, and q within the first 100 s of rinsing. All sensor readings increase. Undoubtedly heat is lost to the system and the surroundings. This effect is likely to be related to the stabilisation time of the system. At lower temperatures the duration of this effect would be shorter.
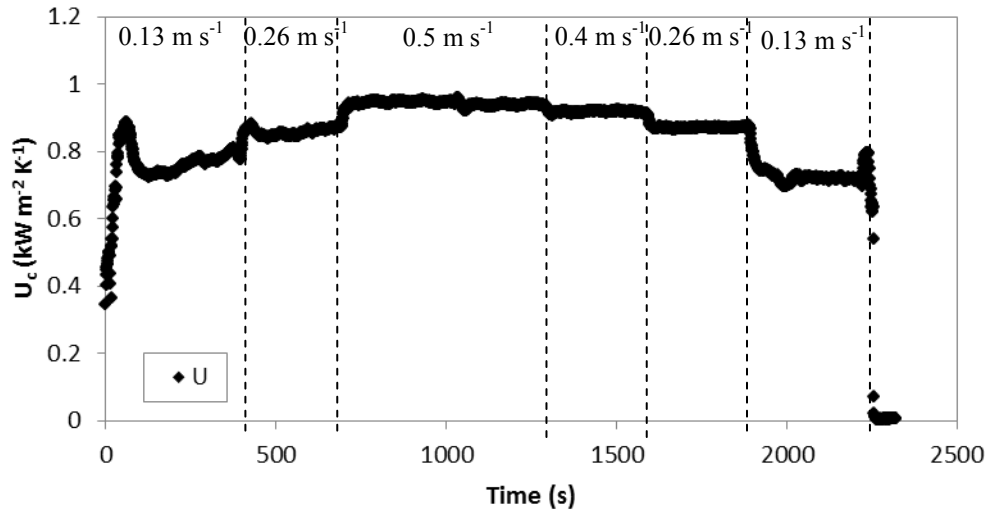
(a)
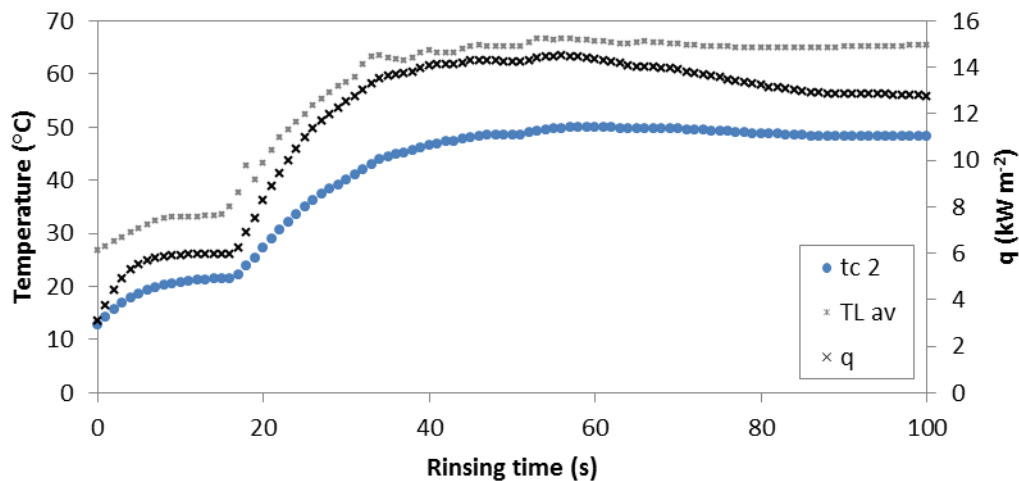
(b)

Figure 3.12: (a) Response of U the MHFS at different flow rates at 70°C; (b) Response of Tc_2, Tc_4 and Tc_5 average (TL av) and q readings during the first 100 s of rinsing.

Figure 3.13 illustrates characterisation of U_c when the MHFS was in contact with different media. This was done to give as much background information on the behaviour of the MHFS as possible, to ensure the sensor was in contact with the coupon during experiments and there were no leaks. Actual cleaning behaviour (measured by plotting U values) can therefore be clearly identified. The response time of the MHFS in the ice bath in contact with either the general surroundings or the coupon in flowing and non-flowing conditions was characterised.
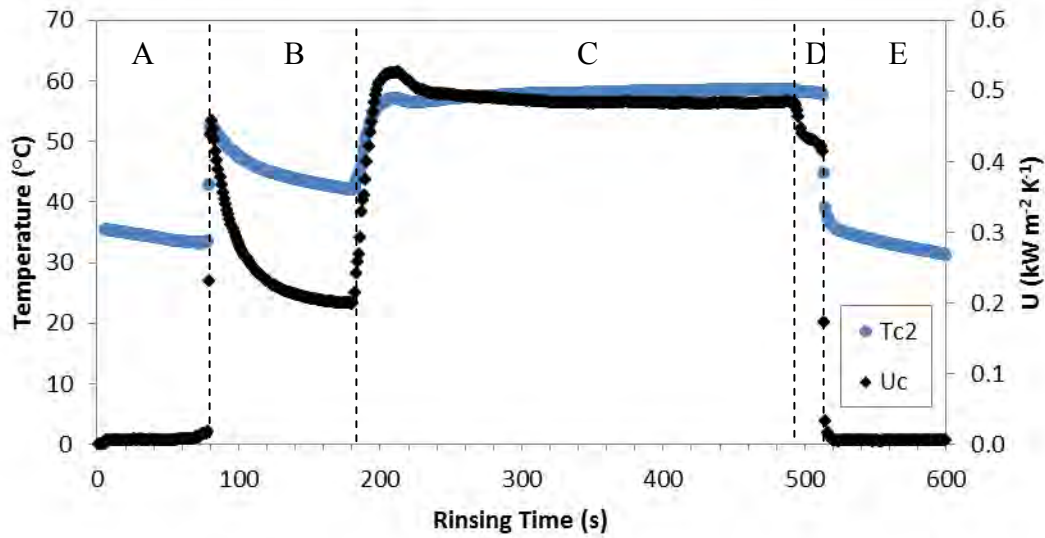
Figure 3.13: Response time of the MHFS in ice under different conditions. A: MHFS in contact with surroundings; B: MHFS in contact with the coupon; C: MHFS in contact with the coupon when water is flowing through the test section at 70˚C, 0.26 m s⁻¹; D: MHFS in contact with the coupon when flow stopped, E: MHFS in contact with the surroundings.

The phases identified in Figure 3.13 correspond to:

A. MHFS response in contact with the surroundings,

B. MHFS response in contact with the coupon positioned within the test section (no flow),

C. MHFS response in contact with the coupon positioned within the test section (flowing system at 70°C),

D. MHFS response in contact with the coupon when the flow was stopped,

E. MHFS response in contact with the surroundings.

When the MHFS is in contact with the general surroundings, U is measured at $0 \text{ kW m}^{-2} \text{ K}^{-1}$. This illustrates effective cooling of the sensor to 0°C using the block, copper stub and the ice bath set up. Tc_2 is cooling down in phase A and E. Then the sensor is in contact with the coupon during

phase B and the U_c and Tc_2 both increase and then decrease as the coupon is also cooled. At the start of phase C, an increase in U_c, occurs for a similar duration as in Figure 3.13, and U_c then becomes constant. When the flow is stopped U_c decreases and Tc_2 remains at a constant temperature.

To ensure that cooling the MHFS had minimal effect on the cleaning behaviour of yeast a comparison of two cases of cleaning 30°C, 0.4 m s^{-1}, for the MHFS cooled and not cooled in ice was done at by plotting the average area vs. cleaning time, illustrated in Figure 3.14. The profiles appear similar; certainly within the error of the experiment.

Water rinsing of yeast slurry films that had been aged revealed a thinner film of deposit that could not be removed completely with water. Measuring complete removal of this thin film using chemical cleaning was not possible using heat transfer as the film was removed within a couple of seconds. As such the effect of chemical cleaning on wholly fouled coupons was investigated.
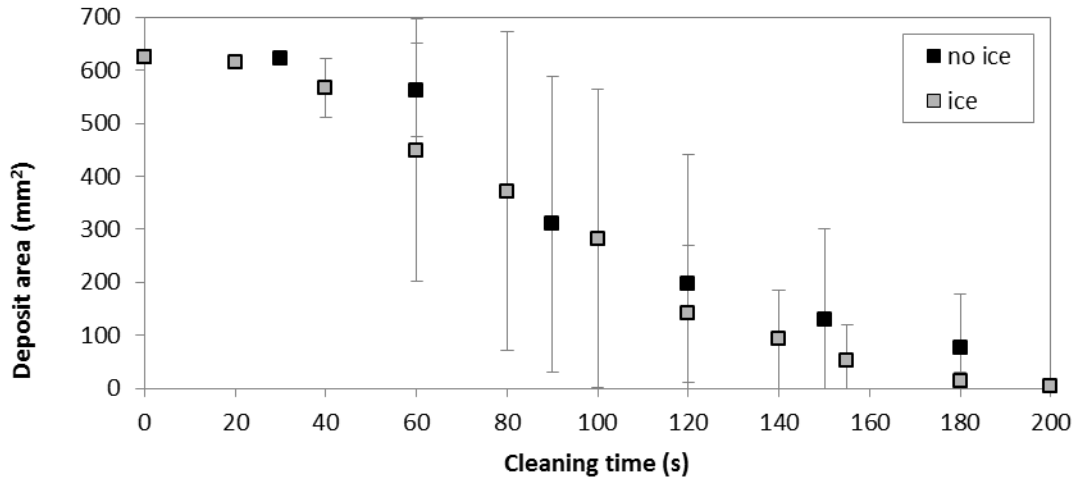
Figure 3.14: Removal behaviour of yeast at 0.4 m s^{-1}, 30°C rinsed with 2 wt% Advantis 210 when the MHFS was cooled in ice and not cooled in ice.

3.3. Pilot plant CIP system

The pilot plant used in CIP experiments is discussed in detail in Cole et al., (2010). A schematic of the pilot plant CIP unit and the associated mains is illustrated in Figure 3.15 (a). The layout of the test section which incorporates the fouled pipe is shown in Figure 3.15 (b).

(a)

(b)
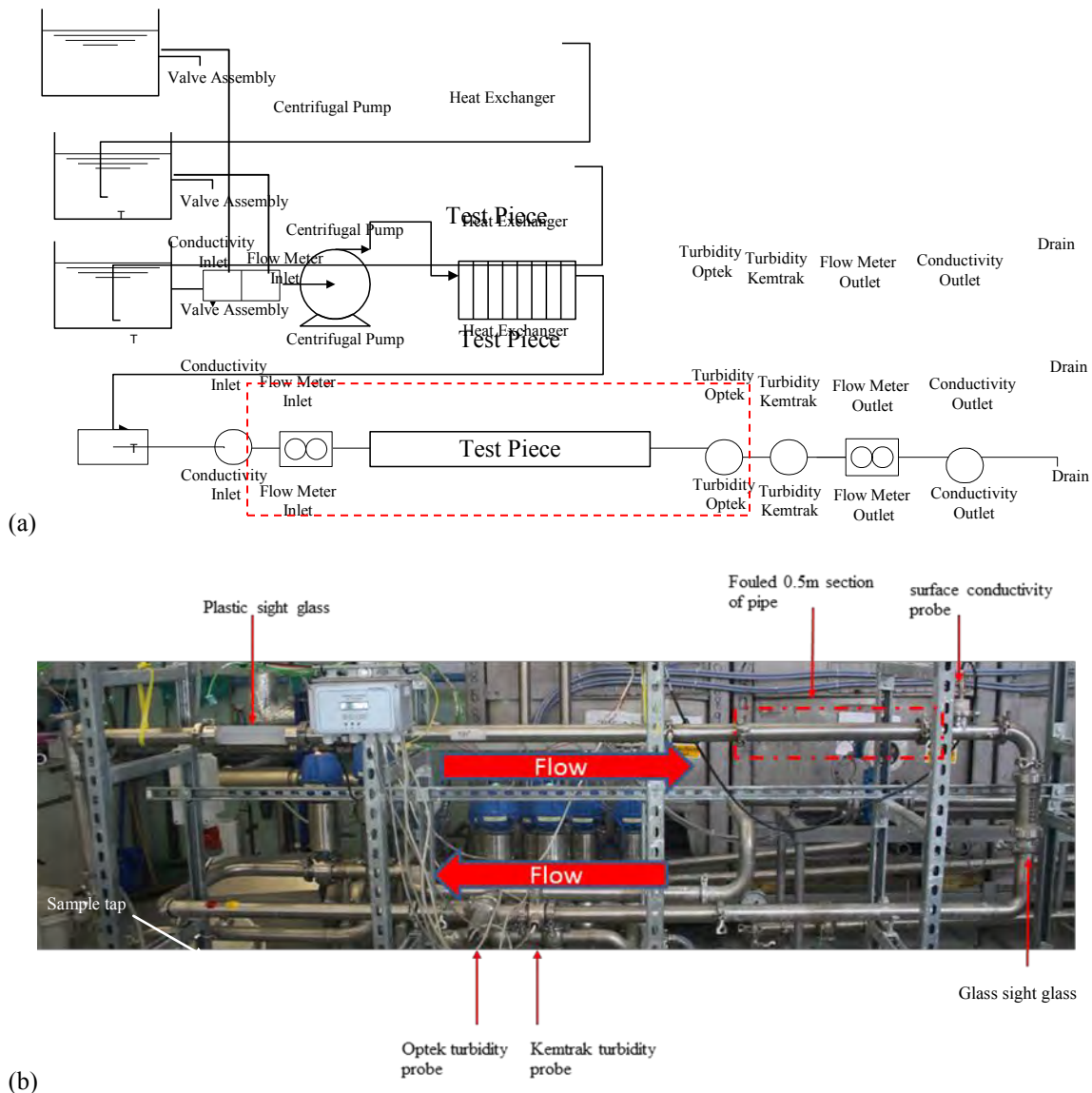
Figure 3.15 (a): Schematic of the pilot plant (Cole et al., 2010) with the test section highlighted with the red dashed box. There are three tanks: Tank 21, 22 and 23; (b) Pilot plant test section layout with fouled caramel pipe in line.

The CIP unit is a three tank system. Tank 21 automatically fills to the level switch with fresh water from the mains, tank 22 was used as a pre-rinse tank, and tank 23 was used as the chemical tank. The system is a 2" (OD) system constructed of 316 stainless steel pipe work. The test section was made of modular sections of pipe up to 2 m in length. This allows the study of different geometries in this 2 m space. The cleaning fluid is transferred through the system by a

centrifugal pump (Alfa Laval) capable of delivering up to 20 m^3 h^{-1} in the 47.7 mm (ID) 2" (OD) system. Operational routes used are detailed in Appendix C, Table C.1. The test sections investigated in this thesis were;

(i)   1 m of stainless steel pipe for yeast slurry cleaning,

(ii)   0.5 m of stainless steel pipe for cooked caramel cleaning.

The flow rates ranged from 4 - 18 m^3 h^{-1} (0.7 - 3.2 m s^{-1}). The relationship between flow velocity, Re, and wall shear stress in the 2" pipe system is illustrated in Figures 3.16 (a) and (b) respectively. The routes available for tank filling, heating, pipe work rinsing and circulation are listed in Appendix C, Table C.2. The tanks were filled to the same level, heated, and chemical was dosed to the chemical tank to the required concentration (details given in Appendix C). After each experiment residual chemical was rinsed from the line and the test section drained. For yeast slurry rinsing experiments the yeast was poured into the pipe work. Caramel was fouled onto 0.5 m sections of pipe which were incorporated into the test section. Before and after each experiment the pipe and fouling were weighed. Fouling protocol for caramel is detailed in Section 3.6.

Operation of the pilot plant was done through Matlab R2007b by selecting the directory: C:\Matlab Files\zeal_pilot and selecting the required route by typing run_zeal. The route function is given in Appendix C, Table C.2. Matlab R2007b was operated from a laptop (Toshiba Satellite Pro L40, model: PSL4BE – 00S00WEN) connected to the signalling panel (GEA Tuchenhagen).

A detailed description of the pilot plant operation and data export to Excel is given in Appendix C.
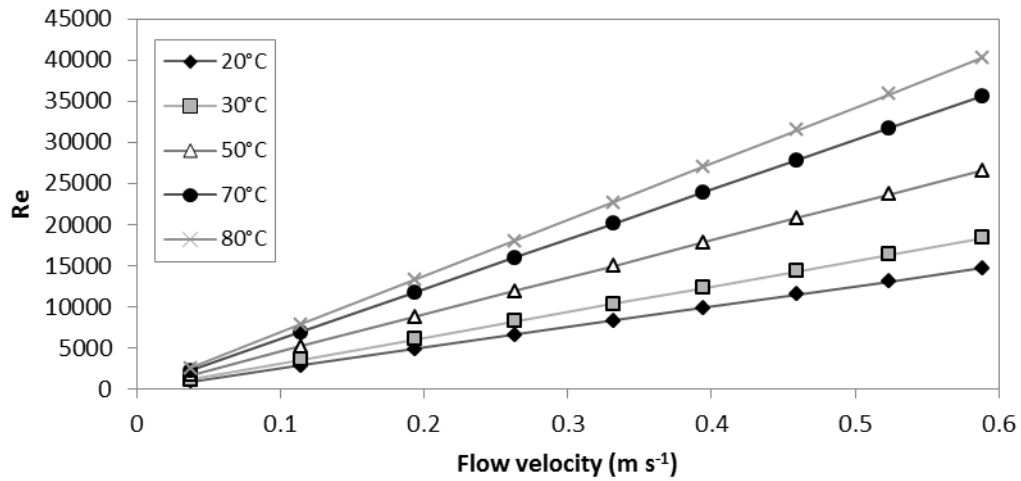
(a)
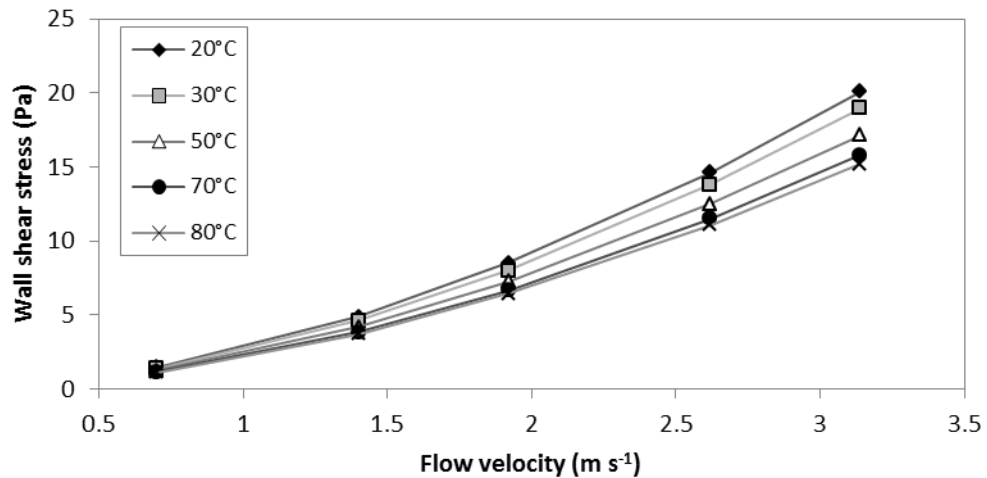
 (b)

Figure 3.16: Pilot plant (a) Re for 1" diameter pipe (calculated from Eqn [3.2] and (b) wall shear stress (calculated from Eqn [3.3]) vs. flow velocity at 20, 30, 50, 70°C and 80°C.

3.3.1 Chemical concentration

Section 3.2.1 described how the concentration of NaOH in Advantis 210 was related to in-line conductivity measurement. In the pilot plant system, chemical was dosed from the skid (Ecolab, Cheadle) into the circulating water at the outlet pipe of tank 23 in increments of up to 1 litre.

Figure 3.17 (a) chemical addition to achieve a conductivity of 7 mS cm^{-1}. A flow velocity of at least 2 m s^{-1} was used to circulate the chemical in the plant to ensure complete mixing in around 50 s. Figure 3.17 (b) shows that at the lowest velocity, 1 m s^{-1}, the chemical did not mix well; the slug of chemical is clear from the oscillation in the conductivity reading. The amplitude becomes smaller with increasing circulation time due to some mixing of the water and chemical.
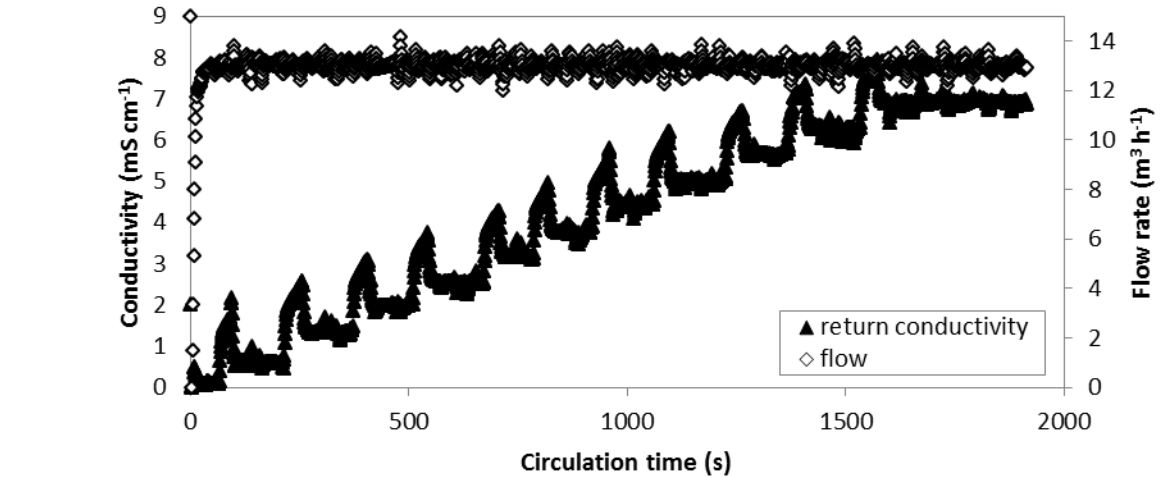
(a)
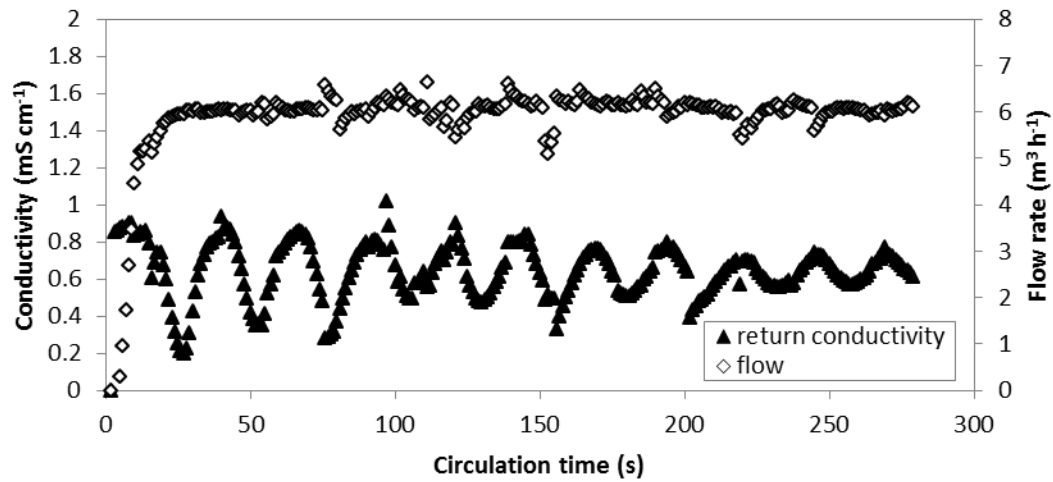
(b)

Figure 3.17: (a) Advantis 210 dosing during route 4b (1L approximately every 150 s), (b) Advantis 210 circulation at 6 $m^3 h^{-1}$. Once dosed the Advantis 210 did not mix effectively.

3.3.2 Measurement technologies

A series of bulk measurements were made at the positions indicated in Figure 3.15 (a) during cleaning;

(i)   Inductive conductivity (LMIT 08, Ecolab) measuring the conductivity of the cleaning solution before and after the test section,

(ii)   Temperature (LMIT 08, Ecolab) before and after the test section,

(iii)   Flow rate (Promag 51P, Endress-Hauser) before and after the test section,

(iv)   Turbidity (Kemtrak TC007, Kemtrak ab; Optek TF16, Optek-DanulatGmbH) after the test section.

The error estimated for each measurement technique is given in Table C.3 in the appendix.

Conductivity (Inductive)

Conductivity is defined as conductance in a given volume (or probe measuring distance). In this case measured in μS or $mS\ cm^{-1}$. The conductivity of acid and alkali at the concentrations used in this study is significantly different to water. As such the chemical phases of cleaning can be clearly identified. The electrolyte solution flows through two electric coils within the probe. An electric current applied on one coil and an electric current is induced in the second coil. The strength of this induction is directly proportional to the applied current and the conductivity of the electrolyte.

Turbidity

Turbidity is a measure of the light absorbed or scattered by a liquid from a known light source. The two turbidity sensors measure different units. The Kemtrak sensor measures FTU. FTU stands for Formazin turbidity unit and is a non-descript measure of scattered light at 90° to the light source. Scattered light was calculated by the manufacturer by multiplying the calibration constant by the detector current (Kemtrak user guide). The Optek turbidity meter gave a numerical output that saturated at 241 ppm.

3.4 Rheology

An AR 500 rheometer (TA instruments) and stainless steel plate geometry (40 mm diameter, 250 μm gap) was used to characterise the flow properties of yeast soils. An AR 1000 rheometer (TA instruments) and stainless steel cone geometry (40 mm diameter, 52 μm gap) was used to characterise the flow properties of cooked caramel. The moisture trap was placed over the geometry and sample and left to equilibrate for up to 5 minutes before testing. The set up and operation of both rheometers was the same and is standard, detailed in Appendix D.

3.5 Micromanipulation

The micromanipulation device is illustrated in Figure 3.18. This rig has been used previously to characterise the adhesive and cohesive forces of tomato paste, whey protein, egg albumin (Liu et al., 2002 - 2007), toothpaste, caramel and SCM (Akhtar, 2010). The principle and operation of the rig has been described in detail by Liu et al., (2002). The T-shaped probe was passed through the yeast deposits at different cut heights from the stainless steel surface; 20, 200, 400 and 600

μm, and the force to remove the deposit measured. A 10 g transducer was used that was suitable

for yeast slurry. The 10 g transducer measured within the force range 0 – 100 mN. The force

transducer calibration is illustrated in Figure 3.19. All experimental runs used a probe speed of

1.11 mm s^{-1}. Five measurements were performed per cut height. The coupons used for

micromanipulation experiments were circular with a diameter of 30 mm. The milled ridge was 5

mm x 1 mm resulting in a fouled surface area of 314 mm^2. This represents approximately half the

area investigated in cleaning rig experiments.
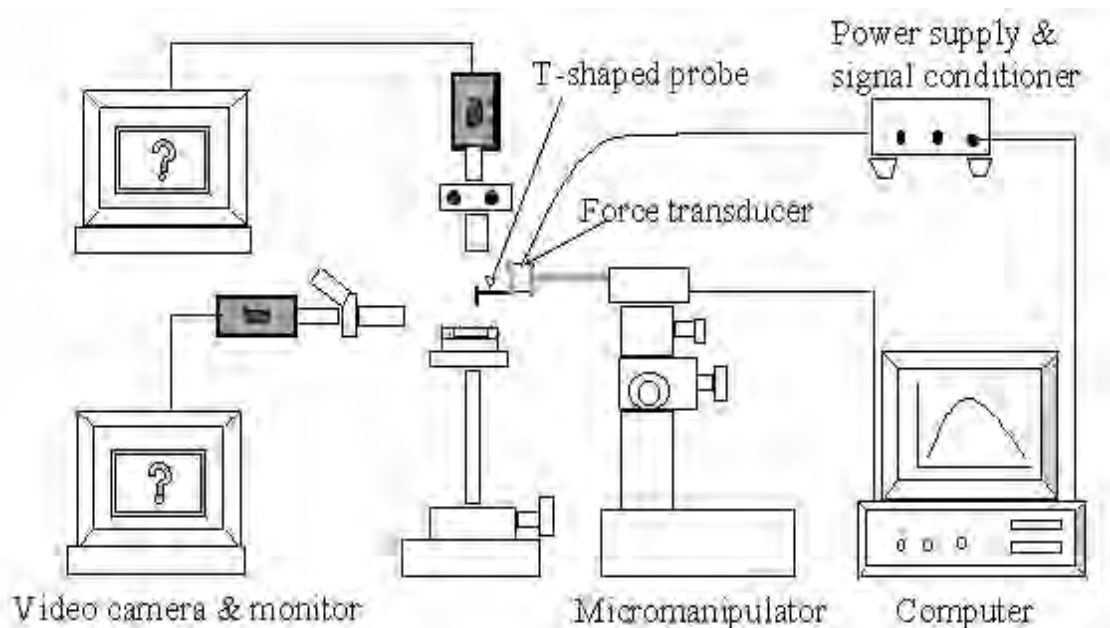
Figure 3.18: Schematic of the Micromanipulation rig (Liu et al., 2002).
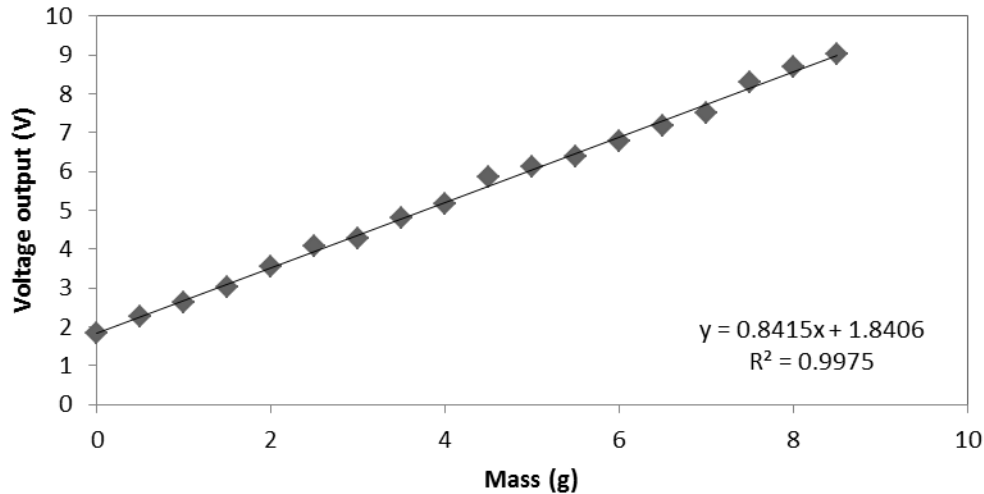
Figure 3.19: Calibration of the 10 g force transducer.

3.6 Caramel type and fouling

Caramel was supplied by Cadburys (Bourneville, Birmingham). The main components of the caramel included vegetable oil, sugar, glucose-fructose syrup, dried whey powder, flavour and emulsifier (Cadburys, Birmingham). In the brewery caramel can be added to some beers to modify the flavour and to darken the colour. There are four different types of caramel used in the food and beverage industry (Briggs et al., 2004):

- Class I - *used in spirits and liqueur.* Caramel prepared by controlled heat treatment of carbohydrates with or without the presence of food quality alkali or acid.
- Class II – *used in vermouths and other aperitifs*. Caramel prepared by controlled heating of carbohydrates with caustic sulphites.
- Class III - *used in bakery, meat products and in brewing*. Caramel prepared by the controlled heating of carbohydrates with ammonia.

- Class IV - *used in soft drinks*. Caramel prepared by controlled heating of carbohydrates with ammonium and sulphite containing compounds.

The caramel used in this work is most likely a class IV caramel and electronegative. Caramel used in brewing is electropositive. Electronegative caramels cannot be used in beer due to reaction with the electropositive finings. Brewery caramel was not readily available for this work only available in small quantities from the tanker during delivery to the brewery. Confectionary caramel was readily available and has already been characterised at nano-meter and micro-meter length scale by Akhtar (2010) using AFM and micromanipulation. Thus parallels may be seen between meter length and smaller length scale cleaning forces.

3.6.1 Fouling pipes

The caramel was heated at 70˚C for up to 1 h to decrease viscosity so that it could be easily poured into the annulus of the pipe-in-pipe system (Holroyd, UK) illustrated in Figure 3.20. Both ends were clamped in place using tri clamps (Alfa Laval). The top tri clamp was attached to the temperature control box by an earth wire. The heating jacket was designed to wrap around a section of 0.5 m pipe, 2" OD. The heated jacket was covered with a layer of insulating foam to minimise heat loss which was held in place by a series of ties. The caramel was heated in the pipe-in-pipe system for up to 20 h.
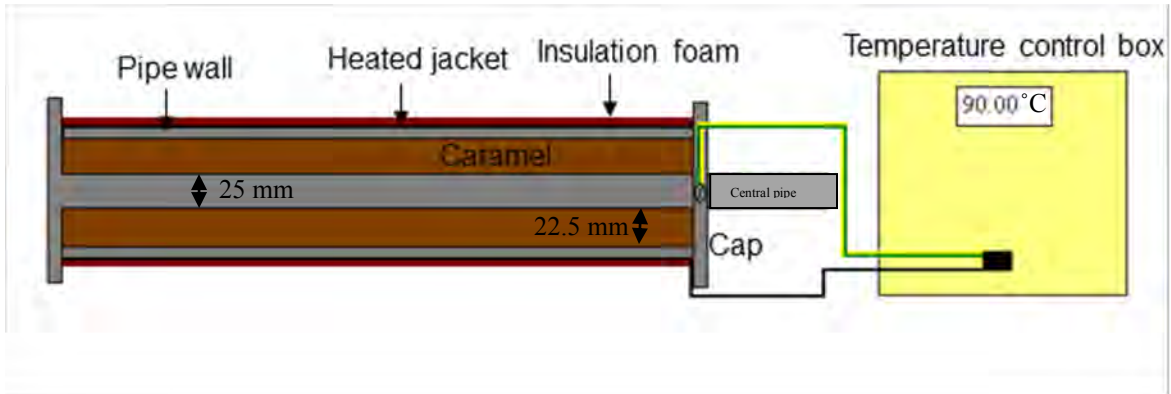
Figure 3.20: The pipe-in-pipe system used to heat the caramel up to 90˚C.

The temperature of the caramel at the inner pipe surface was measured during heating using Tc_5, and the temperature monitored illustrated in Figure 3.21. The caramel used in rheology and coupon rig experiments was taken from this surface. The temperature of the heated jacket was set to 90˚C, which fluctuated by 5˚C. In the first 600 s the temperature of the caramel increased 2˚C per minute, it then increased by 1˚C per minute for 2400 s. The temperature remained constant at 98˚C for 10 minutes. In the following 65 minutes the temperature decreased by 15˚C. For the remaining heating time (105 minutes) the temperature remained constant at approximately 82˚C. The caramel then cooled to 43˚C in 45 s.
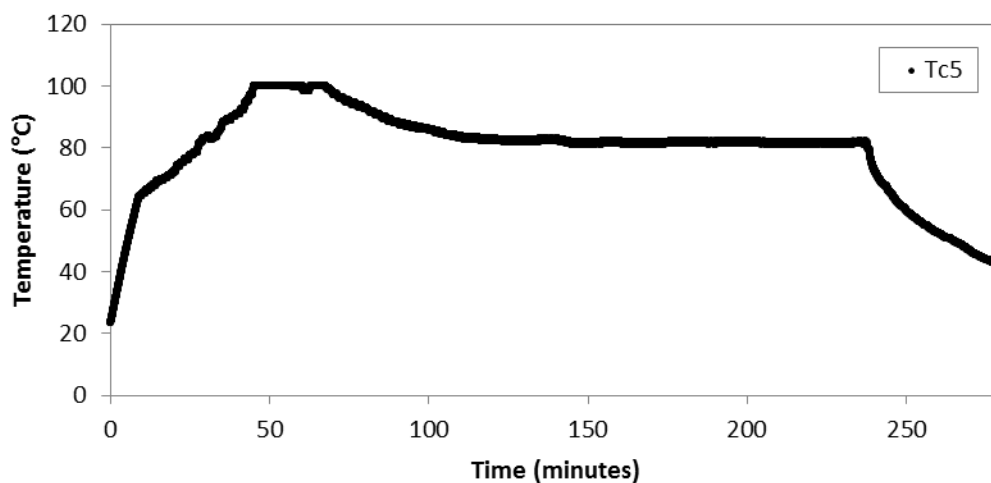
Figure 3.21: Temperature of caramel at the inner pipe surface.

The mass of caramel on the pipe wall after fouling is illustrated in Figure 3.22. The average mass of caramel fouling was 0.57 kg ± 0.1 kg with a standard deviation of 0.06. This gives an average loading of 8.14 kg per unit m^2.
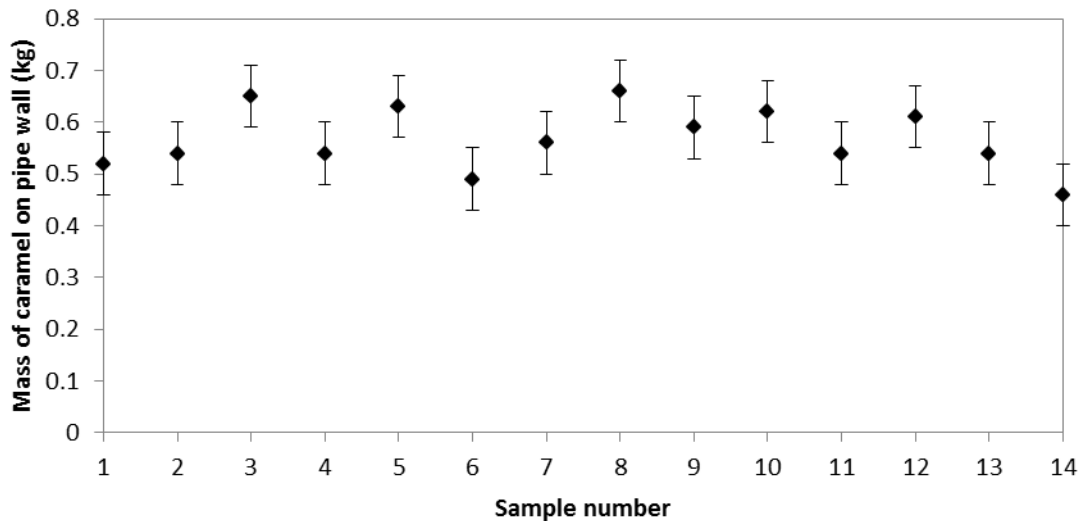
Figure 3.22: Mass of caramel on the pipe wall for each fouling batch. The average was 0.57 kg ± 0.1 kg and a standard deviation of 0.06.

3.6.2 Fouling coupons

Heated caramel was too fluid to foul coupons consistently. The pipe-in-pipe fouling system revealed cooked caramel loosely attached to the central pipe. This caramel spread evenly on coupons to give a repeatable mass of 1 g (±0.03 g). This caramel was heated to become more solid but not cooked like the caramel at the outer wall of the pipe. The heating mat was set up as in Section 3.6.1 however the pipe was not present. 10 coupons were placed along the length of the heated jacket so the back of the coupons were in contact with the heating surface. Each coupon was covered with a foil lid to isolate the caramel and mimic the conditions in the pipe-in-pipe system. The ends of the heater were wrapped with tinfoil to contain the heat. The caramel

was cooked on the coupons for 8 h. Figure 3.23 shows the initial mass of caramel and the mass after cooking (0.08 g ± 0.06 g).
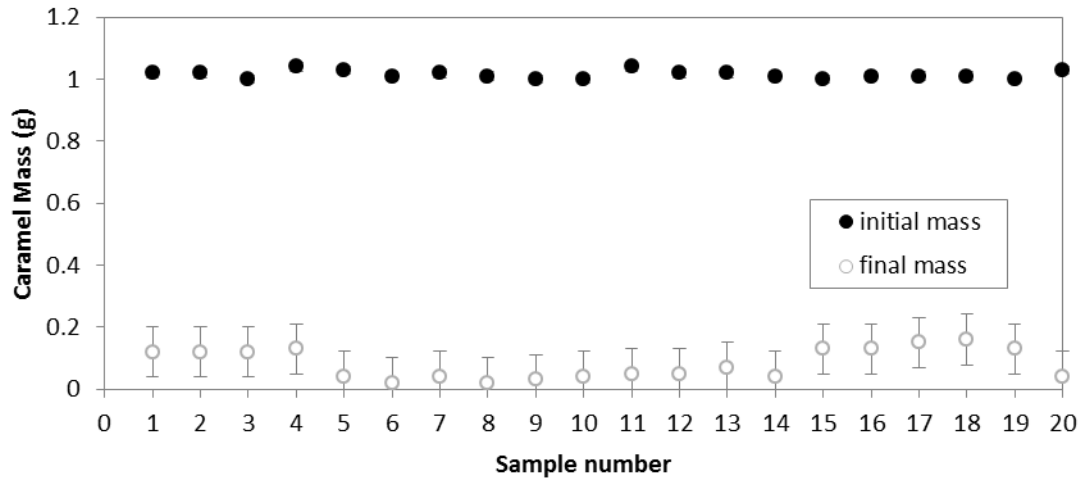
Figure 3.23: Caramel deposit mass before (initial) and after (final) fouling on the coupons (by heating).

3.7 Yeast fouling and cleaning pilot study

Yeast slurry was used to mimic the fouling encountered in brewery fermentation vessels. Observation of the fouling layers in fermenters prior to CIP revealed two types of fouling termed type A and type B (Goode et al., 2010) and illustrated in Figure 3.24. Type A deposit was formed during fermentation and type B deposit was formed after fermentation as the vessel was emptied.
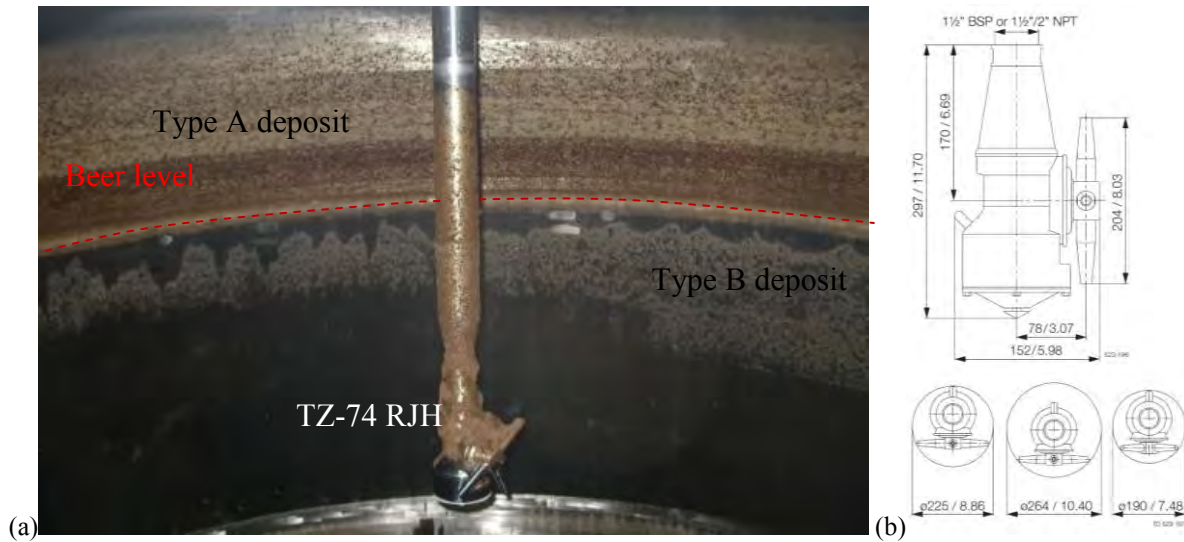
Figure 3.24: (a) Type A and type B fouling present in a brewery fermenter prior to CIP, (b) the dimensions of the TZ-74 cleaning head.

Figure 3.25 illustrates the removal behaviour of both deposit types during CIP. Type B deposit was removed after the first 45 s of the pre-rinse. Type A deposit was removed after the chemical circulation phases. However a patch of deposit remained on the cleaning head in this case indicating that it was not functioning as prescribed by the supplier. The head could have been blocked or the pressure delivered to the head insufficient. The cleaning head should be self cleaning.

Figure 3.25: Phases of CIP (a) After 1 minute of pre-rinse, (b) after 8 minutes of pre-rinse (c) after the chemical phase and final rinse.

Fermentation foaming transports materials like yeast and protein to the tank surface above the beer level. Yeast cells were extracted from 1 g of deposit (taken at day 7 of fermentation) by grinding the sample in a pestle and mortar and extracting and quantifying cells according to the protocol given in Section 3.7.2. 1 g of deposit was found to contain 10^6 cells, all of which were dead. Type A deposit was collected on stainless steel coupons using a bespoke rig suspended in the fermenter head space during fermentation. A bench top experiment presented in Figure 3.26 revealed that substantial deposit could be removed by soaking in water and that all deposit could be removed by soaking in 2 % (w/v) NaOH for 2 minutes at room temperature.

(Clean)   2 min caustic rinse (2%),   (Fouled)   2 min water rinse,   10 min water rinse,   20 min water rinse, cold   No fu
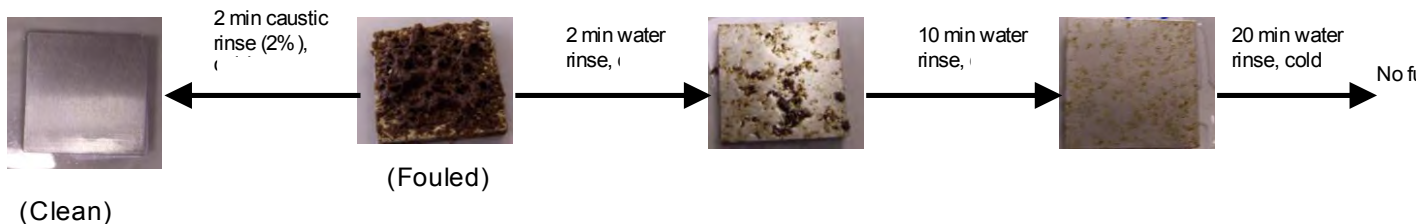
Figure 3.26: The effect of soaking the type A deposit with 2 % (w/v) sodium hydroxide at room temperature for 2 minutes and with water at room temperature for 2 minutes, then 10 minutes. No further deposit was removed with water soaking for 20 minutes.

3.7.1 Mimicking type B fouling

Yeast slurry was used to mimic type B fouling (from handling yeast slurry and the type B deposit on site and in lab scale fermentations (Section 3.7.5)). The viscosity and consistency of the products appeared similar. It took 7 - 8 hours on average to empty the fermentation vessels. To examine type B deposits on the same day of fouling, yeast slurry was aged on surfaces for up to 5 hours before removal was assessed.

3.7.2 Yeast slurry collection and handling

Yeast slurry was collected from yeast storage tanks at the Brewery. The tank was selected from brewery records and agitated prior to sample collection. The same strain (SA/JS) viability 90 % (±5 %) and solids content 37 % (± 3 %) was collected each time. The sample point was rinsed using de-aerated liquor and chemical sterilised for 5 minutes using Savlon. Parameters recorded by the brewery were tank number, storage time, strain type, generation, sample solids, viability, temperature and pH. Cell density and viability was calculated prior to fouling using a haemocytometer (Neubauer, Sussex) and light microscope (Olympus BX50, Japan). The cell density was on the order 10^8 cells ml^{-1}; the viability was 90 ±5 %. 1 ml of yeast slurry was added to 9 ml of distilled water using a pipette (BioHit) with a widened tip, vortexed, and 1 ml immediately extracted and added to a further 9 ml of distilled water. This serial dilution was repeated once more, 1ml extracted and added to 1 ml of methylene violet. The mixture was vortexed and 20 µl extracted. This was pipette between the haemocytometer slide and the cover slip to fill the counting chamber.

Yeast slurry collected in Sterilin pots was transported from the brewery in an electric coolbox (Halfords, Birmingham). 250 ml quantities of yeast slurry were collected in plastic containers and stored in a refrigerator at 4°C until use. Samples were kept no longer than a week due to decreased viability.

From trial and error it was found that 1 ml of yeast slurry gave complete coverage of cleaning rig coupons (625 mm^2) and generated deposits of similar appearance, visible thickness and mass. As such 0.5 ml of yeast slurry gave complete coverage of the micromanipulation coupons with a

surface area of 314 mm^2. Yeast slurry was applied to the surfaces using a pipette (BioHit) with a widened tip. To recreate type B fouling, the fouled coupons were placed in Petri dishes in an incubator at 30°C for 5 h. The coupons were weighed prior to experiments. Figure 3.27 illustrates the initial yeast slurry mass and the mass after 24 h and 120 h. The average yeast slurry mass was 1.13 g ± 0.05 g, at 24 h was 0.35 g ± 0.15 g, and at 120 h was 0.11 g ± 0.03 g.
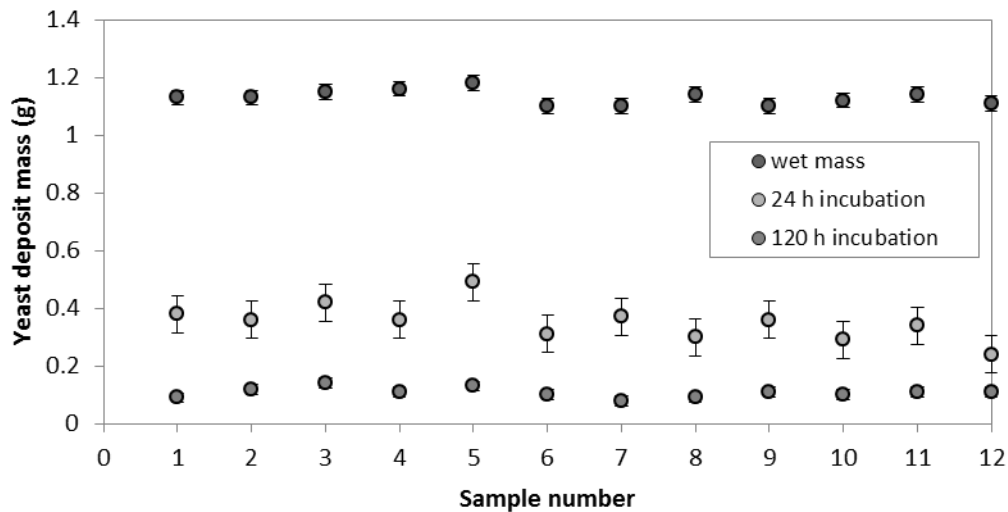
Figure 3.27: Deposit mass in one batch at 0 h (wet mass), 24 h incubation and 120 h incubation.

3.7.3 Mimicking type A fouling

Fouled coupons from industrial fermentation had variable amounts of fouling. In some instances fouling did not cover the entire coupon area. There was a need to generate repeatable deposits. Yeast slurry was applied to the surfaces according to Section 3.7.2 and aged in the incubator at 30˚C for 5 days. Figure 3.28 illustrates the viability of yeast on the surface and the deposit appearance vs. incubation time at 1, 3, 5, 48, 72, and 120 h. Viability measurement was repeated twice. As the aging time was increased the deposit became less fluid and the viability decreased exponentially with a R^2 value of 0.98.
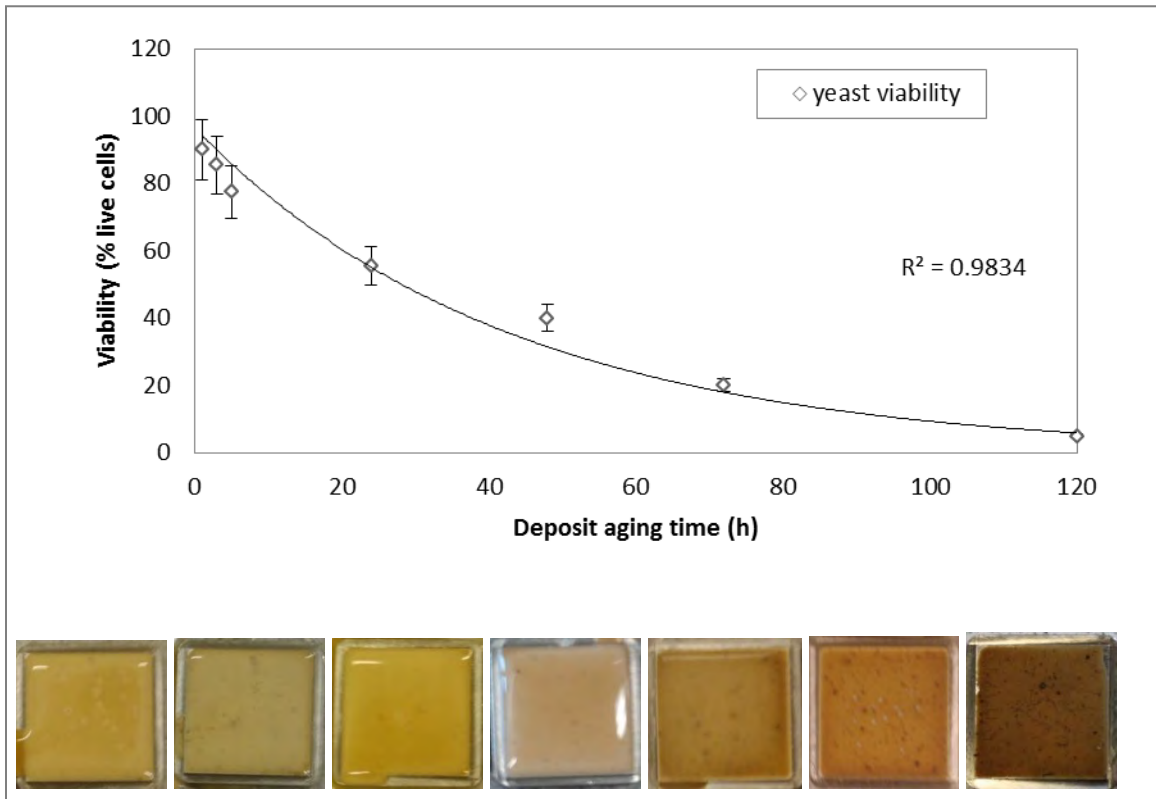
Figure 3.28: Viability of yeast on the coupon surfaces at 1, 3, 5, 25, 48, 72 and 120 h. 1 ml of yeast slurry aged on the coupons at 30°C.

3.7.4 Rheology of yeast and fermenter deposits

For Newtonian fluids τ_y is 0 and n is 1, for Power Law materials τ_y is 0 and n is greater or less than 1, and for Bingham plastic materials τ_y is finite and n is 0.

Type A fouling recovered from fermentation vessels was characterised using an AR 500 rheometer detailed in Section 3.4. This behaviour was compared to yeast slurry and to type A fouling recovered from lab scale fermentations done in Cornelius flasks (Section 3.7.5) called the miniature fermenter in this thesis. Figure 3.29 illustrates the apparent viscosity of the deposits as the shear rate was increased from 0.1 to 1000 s^{-1}. The three deposits show:

(i)   significantly different behaviour at low shear rates,< 1 s^{-1}, with the industrial deposit having a higher viscosity by a factor of 10 than that from the pilot fermenter, and the yeast slurry having a viscosity a factor less;

(ii)   in the range >2 s^{-1}, the three materials show similar, shear-thinning behaviour. Here the industrial deposit has a lower viscosity.

(iii)   At higher shear rates, >100 s^{-1}, the three again diverge.
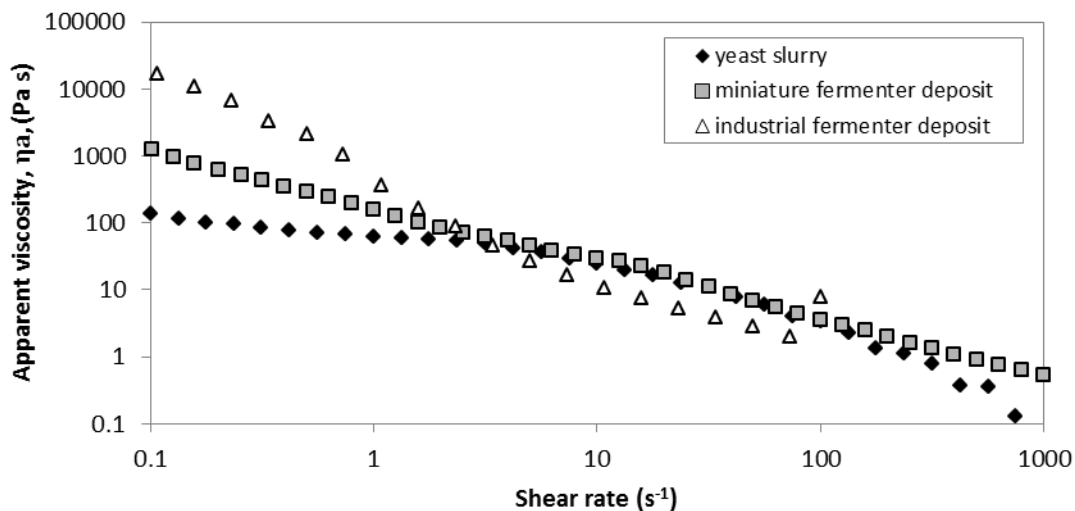
Figure 3.29: Apparent viscosity of yeast slurry at 30˚C, miniature fermenter deposit at 25˚C, and industrial deposit at 30˚C.

From the data it is clear that the industrial deposit has the highest viscosity at low shear, followed by the miniature fermenter deposit, then the yeast slurry. This may reflect the length of time the deposit was aged on the surface, which for the industrial deposit was at least 141 h, at least 72 h for the miniature fermenter deposit, and only 1 h for yeast slurry. The longer the deposit was aged on the surface the more viscous it became (illustrated in Figure 3.29). Mercier-Bonin et al., (2004) discovered the longer yeast cells were left to contact a glass surface the more strongly the

cells were attached. All deposits demonstrated shear-thinning behaviour. The yeast slurry commenced shear-thinning behaviour at a much larger shear rate than the miniature fermenter deposit, around 7 s^{-1}. This was due to the yeast slurry sample retaining liquid. These findings could suggest that an increase in flow velocity could remove the deposits similarly because they flow similarly at higher shear rates.

Oscillatory stress sweeps of the yeast slurry, miniature fermenter deposit and industrial fermenter deposit were conducted at 15, 18 and 20˚C respectively as illustrated in Figure 3.30 (a) – (c). The curves have similar shapes with *G'* > *G"* at lower oscillatory stress and *G'* = *G"* at higher oscillatory stress. The crossover point was found to be at approximately 500 Pa for the industrial deposit, 5.5 Pa for the miniature fermenter deposit and 1.5 Pa for yeast slurry. This indicates that the yield stress of the deposit is likely to increase as the aging time increases. The magnitude of the low shear modulus is much greater for the fermenter deposits at around 5000 and 500 Pa as opposed to 140 Pa at an oscillatory stress of 0.1 Pa for yeast slurry. The maximum surface shear stress achieved in the cleaning rig system was 1.2 Pa and 20 Pa in the pilot plant at ambient temperature (estimated from Equation [3.3]) suggesting the deposits would remain elastic during cleaning rig rinsing experiments.
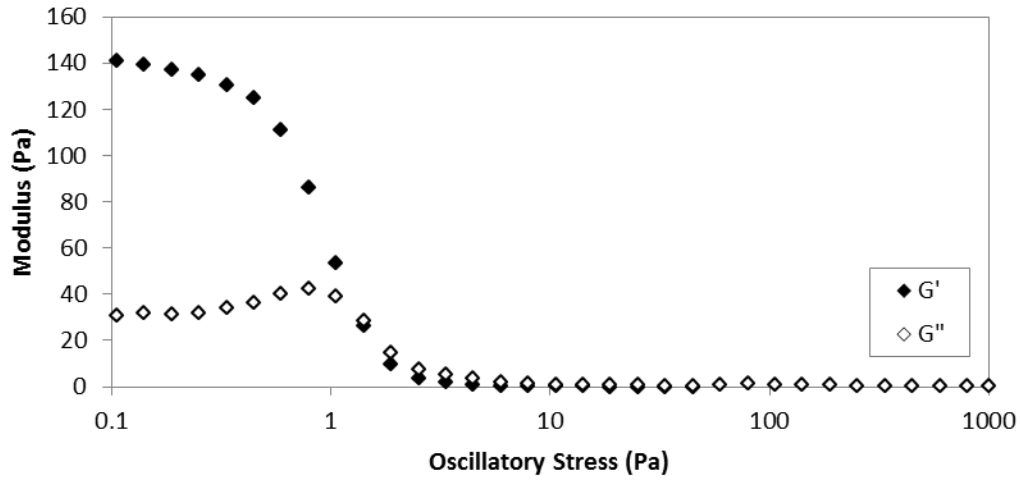
(a)
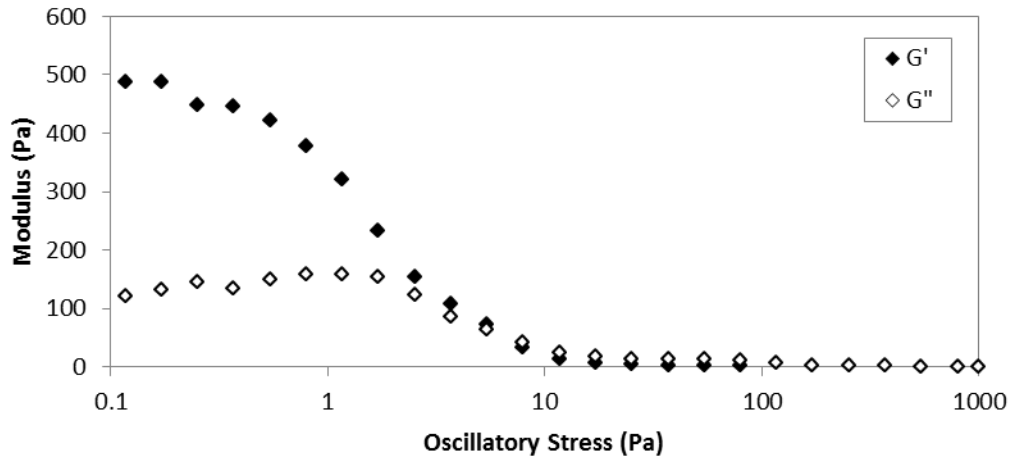
(b)
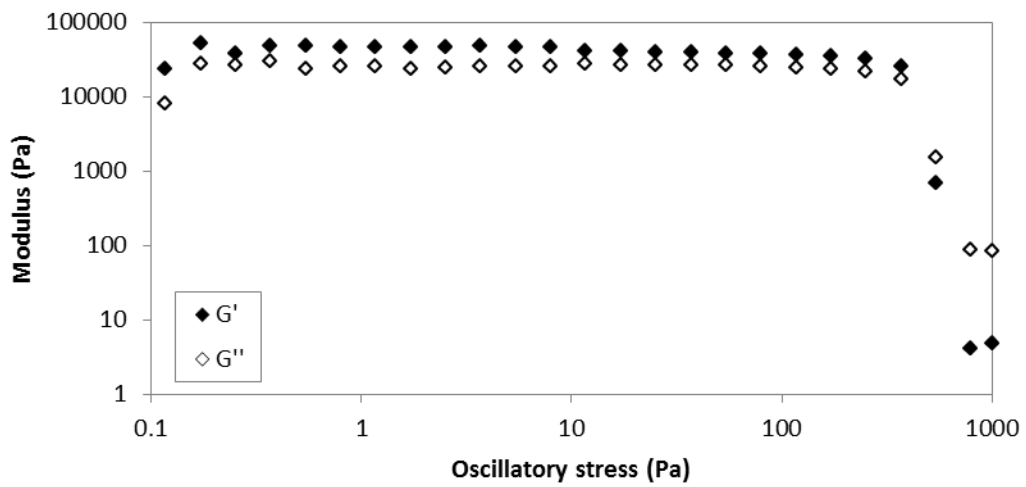
(c)

Figure 3.30: Oscillatory stress sweeps of (a) yeast slurry at 15˚C (b) miniature fermenter deposit at 18˚C (c) industrial fermentation deposit at 20˚C.

An oscillatory stress of 0.5 Pa was selected for further investigation of the linear viscoelastic region (LVR) of yeast slurry and the miniature fermenter deposit. Figure 3.31 (a) and (b) illustrate that G' remained greater than G'' for both deposits when the temperature was ramped from 20 to 70˚C at a shear stress where the structure was consistent. Increasing the temperature increased the magnitude of the measured modulus; more so for the miniature fermenter deposit than the yeast slurry. This effect may have been due to the gelation of proteins within the deposits and greater moisture retention in yeast slurry. Similar rheological behaviour was shared by the two deposits, indicating that yeast slurry could be used to mimic industrial type A deposit if the aging time was increased.
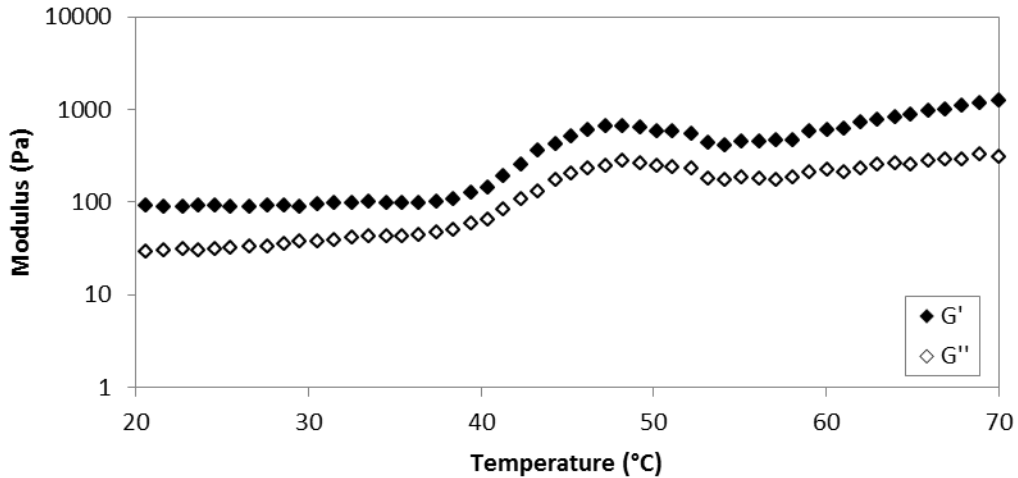
(a)
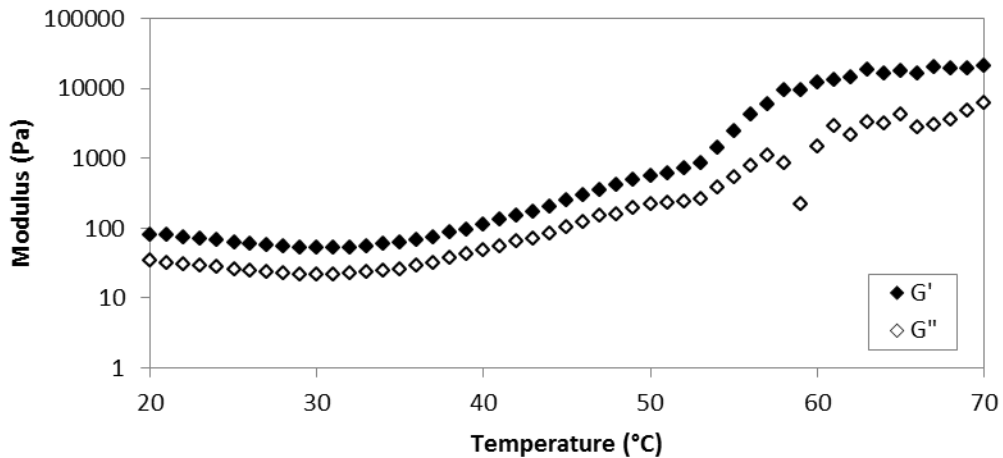
(b)

Figure 3.31: Temperature ramp of (a) yeast slurry and (b) miniature fermenter deposit.

3.7.5 Fermentation and scalable fouling

During fermentation, temperature is controlled and specific gravity is monitored. The two parameters are expected to conform to a profile which has been determined from historical fermentation data. Figure 3.32 illustrates an example of an ale fermentation profile. Three stages of the fouling process were identified during pilot scale fermentations that can be applied to the industrial curve:

(1)   Mass transport of the yeast cells in the foam to the surface within the head space,

(2)   Foam collapse, and

(3)   Deposit aging on the surface

The deposit could have attached to the tank surface above the beer at any point during phase 1 after the approximate lag time of 5 h. Foam collapse was seen at around 20 h but could have occurred earlier. The measured temperature can be related to the metabolic state of the yeast in fermentation. Fermentation is most rigorous at the start after the initial lag phase. The point where yeast metabolism slows could be the point where the foam collapses. In industrial ale fermentation this would be around 30 h. In ale fermentation when the cooling rate is increased at 60 h the foam has certainly collapsed. In lager production however the vigour of the fermentation can still be seen at 66 h, and slightly at 107 h. A schematic of the foam collapse observed is illustrated in Figure 3.33. This is a simple cross sectional view of the fermentation media in a cylindroconical vessel if looking in from the top. The convection currents that were seen to push the foam out from the centre of the vessel towards the wall are indicated by the arrows. The volume of foam decreases with fermentation time and cooling rate.
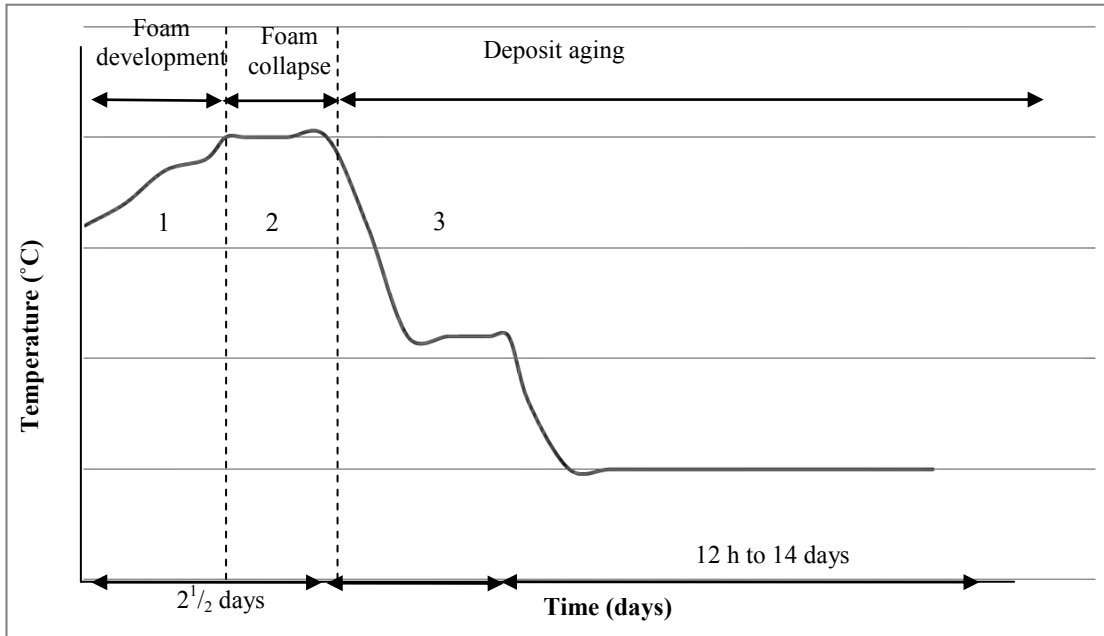
Figure 3.32: Ale fermentation profile. 1: foam development, 2: foam collapse, 3: deposit aging.

(a)   (b)   (c)
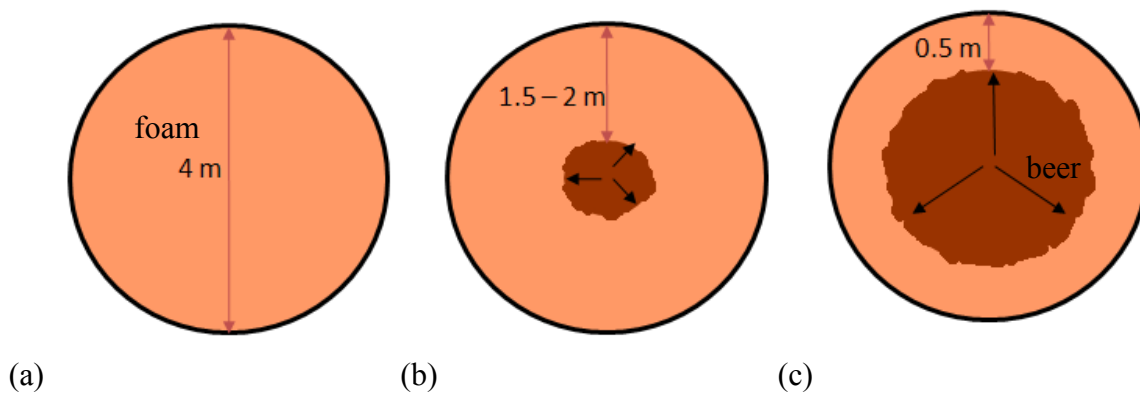
Figure 3.33: cross section schematic of foam collapse observed in lager fermentation vessels. (a) Foam fully covering the beer, (b) foam volume decreased at 66 h, (c) foam volume further decreased at 107 h and the vigour of fermentation decreased.

Visualisation of the point where the deposit attached to the surface was not possible in closed fermentation vessels. To visualise the fermentation fouling process directly and safely bench top fermentations in modified Cornelius Flasks were done; modified so that a portion of the top section was removed. Foam was seen to develop within 5 h of aeration. Foam recession was seen

at approximately 20 h, although this could have occurred at less than 20 h. The resulting fouling

layers are shown and labelled in Figure 3.34.
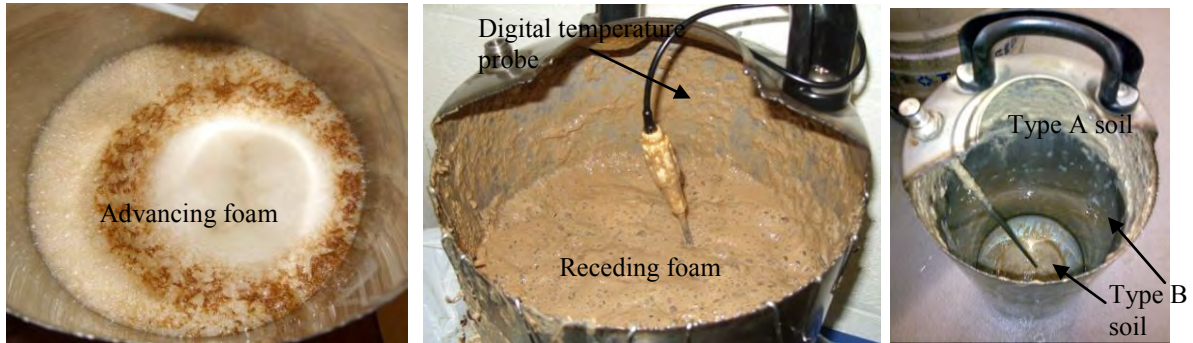
Figure 3.34: Bench top fermentation in a modified Cornelius flask (20 L capacity).

Table 3.1 illustrates the similarities between the thickness and coverage of industrial and

miniature fermenter fouling (bench top scale).

Table 3.1: Characteristics of fouling deposits formed during fermentation.

Fermentation	Fouling thickness (mm)	Geometry surface area (m²)	Surface area fouled (m²)	Fouling coverage (%)
Plant scale	3	135.0	25.45	18.9
Bench top scale	3	0.3	0.06	20

To carry out bench top fermentations, cooled wort was collected from the plate heat exchanger

sample tap which was heat sterilised. The wort was collected in tetrahop drums using an

autoclaved silicone rubber tube connecting the sample tap to the drum. The specific gravity of

wort samples was recorded for reference. The mass of yeast slurry (M_y) required for fermentation

was calculated according to Equation [3.6], where L_w is the volume of wort, u_y is the yeast

addition rate to the flask (g l^{-1}), C is the percentage solids of the yeast slurry and V is the

percentage viability of the yeast slurry.

$$M_y = \frac{L_w u_y}{CV}$$
[3.6]

Yeast addition rate was 7 g l^{-1}, as calculated from brewery fermentation parameters; volume, yeast mass, viability and percentage solids. Fermentations were covered with an autoclaved transparent bag, agitated at 110 rpm for up to one day and held at 20°C for 3 − 5 days. Yeast slurry was collected according to Section 3.7.2. The flask was manually cleaned using hot water, a hypochlorite washing up liquid and autoclaved sponge. The vessel was sterilised using steam for 10 minutes.

3.7.6 Fermentation in other systems

Various methods were used to assess the feasibility of fouling pipelines with yeast slurry. Fermentation was attempted in stainless steel pipes (0.3 m, OD of 2") in the upright and horizontal positions with a head space of 25% (typical of fermentation), 50%, 75%, and 90%. Fermentations followed the same protocol as detailed in Section 3.7.5.

No type B fouling was seen when the pipes were emptied from the bottom, similar to fermentation vessel emptying. The lack of type B fouling was expected due to the fast emptying time of the pipe. In the miniature fermenter the emptying time was at least 30 minutes and in industrial fermentations ranged from 4 to 11 hours. It was hoped that increasing the head space would increase the surface area for fouling contact for type A deposit. However fouling was limited to 2 - 3 centimetres above the level of the medium. Pipes fermented in the horizontal

position revealed no fouling. The fouling layer obtained using a head space of 25 % is illustrated in Figure 3.35.

Figure 3.35: Fouling layers obtained from vertical pipe fermentation with head space of 25 %.

3.7.7 Maximising yeast cell transport to the surface

Yeast slurry was applied to the inner surface of stainless steel pipes (0.3 m, of 2" OD) using;

(i)   an autoclaved paintbrush, and

(ii)   a garden trigger sprayer (Homebase, Birmingham),

10 applications were done 5 minutes apart and the pipes were left at room temperature, approximately 25˚C. The pipe applied with yeast slurry using a paint brush was left in the upright position in between applications and the pipe sprayed with yeast slurry was left in the horizontal position. Within seconds of each application the yeast slurry ran out of the bottom of the pipe or collected in the bottom of the pipe respectfully. No visible fouling was generated. The yeast

slurry did not stick to the pipe wall. Sections of pipe in stainless steel and plastic (0.3 m, 2" OD) were coated with yeast slurry. 71 ml of slurry was used to foul an internal surface area of 0.08 m^2. This was determined from lab scale fouling experiments where 1 ml of slurry was found to evenly coat 625 mm^2 surface area (Section 3.7.2). The capped pipes were modified at one end to relieve pressure. The mixer and pipes were placed in an incubator at 30°C. The mixer rotated at a fixed speed of 50 rpm for 5 days. A schematic of the system is illustrated in Figure 3.36. Both the stainless steel and the plastic pipe revealed limited fouling. More slurry appeared to have adhered to the plastic pipe than the stainless steel pipe.

Figure 3.36: Section of 0.3 m pipe (stainless steel and plastic, 2" OD) on the roller mixer placed in an incubator at 30°C.

3.8 Conclusions

The variable fouling of industrial deposit in fermenters will lead to significantly variable cleaning behaviour. As such a way of generating representative deposits was required. This Chapter has investigated the feasibility of using yeast slurry to mimic both type A and type B fermenter deposits. Rheological characterisation of type A soil from both scale fermenters and yeast slurry has revealed that yeast slurry can be used to mimic industrial yeast deposit if aged on the surface, increasing yield stress. The use of rheology and micromanipulation in predicting cleaning behaviour should be further investigated. Micromanipulation and rheology is next used to characterise yeast slurry and caramel respectively.

The bench top cleaning rig can be used to study the removal of both type A and B deposits, and cooked caramel from a surface under different flow, temperature and chemical regimes, and the behaviour quantified by U and deposit area. The dissolving effect of water and chemical is demonstrated at the micro-scale in the following Chapters. Deposit swelling, erosion and total cleaning times are also discussed in the following Chapters.

The pilot plant can be used to study deposit removal from a pipe under different flow, temperature and chemical regimes and the behaviour quantified by turbidity, conductivity, mass and visual observation. Un-aged yeast slurry, and cooked caramel can be studied at the pilot plant scale. It was not possible to foul pipes with yeast slurry. Yeast slurry removal behaviour is studied in Chapter 4.

Aged yeast slurry removal behaviour from coupons is next studied in Chapter 5. Cooked caramel removal behaviour is studied in Chapter 6. The fouling trials using glucose, glucose and whey protein, and caramel are discussed initially, followed by the rheology of cooked caramel. The effectiveness of alkali chemical on deposit removal following a pre-rinse and the measurement of this effectiveness by turbidity and mass on the pilot plant are discussed.

CHAPTER 4: REMOVAL OF YEAST SLURRY FROM STAINLESS STEEL PIPES AND SURFACES

4.1 Chapter Introduction

The aim of this Chapter is to report the cleaning behaviour of a type 1 soil, yeast slurry, from pipes and from coupons. The previous Chapters have;

Chapter 1:　Highlighted the importance of optimising CIP to the manufacturer.

Chapter 2:　Presented broad knowledge of fouling and cleaning methods, and the factors important in optimising CIP.

Chapter 3:　Detailed the methods, equipment and procedures used to generate and analyse the results presented throughout the remainder of this thesis.

This Chapter reports the cleaning times of yeast slurry, Type B soil (see Chapter 2 and Chapter 3), from coupons and pipes. Preliminary cleaning studies of yeast slurry from coupons in the cleaning rig system revealed the slurry could be removed with water alone, i.e. type B yeast deposit is a type 1 deposit by the criteria proposed by Fryer and Asteriadou (2009). The current

CIP regime for yeast slurry storage tanks involves a pre-rinse, hot caustic circulation, intermediate rinse, sanitiser circulation and final rinse. A CIP regime using only water and a final sanitisation would reduce chemical, water, energy and effluent from this CIP process.

The effect of flow, wall shear stress and temperature on the removal time of yeast slurry is presented in this Chapter. Cleaning times from surfaces were determined by visual observation, deposit area and compared to U data (the heat transfer coefficient). Cleaning times in pipes were determined by visual observation and compared to online conductivity and turbidity data. The effectiveness of measurement devices in measuring yeast slurry removal is reported. Rheological and micromanipulation studies of the yeast slurry were done to assess yeast slurry structure and behaviour. If the cleaning times on the cm scale relate to cleaning times on the meter scale, relevant cleaning research can be done at much lower cost and in less time.

4.2 Measurement device characterisation

Water was rinsed through the cleaning rig (see Chapter 3, Section 3.2) and the pilot plant system (see Chapter 3, Section 3.3), both developed at the University of Birmingham as part of project ZEAL (see Chapter 1, Section 1.6), to determine the response of the measuring probes in flowing water (RO water) with and without yeast present.

4.2.1 Heat transfer coefficient (U) response

In the clean system (with an un-fouled coupon in place in the cleaning rig duct) U was measured from the MHFS and temperature readings, detailed in Chapter 3 Section 3.2.5. The response of U was calculated from Equation 3.5. This Section also detailed the effect of flow rate on U at high cleaning temperature, 70°C. It is feasible that coupons fouled with yeast slurry will be removed

as easily at 20°C. As such, the response of U in the flowing system at 20°C was characterised and is illustrated in Figure 4.1. The flow rate was increased in increments and held at each flow rate for a period of time to see the effect. As the flow rate was increased (or decreased, at 160 s) the value of U increased (or decreased) similarly. When the flow rate was held at a constant value, U remained reasonably constant. This finding illustrates the temperature differential is only reasonably constant when the flow rate is constant. The step change in the flow rate, up and down, is clear. The step changes in U are not so obvious. The change in U is more of a slope than a step, reflecting the response time and change in temperatures in the device.
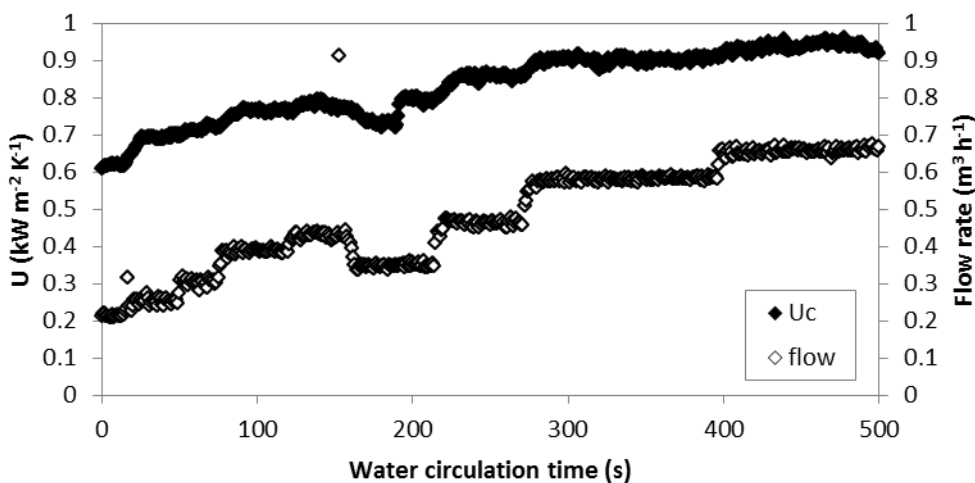
Figure 4.1: Clean heat transfer coefficient (U_c) and flow rate vs. time using an un-fouled coupon in the cleaning rig system.

Figure 4.2 illustrates the stability of U measured at (a) 0.46 m³ h⁻¹ (0.26 m s⁻¹) and (b) 0.85 m³ h⁻¹ (0.5 m s⁻¹) after yeast slurry was removed from coupons at 20°C. In Figure 4.2 (a) the flow rate is initially stable and gradually increases during the experiment. This is because the flow rate was set manually at the start of the experiment in this case. It can be seen from this Figure that the

effect on U appears small. U_c is consistent although there is a small deviation in the flow rate. The visual cleaning time for (a) was 52 s and for (b) was 28 s.
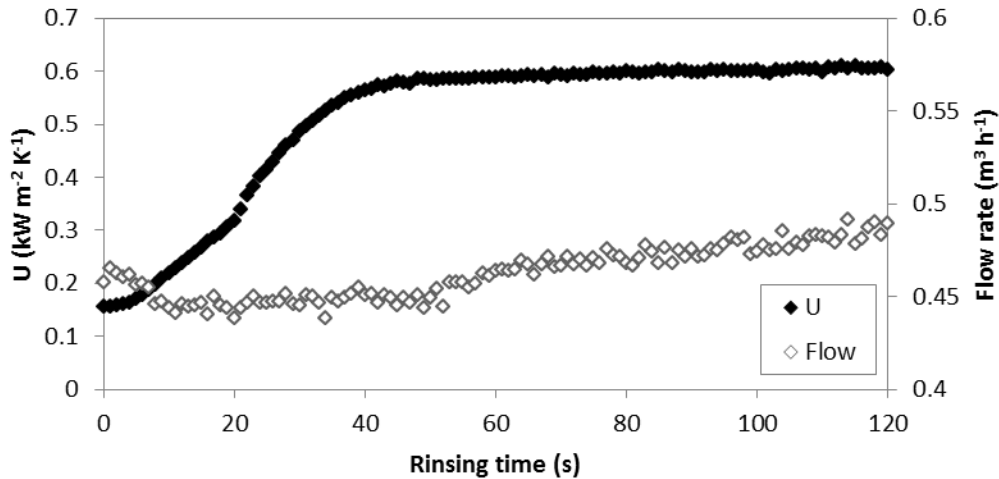
(a)
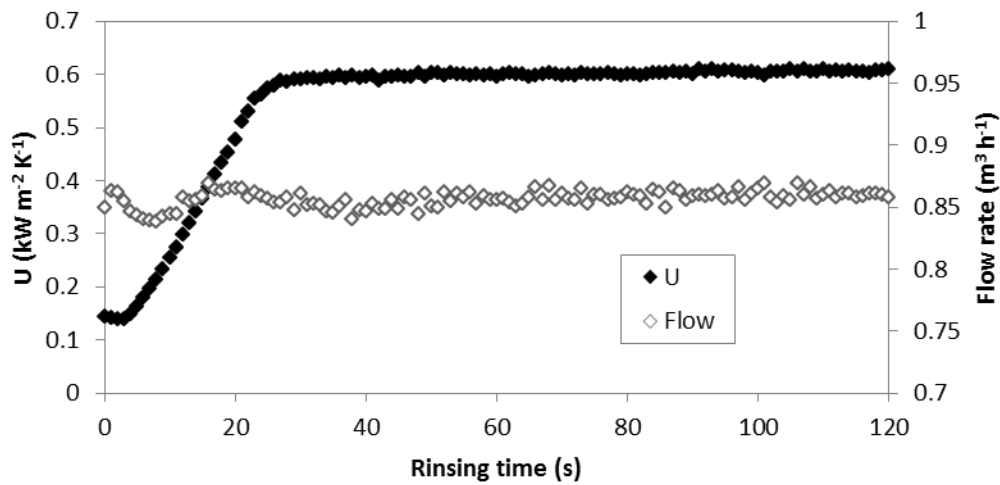
(b)

Figure 4.2: U measured during yeast slurry removal from a coupon at 20°C at (a) 0.85 m^2 h^{-1} (0.5 m s^{-1}) and (b) 0.46 m^3 h^{-1} (0.26 m s^{-1}).

4.2.2 Conductivity and turbidity response

In the cleaning rig and pilot plant, both run clean (i.e. with un-fouled coupon of pipe work in the test section). The flow rate was increased in increments with and without stopping the pump at 20°C. The response of the conductivity and turbidity probe was investigated. Figure 4.3 shows:

(a)   Continuous flow with step changes in flow rate from 0.2 to 0.46 m^3 h^{-1} (0.13 to 0.26 m s^{-1}) 0.46 to 0.85 m^3 h $^{-1}$ (0.26 to 0.5 m s^{-1}) within the cleaning rig system.

(b)   Three independent experiments where the flow was set first, at 0.2, 0.46 and 0.85 m^3 h^{-1} (0.13, 0.26 and 0.5 m s^{-1}) in the cleaning rig system.

(c)   Four independent experiments where the flow was set first, at 6.5, 7.7, 10.0 and 15 m^3 h^{-1} (0.6, 1.8, 2.4 and 2.9 m s^{-1}).

Some features of Figure 4.3 can be described:

(i)   Conductivity does not exceed 0.16 mS cm^{-1} in either system, so any conductivity measured greater than 0.16 mS cm^{-1} will suggest the detection of deposit. The base line conductivity data measured in the cleaning rig system also appears more variable than in the pilot plant system.

(ii)   Turbidity data did not exceed 16 FTU (Formazin turbidity unit) in the cleaning rig and 80 FTU in the pilot plant. Therefore turbidity values greater than this will suggest the presence of deposit in the system. An increase in turbidity did however appear to be linked to the onset of flow in some cases (i.e. in Figure 4.3 (a) and (c)).

(iii)   Turbidity measured after the onset of flow read between 0 and 3 FTU for both the cleaning rig and the pilot plant systems and was taken as the baseline for clean water.

(a)

(b)

(c)
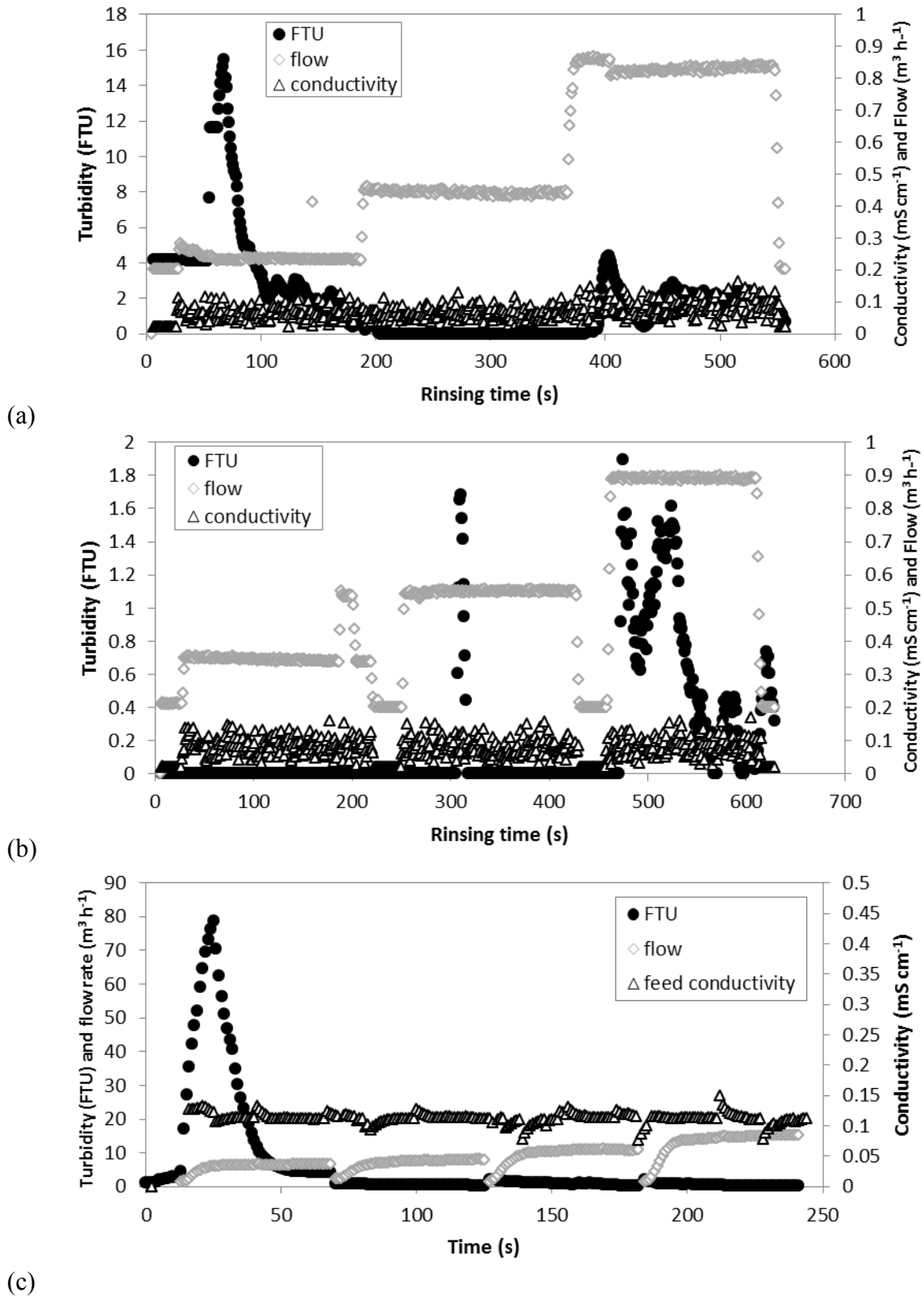
Figure 4.3: The effect of flow rate on turbidity and conductivity measurements in the cleaning rig (a) and (b) and pilot plant (c) systems with clean water.

4.2.3 Measuring yeast slurry

On the pilot plant, the fouling loop was filled with 20 L of yeast slurry (John Smiths Brewery). The cell density of this yeast was on the order of 10^8 cells ml^{-1}. This volume of yeast was circulated around the plant at 6 and 18 m^3 h^{-1} and the conductivity and turbidity responses measured. Figure 4.4 illustrates the measurement of yeast slurry circulation by (a) turbidity and (b) conductivity at 20°C at 6 m^3 h^{-1} (run 1) and 18 m^3 h^{-1} (run 2). The two runs are plotted adjacent on each graph for easy comparison of the effect of flow rate (185 s is actually time 0 for run 2). Visually the yeast slurry was observed through the sight glass at the outlet of the test section to be pushed around the plant as a "slug" at 6 m^3 h^{-1}, and appeared mixed at 18 m^3 h^{-1}. The presence of a "slug" of yeast at low flow velocity (< 1 m s^{-1}) suggests that yeast can preferentially stick together rather than be broken up in the flow.

(a)

(b)
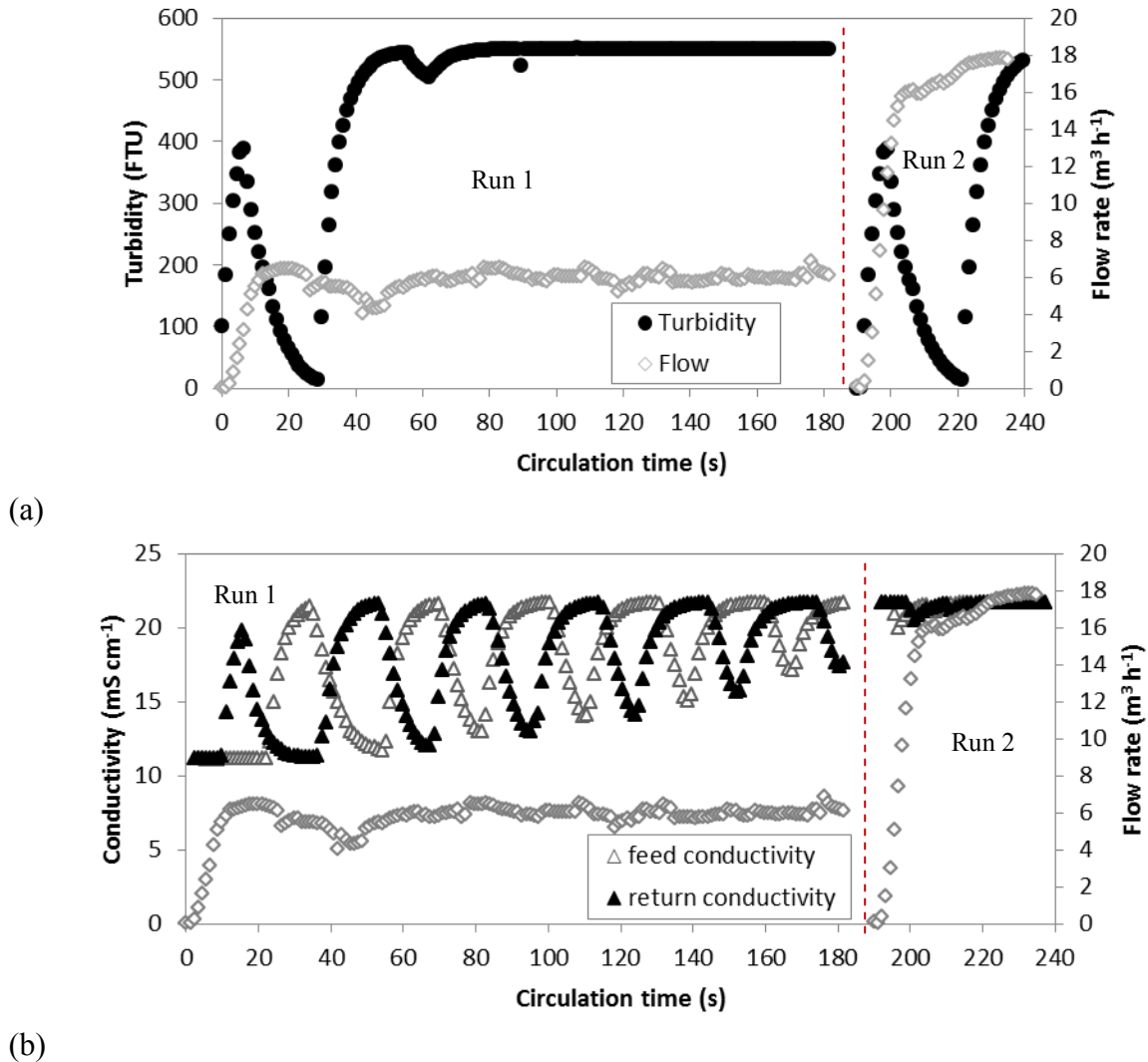
Figure 4.4: Yeast slurry circulation measured by in line (a) Turbidity and (b) conductivity at 6 m³ h⁻¹ for Run 1 followed by 18 m³ h⁻¹ for Run 2.

Turbidity

Figure 4.4 (a) reveals that as the yeast slurry was circulated the turbidity value increased to saturation. The Optek turbidity meter saturated at 241 ppm at both flow rates (data not shown), and the Kemtrak turbidity meter saturated at 550 FTU at both flow rates. This occurred at approximately 75 s during both runs. Turbidity measurement suggests there is no difference in the yeast slurry mixture in the pipe at the two flow rates although visually there was a difference.

The concentration of yeast within the system was probably too high and thus the fluid was too turbid.

Conductivity

Figure 4.4 (b) reveals that at 6 and 18 m^3 h^{-1} the yeast slurry mixture in the system appears different when measured by conductivity. At 18 m^3 h^{-1} the conductivity is constant suggesting the yeast has mixed whilst at 6 m^3 h^{-1} the conductivity is not constant. The amplitude of the waveform decreased with increasing circulation time, but the wavelength did not change (because the position of the sensors and the flow rate remained the same). This suggests yeast slurry mixes into the water much slower at this flow rate. The data suggests yeast slurry cleaning could be monitored using both conductivity and turbidity: conductivity at the start of removal when yeast concentration is high and turbidity as removal progresses and yeast concentration decreases.

4.3 Characterisation of yeast slurry

Rheological characterisation of yeast slurry was measured using the AR 500 rheometer (TA Instruments). Figure 4.5 suggests that yeast slurry is a stable over 600 s. The yeast slurry appeared more elastic than viscous at low wall shear stress (0.4 Pa). Yeast slurry removal times presented in the Chapter are less than 600 s.
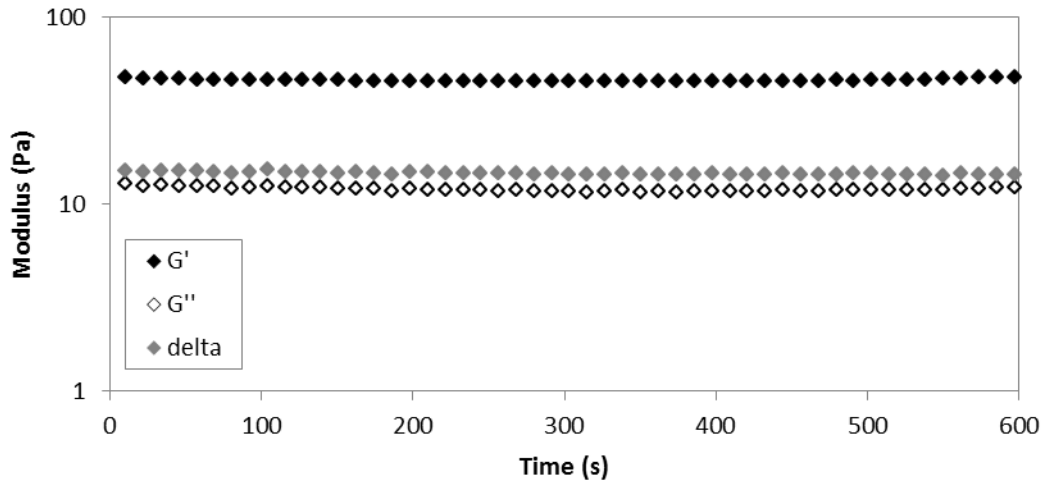
Figure 4.5: Modulus behaviour of yeast slurry with respect to time at 18°C and 0.4 Pa.

The viscosity of yeast slurry at ambient temperature is presented in Figure 4.6. The data suggests that the structure of yeast slurry is (i) repeatable and (ii) shear thinning; as the oscillatory shear stress was increased the viscosity of the deposit decreased according to the power law model (R^2 > 0.85). The data when extrapolated back to 1 Pa suggest the deposit viscosity would not exceed 100 Pa. The maximum wall shear stress achieved in the pilot plant was 20 Pa and 1 Pa in the cleaning rig.
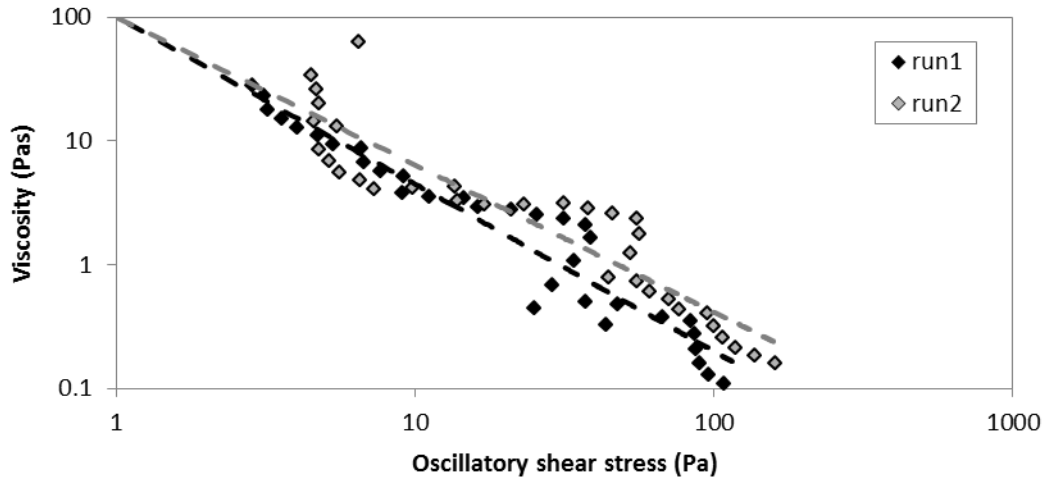
Figure 4.6: Viscosity of yeast slurry vs. Oscillatory shear stress measured at 18°C.

Yeast slurry was incubated at 30°C for up 5 hours to ensure all fouling samples were of a similar mass and appearance and easier to handle at the time of testing on the cleaning rig, as described in Chapter 3. Up to 5 hours of aging is likely for type B deposit on the walls of fermenters, maturation vessels and in yeast slurry storage tanks prior to cleaning. The comparability of un-incubated (un-aged) and incubated (aged for 5 days) yeast slurry was assessed by micromanipulation, described in Chapter 3, Section 3.5. The pulling energy data is presented in Figure 4.7. This plot reveals similarities between un-incubated and incubated samples:

(i) A similar pulling energy to remove the samples from the surface is required.

(ii) A similar variability is seen at each cut height. The largest variability seen at 0 mm in for both samples.

The pulling energy presented in Figure 4.7 is greatest at a cut height of 0 mm suggesting yeast slurry is adhesive rather than cohesive. This measurement however also has the largest variability

as mentioned. Yeast slurry and yeast slurry incubated at 30°C for 5 h have been shown here to be comparable. Rinsing times of yeast slurry from coupons and pipes could also be scalable.
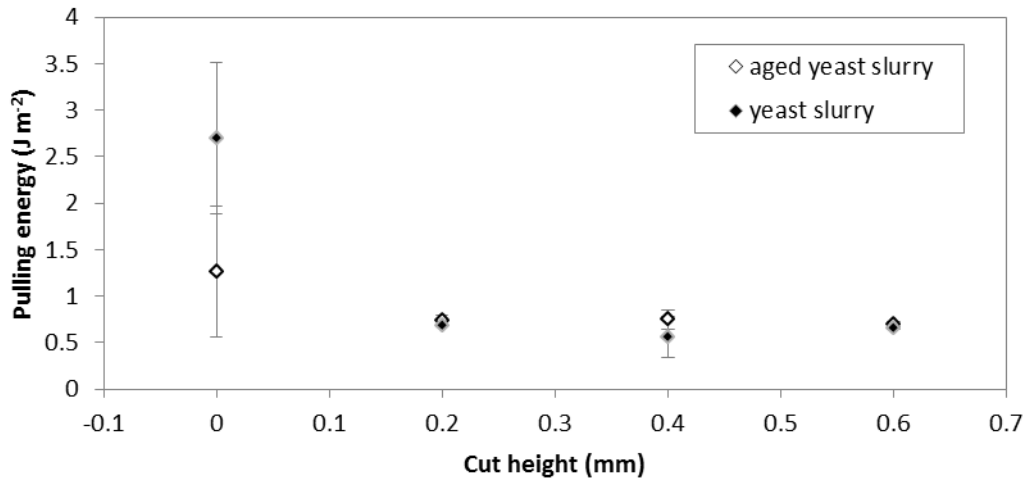
Figure 4.7: Yeast slurry micromanipulation measurements at 0, 0.2, 0.4 and 0.6 mm vs. Pulling energy. Aged yeast slurry was incubated for 5 h at 30°C.

4.4 Yeast slurry removal from stainless steel coupons

A visually clean surface was achieved during water rinsing experiments in all cases. Figure 4.8 gives a selection of images from the series taken during experiments at 0.5 m s^{-1} at four temperatures: (a) 20, (b) 30, (c) 50 and (d) 70°C. The yeast slurry is beige in colour and the coupon is grey.
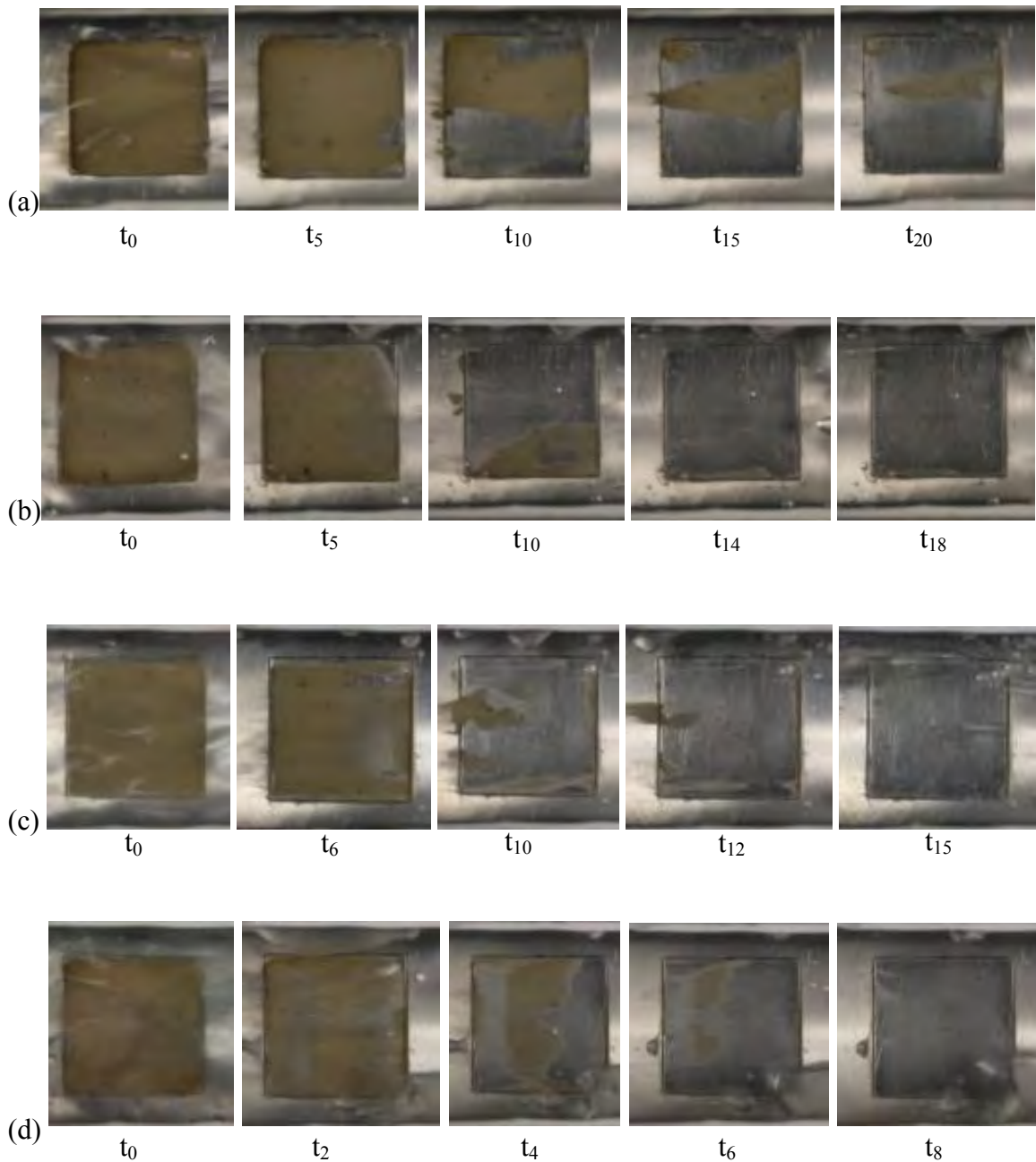
Figure 4.8: Images taken during yeast slurry removal at 0.5 m s^{-1} at (a) 20 (b) 30 (c) 50 and (d) 70°C.

Examples of the area and U profiles from water rinsing yeast slurry from the same experiments are presented in Figure 4.9 (a) – (d). The flow velocity was 0.5 m s^{-1} at four temperatures: 20, 30, 50 and 70°C. This gave a wetting rate of 9.2 l min^{-1} m^{-2}.

Three phases that could be identified:

 (i)   lag phase - where no deposit is removed,

 (ii)   removal phase - where deposit is removed from the surface, and

(iii)   constant phase - where all deposit that is going to be removed has been removed from the

         surface.
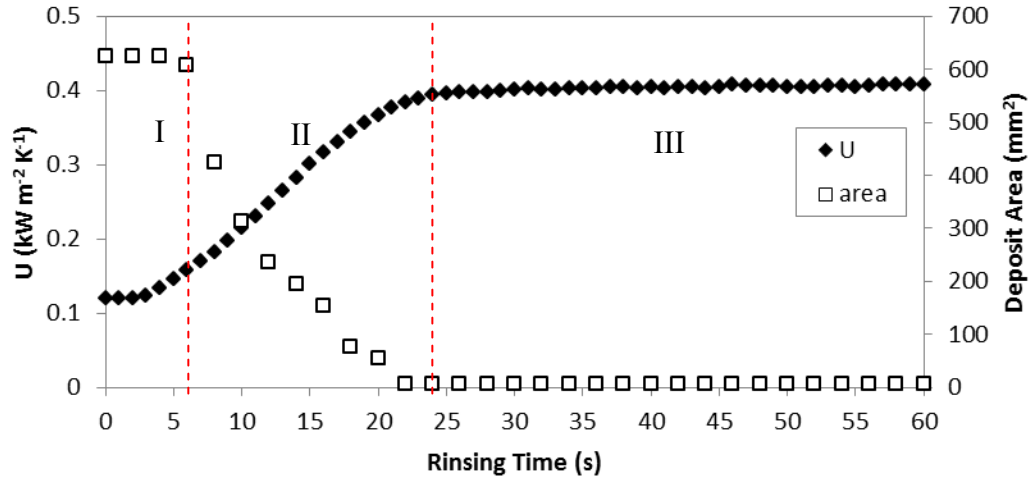
(a)
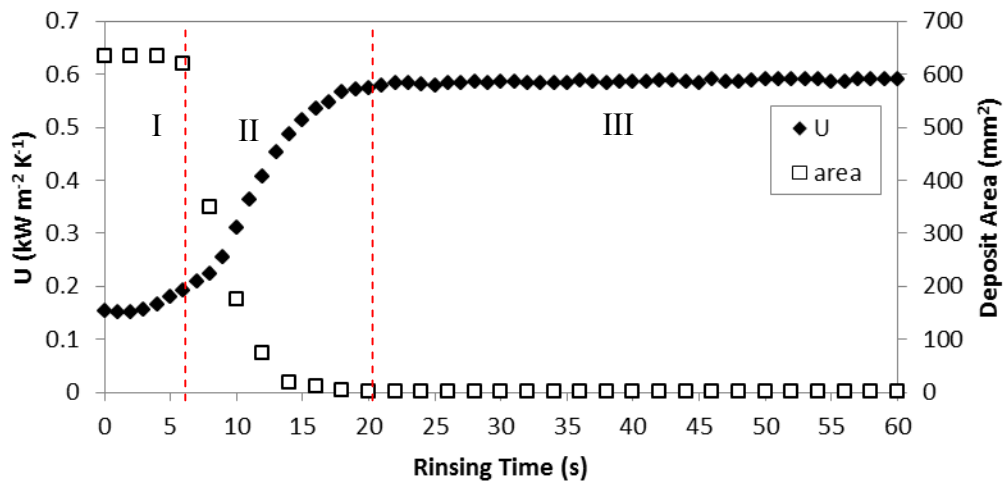
(b)
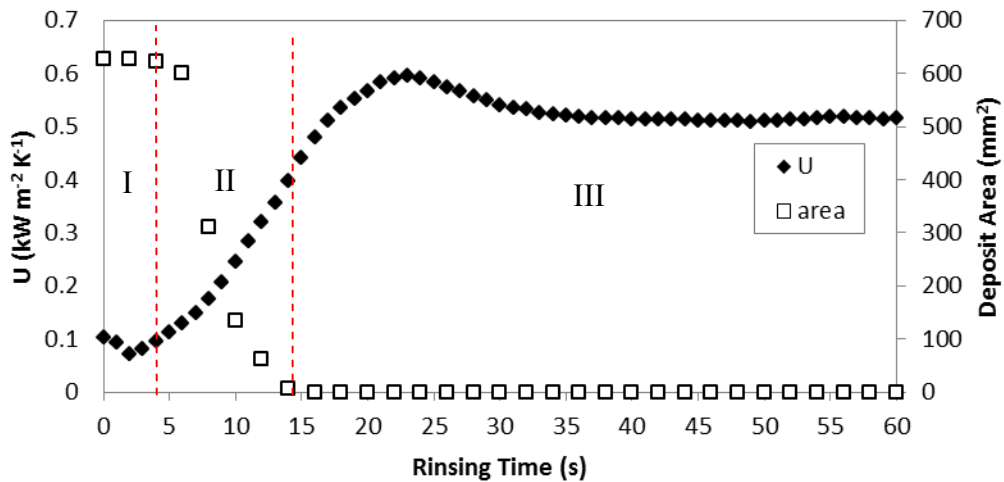
(c)

Figure 4.9: U and deposit area profiles for yeast slurry removed at 0.5 m s^{-1} and (a) 20 (b) 30 (c) 50 and (d) 70°C. Visually determined cleaning time is represented by the dashed line.
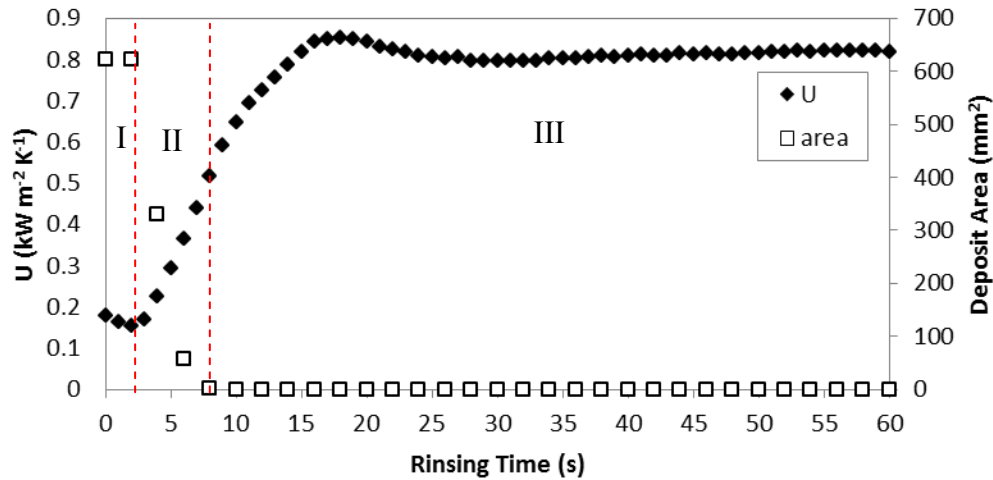
(d)

Figure 4.9 continued: U and deposit area profiles for yeast slurry removed at 0.5 m s^{-1} and (a) 20 (b) 30 (c) 50 and (d) 70°C. Visually determined cleaning time is represented by the dashed line.

The phases are separated by the dashed lines illustrated in Figure 4.9 and the length of these phases is discussed in the following Sections. In all cases the area decreased with rinsing time to 0, indicating the coupon was clean. U increased with rinsing time until the value became constant, indicating that all deposit (that can be removed at these cleaning conditions) has been removed. It can be seen from Figure 4.9 (c) and (d), when rinsing at higher temperatures, 50 and 70°C; the time area become 0 and U becomes constant is different. Cleaning times based on U may overestimate the cleaning time as the onset of the constant phase of U occurs after the point of visually clean. Observation of deposit removal revealed deposit fracture and removal in "chunks" and dissolution in the flow. This supports the micromanipulation finding that yeast slurry aged up to 5 h is adhesive.

4.4.1 Average area profiles and visual cleaning time

Average removal profiles of 4 experiments were plotted to determine average removal behaviour. The average area profiles of yeast slurry removed at 0.26, 0.4 and 0.5 m s^{-1} (4.8, 7.4 and 9.2 l min^{-1} m^{-2} respectively) are illustrated in Figure 4.10 (a) – (d). Dashed lines indicate the lag phase time at each velocity.
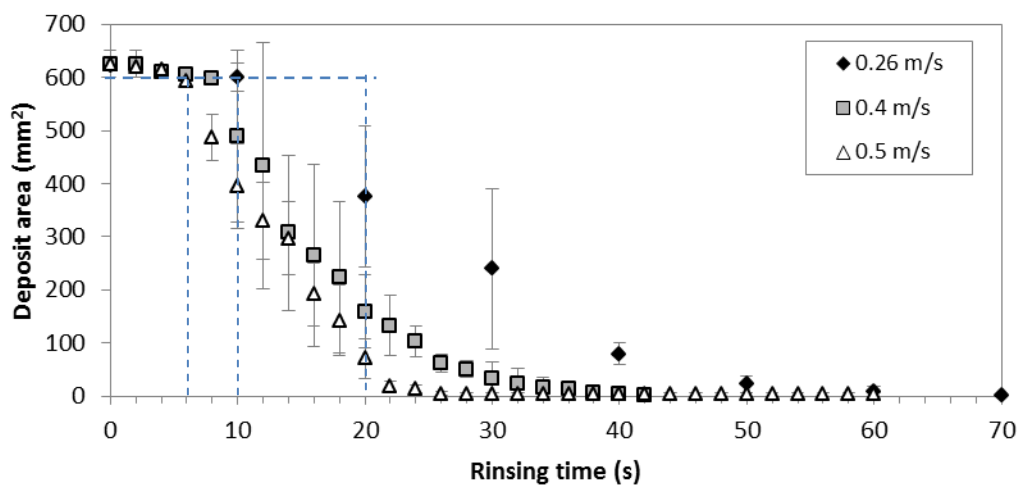
(a)
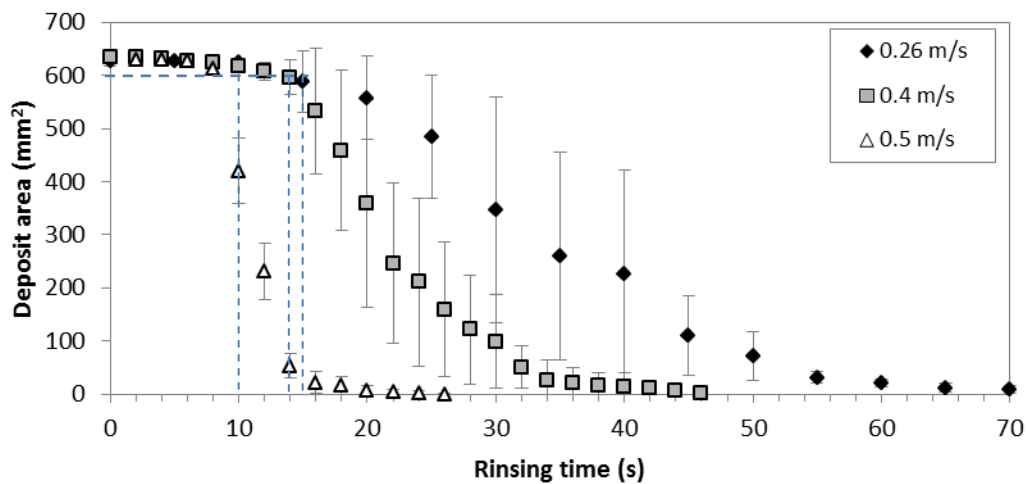
(b)

Figure 4.10: Average area removal profiles of yeast slurry (incubated for 5 h at 30°C) at (a) 20, (b) 30, (c) 50 and (d) 70°C.
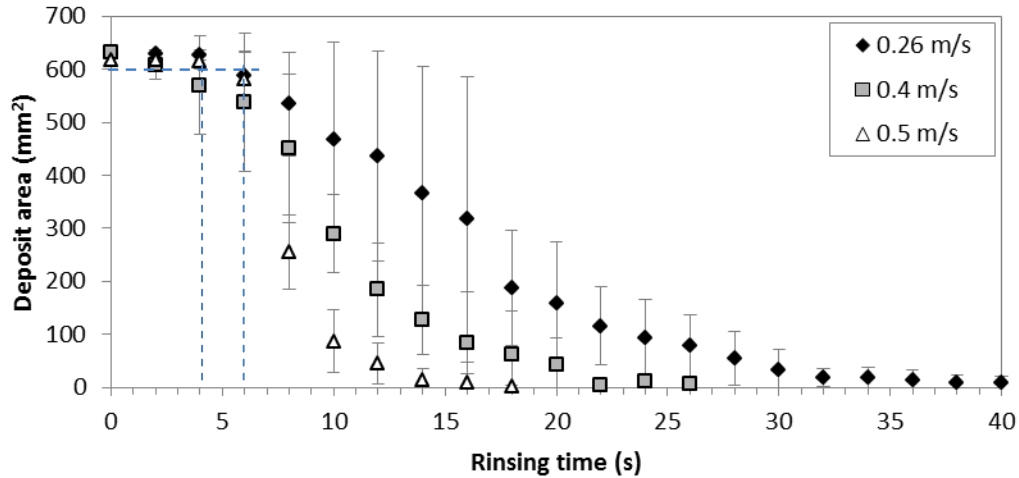
(c)
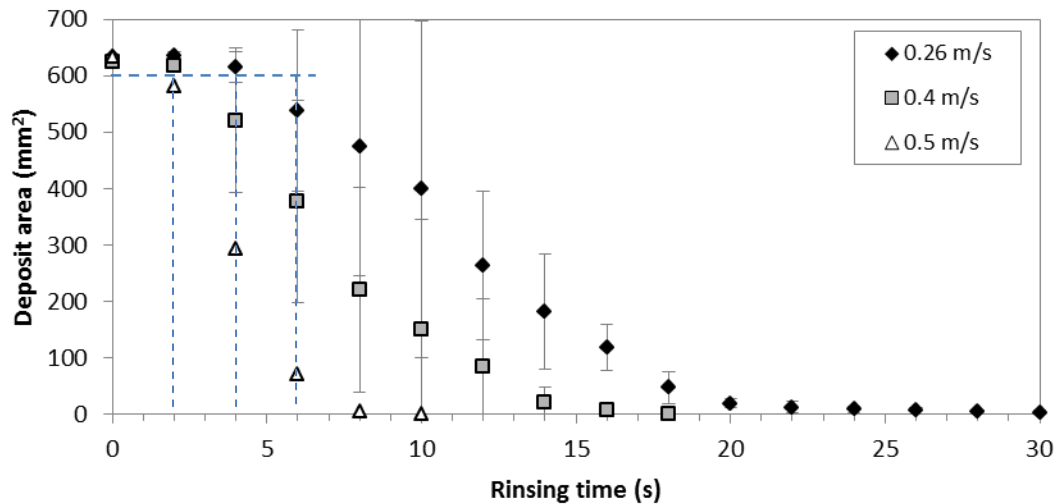
(d)

Figure 4.10 continued: Average area removal profiles of yeast slurry (incubated for 5 h at 30°C) at (a) 20, (b) 30, (c) 50 and (d) 70°C.

Figure 4.10 shows:

(i)   At 20 and 30°C the area profiles have a similar shape. The area profiles at 30°C have a longer lag, phase (i) than at 20°C unless the flow velocity was increased to 0.5 m s^{-1}.

(ii)   Area profiles at 50 and 70°C have a similar shape. The lag phase is shorter than at 20 and 30°C, the shortest being at 70°C lasting 2 – 3 s.

(iii)   At 20°C rinsing at 0.26 m s^{-1} is significantly different from rinsing at 0.4 and 0.5 m s^{-1}.

(iv)   At 30°C each area profile at 0.26, 0.4 and 0.5 m s^{-1} is significantly different after the

soaking period.

(v)   At 50 and 70°C rinsing at 0.5 m s^{-1} is significantly different from rinsing at 0.25 and 0.4

m s^{-1}.

4.4.2 Visual cleaning time

Figure 4.11 illustrates time to remove yeast slurry from stainless steel coupons determined from

images by eye vs. (a) flow velocity, (b) wall shear stress, and (c) Re. The data presented in Figure

4.11 is accurate ± 2 - 10 s at 0.26 m s^{-1} (depending on the temperature) and ± 2 s at 0.4 and 0.5 m

s^{-1}. The data presented in Figure 4.11 shows:

(a)   Increasing the flow velocity, thus increasing wetting rate per m^2, decreases cleaning time

and standard deviation at all temperatures. The cleaning times are most similar at the

highest flow velocity. On average there appears to be a significant effect of temperature at

low flow velocity; increasing the temperature to 70°C significantly decreases cleaning

time compared to rinsing at 20°C at 0.26 m s^{-1}. The difference in cleaning time becomes

insignificant as the flow velocity is increased. Increasing the temperature at higher flow

velocity (0.5 m s^{-1}) only decreases cleaning time by a second or two.

(b)   The plot of cleaning time vs. τ_w (wall shear stress) reveals temperature has a significant

effect on the cleaning time. Both an increase in temperature and an increase in τ_w decrease

the cleaning time.

(c)   The plot of cleaning time vs. Re reveals that data overlap for temperatures 30, 50 and

70°C. Data at 20°C does not overlap, it is significantly different.

(a)

(b)

(c)
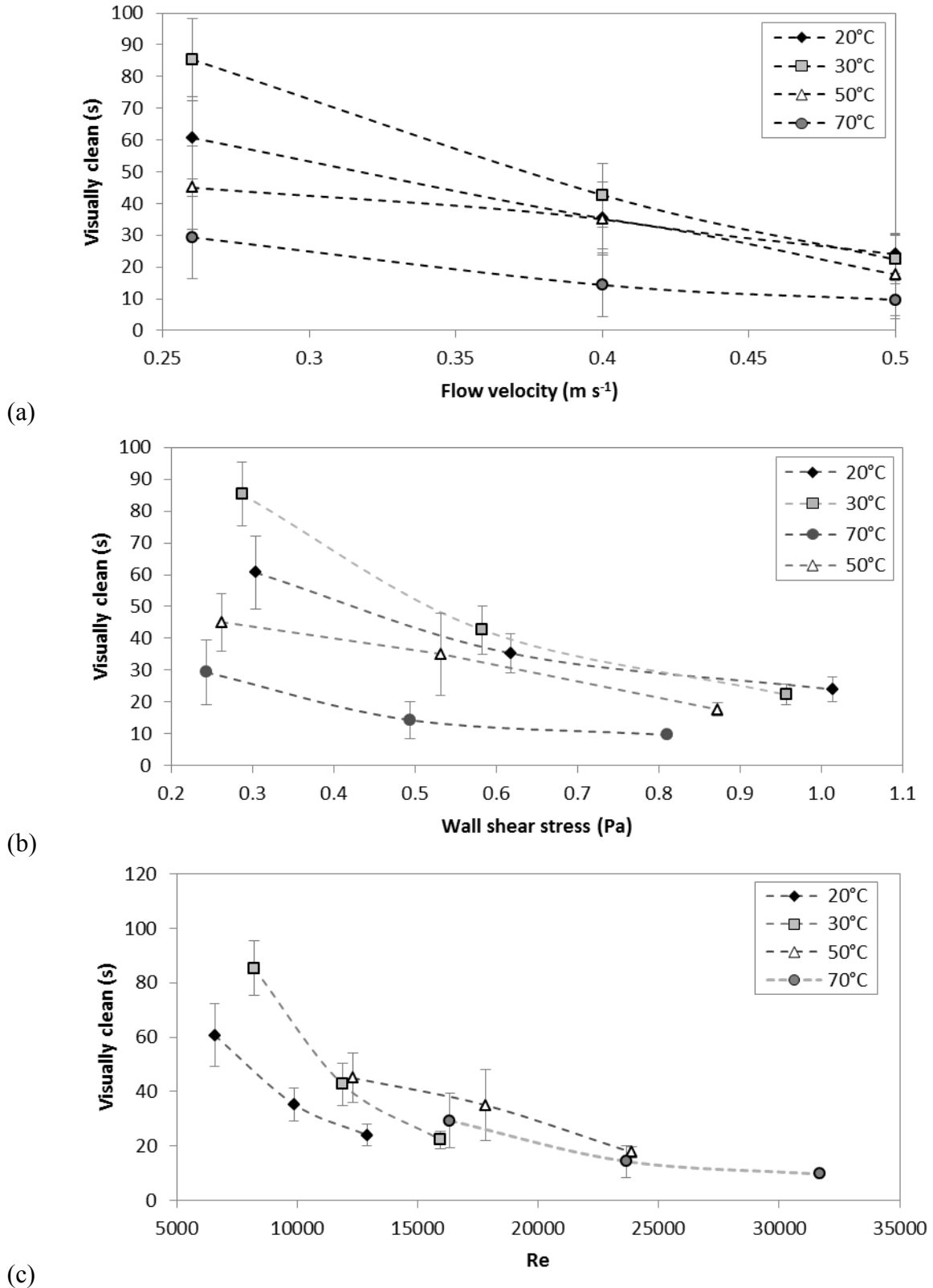
Figure 4.11: Visually determined cleaning time vs. (a) flow velocity, (b) τ_w and (c) Re at 20, 30, 50 and 70°C. Each data point is averaged from 4 experiments and the standard deviation plotted as error bars.

A hypothesis can be generated: At lower flow velocities, 0.26 m s^{-1} and higher temperatures i.e. 70°C, water will penetrate the yeast deposit enabling rapid hydration. The hydrated deposit will be removed more easily by lower fluid shear forces than the drier deposit. Increasing the temperature at low flow rate appears beneficial here. The data indicates that rinsing at faster flow rates or wall shear stress achieve a visually clean surface in the quickest time irrespective of temperature. Thus beyond a certain flow rate hydration occurs to a much lesser extent and shear force acts on the deposit rather than hydration. A flow velocity of 0.5 m s^{-1} is equivalent to τ_w of 1 and 0.8 Pa at 20 and 70°C respectively. τ_w achieved on a tank wall using a static spray ball in a tank can be between 1 and 4 Pa depending on the vessel diameter and water pressure (Alfa Laval personal communication, 2010). Data here suggests yeast slurry can be removed from the wall of a vessel using τ_w less than 1 Pa. The flow rate into the spray ball could be reduced to save water as long as the spray fully covers the tank interior.

Phase I and II of yeast slurry cleaning from coupons (identified in Figure 4.9) was determined from the area data. Area > 600 mm^2 was chosen to signify phase I. Visual assessment of the images agrees with this quantification. An area of 0 mm^2 signifies the end of the removal phase. Thus the time taken to reach 0 mm^2 minus the time area > 600 mm^2 is indicative of phase II on yeast slurry cleaning. The effect of temperature and flow velocity on (a) the lag and (b) removal phase times is presented in Figure 4.12.
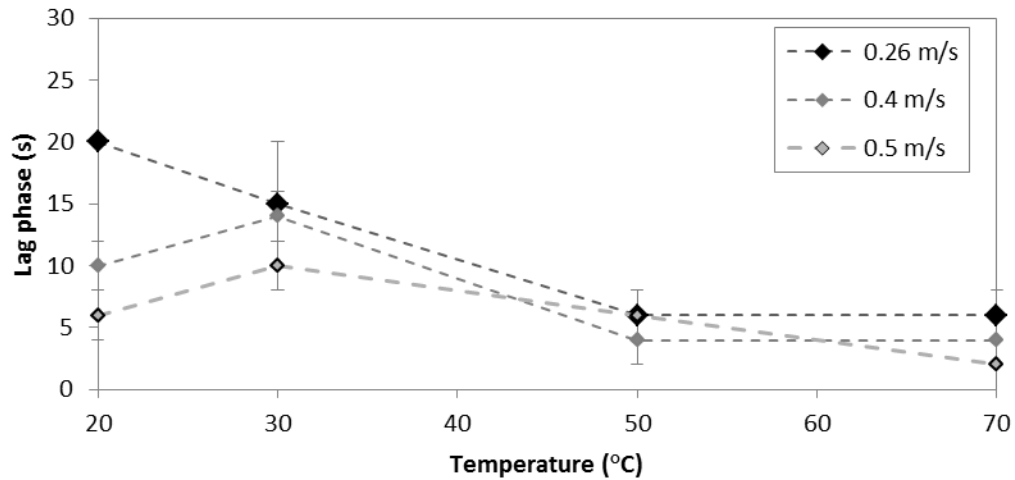
(a)
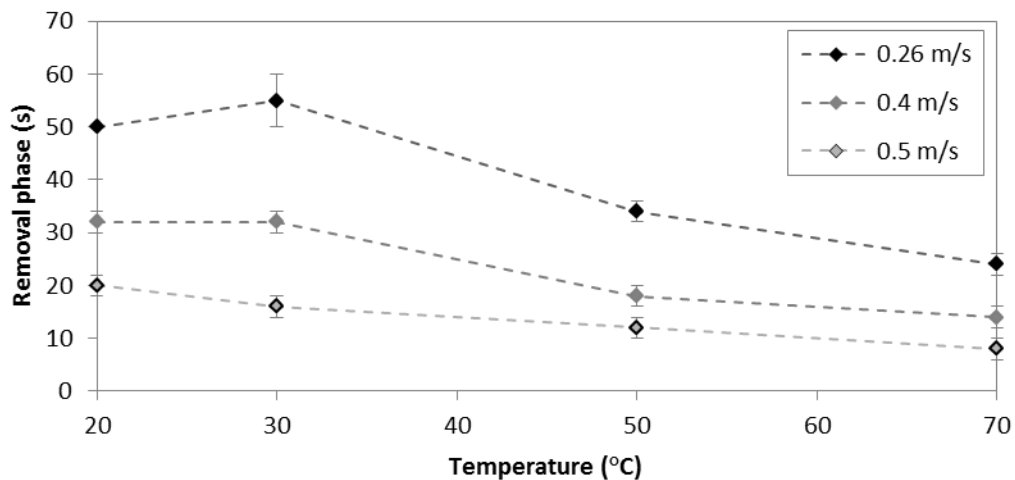
(b)

Figure 4.12: Duration of the (a) lag phase, (b) removal phase vs. Temperature at 0.26, 0.4 and 0.5 m s^{-1}. Each data point is averaged from 4 experiments and the standard deviation plotted as error bars.

There is no significant effect of flow velocity on lag phase time at each temperature except at lower temperature (20°C) where there is a significant difference in time between 0.26 and 0.5 m s^{-1}, 20 and 6 s respectively. An increase in temperature to 50 or 70°C decreases the lag phase time to less than 10 s, however this effect can also be achieved by increasing the flow velocity to 0.5 m s^{-1} at 20°C.

The removal phase time presented in Figure 4.12 (b) demonstrates an increase in flow velocity at each temperature significantly decreases the cleaning time. This was also true for reducing the duration of the removal phase at the test temperatures. Rinsing at the highest flow velocity, 0.5 m s^{-1}, gave the shortest and most similar removal phase times irrespective of the temperature. Generally an increase in temperature decreased the duration of the lag phase most significantly and an increase in flow velocity decreased the duration of the removal phase most significantly.

4.4.3 Cleaning phases and time determined by plotting Rd and U

Average R_d, deposit resistance, profiles were plotted to indicate overall cleaning measured by the MHFS. R_d is calculated from the heat transfer coefficient at time t (U_t) and the time when a clean surface is achieved (U_c) according to Equation 4.1.

$$R_d = \frac{1}{U_t} - \frac{1}{U_c}$$ [4.1]

Figure 4.13 illustrates average R_d values (from four repeats) vs. rinsing time at (a) 20 (b) 30 (c) 50 and (d) 70°C. The lag phase is not obvious from the plots, but is a maximum of only 20 s for this deposit at the lowest temperature and flow velocity, 20°C and 0.26 m s^{-1}. At 50 and 70°C at the higher flow velocities, R_d increases slightly and then decreases. In all plots zero time is determined as the point where water enters the test section and is accurate ± 5 - 10 s at 0.26 m s^{-1} (depending on the temperature) and ± 2 s at 0.4 and 0.5 m s^{-1}.

(a)

(b)

(c)
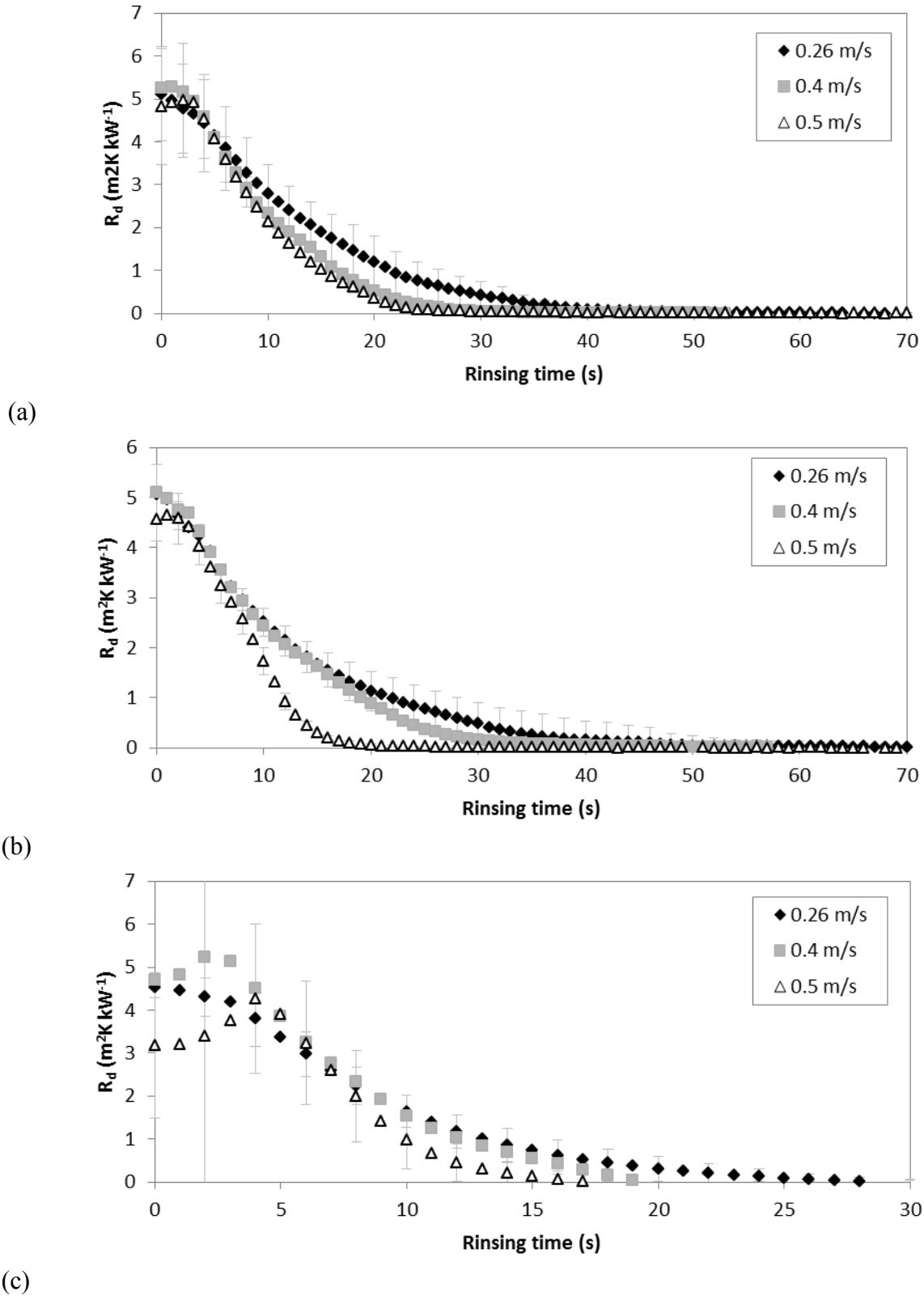
Figure 4.13: R_d vs rinsing time of yeast slurry deposit on coupons at (a) 20, (b) 30, (c) 50°C as a function of flow velocity. Each data point is averaged from 4 experiments and the standard deviation plotted as error bars.
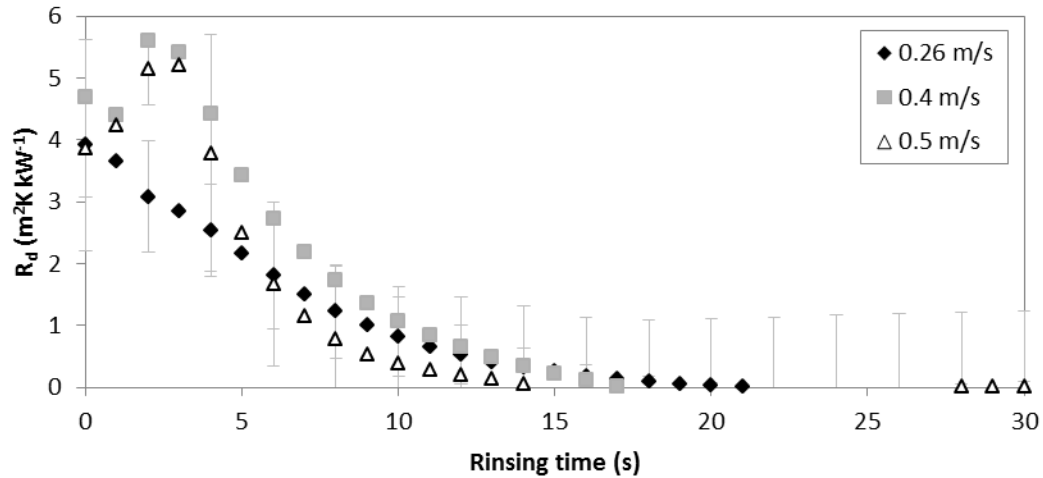
(d)

Figure 4.13 continued: R_d vs rinsing time of yeast slurry deposit on coupons at (d) 70°C as a function of flow velocity. Each data point is averaged from 4 experiments and the standard deviation plotted as error bars.

The values of U in equation 4.1 depend on Tc_2, MHFS voltage output and the average of Tc_4 and Tc_5 (T_{av}). Figure 4.14 reveals in the first 5 s, the value of T_{av} increases more rapidly than Tc_2 and the voltage output when rinsing at 0.5 m s^{-1} at 50 and 70°C. This causes smaller values of U in the first 5 s, which in turn gives larger values of R_d. The end of the removal phase is fairly obvious but was under-estimated from R_d values when compared to visual cleaning times.
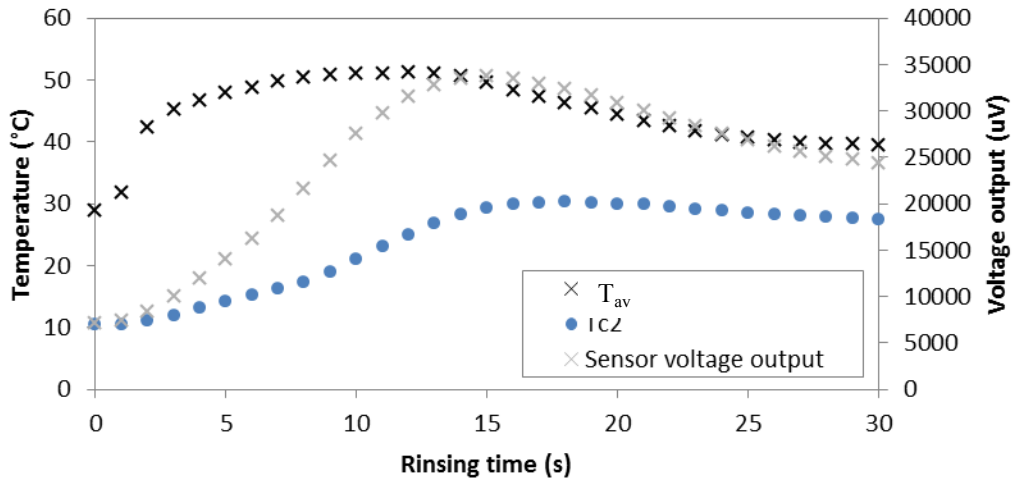
(a)
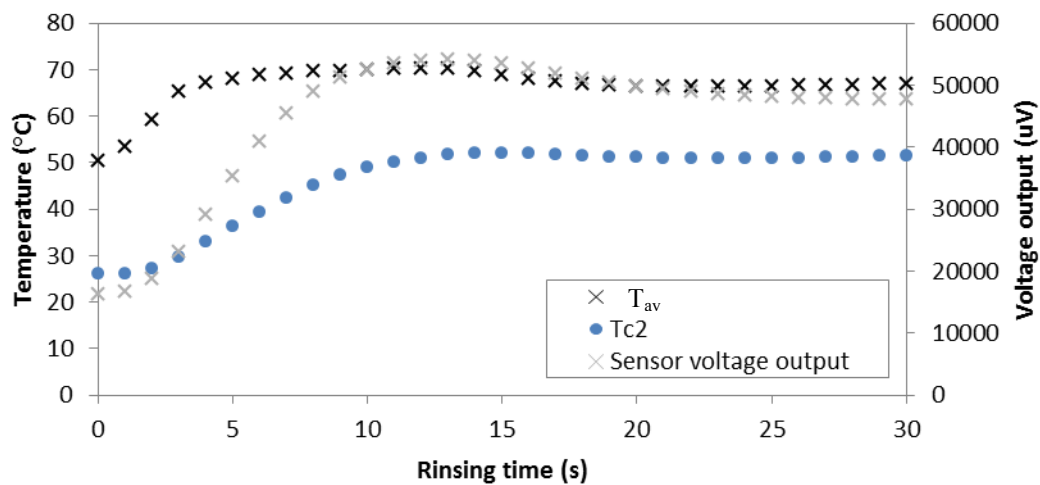
(b)

Figure 4.14: T_{av}, Tc_2, and sensor voltage output vs. rinsing time at (a) 50 and (b) 70°C.

The point of clean, U_c, was determined as the time when U was constant (for at least 3 minutes) minus 1 standard deviation. Figure 4.15 presents yeast slurry rinsing time (clean time), U_c vs. flow velocity.
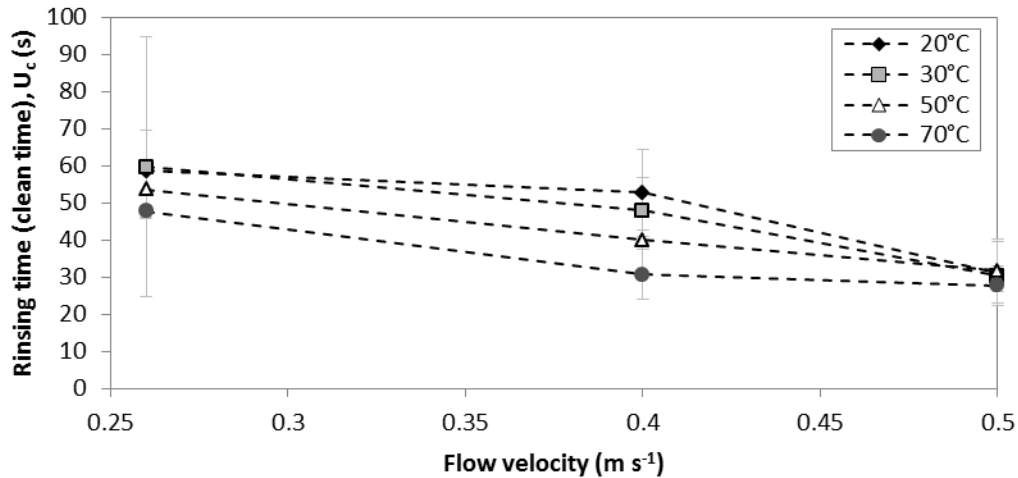
Figure 4.15: Cleaning time, U_c, of yeast slurry vs. rinsing time at 20, 30, 50 and 70°C.

From Figure 4.15 it is clear that:

(i) The same trend is seen in the data as for visual cleaning time: increasing flow velocity decreases cleaning time on average; although this trend is within the variation of the data.

(ii) When comparing the visual cleaning time (presented in Figure 4.11), at the lowest flow velocity, 0.26 m s^{-1}, U_c over estimates cleaning time at 70°C by 20 s and at 50°C by 10 s. U_c underestimates cleaning time at 30 and 50°C by 25 s at 30°C. At higher flow velocities, 0.4 and 0.5 m s^{-1}, U_c also over estimates cleaning time.

The method used to cool the block and copper stub may not have been given consistent cooling throughout cleaning experiments. This is because the spring and the hole housing the copper stub and MHFS (see Figure 3.4) could not be replenished with ice during any experiment.

4.5 Yeast slurry removal profiles from pipes

The fluid like nature of yeast slurry meant that it could be poured directly into test pipes for rinsing experiments. Pipe filling protocol is given in Appendix C.2.1. A visually clean sight point was achieved during all water rinsing experiments. Inspection of the pipes at this point in rinsing experiments also revealed a visually clean pipe. It was found in some instances that if the pipe became hot before filling, yeast slurry could stick to the pipe wall. To mitigate this, the pipe was always rinsed with cold water in between experiments.

The sight point was located at the outlet of the test pipe. In the cleaning rig this sight point was a silicone pipe, and in the pilot plant was a sight glass. Images taken during experiments are seen in Figure 4.16 and 4.17. A flow velocity of 0.5 m s^{-1} was used in the cleaning rig and 1 m s^{-1} in the pilot plant, both at 20°C. The yeast slurry is beige in colour.

From Figure 4.16 in the cleaning rig, it can be seen that water initially pushed some yeast slurry from the pipe and flowed over the top of the product. The sight point was then seen to be full of yeast slurry within 6 s of the onset of flow. At 8 s the water was visually turbid indicating yeast was still being rinsed from the pipe. This phase lasted approximately 16 s, at 24 s the sight point appeared clean.

Direction of flow
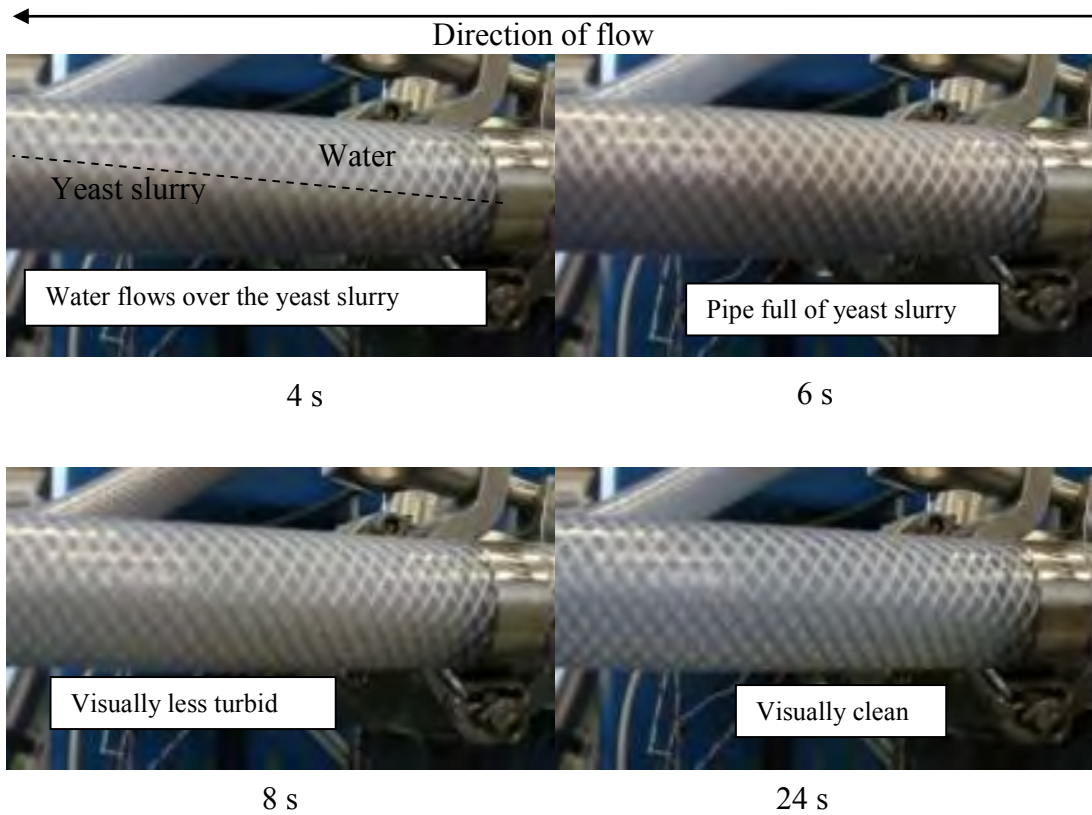
Figure 4.16: 1" outlet silicone pipe in the cleaning rig used as the sight point to determine visual cleaning times during yeast slurry rinsing experiments from 1 m pipe. This experiment was done at 0.5 m s^{-1} at 20°C (run 2 on Figure 4.18 (a)).

From Figure 4.17 in the pilot plant, it can be seen that the sight glass first appears turbid before the sight glass become full of yeast slurry. At 9 and 10 s the yeast slurry was also seen to smear across the sight glass in the direction of flow. This was not seen in the cleaning rig system. The sight glass was full of yeast at 12 s and appeared visually clean at 15 s. The different removal behaviour could be due to the flow velocity, the pipe diameter or the properties of silicone and glass.

Direction of flow

5 s	Visually more turbid 8 s	Yeast smearing the glass 9 s
Further smearing 10 s	Pipe full of yeast slurry 12 s	Visually clean 15 s
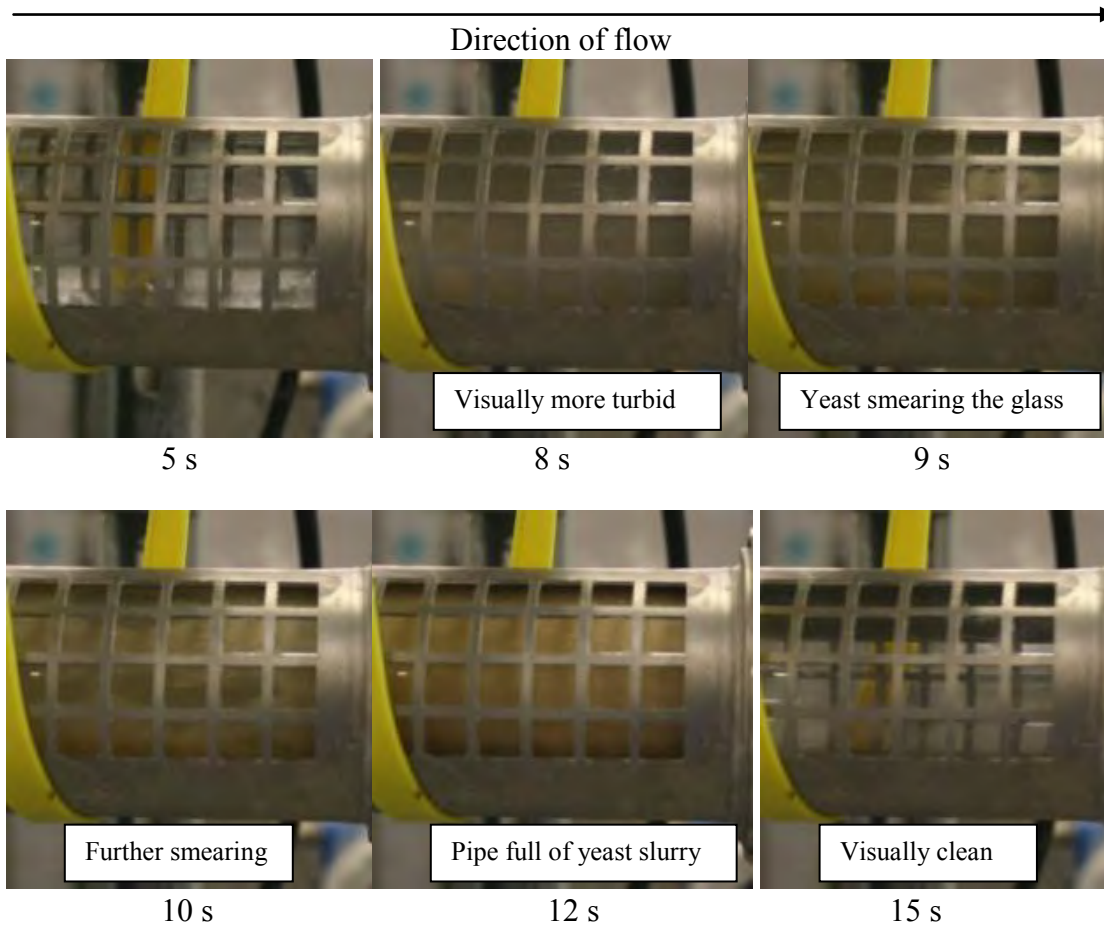
Figure 4.17: 2" outlet sight glass in the pilot plant used as the sight point to determine visual cleaning times during yeast slurry rinsing experiments from 1 m pipe. This experiment was done at 1 m s^{-1} at 20°C (run 4 on Figure 4.18 (b)).

The removal profile of yeast slurry from a 1 m stainless steel pipe is presented in Figure 4.18, which illustrates conductivity and turbidity data of three identical runs in (a) the cleaning rig and (b) the pilot plant. The flow velocity was 0.5 m s^{-1} in the cleaning rig and 1 m s^{-1} in the pilot plant and the temperature was 20°C. Conductivity from "run 1" is plotted in both (a) and (b).
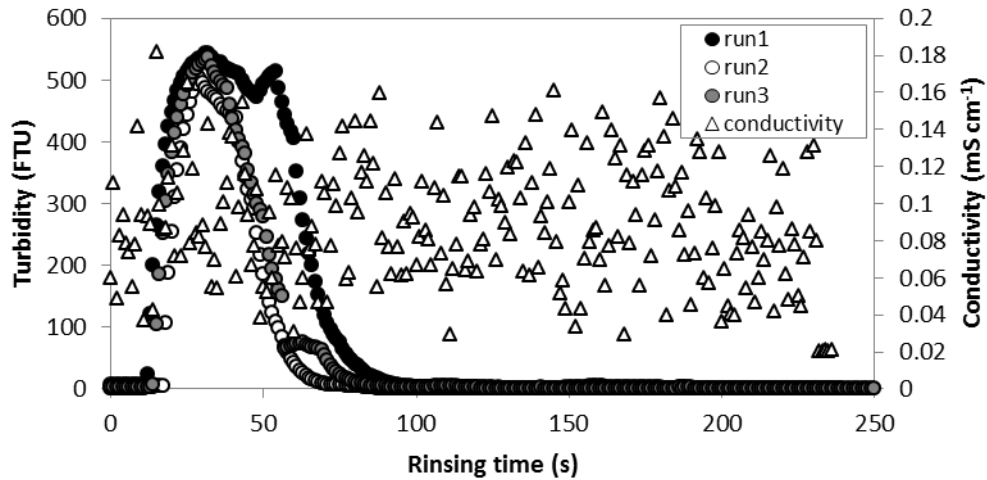
(a)
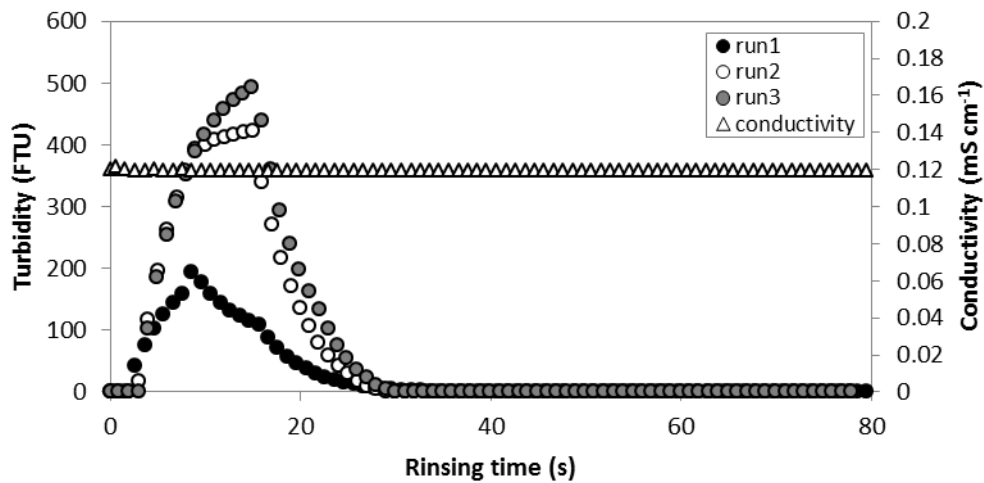
(b)

Figure 4.18: Rinsing of yeast slurry from a 1 m pipe at ambient in (a) the cleaning rig at 0.5 m s^{-1} and (b) the pilot plant at 1 m s^{-1}. Turbidity measured in three repeats is plotted and the conductivity measured in the 1st run is also plotted.

The conductivity data measured in the cleaning rig system also appears more variable than in the pilot plant system. It is clear from Figure 4.18 (b) that the volume and density of yeast washed away during the rinse did not have a measurable conductivity.

The turbidity data exceeded 16 and 80 FTU in the cleaning rig and pilot plant respectively, the base line for water, given in Section 4.2.2. The turbidity measured was attributed to yeast slurry removal. Visual cleaning times were determined at the sight point at the outlet of the pipe from the series of images taken during each experiment and are accurate ± 1 s. In all cases a visually clean pipe was achieved.

4.5.1 Determining removal time

The point at which the 1 m pipe was determined to be clean was taken at two points that could be compared; the time when,

(i) the sight point appeared visually clean (at the outlet of the test pipe) from the series of images taken during each experiment, accurate ± 1 s in most cases,

(ii) the turbidity probe (Kemtrak) was clean, determined as the time when FTU was constant (at least 3 minutes) minus 1 standard deviation, termed FTU_p, accurate ± 1 s.

Visual cleaning times determined at the sight point reported are accurate ± 1 - 5 s according to the image series time interval. The turbidity probe was positioned approximately 1 m and 2 m after the 1 m pipe in the cleaning rig and pilot plant respectively. Turbidity measured in FTU was found to increase with the onset of flow although the slurry had not yet reached the turbidity probe, therefore the rinsing times include a lag time prior to deposit rinsing. Conductivity data did not exceed 0.16 mS cm^{-1} for any experiment reported here. Therefore conductivity is not reported here.

4.5.2 Effect of flow and wall shear stress

The removal time of yeast slurry from the 1 m pipe at 20°C determined visually and as FTU_p is shown in Figure 4.19 with respect to (a) flow velocity and (b) wall shear stress (calculated from Equation 3.3).
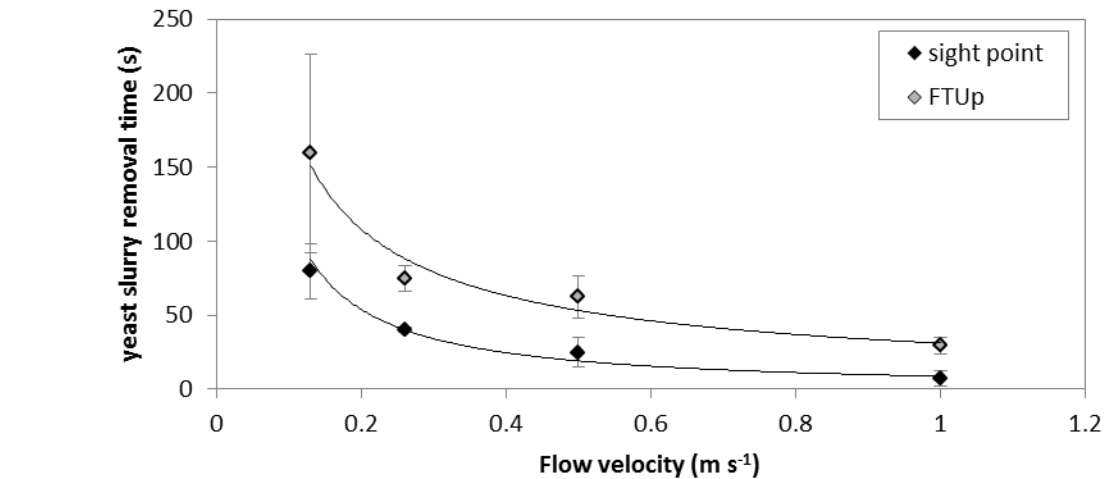
(a)
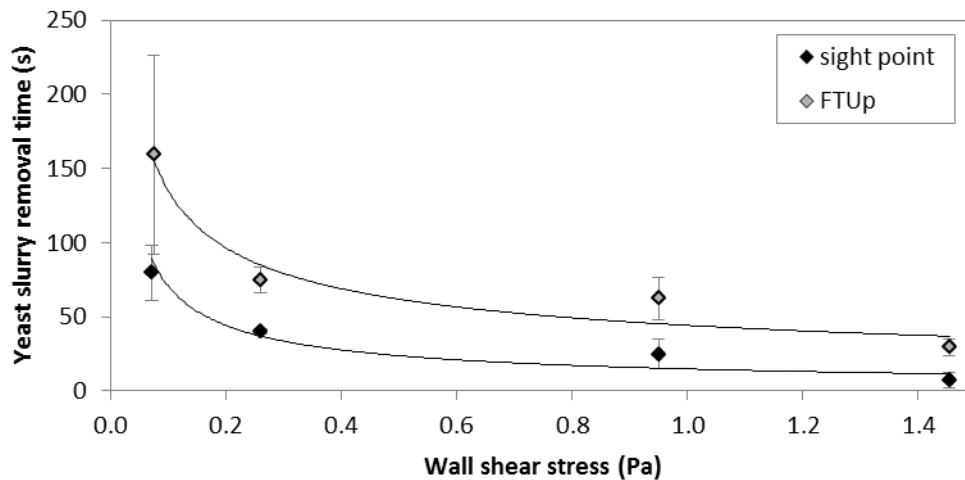
(b)

Figure 4.19: Time taken to remove yeast slurry from a 1 m pipe (sight point) and from the turbidity probe (FTUp) at 20°C vs. (a) flow velocity and (b) vs. wall shear stress.

The removal time of yeast slurry from the sight point (and thus the pipe) and the turbidity probe (FTU$_p$) vs. flow velocity appears to follow the same power law shaped curve with confidence, R^2

> 0.9; lower confidence with respect to wall shear stress > 0.84. As the flow velocity was increased the cleaning time decreased. It could be suggested that doubling the flow velocity halved the cleaning time. The time to clean the turbidity probe was significantly longer than the time to clean the pipe. This difference in time could be attributed to either (i) the time taken for water (rather than yeasty water) to pass the probe, or (ii) the cleaning time of the probe itself; yeast maybe fouling the probe during the experiments. Hence, if FTU_p was the time taken for water (rather than yeasty water) to pass the probe then the time difference between sight point and probe cleaning time and the time taken for the cleaning fluid to pass from the 1 m pipe to the turbidity probe would be the same. Figure 4.20 illustrates that the "time difference" i.e. the difference in time between cleaning the pipe (determined visually) and the turbidity probe (determined by the probe FTU reading), is greater than the time taken for water to flow from the pipe to probe: "lag time". This indicates FTU_p is a measure of cleaning the turbidity probe of residual yeast. The probe takes longer to clean than the pipe.
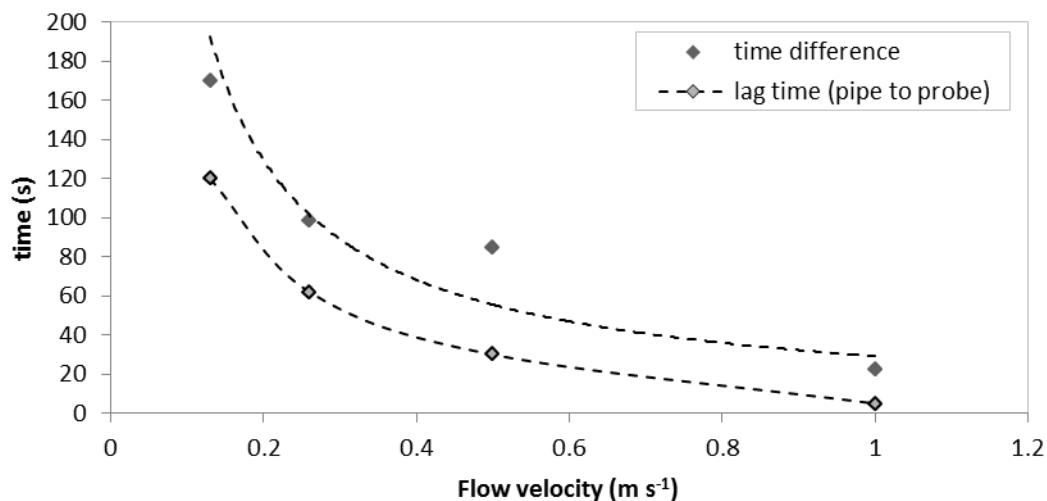
Figure 4.20: Time vs. flow velocity: The time difference between cleaning the pipe and the probe is plotted, and the lag time from the pipe to the probe is plotted.

4.5.4 Effect of temperature

The removal time of yeast slurry from the sight point and the turbidity probe at 20, 30, 50 and

70°C is shown in Figure 4.21 with respect to flow velocity.
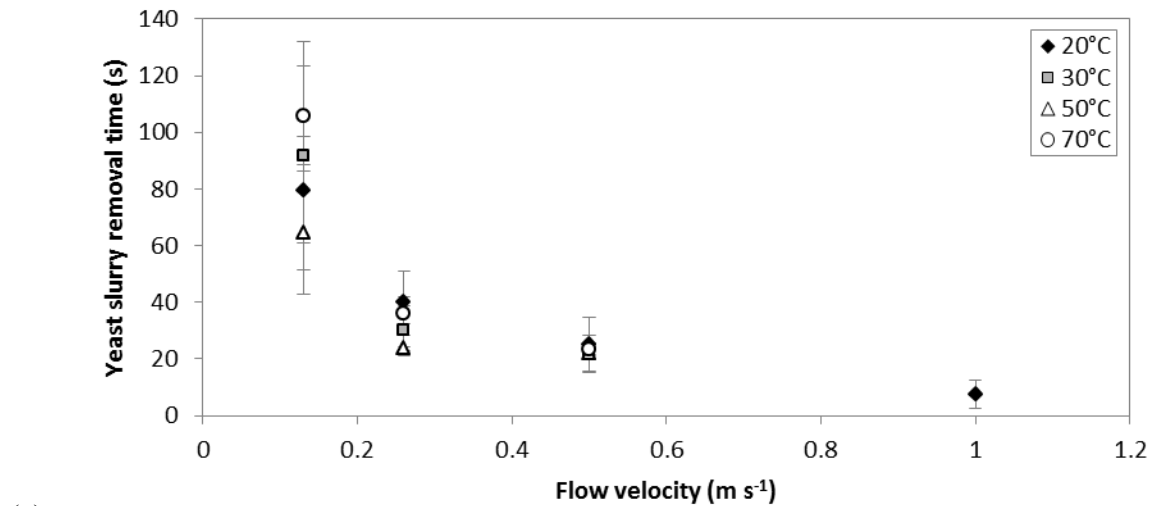
(a)
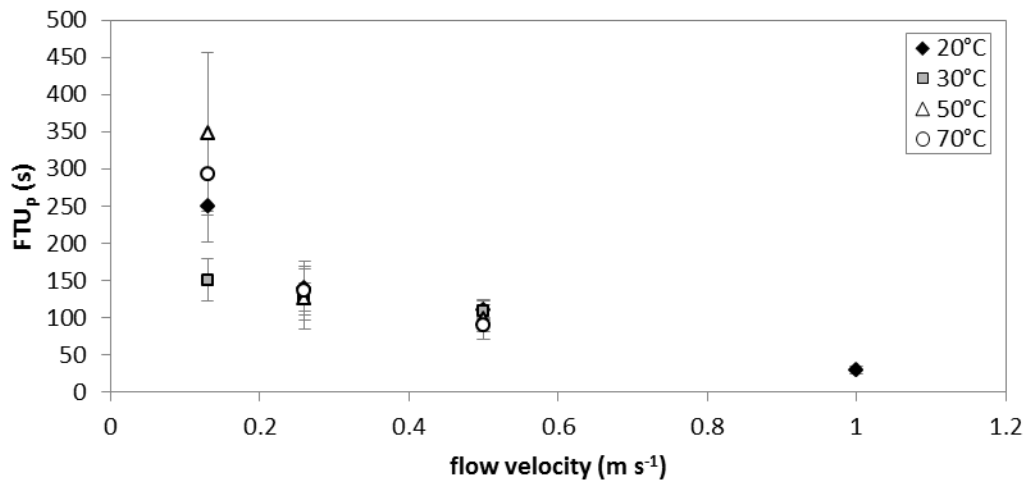
(b)

Figure 4.21: Time taken to remove the yeast slurry from (a) 1 m pipe and (b) probe (FTU_p) at 20, 30, 50, and 70°C with respect to flow velocity.

The temperature has no significant effect on the removal time of yeast from the sight point (thus

the pipe); thus the data correlates well with flow velocity at ambient temperature (see Figure 4.19

(a)). The trend seen for visual cleaning time is also seen for probe cleaning time. However at the lowest flow velocity, 0.13 m s^{-1}, there is a significant difference between rinsing at 30°C and other temperatures. This removal time was quickest. Rinsing a coupon of yeast in the cleaning rig at the lowest flow velocity, 0.26 m s^{-1}, the removal time was significantly slower than at other temperatures (see Figure 4.11 (a)). This is the opposite effect to that seen here at 30°C. Rinsing at 0.13 m s^{-1} was not investigated for coupon cleaning on the cleaning rig equipment. Figure 4.22 illustrates the visual cleaning times of the coupon and the pipe at 20, 30, 50 and 70°C at each flow velocity (0.13, 0.26 and 0.5 m s^{-1}). There appears to be a relationship between coupon and pipe cleaning times, $R^2 > 0.95$ in all cases.
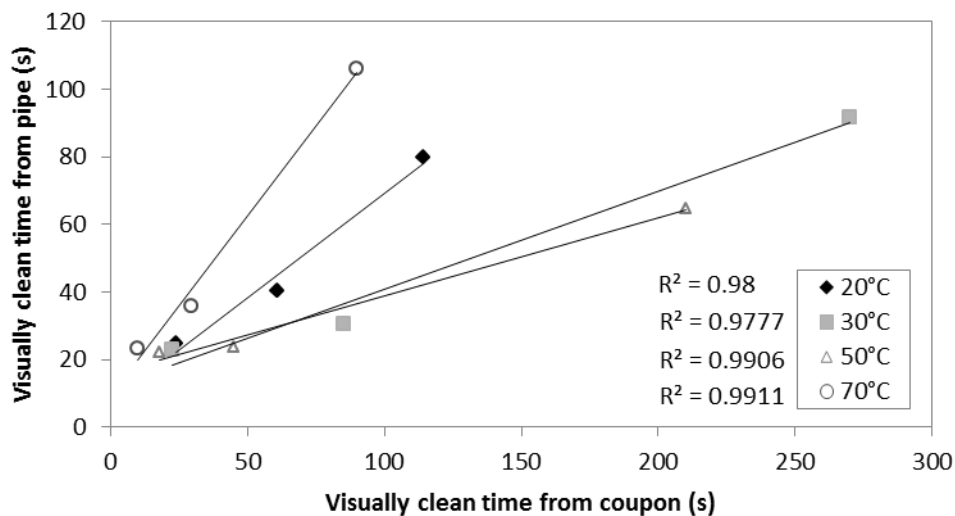
Figure 4.22: visual cleaning times of yeast slurry from the coupon vs. visual cleaning times of yeast slurry from 1 m pipe.

4.5.5 Effect of Re

Figure 4.23 (a) reveals the relationship between removal time from the pipe and probe vs. Re (irrespective of temperature). There appears to be a correlation between Re and removal time however the R^2 value was less than the correlation between flow velocity and cleaning time for

both pipe and probe cleaning; 0.68 and 0.56 respectively. The outliers on the probe cleaning plot are the lowest flow velocity, 0.13 m s^{-1} and highest temperature, 50 and 70°C. The outlier on the visually clean plot is also the lowest flow velocity and the highest temperature. At low flow rate and high temperature the yeast removal time is actually slower than other experiments. Removing these outliers and re-plotting in 4.23 (b) reveals a better data fit.
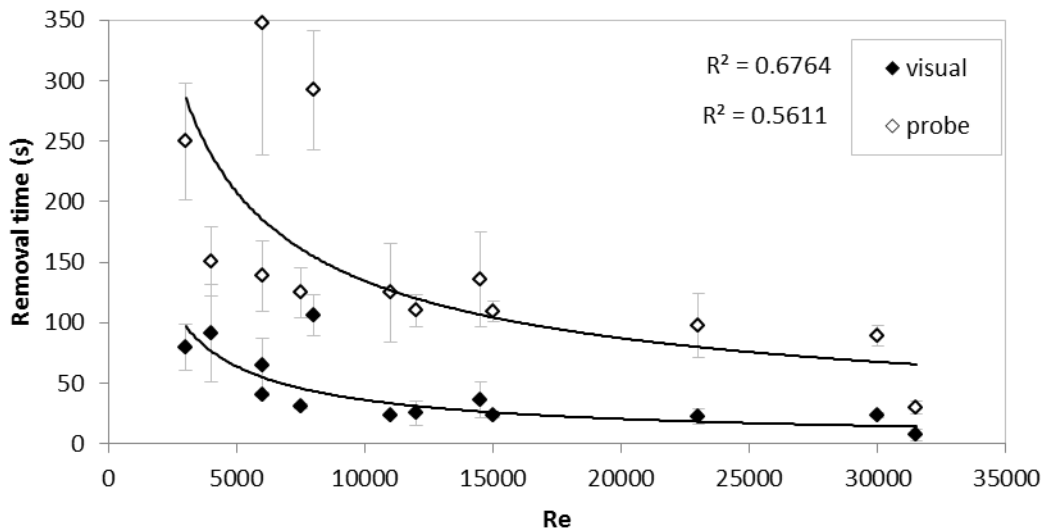
(a)
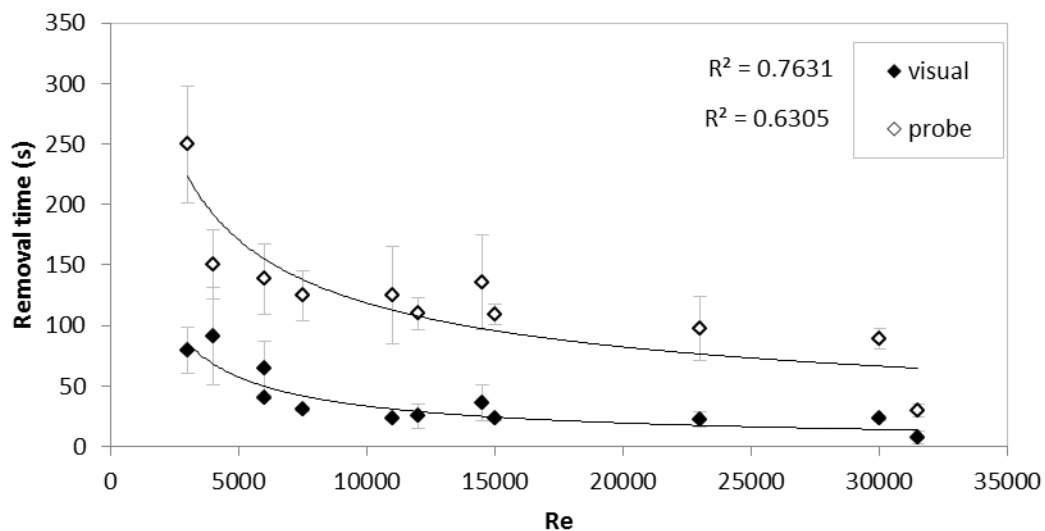
(b)

Figure 4.23: (a) Removal time for pipe and probe vs. Re. (b) re-plot of Figure 4.23 (a) without outliers.

4.6 Relating coupon and pipe cleaning times

Cleaning times of coupons, the pipe, and the turbidity probe were found not to be significantly affected by temperature. As such all cleaning times could be plotted as a function of Re. Figure 4.24 illustrates the trend. As the Re is increased the cleaning time decreases in all cases. Pipe cleaning times appear to be 4 times greater than coupon cleaning times. Probe cleaning times are more variable.
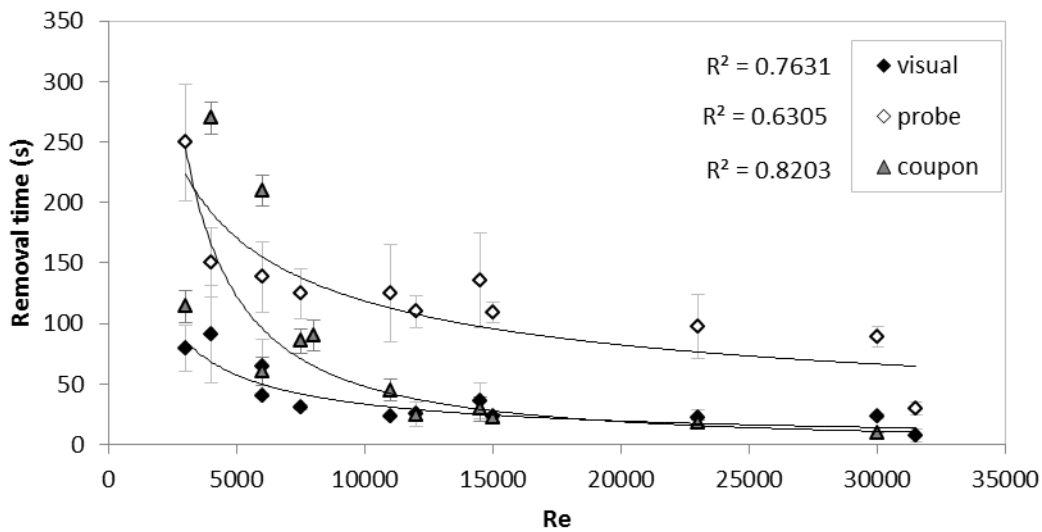
Figure 4.24: Removal time for the pipe, probe and coupon vs. Re

4.7 Conclusions

This Chapter show that yeast slurry from the brewery un-incubated and incubated for up to 5 hours clean comparably from coupons and from pipes. The results presented here reveal at all flow velocities and temperatures tested that yeast slurry was removed to give a visually clean surface using water. As such yeast slurry can be classified as a Type 1 soil according to Fryer and

Asteriadou (2009) when in pipes, and on stainless steel coupons. The visual cleaning times of the pipe and coupon also appear the same at 0.5 m s^{-1}.

Micromanipulation data suggested yeast slurry was adhesive. This was supported by visual observation of chunks of yeast slurry of deposit being removed from the coupon and smearing of the sight glass. Three distinct phases were identified during yeast slurry removal from coupons; (i) a lag phase, (ii) a removal phase, (iii) constant phase. The lag and removal phases determine the total cleaning time. An increase in temperature appeared to decrease lag phase time most significantly. However as this phase represented no more than 14 % of the total cleaning time the effect of temperature was not significant in overall cleaning time. As such cleaning of this deposit appears to be minimally affected by temperature; more so as the flow velocity was increased. As the flow velocity was increased the cleaning time decreased according to the power law model overall.

Yeast slurry was characterised as shear thinning and time independent over 600 s. Thus viscosity decreased with increasing shear. The cleaning times suggests the same trend, whereby as the wall shear stress increases the cleaning time decreases. At higher flow rates the deposit is simply forced out of the pipe quicker and the flow velocity can overcome the adhesive force of the yeast slurry so that no yeast film remains on the inner pipe surface.

To remove yeast slurry from storage tanks and transfer lines in breweries, a CIP regime consisting of a cold water rinse, hot alkaline detergent phase, and chemical sterilisation is supplied at 1.5 m s^{-1} through a spray ball. The data suggests that the yeast can be removed from

the system at flow velocities less than 1.5 m s^{-1} (this is most likely because the Re in both the cleaning rig and pilot plant system is > 3000). Increasing the flow velocity removed the yeast more quickly. If all yeast is removed by water rinsing as suggested here, the alkaline detergent phase could be omitted from the CIP regime in the plant. The surfaces would be sanitised by acid based chemical or heat after the water rinsing step. Rinsing the yeast using hot water (60 – 70°C) may have the dual effect of removing the yeast while sanitising at the same time. The cleaning time could be further reduced. The annual cost of cleaning yeast storage tanks at the Brewery is approximately £8 K (see Appendix A Section A.2.10). Omitting the detergent phase would save 71 % of this cost and significantly reduce the environmental impact associated with caustic generation and use. Current use of sanitiser is already included in this cost.

Yeast removal from pipes was well represented using turbidity measurement (if flow rate sufficient) and showed the cleaning time of the whole system adequately. Breweries often have turbidity meters in yeast process lines already. Turbidity measurements can potentially be used to measure soil loading of the cleaning fluid and soil removal during CIP of yeast type deposits.

The use of a heat flux sensor to determine the removal time of yeast slurry from coupons proved problematic as removal of the yeast slurry was very fast. At temperatures greater than ambient a cooling system that ensures consistent temperature differential is required to improve measurement with the heat flux sensor. If this technology was to be applied onto a plant, the position of the MHFS in the system must represent the cleanliness of the whole system, which is difficult to do and even to measure offline.

CHAPTER 5: CLEANING OF TYPE 2 DEPOSIT, AGED YEAST SLURRY

5.1 Chapter Introduction

The aim of this Chapter is to report the cleaning behaviour of a type 2 soil, aged yeast slurry, from coupons when rinsed with water and a sodium hydroxide based cleaning chemical. This Chapter reports the removal behaviour of aged yeast slurry from stainless steel coupons in the cleaning rig system. This deposit was found to mimic brewery fermenter fouling (see Chapter 3, Section 3.7), termed type A yeast deposit because chemical action is required to fully remove it in industry. Preliminary cleaning studies of the deposit from coupons in the cleaning rig system revealed around 80 % of the deposit area could be removed with water. The remaining 20 % required chemical action. The need for chemical action is illustrated in Figure 5.1. A selection of images from the series taken during experiments is given in Figure 5.1 using water at 0.5 m s^{-1} (a) 20°C and (b) 70°C and using 0.2% Advantis 210 at (c) 20°C and (d) 70°C, and 2% Advantis 210 at (e) 20°C and (f) 70°C. The yeast deposit is coloured black and the coupon is grey. This defines the type A yeast deposit as a type 2 deposit by the criteria proposed by Fryer and Asteriadou (2009). The current CIP regime for fermentation and maturation tanks involves a pre-rinse, hot caustic circulation, intermediate rinse and sanitiser circulation. A CIP regime enhancing the

effect of the water phase would reduce chemical, energy and effluent BOD and COD from this CIP process.

The effect of flow, wall shear stress, temperature and chemical concentration on the removal time of aged yeast slurry is presented here. Removal was investigated at 0.26, 0.4 and 0.5 m s^{-1} (4.8, 7.4 and 9.2 l min^{-1} m^{-2} respectively) and temperatures of 20, 30, 50, 70°C using water and Advantis 210 concentrations of 0.2 and 2 (wt%). There are at least three repeats for all data sets presented. The cleaning behaviour was quantified from deposit area measurement and compared to U data (the heat transfer coefficient). The ability of U to trend deposit removal is reported and the limitations discussed. A microbiologically clean surface was not quantified for two reasons:

1. Industrial CIP is followed by a sanitisation step, after which the cleanliness of the surface is determined by microbe enumeration from rinse samples and surface swabs.
2. The yeast on the surface was not alive at the time of cleaning.

The use of Advantis 210 at both 0.2 and 2 wt % was found to remove all deposit from the coupon to give a visually clean surface at all temperatures and flow velocities presented.
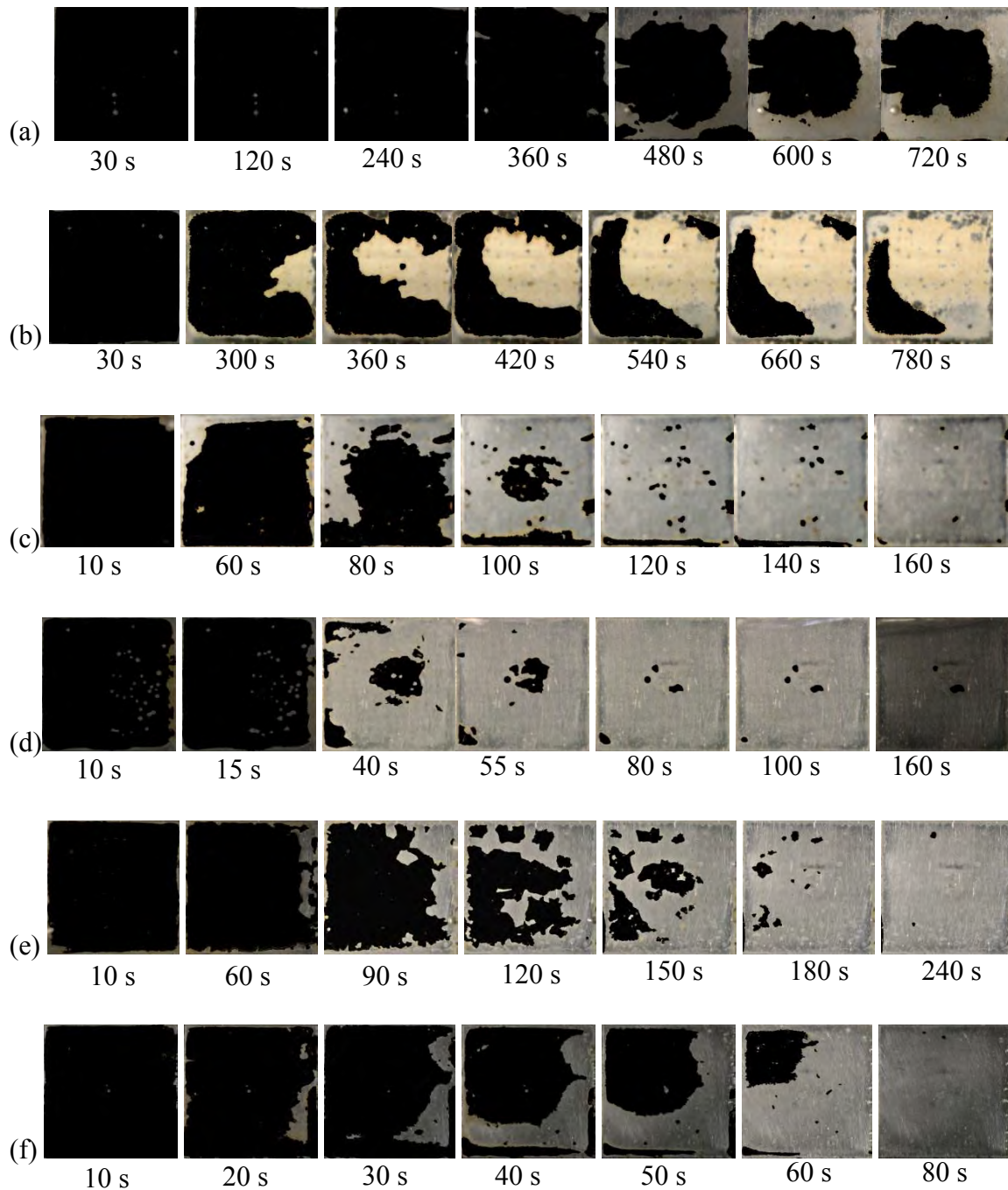
Figure 5.1: Images taken during yeast slurry removal at 0.5 m s^{-1} using (a) – (b) water at (a) 20°C and (b) 70°C; (c)-(d) using 0.2% advantis at (c) 20°C and (d) 701°C; using (e)-(f) 2% Advantis 210 at (e) 20°C and (f) 70°C. The yeast deposit is coloured black and the coupon is grey. The thin film identified in Figure 5.3 (a) can be seen in (b). Time interval is indicated on each image (light source switched off unintentionally at 160 s in (d)).

5.2 Deposit removal profiles

Figure 5.2 illustrates area and U profiles of deposit removal experiments conducted at a flow velocity of 0.5 m s^{-1} for water ((a), (b)) and chemical rinsing ((c) – (f)) at 20°C and at 70°C. At the temperatures and flow velocities investigated for water and chemical rinsing, the three phases of cleaning could be similarly described for this deposit as in Chapter 4 Section 4.4:

  (II)   Lag phase - Deposit hydration and swelling; during this phase the deposit became lighter in colour.

  (III)   Deposit removal phase - Deposit removal by fluid flow in part by dissolution and in patches.

 (IIII)   Constant phase - A visually clean surface was reached during chemical rinsing, or no further deposit was removed during water rinsing experiments.

As rinsing time increased the area measurement and U increased until the values became constant. Area > 600 mm^2 was chosen to signify phase (I). An area of 0 mm^2 signifies the end of the removal phase in chemical cleaning. However in water rinsing the deposit was not wholly removed, so when the area became constant ($\pm$ 50 mm^2) or the time taken to reach 0 mm^2 minus the length of time area > 600 mm^2 is indicative of phase (II). The phases are separated by the vertical dashed lines in each profile in Figure 5.2.

(a)

(b)

(c)
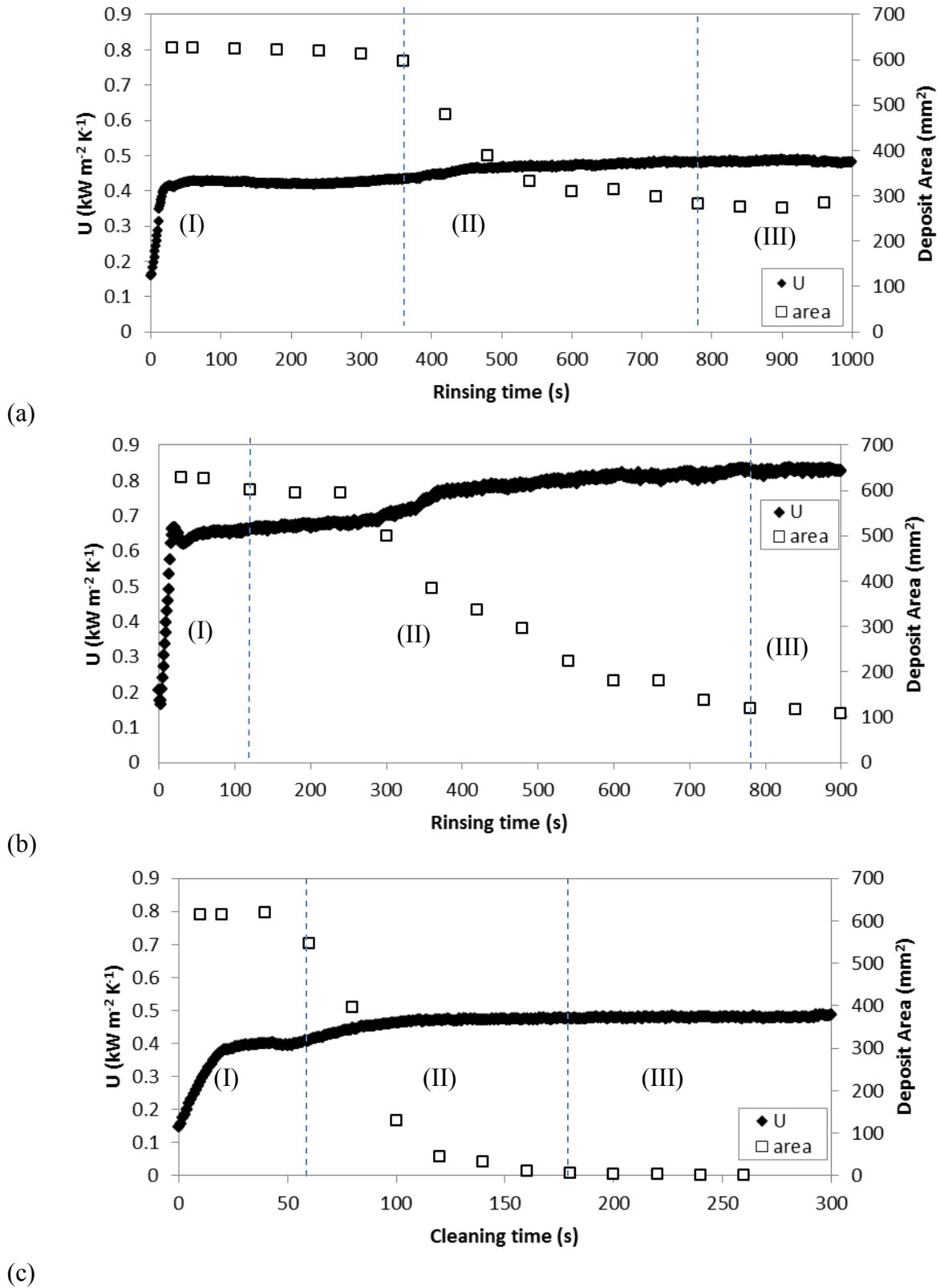
Figure 5.2: Removal profiles of U and area for type A deposit at 0.5 m s^{-1} using water at (a) 20°C, (b) 70°C; using 0.2 wt % Advantis at (c) 20°C and (d) 70°C, and using 2 wt % Advantis at (e) 20°C and (f) 70°C.

(d)

(e)

(f)
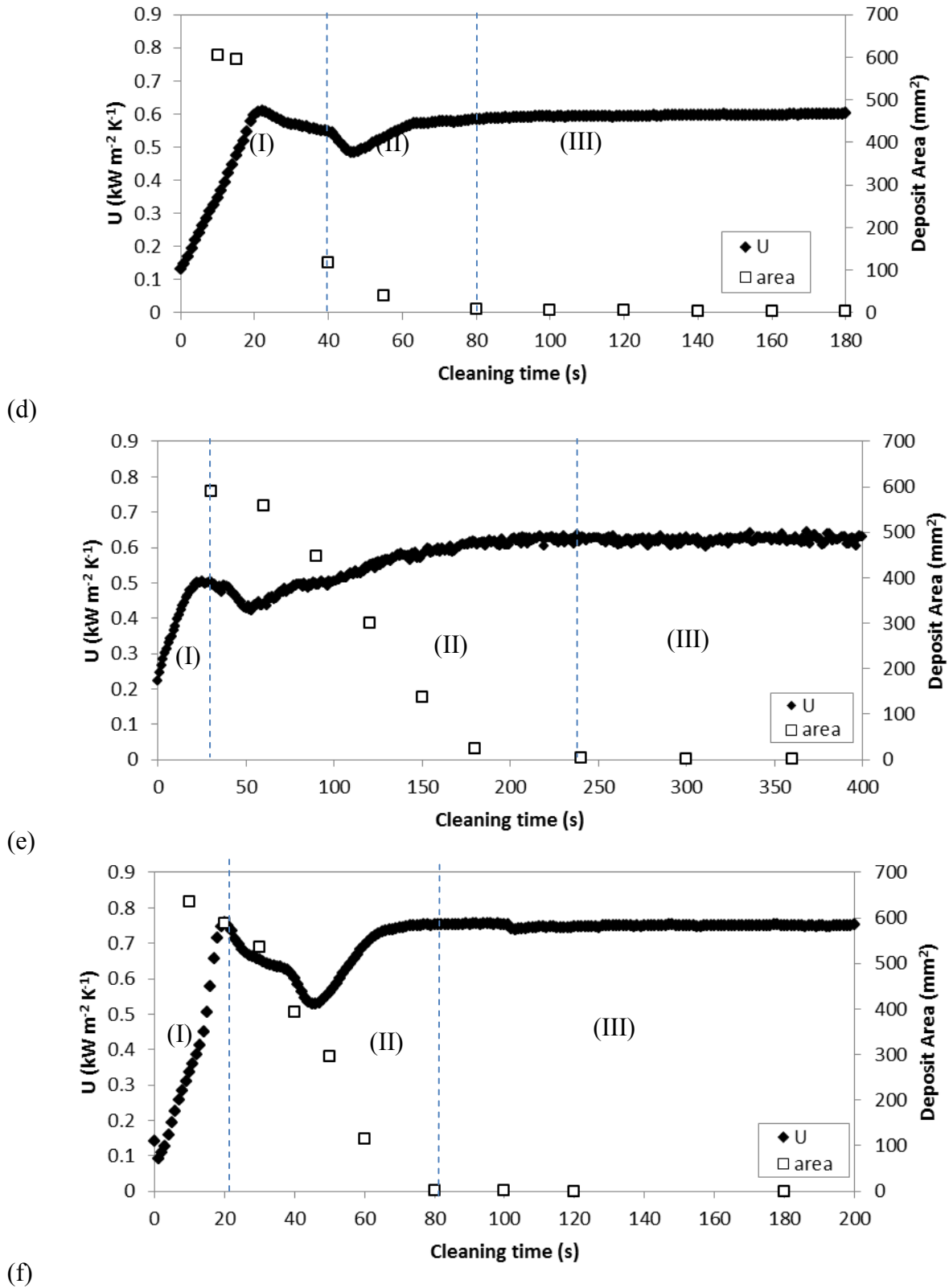
Figure 5.2 continued: Removal profiles of U and area for type A deposit at 0.5 m s^{-1} using water at (a) 20°C, (b) 70°C; using 0.2 wt % Advantis at (c) 20°C and (d) 70°C, and using 2 wt % Advantis at (e) 20°C and (f) 70°C.

5.3 Water rinsing

In all cases of water rinsing the surface did not reach a clean state visually; an adhesive film that could not be removed by further water rinsing remained. A typical coupon after water rinsing is illustrated in Figure 5.3 (a) showing the surface is not visually clean. A section of this coupon surface obtained using a surface reflectance microscope is shown in Figure 5.3 (b). The film appeared to be clusters of yeast cells (in green) on the surface (in yellow). As water rinsing time increased the deposit became lighter in colour. There was some deposit erosion at the coupon edges and the majority of deposit was removed in patches in the flow in all cases. Initially large patches of deposit were removed. The size of the removed material decreased with time. In all cases as the water rinsing time increased the amount of deposit on the coupon decreased to a point where no further deposit was removed by the flow.
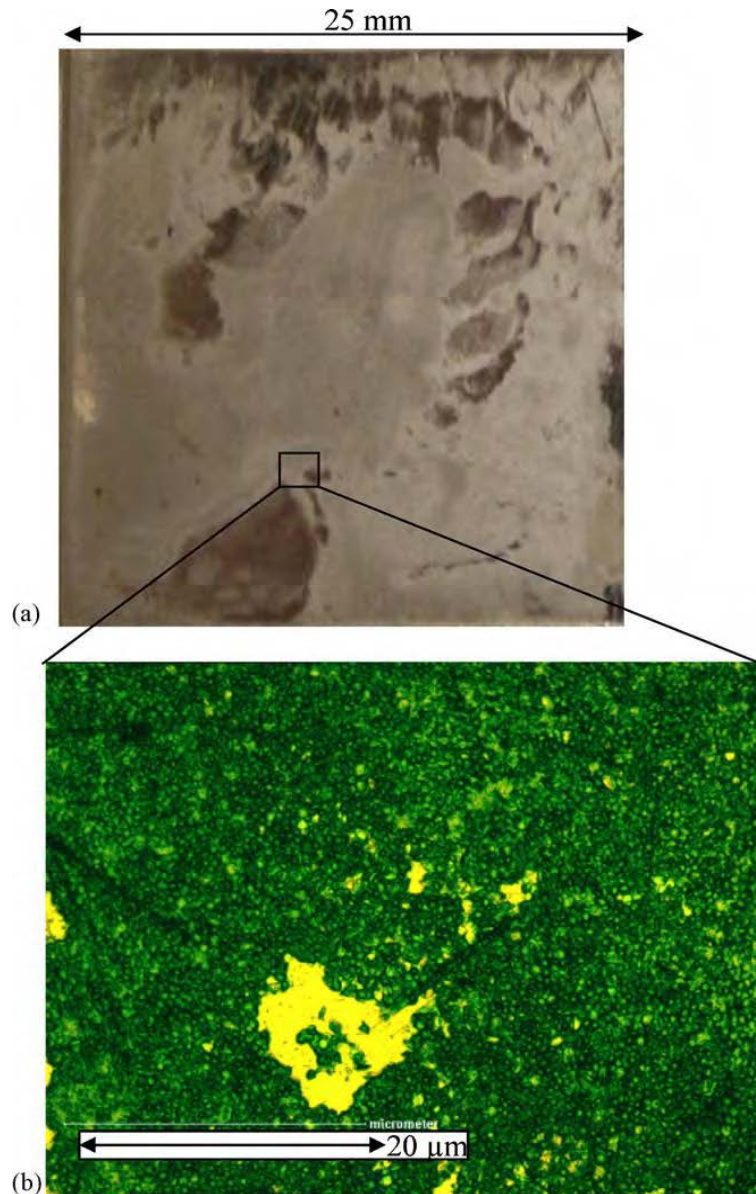
Figure 5.3: (a) Fouled coupon rinsed with water showing that the surface is not visually clean. A section of this coupon surface is shown in (b) on the surface using a surface reflectance microscope. The yeast cells are green and the surface is yellow.

5.3.1 The effect of temperature and flow on the lag phase

Figure 5.4 illustrates the effect of temperature on the lag phase time at different flow velocities.

There is a clear difference between 20°C and the other temperatures, with a significantly lengthy

lag period ca.400 s at 0.4 and 0.5 m s^{-1} before deposit removal starts visually. At other temperatures, removal starts more quickly and the effect of flow velocity is insignificant. Water will diffuse more quickly into the deposit at temperatures greater than ambient at even at higher flow rates, 0.4 and 0.5 m s^{-1}. However rehydration of the deposit at lower flow velocity, 0.26 m s^{-1}, appears less dependent on temperature.
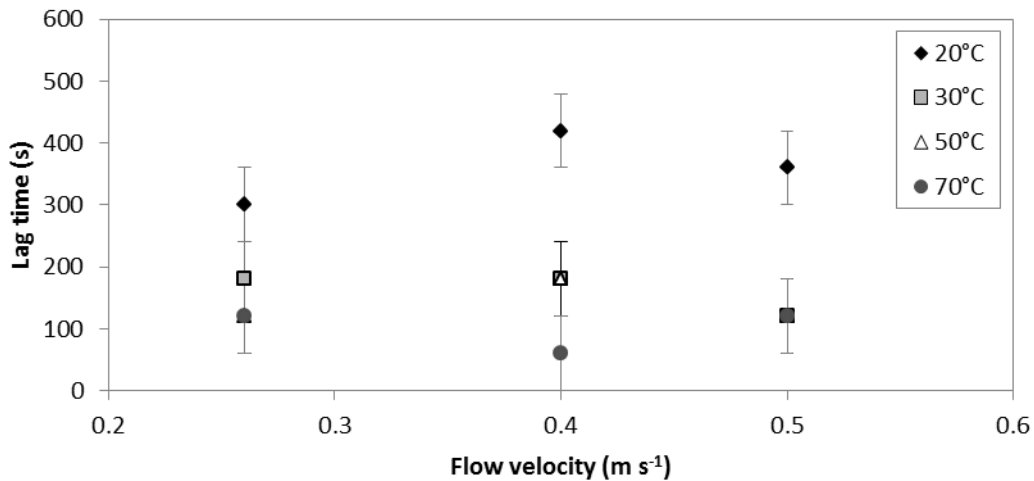
Figure 5.4: Lag phase time of deposit removal vs. Flow velocity for water rinsing yeast deposit.

During water rinsing of the deposit, phase (I) the lag phase could be accurately distinguished. However, the end of the removal phase (II) and the amount of deposit removed were difficult to identify clearly and accurately.

5.3.2 The effect of temperature and flow on removal

Average area measured during water rinsing of the type A deposit at 20, 30, 50 and 70°C is illustrated in Figure 5.5 (a) – (d).

(a)

(b)

(c)
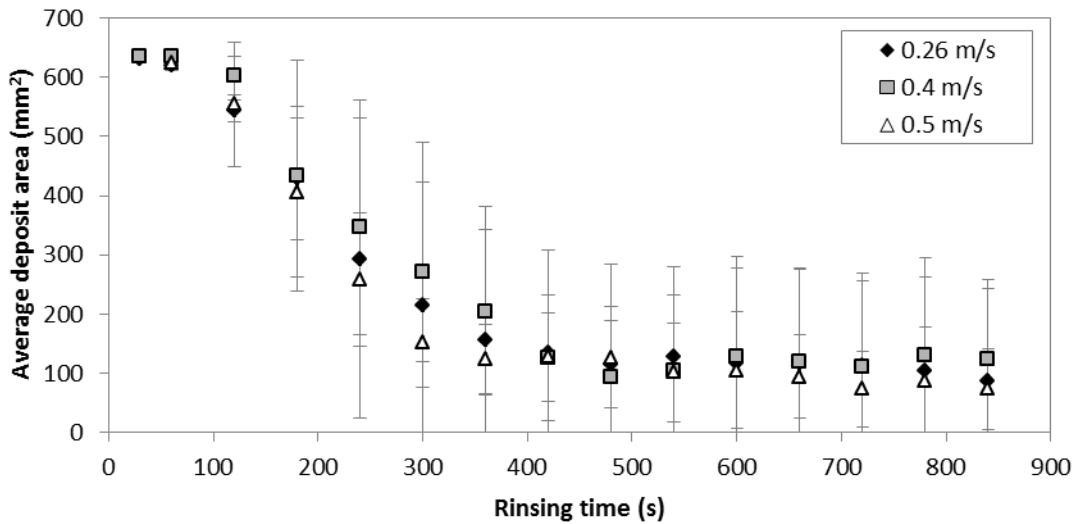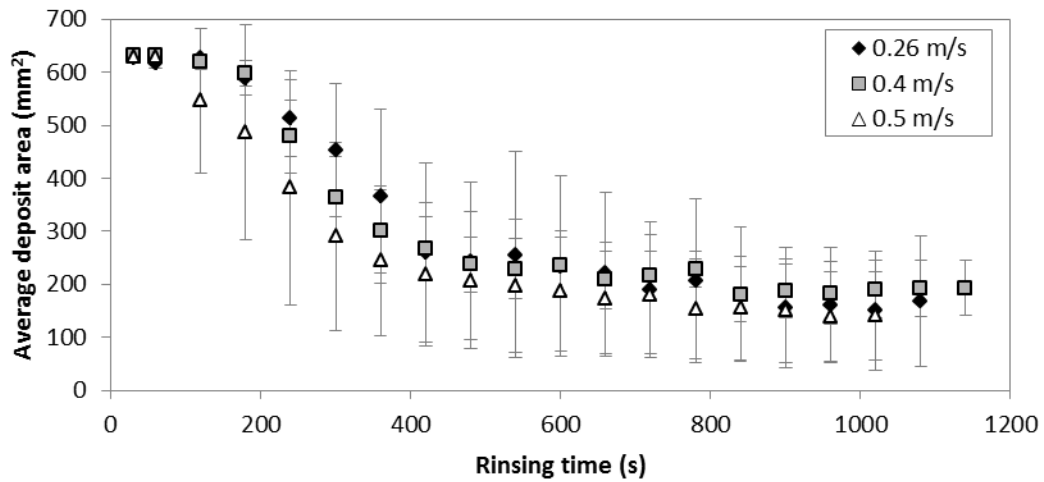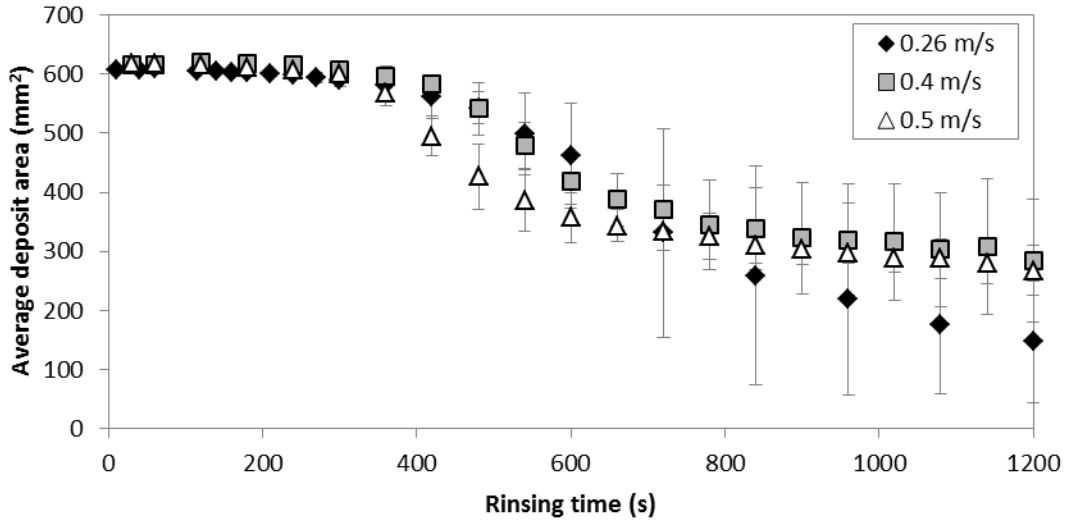
Figure 5.5: Average area of aged yeast slurry removed vs. Rinsing time at (a) 20, (b) 30, (c) 50 and (d) 70°C.
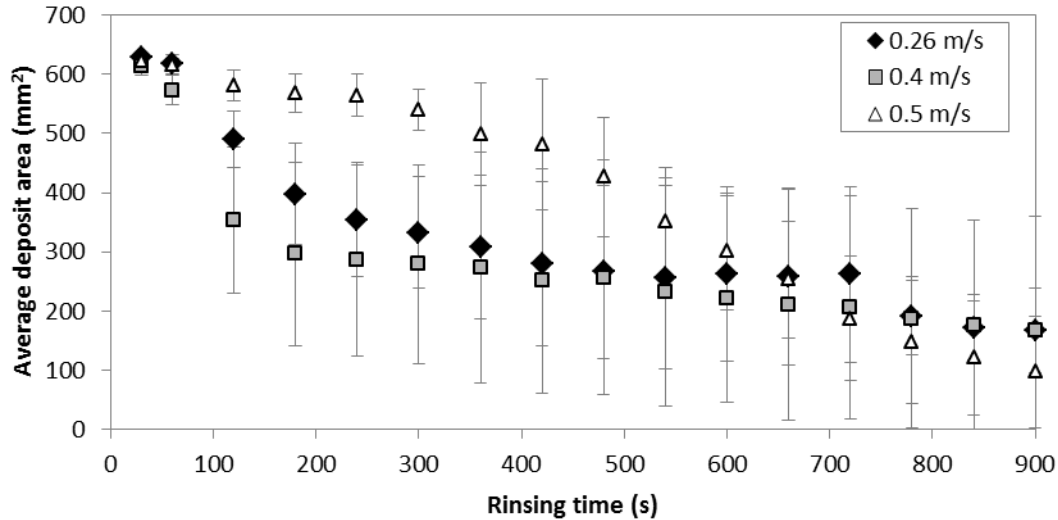
(d)

Figure 5.5 continued: Average area of aged yeast slurry removed vs. Rinsing time at (a) 20, (b) 30, (c) 50 and (d) 70°C.

From the average area removal profiles presented in Figure 5.5 it was found that:

(i) Most of the velocity data shows no trend at each temperature, except at 70°C where there is a clear difference in the removal phase of rinsing at 0.26 and 0.5 m s^{-1} (4.8 and 9.2 l m^{-2} min^{-1}).

(ii) Rinsing at 30 and 50°C removed the most deposit in the shortest times. There is some evidence that the deposit is removed most quickly at these two temperatures.

(iii) Data at 70°C is most scattered. There is some evidence that rinsing at 70°C and 20°C removed deposit most slowly. Rinsing at high temperatures like 70°C could bake the yeast to the surface.

During water rinsing, increasing the temperature to 50°C decreased both the duration of the lag phase and the time at which no further deposit appeared to be removed. At 70°C the time at which no further deposit appeared to be removed was greater than at other temperatures even

though lag phase time was similar to that at 30 and 50°C (see Figure 5.4). These findings suggest that:

 (i)   temperature has a bigger impact on deposit removal than flow velocity,

 (ii)   the removal phase time controls the overall time at which no further deposit is removed
         during water rinsing, and

(iii)   rinsing at mid-range temperatures removed deposit most quickly.

This suggests that heating the pre-rinse to 30 – 50°C would remove deposit more quickly than at ambient. This could reduce the deposit load carried over into the chemical cleaning phase and potentially the overall cleaning time. The average area removal profiles suggest most deposit is removed at 50°C although this cannot be stated for sure due to the large variation of the results.

5.3.3 Determining of the removal phase (II) by R_d

Average R_d, deposit resistance, profiles were plotted to indicate removal phase (II) time. R_d is calculated from the heat transfer coefficient at time t (U_t) and the time when a clean surface is achieved (U_c) according to Equation 4.1. In this case because a clean surface is not achieved during water rinsing R_d is inversely proportional to U_x, the heat transfer coefficient at the time where no further deposit was removed determined from U_t values of the last portion of each rinse (at least 1 minute) minus 1 standard deviation.

Figure 5.6 illustrates average R_d values (from four repeats) vs. water rinsing time at (a) 20 (b) 30 (c) 50 and (d) 70°C. The lag phase has been omitted from the plots to simply illustrate the removal phase (II). This is why the plots start at 300 s (20°C) or 100 s (30, 50, and 70°C). The

accuracy of the point determined at the end of the removal phase is ± 1 s. The variation in R_d is large and omitted from the plots; the variation in R_d itself is not of interest here, more the variation in the time where R_d becomes zero.
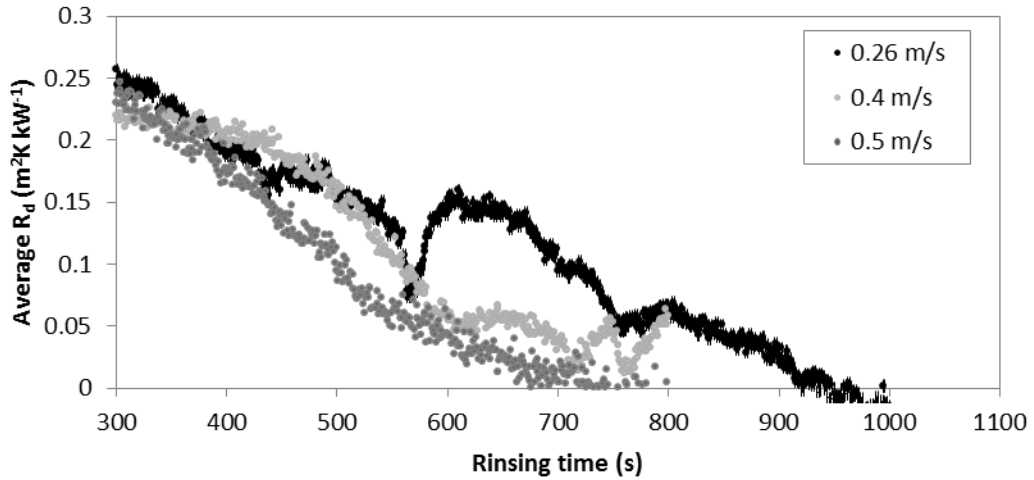
(a)
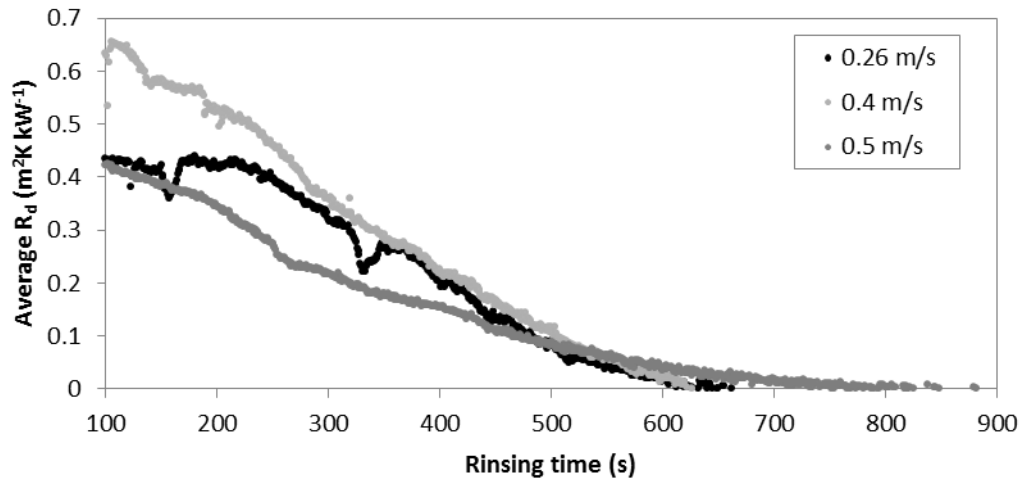
(b)

Figure 5.6: Average R_d removal profiles for aged yeast slurry vs. Rinsing time at (a) 20, (b) 30, (c) 50 and (d) 70°C.
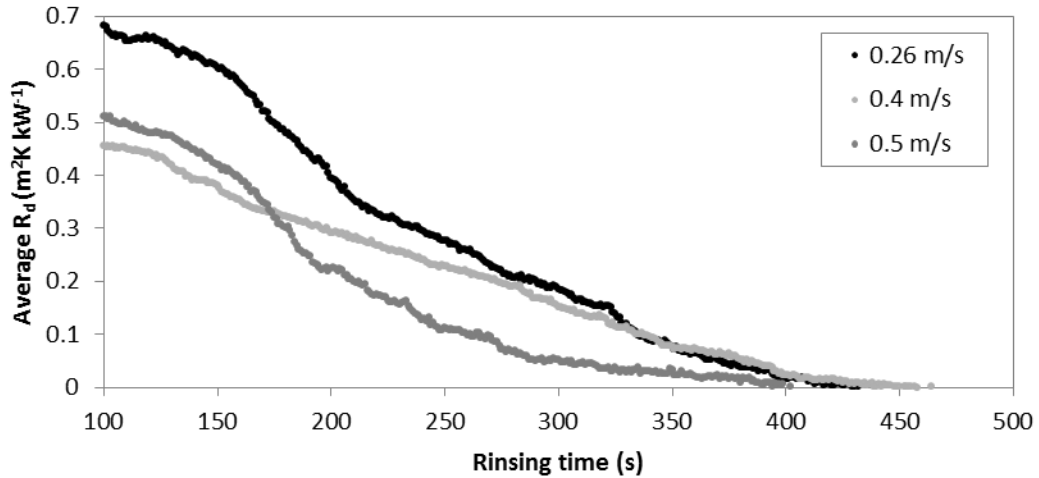
(c)
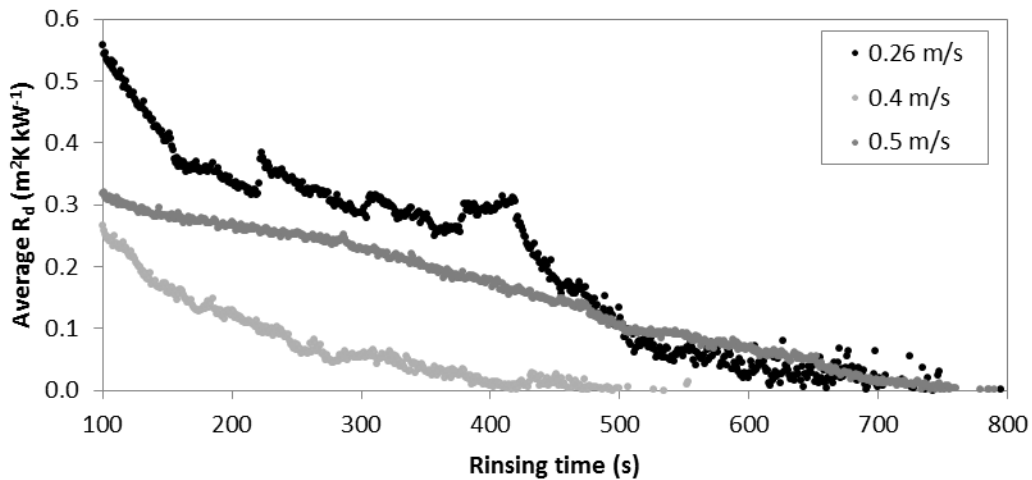
(d)

Figure 5.6 continued: Average R_d removal profiles for aged yeast slurry vs. Rinsing time at (a) 20, (b) 30, (c) 50 and (d) 70°C.

It can be seen from Figure 5.6 that the time at which R_d reached zero at 50°C is much shorter than the other temperatures. Depending on the flow velocity it is between 400 and 450 s. At 20°C R_d becomes zero between 700 and 1000 s; at 30°C R_d becomes zero between 600 and 800 s and at 70°C between 500 and 800 s. This finding agrees with area removal in Section 5.3.2 suggesting removal of deposit occurs most quickly at 50°C.

5.4 Chemical cleaning

In all cases of Advantis 210 cleaning, the surface reached a visually clean state. Images taken during yeast slurry removal at 0.5 m s^{-1} using 0.2 and 2% Advantis 210 at 20°C and 70°C are presented in Figure 5.1 (c) - (d) and (e) – (f) respectively.

5.4.1 Average cleaning times

The deposit could be removed with Advantis 210 at all temperatures and flow rates investigated including at both chemical concentrations 0.2 and 2 wt %. During chemical rinsing the deposit became lighter in colour as the cleaning time increased. Similarly to water rinsing, the majority of deposit was removed in patches in the flow and by dissolution. The average area of deposit removed with respect to cleaning time using 0.2 % Advantis 210 is presented in Figure 5.7 (a) – (d). Rinsing at 2 % is presented in Figure 5.8 (a) – (d). The Figures can be summarised;

(i)   At low and high temperature, 20 and 70°C, rinsing at 0.26 m s^{-1} is significantly different to that at 0.4 and 0.5 m s^{-1} at both chemical concentrations. There is no significant difference between rinsing at 0.4 and 0.5 m s^{-1} at these temperatures.

(ii)   The area profiles at 20°C and 50°C at 2 % concentration are significantly different to the other area profiles presented (except at 50°C, 0.4 m s^{-1}) showing linear reduction in area rather than a sigmoid shape.

(iii)   At 30°C, 0.2 % concentration there is no significant difference between 0.4 m s^{-1} and 0.26 m s^{-1} except for the longer lag period at 0.4 m s^{-1}. At 30°C, 2 % concentration there is no significant difference in 0.4 m s^{-1} and 0.5 m s^{-1}.

(iv)   At 50°C, 0.2 % concentration, there was no significant difference in the area profiles only

the cleaning time. A 50°C, 2 % concentration, rinsing at 0.4 m s^{-1} had a sigmoidal curve

rather than linear.

These findings suggest there are effects both of temperature and flow. At low and high

temperatures doubling the flow velocity produced a significantly different profile. At 30°C an

increase in concentration causes a shift of area profile at 0.4 m s^{-1} to be more similar to the higher

flow velocity. At 50°C an increase in concentration reveals rinsing at 0.4 m s^{-1} to be significantly

different to the other flow velocities.
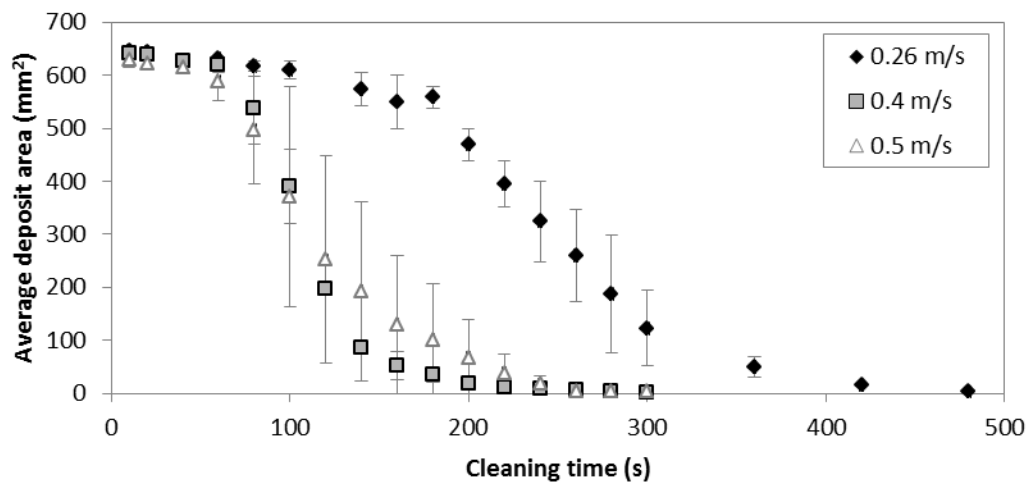
(a)

Figure 5.7: Average area removal profiles of yeast slurry film using 0.2 % Advantis 210 at (a) 20 (b) 30 (c) 50 and
(d) 70°C.
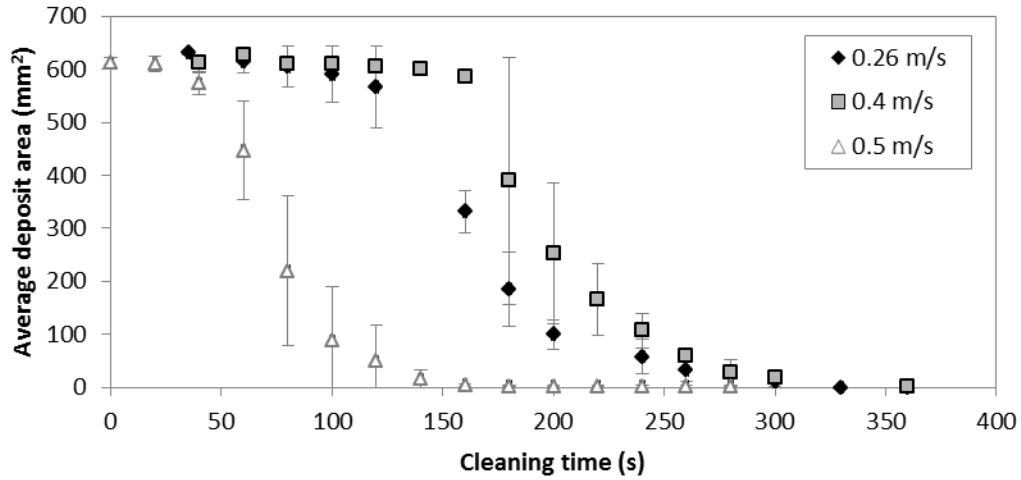
(b)
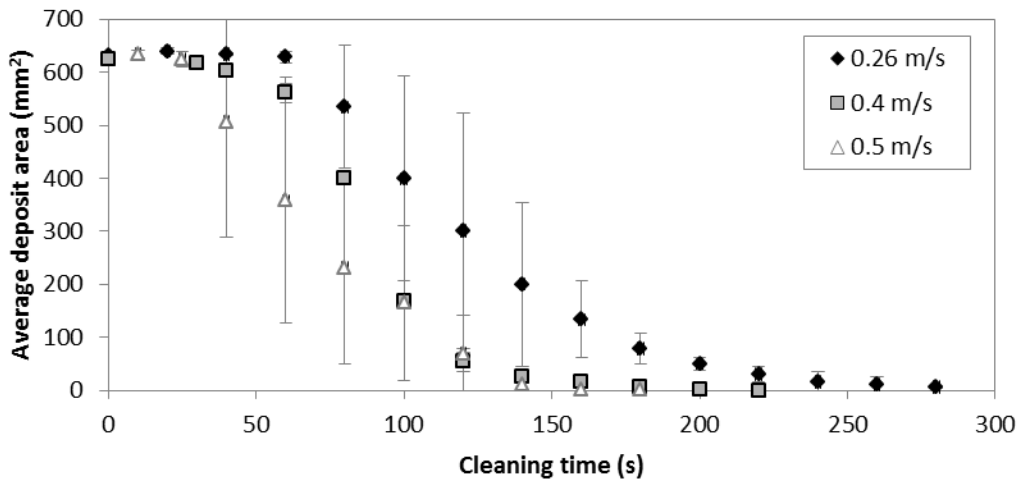
(c)
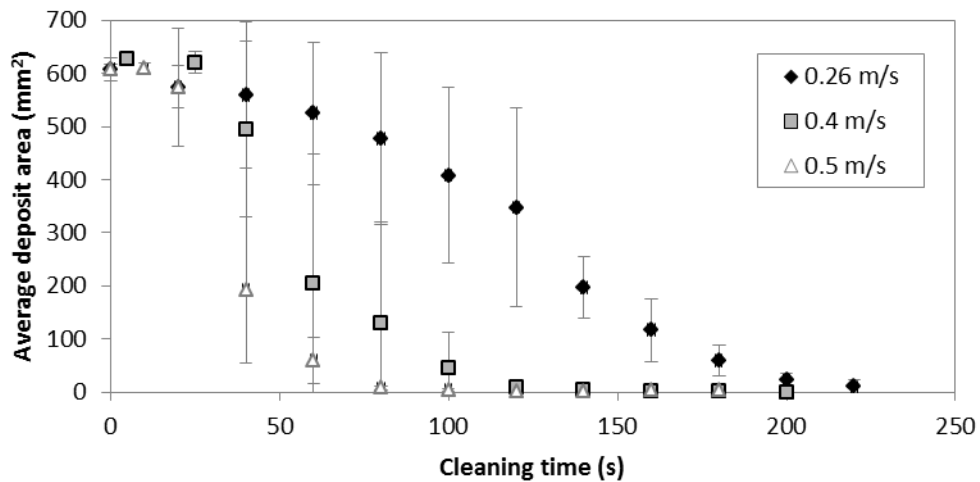
(d)

Figure 5.7 continued: Average area removal profiles of yeast slurry film using 0.2 % Advantis 210 at (a) 20 (b) 30 (c) 50 and (d) 70°C.
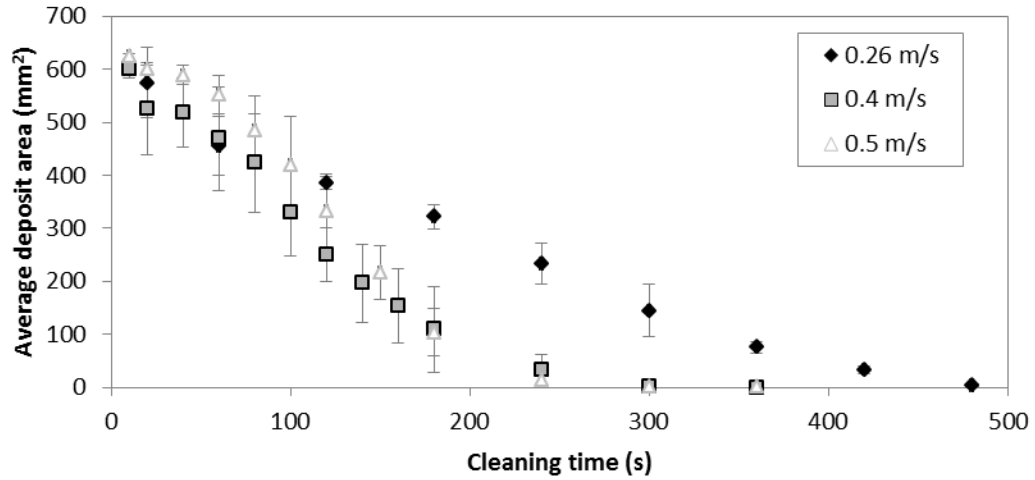
(a)
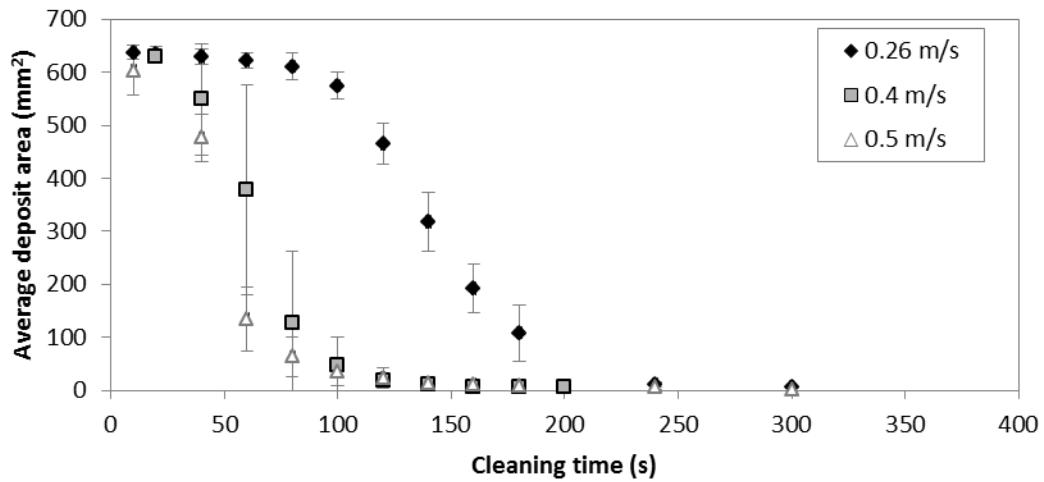
(b)
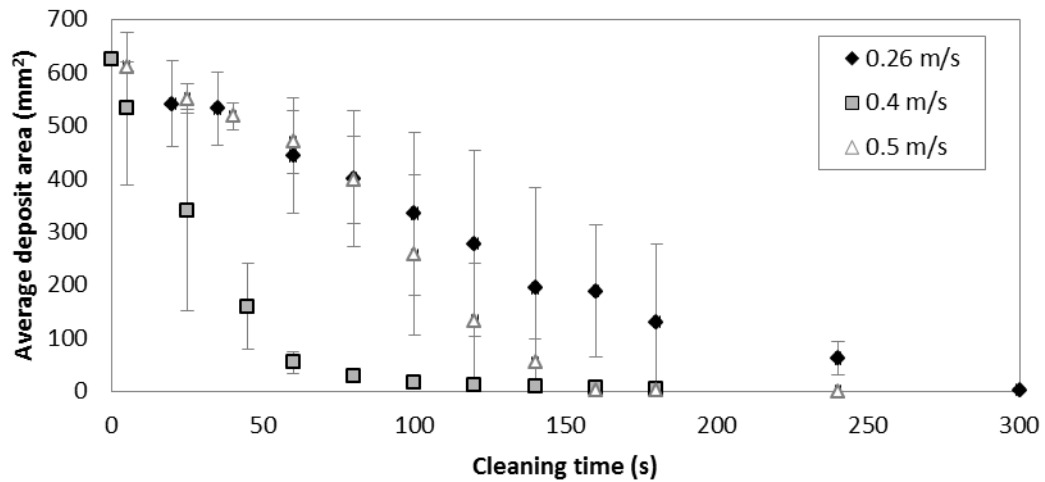
(c)

Figure 5.8: Average area removal profiles of yeast slurry film using 2 % Advantis 210 at (a) 20 (b) 30 (c) 50 and (d) 70°C.
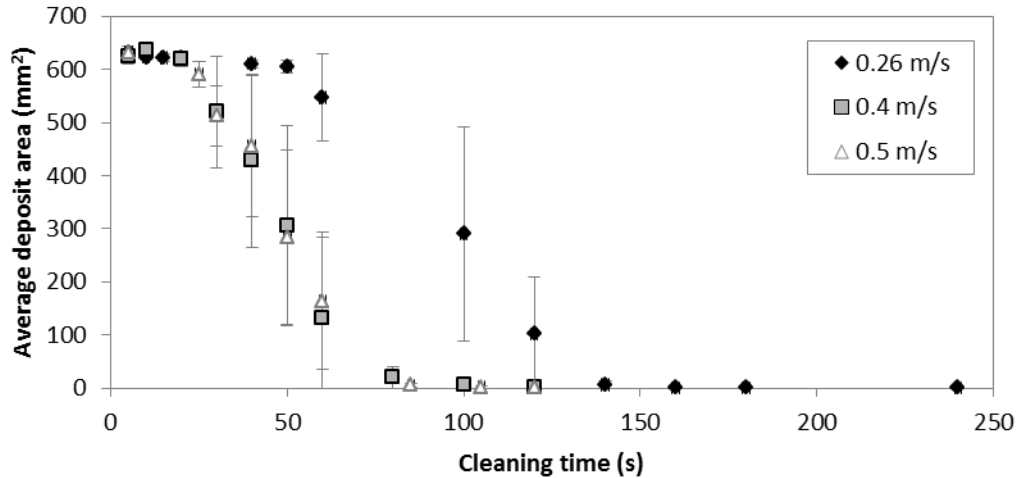
(d)

Figure 5.8 continued: Average area removal profiles of yeast slurry film using 2 % Advantis 210 at (a) 20 (b) 30 (c) 50 and (d) 70°C.

5.4.2 Rinsing using 0.2 % Advantis 210

The lag phase, phase I, can be reduced by increasing the temperature and by increasing flow velocity at 20, 30, and 50°C. At 70°C the lag phase lengths are similar and shorter than other temperatures. Figure 5.9 illustrates the duration of phase II, the removal phase, of the deposit. As with the lag phase, the shortest removal phase was seen at the highest temperature at all flow velocities. Increasing the temperature at 0.26 m s^{-1} significantly decreased the duration of the removal phase similarly at 30, 50 and 70°C. At 0.5 m s^{-1} rinsing at 70 and 20°C revealed the fastest and slowest removal time. Rinsing at 30 and 50°C revealed a similar removal time in between that of 20 and 70°C.
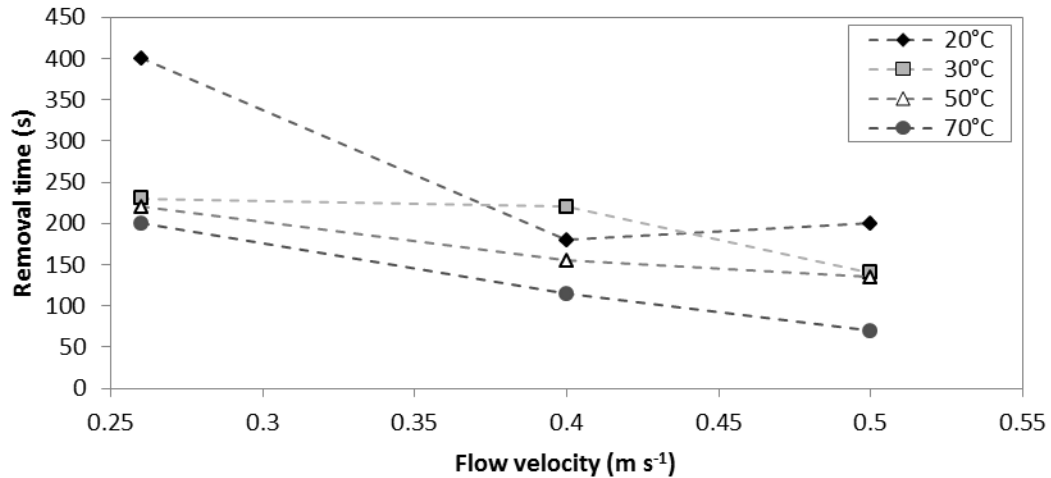
Figure 5.9: Removal phase time vs. flow velocity for cleaning with 0.2 % Advantis 210.

5.4.3 Rinsing using 2 % Advantis 210

The lag time, phase I, of deposit removal was minimised at 20 and 50°C. The lag time could be reduced at 30 and 70°C by increasing the flow rate. Figure 5.10 illustrates the removal phase time of the deposit. Increasing the temperature clearly decreases cleaning time. At 0.5 m s^{-1} the same relationship is found as rinsing at 0.2%. Rinsing at 70 and 20°C revealed the fastest removal time and slowest removal time at that flow rate respectfully. Rinsing at 30 and 50°C gave similar removal times between those of 20 and 70°C. This relationship has held at all flow velocities. Again rinsing at 70°C revealed the fastest removal phase times.
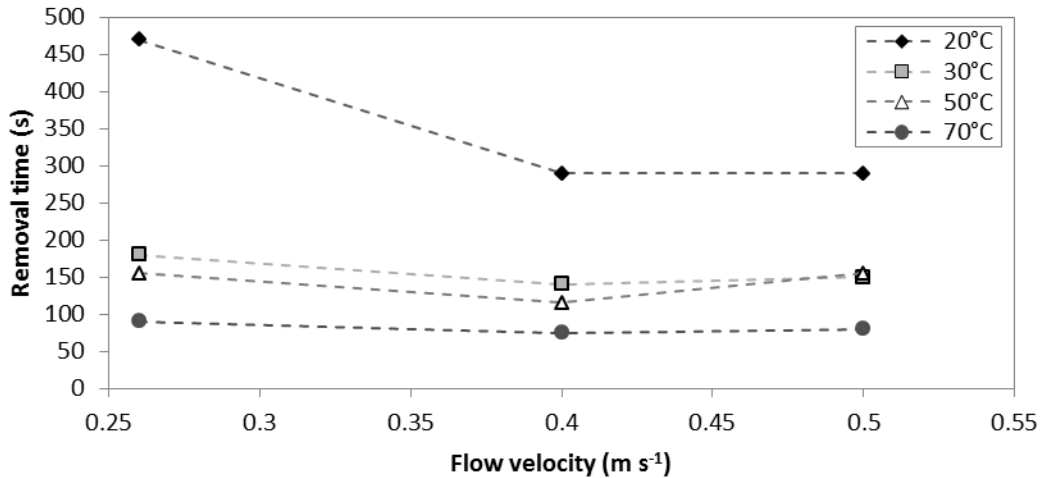
Figure 5.10: Removal phase time vs. flow velocity for cleaning with 2 % Advantis 210.

5.4.4 Cleaning time

The overall cleaning times for the deposit at 0.2 and 2 % Advantis are presented in Figure 5.11 (a) – (c). The data shows;

(i)   At 0.26 m s^{-1} an increase in temperature decreased the cleaning time non-linearly. The effect of concentration was only obvious at 70°C. A decrease in cleaning time of 90 s was achieved by increasing the chemical concentration from 0.2 to 2%.

(ii)   At 0.4 m s^{-1} an increase in temperature decreased the cleaning time. The effect of concentration was evident at lower temperature 20 and 30°C where the higher chemical concentration decreased cleaning time. At 50 and 70°C there was no evidence of concentration effect.

(iii) At 0.5 m s^{-1} an increase in temperature decreased cleaning time. There was no evidence of concentration effect at any temperature.

Figure 5.11 (d) illustrates (a) – (c) on one plot. These findings suggest the effect of temperature has the biggest impact on cleaning time. The effect of flow velocity (and wetting rate per m^2) and concentration has less impact on cleaning time. This is an important finding because potentially lower chemical concentrations can be used to achieve similar cleaning times by optimising operation temperature and flow velocity or wetting rate per m^2.
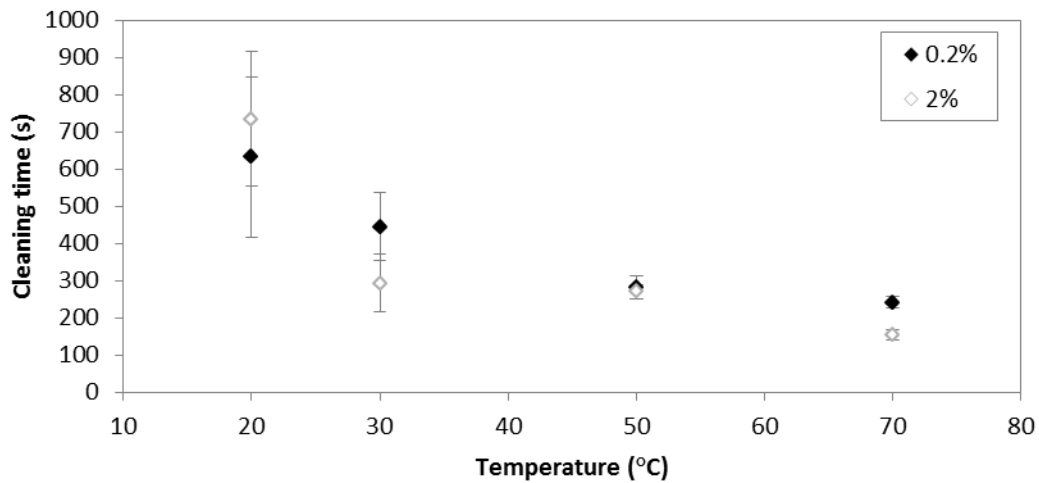
(a)
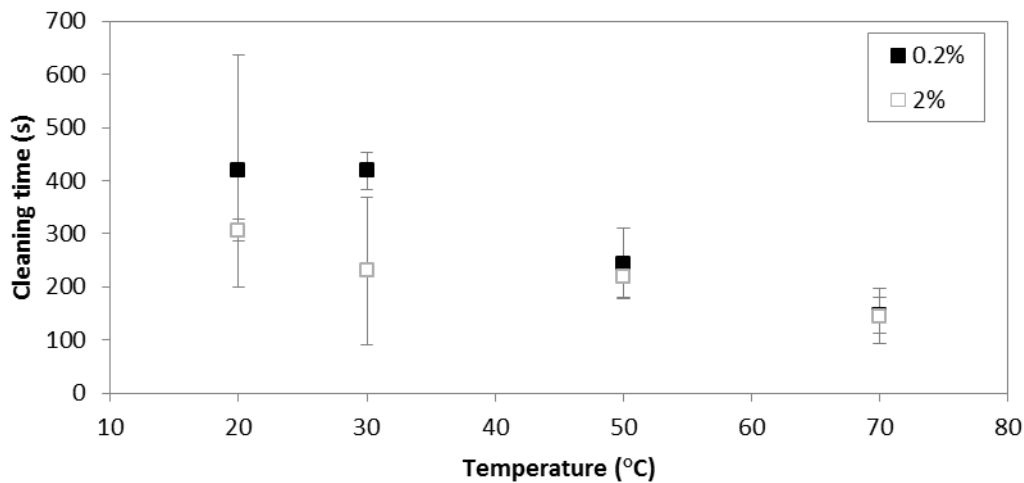
(b)

Figure 5.11: Cleaning times (a) 0.26 m s^{-1} (b) 0.4 m s^{-1} (c) 0.5 m s^{-1} (d) Plot of all the cleaning times vs. Temperature.
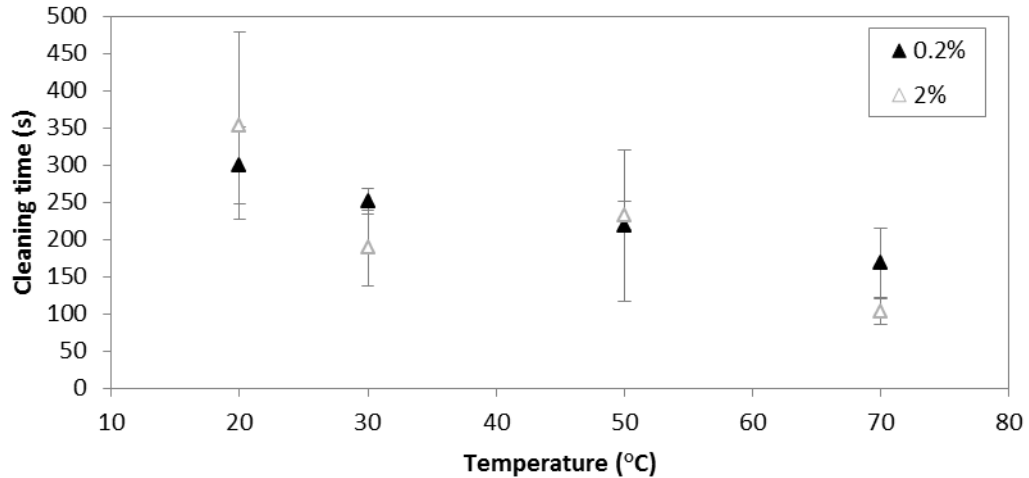
(c)
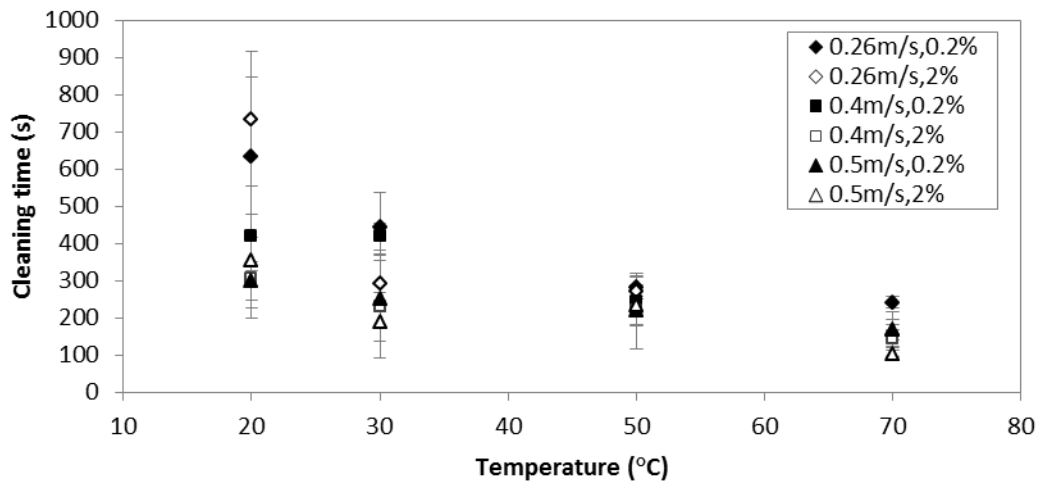
(d)

Figure 5.11 continued: Cleaning times (a) 0.26 m s^{-1} (b) 0.4 m s^{-1} (c) 0.5 m s^{-1} (d) Plot of all the cleaning times vs.Temperature.

5.5 Deposit rheology

Figure 5.12 illustrates samples of deposit soaked in water, 0.2% and 2% Advantis. Clearly the addition of chemical dissolved the semi solid structure more so for 2% than 0.2% characterised by the darker solution surrounding the deposit. The effect of shear rate, water soaking and chemical action on deposit structure during cleaning can be studied by rheology experiments.
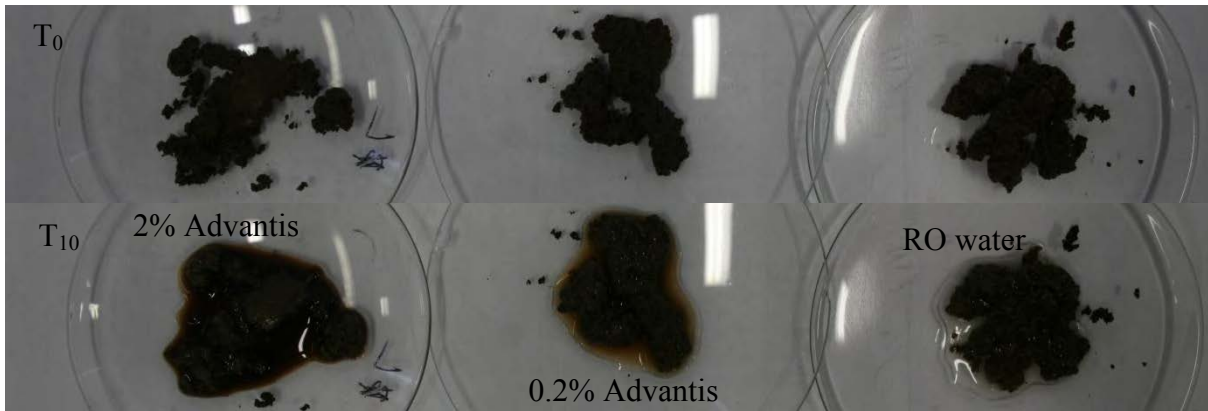
Figure 5.12: The effect of soaking deposit in water,.0.2% Advantis and 2% Advantis at ambient. Image taken after 15 minutes.

Figure 5.13 (a) illustrates viscosity vs. shear rate at 20, 30, 50 and 70°C of industrial type A fouling. The deposit was shear thinning at all test temperatures, more so at higher temperatures. This suggests that as the shear rate and thus shear stress increases the viscosity of the product decreases, more so at higher temperatures.

Figure 5.13 (b) illustrates the rheology of diluted deposit at ambient temperature. Again the deposit remains shear thinning over the shear rate and dilution range. The viscosity of the deposit decreases as the amount of dilution increases. Figure 5.11 (c) illustrates viscosity vs. shear rate for the deposit at ambient at different chemical concentrations, 0, 0.2 and 2 % Advantis. When the deposit was soaked in 2 % Advantis 210 a marked effect on viscosity was shown at corresponding shear rates. The viscosity of the deposit was greatly reduced. The viscosity profile of 0 % and 0.2 % was similar. The deposit remained shear thinning under all conditions suggesting an increase in flow velocity would decrease deposit viscosity.
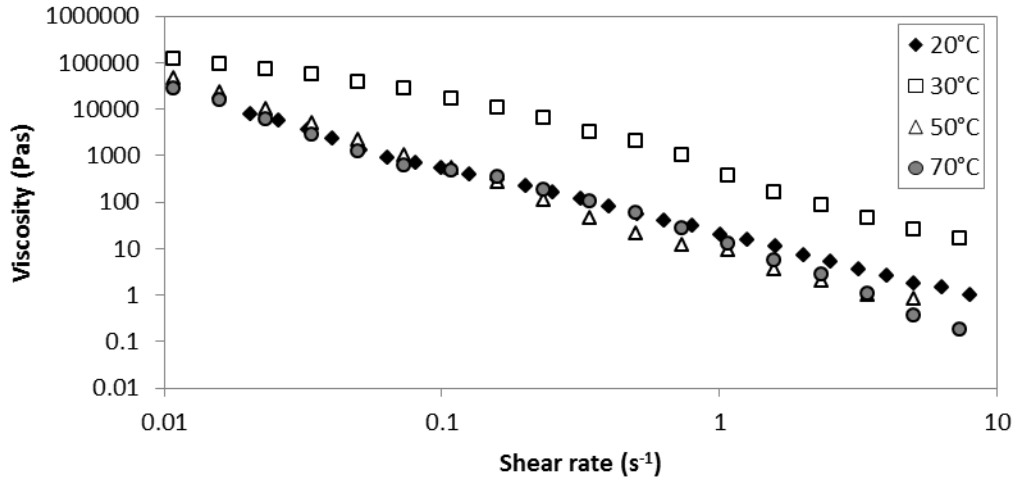
(a)
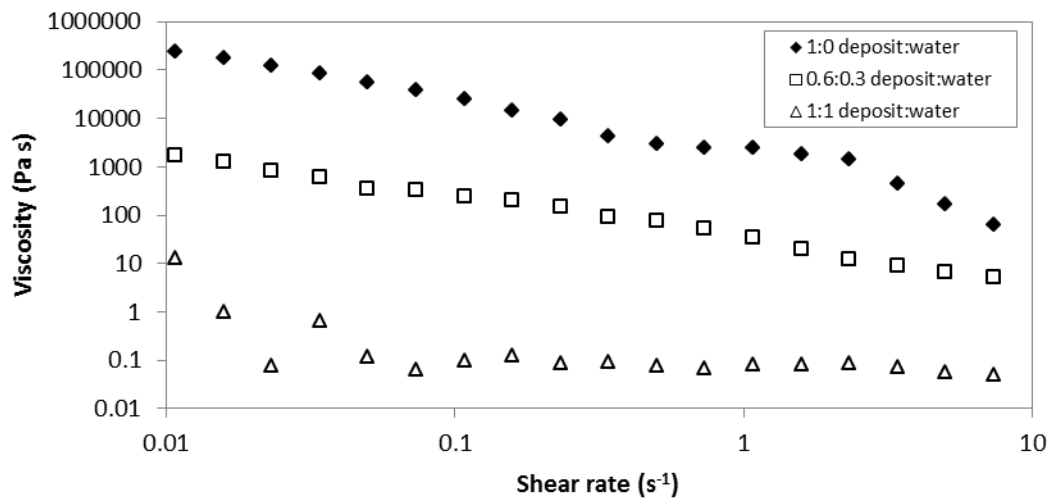
(b)
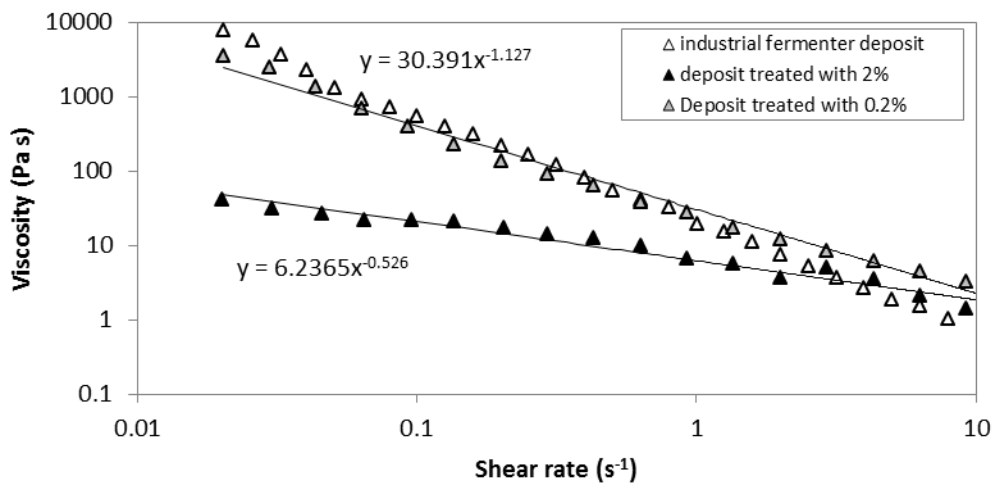
(c)

Figure 5.13: Effect of (a) temperature (no chemical), (b) dilution in water at 15°C (for 10 minutes) and (c) chemical at 20°C.

5.6 Monitoring cleaning using U

The efficacy of U to indicate cleaning behaviour and cleaning times was assessed during water and chemical rinsing.

5.6.1 Water rinsing

Monitoring U revealed that the lag phase (i) and removal phase (ii) could be characterised, however the end of phase (ii) could not be easily identified in the majority of water rinses. This was because the small deposit erosion at the end of rinsing that could be seen in area measurement was not determined by U. U showed unexpected fluxes and increases when no deposit was being removed; accurate measurement of U was highly dependent on the microfoil heat flux sensor (MHFS) remaining cold during the experiment. Due to the set up of the system this was not possible for longer than 10 minutes at ambient and 5 minutes at 70°C when the ice melted. The ice surrounding the block could be replenished during the experiment however the ice directly cooling the copper stub could not be replenished.

5.6.2 Chemical rinsing

In all cases, chemical cleaning times were less than eight and a half minutes. The average value of U increased initially, lasting less than 40 s in all cases. The lag time, phase I, could not be distinguished from this. In many cases U did not become constant (to determine the point of clean within 1 SD) and removal phase times, phase II, could not sensibly be determined. The reason for this is most likely due to the impractical method used to cool the MHFS.

5.7 Conclusion

The results presented here illustrate that for a type 2 deposit found in the brewing industry, chemical action is required for complete removal. There are three characteristic phases for water and chemical rinsing, (i) lag time, (ii) removal phase, (iii) no further removal or clean surface. Unfortunately U was not an effective measure for cleaning time and identifying phase times. Rheology suggests that the deposit is shear thinning under both water and chemical treatment at all the test temperatures. As such viscosity was seen to decrease with increasing shear rate. The addition of 2% Advantis 210 reduced viscosity significantly at low shear rates compared to 0.2% Advantis and water. At constant low shear stress (0.4 Pa) the deposit became more elastic with temperature (Chapter 3) suggesting it would be harder to move at higher temperatures without treatment. In the cleaning rig a wall shear stress of up to 1 Pa could be reached.

Water rinsing did not reveal a clean surface, even at higher wetting intensities than recommended in industry (1.5 l min^{-1} m^{-2}), although most of the deposit was removed using water. To remove deposit using water the lag and removal phase times need to be minimised. Generally speaking increasing the temperature decreased lag time. An increase in flow velocity did not necessarily decrease the lag time. An increase in temperature seemed to minimise the removal phase time, except at 70°C where an increase in the removal phase was seen as average area did not become constant. Most deposit was removed at 30 and 50°C. Flow velocity had no significant effect on the overall removal profiles except at 70°C where an increase in flow velocity did not remove deposit as quickly as the other flow velocities suggesting the deposit was not rehydrated effectively at 70°C.

Chemical rinsing did reveal a clean surface. To remove deposit most effectively rinsing at 70°C was found to give the quickest cleaning times at both concentrations and all flow velocities. The effect of flow velocity and chemical concentration was evident at low flow velocity (low wetting 4.6 l min^{-1} m^{-2}). At higher flow velocity, 0.5 m s^{-1}, the effect of concentration was less significant than the effect of temperature. This is important because lower chemical concentrations can be used to achieve similar cleaning times by optimising CIP operation temperature and flow velocity (or wetting rate per m^2). If the use of chemical can be minimised this will reduce the carbon emissions associated with the production of the chemical which is large due to the large energy requirement (see Table 1.7).

The industrial recommendation from this work is to pre-rinse at 50°C to removal most of the fermenter deposit rather than using ambient water. The caustic concentration can be reduced from 2 % to 1% or even 0.1% (if measureable) and used at ambient temperature (i.e. the detergent tank does not need to be continuously heated) giving a visually clean surface. Terminal sanitisation requires ambient pipe work to be most effective anyway. The cost saving from using 1% NaOH and 0.1% NaOH at the brewery at ambient rather than 2% at 70°C (in FV CIP) would be £45 K and £69 K respectively. Because the impact pressure from the RJH used in the FVs is greater than that tested in these experiments, a visually clean surface could be achieved using only the warm water. It is worth testing in industry.

CHAPTER 6: CHARACTERISING THE REMOVAL BEHAVIOUR OF TYPE 3 DEPOSIT: COOKED CARAMEL

6.1 Chapter Introduction

It was impractical to measure wort fouling and cleaning with existing equipment used in project ZEAL (see Chapter 3, Section 3.1). Caramel was chosen as a relevant type 3 soil for investigation. Caramel is a common additive in confectionary and can be added during the wort boiling process to modify flavour and colour. Removal of caramel cooked onto coupons as in Section 3.6.2, using Advantis 210 at 2.5 and 5.0 wt % at 0.5 m s^{-1}, was monitored by area and U. Removal of cooked caramel from a 0.5 m section of pipe, using water and Advantis 210 at 2.5 wt % at 30, 50, 70, and 80°C, at 1, 1.5 and 2 m s^{-1}, was monitored turbidity, conductivity and mass.

The effect of temperature and concentration of alkali on deposit removal is described from cleaning rig data, and the effect of temperature and flow velocity is described from the pilot plant data. The effect of shear stress, chemical concentration and temperature on cooked caramel was also characterised by rheology.

6.2 Deposit characterisation by rheology

Cooked caramel rheology is shown in Figure 6.1. Oscillatory shear stress measurement of two different cooked caramel deposits collected from the pipe wall is shown. Sample 1 is in black and sample 2 is in blue. The Figure reveals the caramel deposit was structurally similar over a range of 100 Pa. Stresses up to 100 Pa are within the linear visco-elastic region of the deposit.

The effect of increasing temperature on cooked caramel rheology is shown in Figure 6.2. The temperature was increased from $30 - 90°C$ at an oscillatory stress of 5 Pa (within the linear visco-elastic region). G' and G" measured during the temperature ramp reveal;

(i)   G' was greater than G" suggesting the deposit was elastic over the temperature range investigated.

(ii)   The modules (G', G") decreased as temperature was increased. This can indicate less force would be required to move the deposit is the temperature is increased.

Oscillatory stress sweeps done on cooked caramel at 30, 50, 70 and 80˚C revealed the moduli were constant at oscillatory stresses less than 500 Pa. The yield stress decreased as the temperature was increased. This also indicates less force could be required to remove the deposit at higher temperatures. The yield stress was determined as the crossover point of G' and G" during each stress sweep at each temperature.
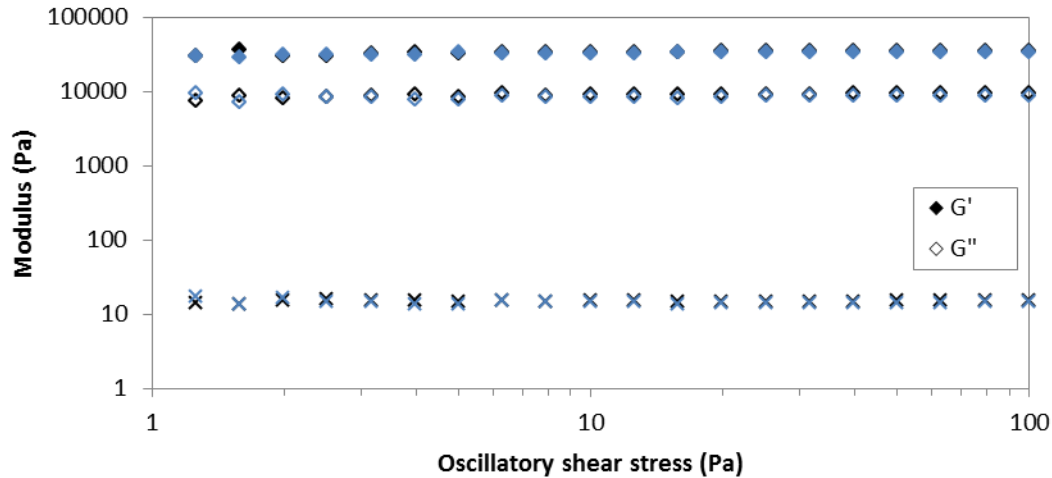
Figure 6.1: Cooked caramel G', G" vs. Oscillatory shear stress at 50˚C. Sample 1: black, sample 2: blue.
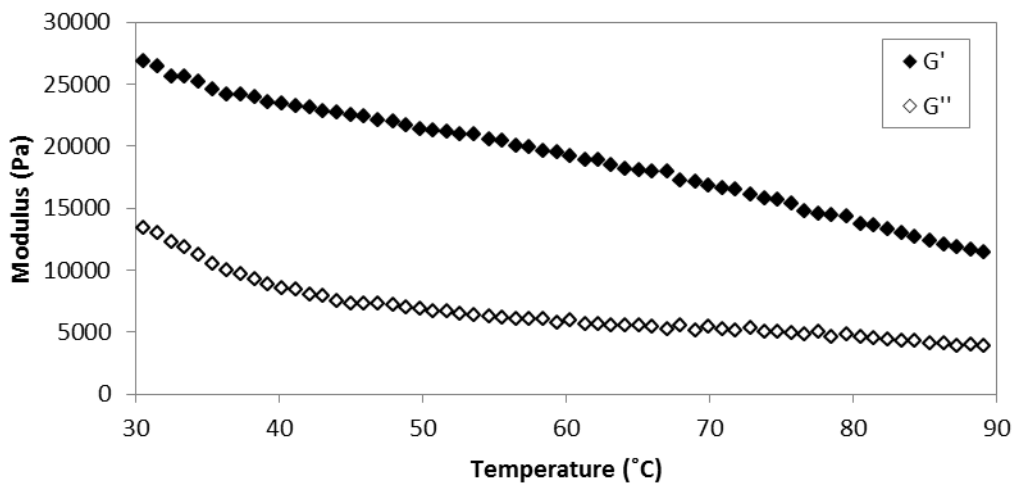
Figure 6.2: Temperature ramp of cooked caramel at an oscillatory stress of 5 Pa.

The caramel deposit structure was assessed by rheology after soaking in Advantis 210 for 10 minutes at a concentration of 2.5 and 5 %, at 30, 50, 70 and 80˚C. Figure 6.3 illustrates the effect of (I) no soaking, and soaking the deposit in 2.5 % (II) and 5 % (III) Advantis 210 at 80°C. The Figure shows;

(i)   The deposit remains elastic at all conditions

(ii)   The moduli increase with time, suggesting the caramel structure is not stable at 80°C whether soaked in chemical or not,

(iii)   The initial value of the moduli are lower in phase III, which is lower than in phase II, which is lower than in phase I.

These finding suggest that chemical action could lower the viscosity of the deposit making it easier to be removed by cleaning fluid shear forces. However these findings also suggest that if the deposit is at high temperature and static, viscosity increases in a short space of time, 10 minutes in this case, making the deposit harder to remove by fluid shear forces
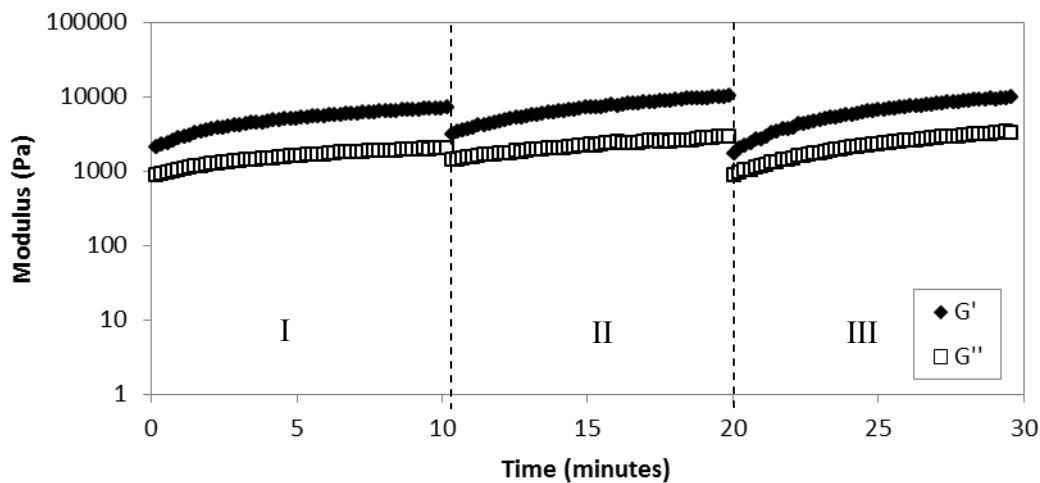
Figure 6.3: Time sweep of cooked caramel at 80˚C at an oscillatory stress of 5 Pa. I - without chemical soaking, II – soaking using 2.5 % Advantis 210, III – soaking using 5 % Advantis.

6.3 Removal of caramel from a pipe by water

This Section reveals the mass or deposit removed by the pre-rinse, turbidity and conductivity measurements of the water during cleaning of cooked caramel, and the feasibility of relating the mass removed to the turbidity measured.

6.3.1 Mass of cooked caramel removed by the pre-rinse

The caramel fouling was prepared as described in Section 3.6.1. The effect of water rinsing on the amount of caramel removed from the pipe was found by flowing 550 l of water (i.e. one full tank) through the fouled pipe, and measuring the resultant weight loss i.e. the amount removed. The temperature of the water rinse was investigated at 30, 50, 70 and 80°C, and the flow velocity was investigated at 1, 4.5 and 2 m s^{-1}. A visually clean surface was not achieved at any temperature using water alone.

Figure 6.4 shows the section of pipe fouled with cooked caramel (a) before and (b) after a pre-rinse where one full tank at 50°C was rinsed through the test section at 1.5 m s^{-1}. It can be seen that most of the deposit was removed by this pre-rinse. After each rinse when the pipe was inspected patches of caramel remained adhered to the pipe wall. This was typical. The mass of deposit on the pipe was initially 520 g (±10 g). The mass of caramel remaining on the pipe wall after the pre-rinse was 60 g (±10 g), thus 88 % of the caramel mass was removed.

Figure 6.4: Cooked caramel deposit in 0.5 m section of pipe (on left) and after a pre-rinse at 1.5 m s^{-1} at 50°C (on right).

The same volume of water was used to rinse cooked caramel deposit from the pipe at different velocities and temperatures. The mass before and after each rinse was measure; the starting mass of caramel in the pipe was 580 g ± 100 g with a standard deviation of 0.06. The mass of caramel removed by the pre-rinse as a function of (a) temperature for all of the flow velocities and (b) flow velocity for all temperatures is plotted in Figure 6.5. It clear that the mass of deposit removed was similar in all cases, and that there is no clear effect of any process variable on removal. The error in mass measured and the variation in the initial mass of deposit obscures any possible relationships between process variables, but the data suggests that any effect is not strong.
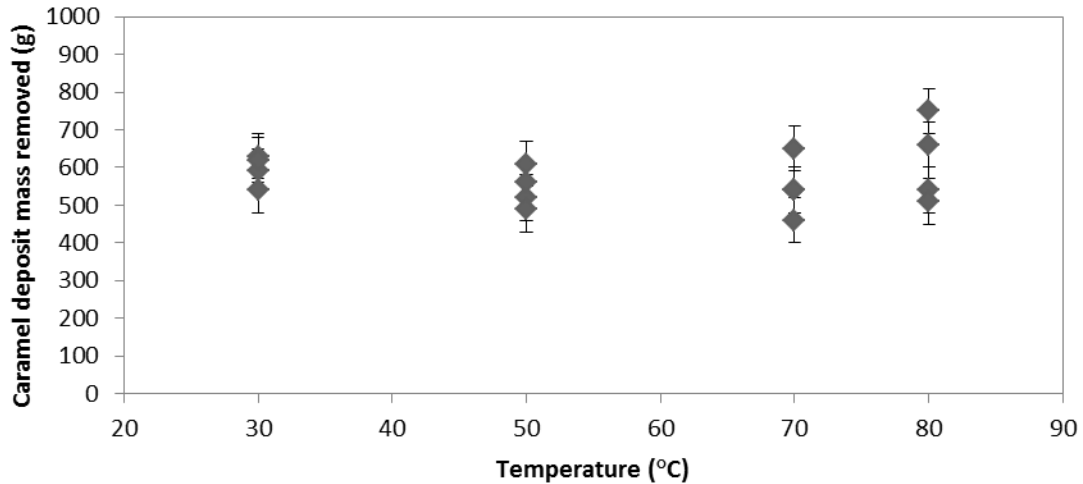
(a)
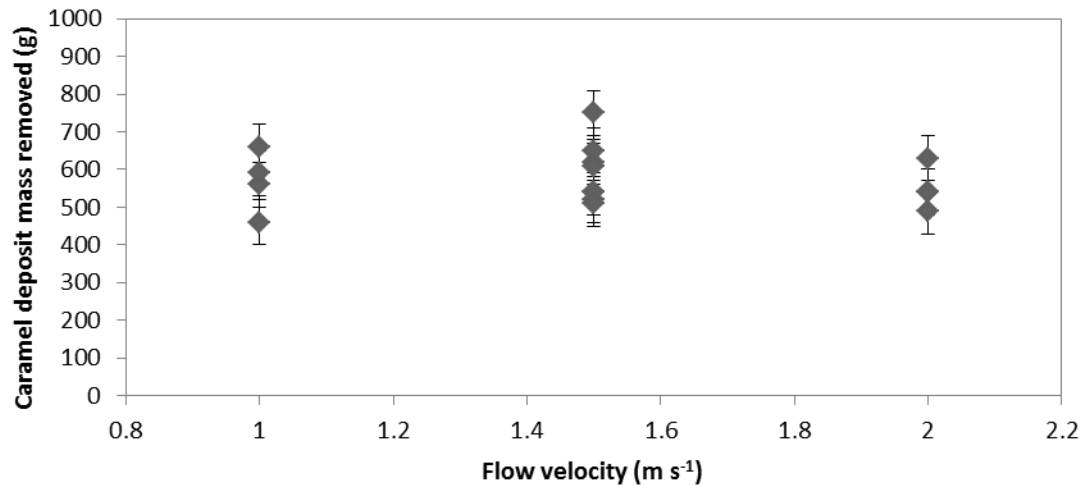
(b)

Figure 6.5: Mass of pipe and deposit after the pre-rinse vs. temperature at 1, 1.5 and 2 m s $^{-1}$.

6.3.2 Conductivity and turbidity measured during water rinsing

A change in conductivity was not measured in most cases of water rinsing caramel deposit. At the start of a small number of runs a sudden increase in conductivity (to 0.3 mS cm^{-1}) was observed before the value dropped suddenly and became constant at 0.16 mS cm^{-1}. The position of the conductivity probe may be too far from the fouled pipe to monitor a clear change in conductivity due to caramel removal. As such conductivity was not used to monitor caramel removal in this case.

Turbidity measured during the pre-rinse

Pre-rinse water was monitored by a turbidity sensor positioned approximately 1 m from the outlet of the fouled pipe. An example of a turbidity profile is shown in Figure 6.6. The Optek and Kemtrak systems measure parts per million (ppm) and formazin turbidity unit (FTU) respectively, and are described in Chapter 3, Section 3.3.2. Figure 6.6 shows the readings for the removal of caramel conducted at 1.5 m s^{-1} and 50°C. Maximum turbidity measured was 241 ppm and 550 FTU for the Optek and Kemtrak probes respectively. During the first 53 s of the rinse the Optek probe was saturated. A reduction in pre-rinse water turbidity is observed at approximately 25 s for the Kemtrak probe and at approximately 53 s for the Optek when the probe was no longer saturated. This point is termed the "point of de-saturation" throughout this Chapter. At this point turbidity was ca. 50 FTU. Turbidity values measured in FTU monitored all of the caramel removed during the water rinse.
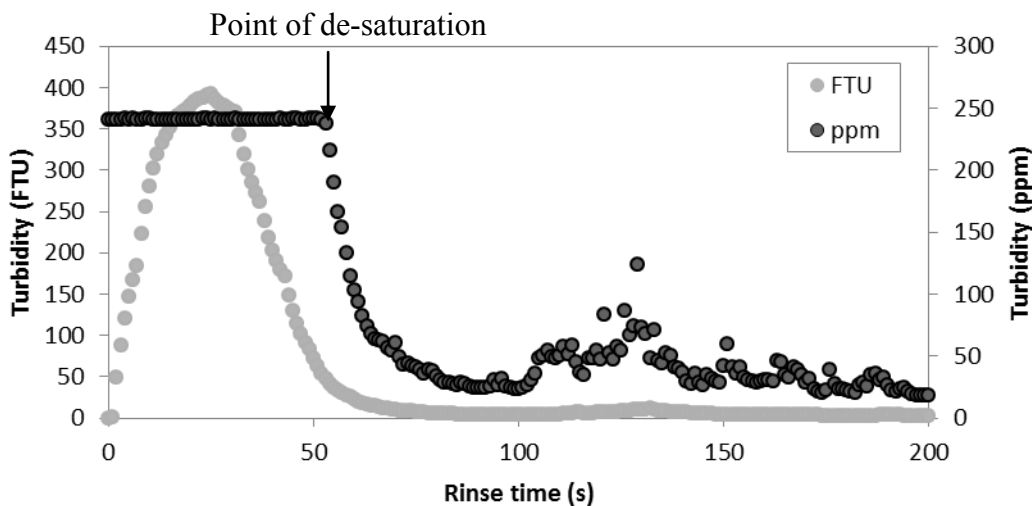
Figure 6.6: Pre-rinse of cooked caramel at 1.5 m s^{-1}, 50°C monitored by turbidity (point of de-saturation labelled).

Turbidity measured during water circulation

Water was circulated around the plant through the fouled section for a total of 100 h at (a) 30 and (b) 70°C. The turbidity profiles are shown in Figure 6.7. The flow velocity at a particular time is indicated in each Figure. Because a fixed volume of water was circulated around the plant the turbidity was seen to increase during each circulation as caramel was being removed. When turbidity drops suddenly to low values, this indicates a point in the experiment where the pump was stopped and the test section drained and opened to observe and weigh the pipe and the deposit. Deposit was remaining in the pipe after both circulations. However, this amount was not quantified and so cannot be compared to the mass removed by the pre-rinse.

Circulating water at 1.5 m s^{-1} revealed saturation or an increase in turbidity at both 30 and 70°C indicating deposit was removed. 50 g (±10 g) of deposit was removed overall when at 30°C and 70 g (±10 g) of deposit was removed overall at 70°C; this was in 50 minutes. The increase in turbidity is greater at 70°C than at 30°C. The turbidity profile suggests more deposit is removed at 70°C than at 30°C, which was the case. Circulating water at 1 m s^{-1} revealed more deposit removed at 70°C than 30°C. 30 g (±10 g) of deposit was removed at 70°C whereas 10 g (±10 g) was removed at 30°C. However the circulation time was 30 minutes longer at 70°C than at 30°C. Circulating water at 2 m s^{-1} was done at 30°C. The ppm value can be seen to increase and saturate suggesting caramel was removed by increasing the flow velocity. As mentioned in the previous Section, the masses are only accurate ± 10 g.

(a)

(b)
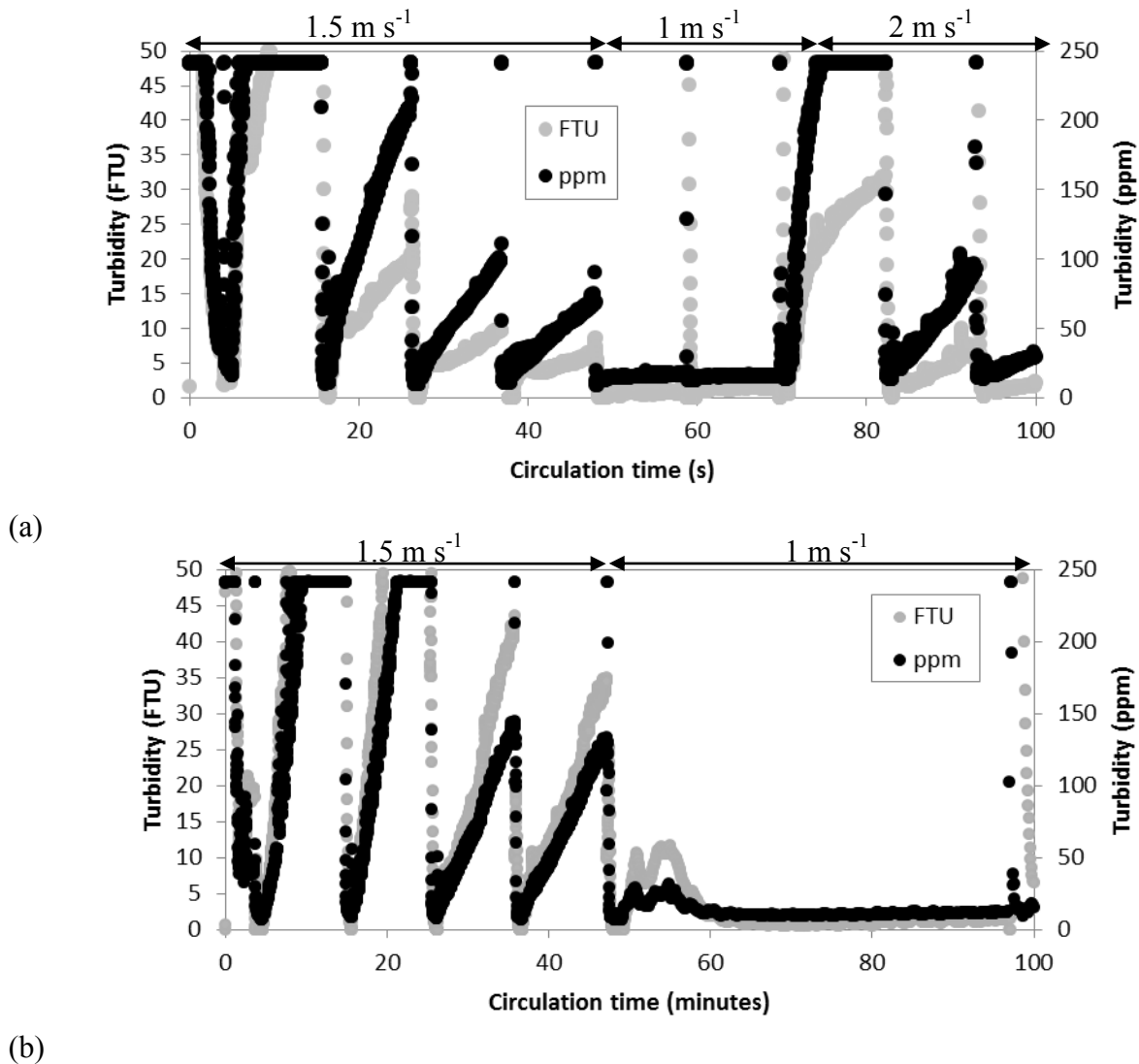
Figure 6.7: Turbidity of water (in FTU and ppm) measured when carmel was removed from the fouled pipe during water circulation at (a) 30 and (b) 70°C. The flow velocity is indicated in each Figure.

6.3.3 Integration of FTU during the pre-rinse.

Turbidity data could be used to monitor caramel deposit removal. Figure 6.8 illustrates the integration of FTU values during the pre-rinse, FTU_{pr} (defined in equation [6.1]) vs. deposit mass removed.

$$FTU_{pr} = \int_{t_0}^{t_{end}} \frac{FTU}{(t_{end} - t_0)} \, dt \qquad\qquad [6.1]$$

Where t_0 is the start time of the experiment (when the pump starts running) and t_{end} is the end of the experiment (when the 550 l of water was rinsed through the test section). FTU_{pr} is thus defined as the sum of FTU over this time divided by the time difference from t_0 to t_{end}. There appears to be a relationship between integrated FTU and mass of caramel removed at both flow 1 and 2 m s^{-1}. The data however is limited and the error large so the finding is not conclusive. Measurement of mass at more frequent time points during rinsing would provide more information on the relationship between FTU measured and mass of deposit removed during water rinsing. This relationship is explored using chemical rinsing data in Section 6.4.
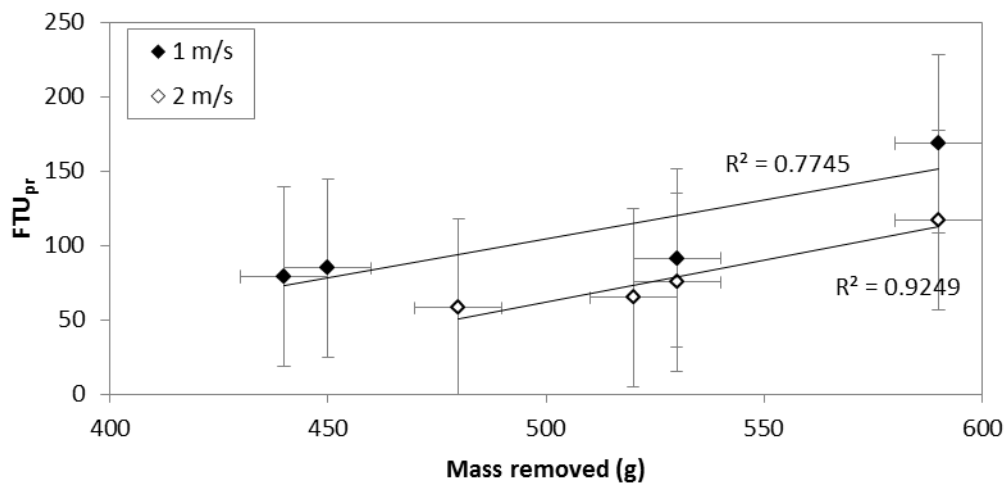
Figure 6.8: FTU integration vs. Mass of deposit removed during the pre-rinse.

6.3.4 Rates of removal during the pre-rinse

A relationship between turbidity and mass of deposit removed during a rinse could exist, as shown in the precious Section. Whether turbidity data could be used to indicate rates of removal is discussed here. A similar point in each experiment can be indicated i.e. the point of de-saturation of the Optek probe. Upon de-saturation of turbidity measurement, a similar amount of mass is being removed from the pipe. The rate of turbidity decrease could indicate if higher temperatures and flow velocities remove the caramel faster. However the results are only indicative due to the lack of repeats. Figure 6.9 shows ppm and FTU values monitored from the point of de-saturation at (a), (b) 1 m s^{-1} (c), (d) 2 m s^{-1} (at 30, 50, 70 and 80˚C). The data in Figure 6.9 shows at 1 m s^{-1} an increase in temperature tends to decrease turbidity more quickly, more so at 70 than 80°C. At 2 m s^{-1} a decrease in turbidity is quicker at 50 and 80°C and turbidity values monitored at 30 and 70°C appear similar. Both types of turbidity measurement (ppm and FTU) give similar indications at least.
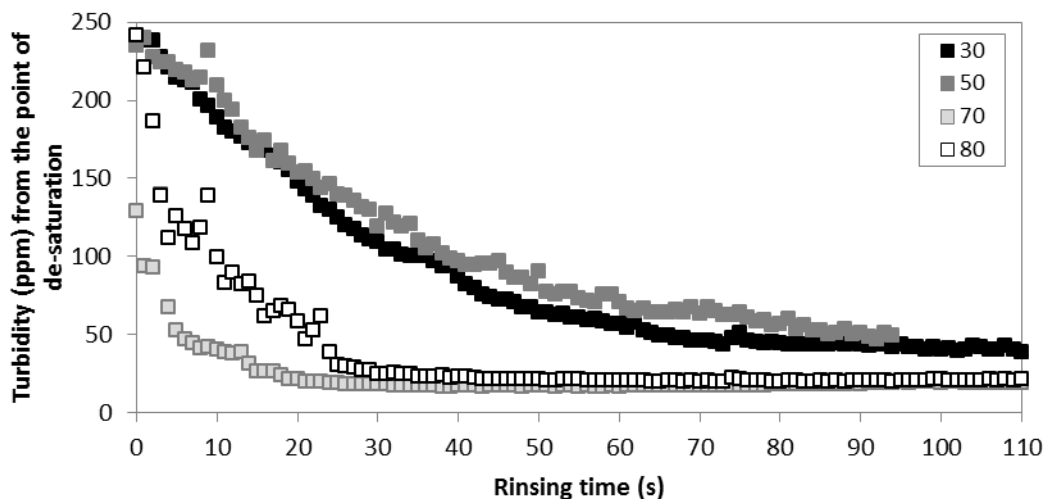
(a)

Figure 6.9: Turbidity values from the point of de-saturation (see Figure 6.6) during water rinsing at (a), (b) 1 m s^{-1} & (c), (d) 2 m s^{-1}.
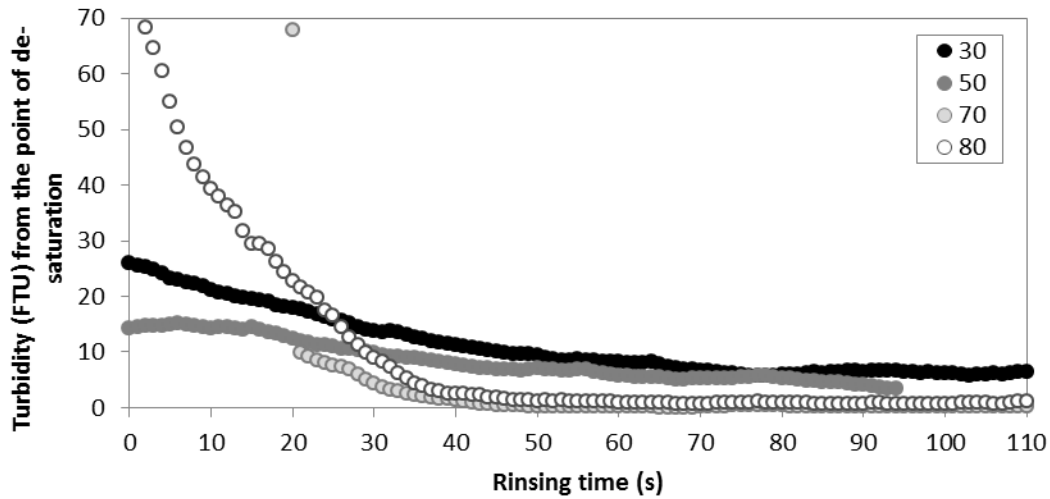
(b)
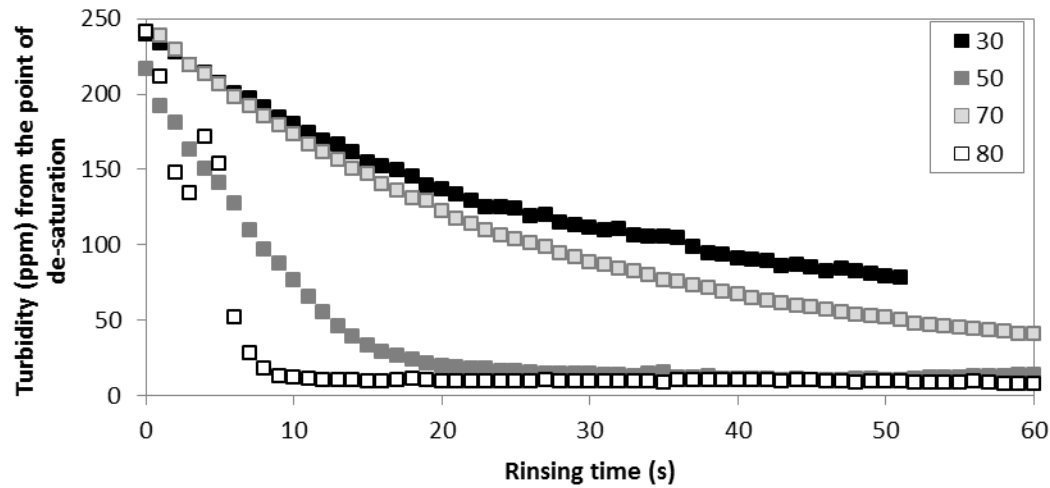
(c)
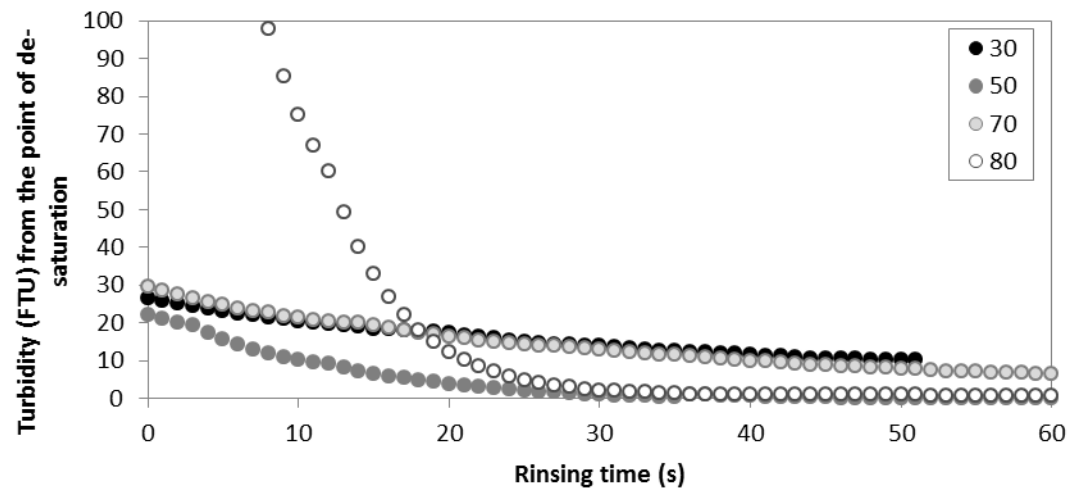
(d)

Figure 6.9 continued: Turbidity values from the point of de-saturation (see Figure 6.6) during water rinsing at (a), (b) 1 m s^{-1} & (c), (d) 2 m s^{-1}.

6.4 Chemical removal of a patch of caramel

Pilot plant experiments revealed that water could not rinse the caramel completely from the pipe to give a visually clean surface. As such caramel rinsing from coupons using water was not investigated. The caramel was cooked onto coupons and weighed as described Chapter 3, Section 3.6.2. The removal of caramel at 0.5 m s^{-1} at 30, 50, 70, and 80°C using 2.5% Advantis 210 is illustrated in Figure 6.10 (a) – (d). The images illustrate the removal behaviour of caramel during 1 hour of chemical circulation. The colour of the caramel was seen to lighten as cleaning progressed. This can be seen in Figure 6.10. This colour change was gradual in all cases, indicating deposit re-hydration with increasing cleaning time. No deposit was removed in any case until the deposit became lighter in colour.

An example of caramel removal in the cleaning rig measured by area (mm^2) and U (kW m^{-2} K^{-1}) during chemical circulation at 50°C, 0.5 m s^{-1} (using 2.5 % Advantis 210) is shown in Figure 6.11. Removal occurred by fracture of the deposit in the flow. This was seen in the other cleaning experiments. It can be seen that a substantial amount of caramel is not removed until sometime between 600 and 1200 s. The area removed becomes constant between 1800 and 2400 s and remains constant after 2400 s until 3600 s suggesting no more deposit is removed at these conditions; i.e. an increase in temperature or conductivity is required to remove further deposit.
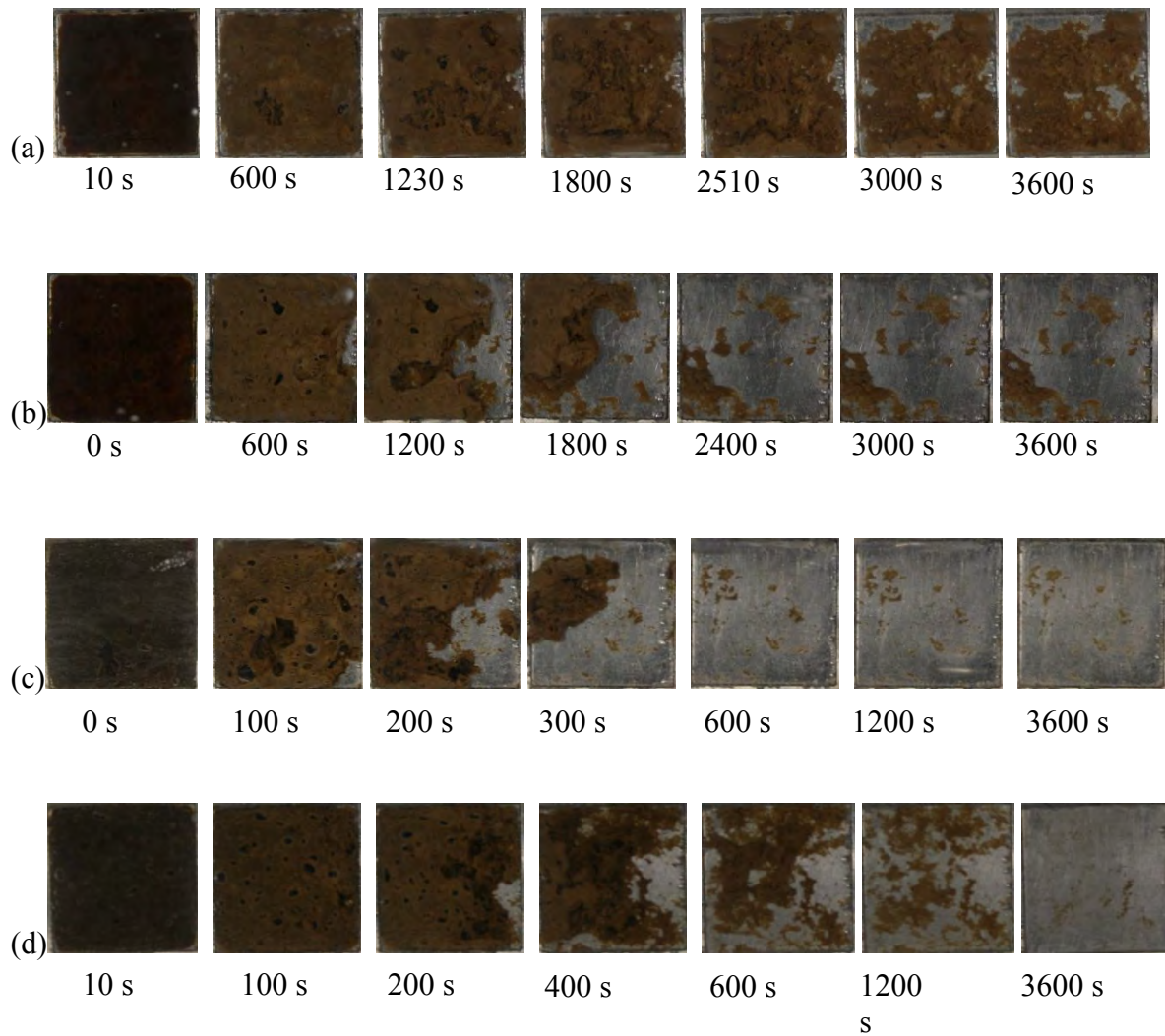
Figure 6.10: Images taken during cooked caramel removal at 0.5 m s^{-1} using 2.5 % Advantis 210 (47 mS cm^{-1}) at (a) 30°C, (b) 50, (c) 70 and (d) 80°C. The caramel is brown and the coupon is grey. Time interval is indicated on each image.
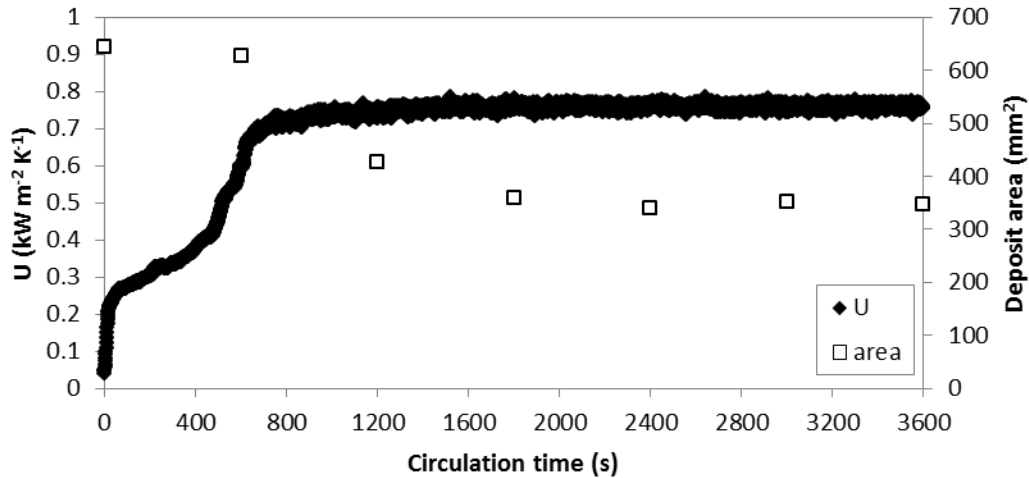
Figure 6.11: Caramel removal at 50°C, 0.5 m s^{-1} measured by U and area, during chemical circulation using 2.5 % Advantis 210 (47 mS cm^{-1}).

The removal of caramel from the coupon was studied at 0.5 m s^{-1} using Advantis 210 detergent at 2.5 % (during the 1st hour of circulation) and at 5 % (during the 2nd hour of circulation). The average area of deposit removed at 30, 50, 70 and 80°C vs. circulation time is illustrated in Figure 6.12. It can be seen from the Figure that;

(i)   Cleaning at temperatures lower than 80°C does not give a visually clean surface. The visually clean surface was achieved using 2.5 % Advantis.

(ii)   Cleaning at 30°C removes significantly less deposit than at higher temperatures using both 2.5 % and 5 % Advantis 210. Increasing the concentration to 5 % revealed only incremental removal, 20% of the deposit area (625 mm^2) was removed.

(iii)   Cleaning at 50 and 70°C appears to remove a similar amount of deposit using 2.5 % Advantis, and significantly different amounts using 5 %. Advantis. More deposit was removed at 70°C than at 50°C.

(iv)   Increasing the temperature significantly increases the rate of deposit removed using 5 %

        Advantis. Rinsing at 80°C gave the fastest deposit removal at both concentrations.
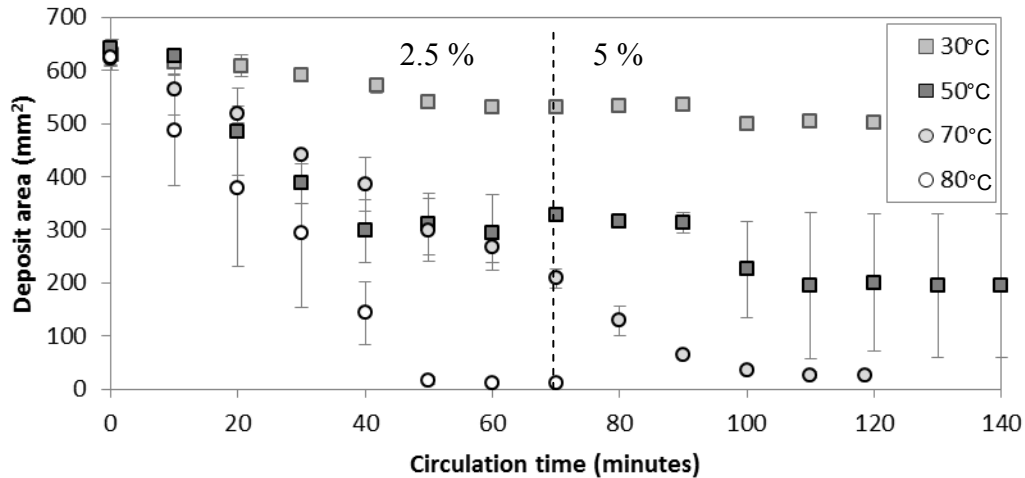
Figure 6.12: Rinsing of cooked caramel at 0.5 m s-1 at 47 mS cm^{-1} (2.5 % Advantis) to 85 mS cm^{-1} (5 % Advantis) at 30°C, 50°C, 70°C and 80°C (2 repeats of each). The dashes line separates the two 1 h chemical circulations at the two different concentrations.

Figure 6.13 illustrates the area of deposit removed vs. Re for all temperatures investigated. As

Reynolds number is increased the area of deposit removed increases. This is true at both chemical

concentrations. It also appears that more deposit is removed using 2.5% Advantis rather than 5 %

Advantis. This finding suggests that increasing the chemical concentration does not increase the

amount of deposit removed.
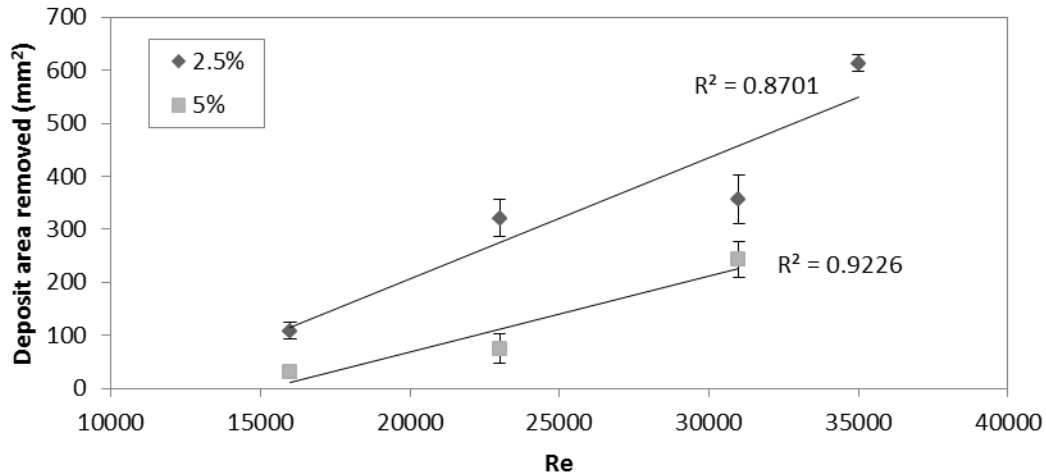
Figure 6.13: Deposit area remaining vs. Re for all temperatures.

R_d is calculated from the heat transfer coefficient at time t (U_t) and the time when a clean surface is achieved (U_c) according to Equation 4.1. In this case because a clean surface was not achieved in all cases, R_d is inversely proportional to U_x, the heat transfer coefficient at the time where no further deposit was removed, determined from U_t values of the last portion of each rinse (at least 1 minute) minus 1 standard deviation. Average R_d values are of 2 repeats. Figure 6.14 shows that the removal profile measured by the MHFS at each temperature is similar. Area profiles show that removal at 30°C and 80°C is significantly different.
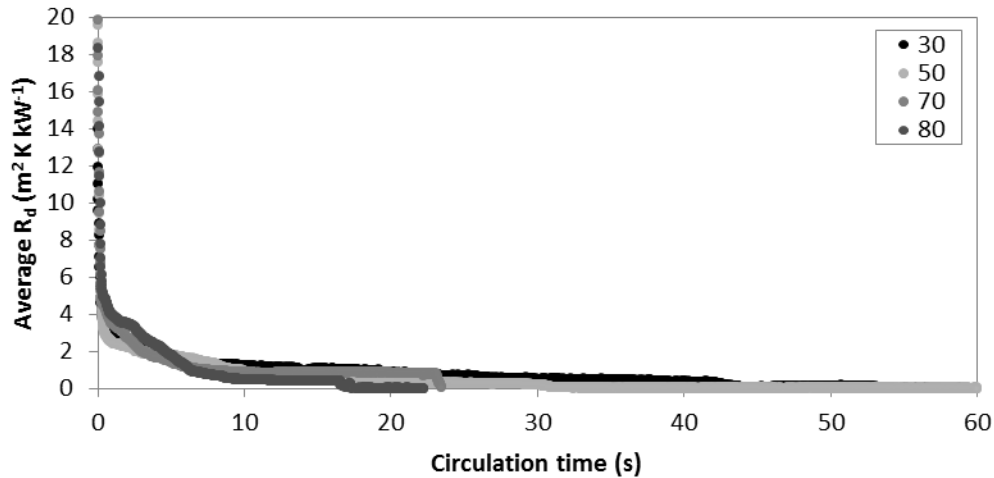
Figure 6.14: Average R_d removal profiles of caramel vs. circulation time at (a) 30, (b) 50, (c) 70 and (d) 80°C.

6.5 Chemical removal of caramel from a pipe

The removal of the remaining material after the pre-rinse was studied using Advantis 210 detergent (Ecolab, Cheadle) at 2.5 %. The experiments conducted and the masses recorded are listed in Table 6.1. The deposit mass was measured after chemical cleaning phases by rinsing the test section with water (using route 2, see Appendix, Table C.2), draining and removing the pipe. The pipe was replaced in the same position in the pipe work and the experiment continued. Caramel mass was recorded in three places;

(a) After the pre-rinse – discussed in Section 6.3.1.

(b) After the 1st detergent circulation - caramel was removed from the pipe by detergent circulation, 2.5 % Advantis, in a closed loop for 1 h (using route 5a, see Appendix, Table C.2).

(c) After the 2nd detergent circulation - caramel was removed from the pipe by detergent circulation, 2.5 % Advantis, in a closed loop for 1 h (using route 5a, see Appendix, Table C.2).

Table 6.1: Summary of mass removed during caramel circulation (circ) experiments using Advantis at 1 and 2 m s-1 at 30, 50 and 70°C. The starting mass (due to pre-rinse) for each experiment indicated. Masses accurate ± 10 g.

Mass on pipe wall after pre-rinse (g)	Temperature (°C)	Caramel mass removed (g) 1 m s^{-1}		Mass on pipe wall after pre-rinse (g)	Temperature (°C)	Caramel mass removed (g) 2 m s^{-1}	
		1st circ	2nd circ			1st circ	2nd circ
150	**30**	60	20	30	**30**	20	10
30		10	0	140		11	10
80	**50**	50	10	80	**50**	60	10
40		0	0	20		20	0
30	**70**	10	0	20	**70**	10	10
10		0	0	40		30	10

It can be seen from Table 6.1 that 0 g of deposit was removed in some cases. During these rinses the colour of the circulating water did have a brown tint and a change in turbidity was seen. Because the scales are only accurate to ± 10 g deposit may have been removed but not measured by mass. Also the initial mass of deposit for the detergent circulations has a large variability. The lowest stating mass was 10 g (± 10g) and the highest 150 g (±10 g). This means results presented in the next Section will have a large error and the final mass may be a result of the starting mass rather than the cleaning conditions.

6.5.1 Deposit mass removed by detergent circulation

Figure 6.15 shows the relationship between the mass present on the pipe wall at the start of each chemical circulation experiment and the final mass at the end of each detergent circulation phase

for all temperatures and flow rates. It does appear that the initial and final mass of deposit is correlated; the larger the starting mass the larger the final mass. A relationship between temperature, concentration and area removed was determined on the lab scale, discussed in Section 6.4, where increasing the temperature and flow velocity increased the area of deposit removed. To determine a relationship between chemical temperature and flow velocity on the pilot plant scale the mass of deposit removed would have to be investigated separately from pre-rinsing. A visually clean surface was achieved at 80°C, 2 m s^{-1} on the pilot plant scale similarly to on the lab scale (2 repeats). Rinsing at 1 m s^{-1}, 80°C was not tested.
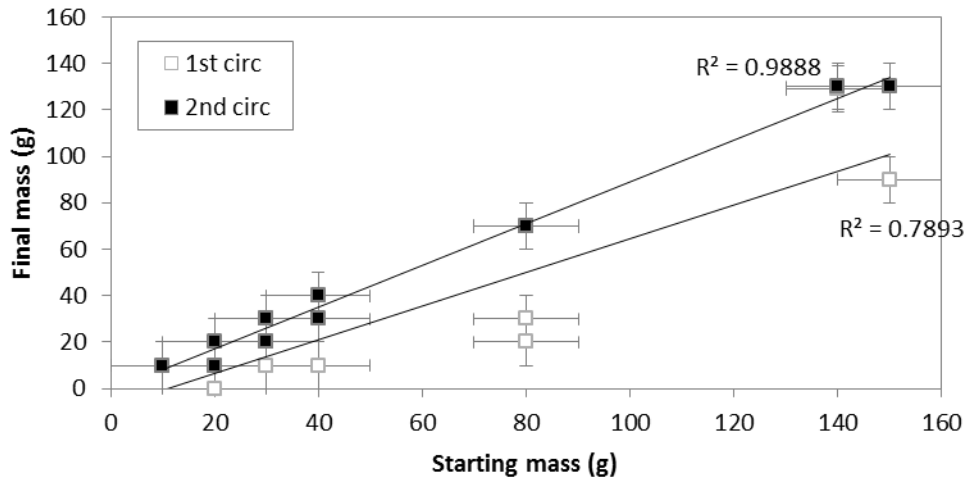
Figure 6.15: The relationship between the mass of deposit at the start of detergent circulation (starting mass) and the mass after detergent circulation (final mass).

Figure 6.16 indicates the average mass of deposit measured at (a) 1 m s^{-1} and (b) 2 m s^{-1} for;

(i)   0 – at time zero, prior to detergent circulation,

(ii)   1 – after the 1st detergent circulation,

(iii)   2 – after the 2nd detergent circulation.

It is clear that at each temperature and flow velocity, as the circulation time is increased, the amount of deposit remaining on the pipe wall decreases as expected. Even though the experiments were conducted at random, unfortunately the initial mass was larger at lower temperatures and smaller at higher temperatures so relationships cannot be sensibly drawn between flow velocity and temperature during chemical removal of caramel. Although the final mass remaining at all temperatures and flow velocities was 10 g or less suggesting that whatever the temperature or flow velocity the same amount of caramel will reaming in the pipe when subjected to two hours 2.5% chemical treatment. The error needs to be minimised by having a similar starting mass of caramel in the pipe (±10 g) for a relationship between chemical temperature and flow velocity to be seen. This means that chemical effects and water effects need to be studied in greater numbers and or separately in the pilot plant. Measuring a small amount of deposit removed from a large mass of pipe will undoubtedly give a large error.
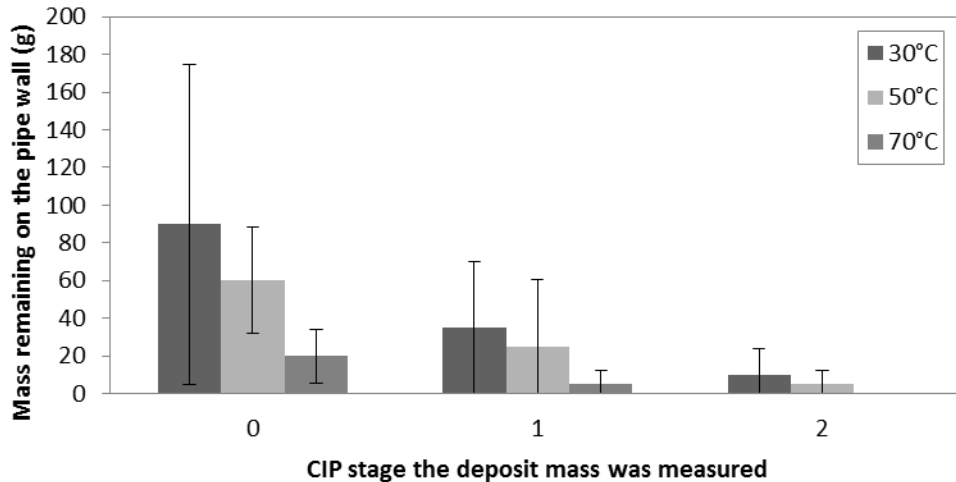
(a)
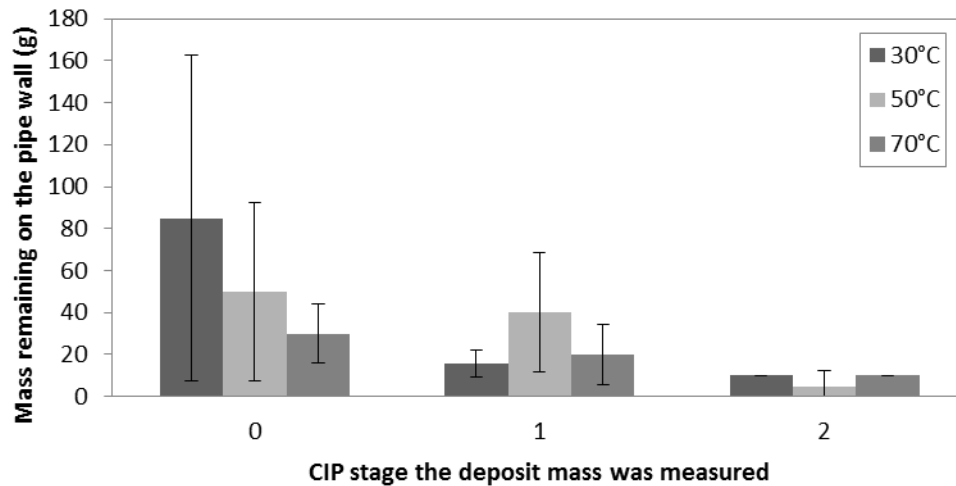
(b)

Figure 6.16: Mass of caramel remaining in the pipe after 0 (indicated on horizontal axis) – the pre-rinse, 1 (indicated on the horizontal axis) – the 1st detergent circulation and 2 (indicated on the horizontal axis) – the 2nd detergent circulation.

6.5.2 The effect of deposit mass on turbidity

Chemical removal of caramel deposit at 2 m s^{-1} is illustrated in Figure 6.17 at (a) 30, (b) 50 and (c) 70°C. The weight of caramel removed during each phase is different and indicated on each graph. The Figure shows;

(i) ppm values measured during each rinse were constant at 241 ppm i.e. the probe was saturated indicating either the deposit was removed immediately or the mass of deposit the probe can detect effectively is less than 30 g.

(ii) FTU values measured were seen to increase at all temperatures gradually, indicating the deposit was removed gradually. This is expected because the amount of deposit in the bulk flow increases with circulation time.

(iii) FTU measured after 1 h was approximately 550 FTU at 30°C, 440 FTU at 50°C and 35 FTU at 70°C. This value will be related to the mass of caramel deposit removed, which was 110 g at 30°C, 60 g at 50°C and 30 g at 70°C.

An increase in FTU may not be a clear indication of removal because an increase in FTU values can mean either;

(i) a portion of caramel is removed from the pipe wall and is measured by the probe in the bulk flow, indicating an actual measurement of deposit removal from the pipe, or

(ii) a chunk of caramel already in suspension dissolves into smaller particles within the measuring size range of the probe. In this case deposit is not actually removed although the increase in turbidity suggests deposit is removed.

(a)

(b)

(c)
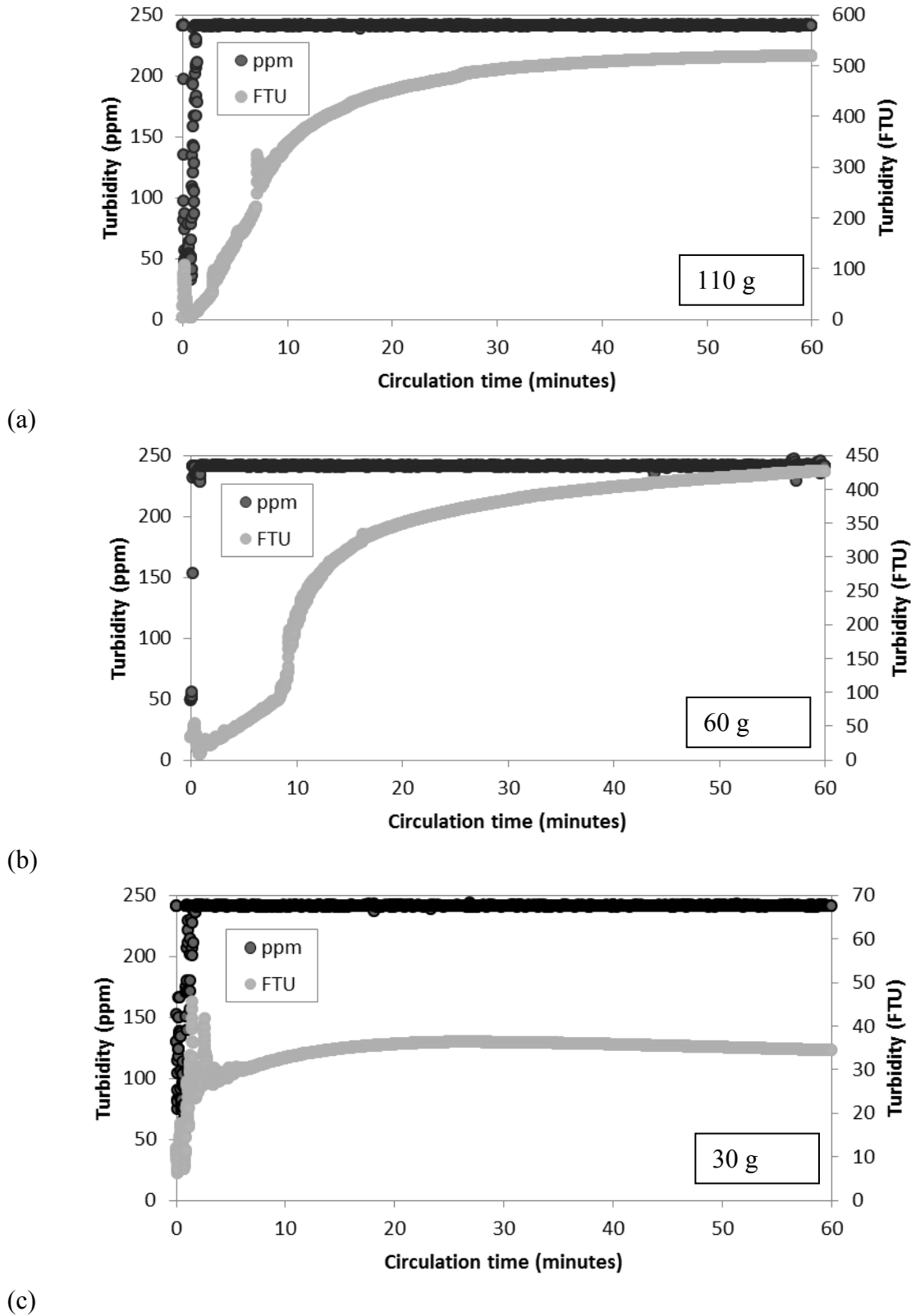
Figure 6.17: Turbidity monitored during chemical circulation at 2 m s^{-1} (2.5% Advantis) at (a) 30, (b) 50 and (c) 70°C. The mass of caramel removed is indicated in each case.

Mass measured is only accurate ± 10 g. If the Optek turbidity probe gives different turbidity values during chemical rinses found to remove 10 g, the sensitivity of mass measurement (± 10 g) may be enhanced in the future. Figure 6.18 shows ppm values measured during three consecutive chemical circulations indicated as I, II and III. The conditions of each circulation are:

(I)   Flow velocity 2 m s^{-1}, 70°C, 10 g of deposit was removed

(II)   Flow velocity 2 m s^{-1}, 70°C, 10 g of deposit was removed

(III)   Flow velocity 2 m s^{-1}, 80°C, 0 g was removed.

Ppm values measured during chemical circulation (I) indicate that more than 10 g was removed because the probe was saturated at 241 ppm. During chemical circulation (II) less than 10 g of deposit may have been removed because the probe was not saturated. A gradual increase in ppm values from 23 to 52 ppm can be seen. During chemical circulation (III) more than 0 g of deposit may have been removed because ppm values increased gradually from 34 to 46 ppm. The pipe was not visually clean until after circulation (III) so removal must have occurred during this phase.
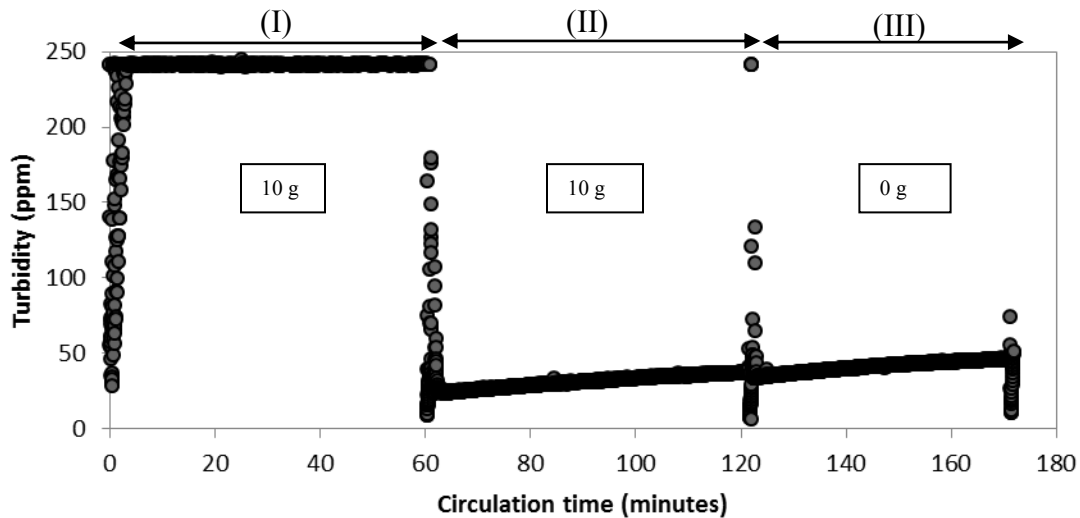
Figure 6.18: ppm values measured during three detergent circulations; I and II at 70°C; III at 80°C.

6.5.3 The effect of flow velocity and temperature on turbidity

Figure 6.19 illustrates the turbidity measured when the same amount of caramel removed was (10 g $\pm$ 10 g) during chemical circulation at 1 and 2 m s^{-1} at (a) 30, (b) 50 and (c) 70°C. The Figure shows that the removal profile is different in each case.

FTU values measured at 1 m s^{-1} increase and decrease during chemical circulation. The flow rate and conductivity were consistent at all three temperatures at 1 m s^{-1} ($\pm$ 0.2 m s^{-1}) and 45 mS cm^{-1} ($\pm$ 2 mS cm^{-1}) respectively. Rinsing at 1 m s^{-1} may not provide sufficient flow through the pipe to measure turbidity accurately. When rinsing at 1 m s^{-1} the deposit removed from the pipe may be deposited further downstream from the test section. This means lower FTU values would be measured over the remaining circulation time even though the same amount of caramel was removed in each case. Figure 6.19 shows the maximum FTU value during 1 m s^{-1} circulations was higher if the temperature was higher. This may suggest that at low floe velocity, using higher rinse temperatures keeps the caramel removed from the test section in suspension.

FTU values measured during circulations at 2 m s^{-1} tend to increase as circulation time increases which is expected as deposit removal is gradual. However the maximum value of FTU obtained at each temperature in 1 h when a similar mass is removed is different. This is 59 FTU at 30°C, 425 FTU at 50°C and 20 FTU at 70°C. There is no decrease in FTU during each rinse suggesting caramel removed from the pipe remains in the bulk flow.
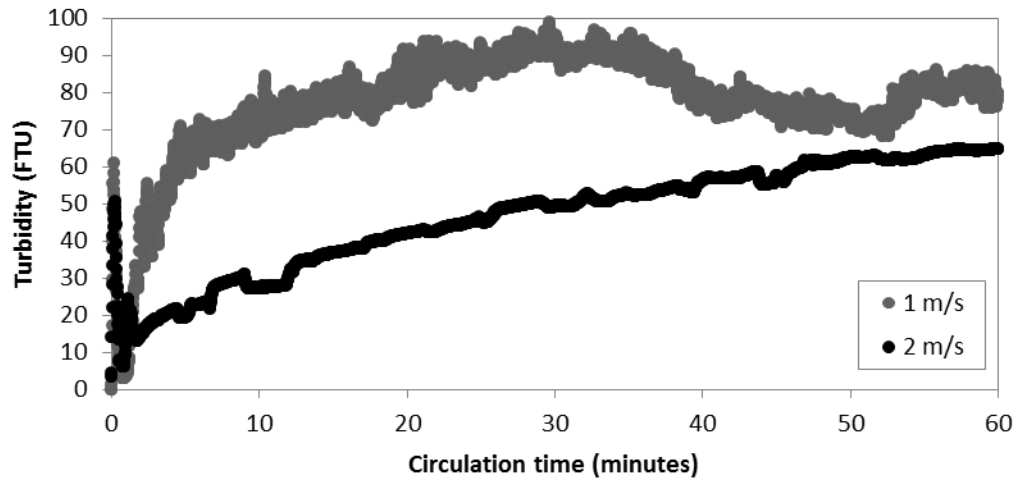
(a)
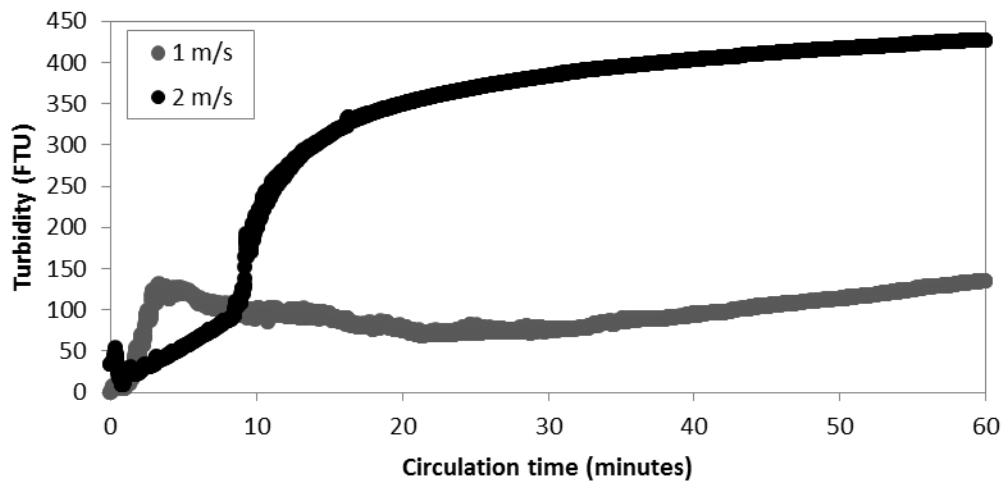
(b)
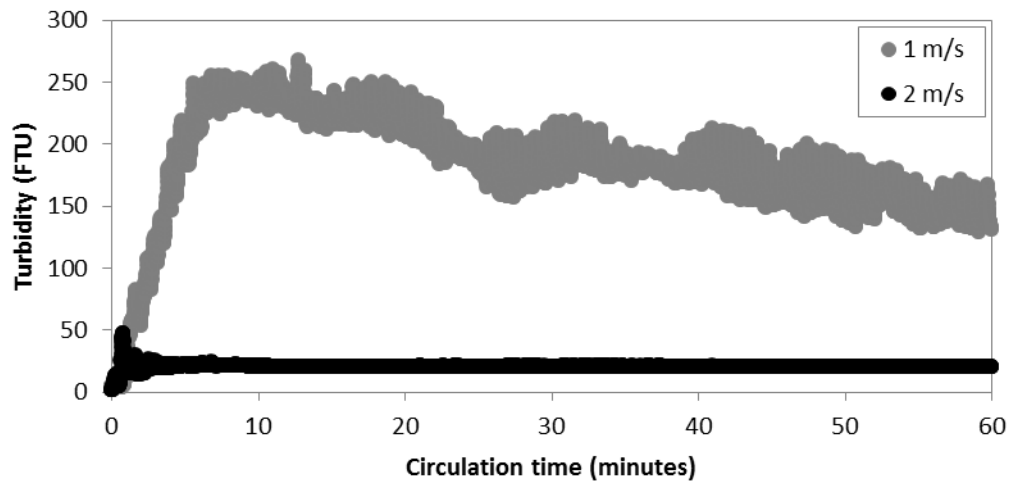
(c)

Figure 6.19: FTU values measured at 1 and 2 m s^{-1} at (a) 30, (b) 50 and (c) 70°C. 10 g of caramel was removed in all cases using 2.5 % Advantis.

6.5.4 Integration of turbidity measurements

The integration of FTU (defined as $FTU_{tcirc-to}$ in equation [6.2]), from the start of detergent circulation, t_0, to the end of detergent circulation, $t_{circ,}$ was calculated by equation 6.2:

$$FTU_{tcirc-to} = \int_{t0}^{tcirc} \frac{FTU}{(t_{circ} - t_o)} \, dt \qquad\qquad [6.2]$$

FTU integrated over the circulation time was plotted against the mass of deposit removed, as in the data shown in Figure 6.8 to determine if a relationship was present, in Figure 6.20 at 1 m s^{-1} and 2 m s^{-1}. It is clear that at 1 m s^{-1} there is no relationship. However at 2 m s^{-1} there is a strong relationship. The lack of correlation at 1 m s^{-1} can be explained by insufficient flow in the pipe work for a long period of time leading to inaccurate FTU values.
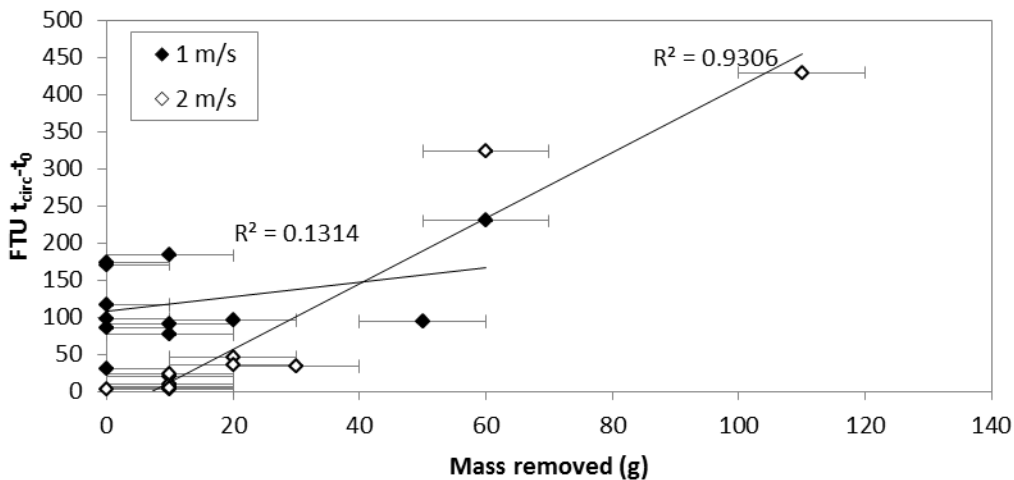
Figure 6.20: $FTU_{tcirc-t0}$ vs. Mass of deposit removed during detergent circulations at 1 m s^{-1} (R^2 0.13) and 2 m s^{-1} (R^2 0.93). Horizontal error bars indicate the mass measurement error (± 10 g).

6.6 Conclusions

Caramel becomes a type 3 soil when heated. The cooked caramel deposit is a semi solid with elastic rather than viscous behaviour. An increase in oscillatory shear stress did not reduce the viscosity of the deposit however an increase in temperature reduced yield stress and chemical soaking reduced viscosity.

The mass of cooked caramel removed by the pre-rinse was similar at all flow velocities (1, 1.5 and 2 m s^{-1}) and temperatures (30, 50, 70 and 80°C) tested. Water rinsing removed most of the deposit but not all.

The removal behaviour of a patch of caramel was effectively monitored by area at 0.5 m s^{-1} using Advantis at 2.5 and 5 %. The colour of the deposit gradually became lighter as the rinsing time was increased. An increase in temperature and Re rather than chemical concentration increased the amount of deposit removed. A visually clean surface was only achieved at 80°C. This was similar to pilot plant experiments where a visually clean pipe surface was only seen when rinsing at 80°C. On the pilot plant higher flow velocities could be investigated; 1 and 2 m s^{-1}, and 10 g of deposit or less (± 10 g) was remaining on the pipe wall after 2 h our chemical circulation at all flow velocities and temperatures.

Evidence has been presented suggesting that the initial mass dictated the final mass of deposit remaining on the pipe in most cases. This effect can be mitigated in future experiments by testing the efficacy of the pre-rinse and the chemical circulation separately. The large error of experiment repeats means conclusive arguments cannot be drawn on the effect of temperature

and flow velocity on caramel removal from a pipe. Currently the conclusion is there is no significant difference.

Integration of turbidity values during removal appears to give an indication of mass of deposit removed provided the flow velocity is sufficient i.e. > 1 m s^{-1}. The integration of FTU had to be a retrospective measure of deposit removed in these cases. If integration of FTU could be monitored on line in real time eventually a consistent value would be reached indicating the cleaning phase has removed all the deposit it can. Data was also presented suggesting ppm values measured may be used in the future to enhance mass measurements of 10 g.

The findings presented here suggest there is no significant effect of temperature or flow velocity at removing caramel from a pipe during water or chemical rinsing. However on the lab scale an increase in Re and temperature increased the amount of deposit removed significantly. The recommendation made to industry it to clean using water and chemical at 80°C to ensure a visually clean surface at flow velocities > 1 m s^{-1} to ensure accurate online measurement.

CHAPTER 7: CONCLUSION AND FUTURE WORK

7.1 The importance of understanding cleaning in breweries

It is clear that it is attractive to manufacturers to minimise energy, water and effluent from CIP. Optimisation can be achieved by understanding the relationships between the different phases involved in fouling and cleaning: the deposit, the surface, cleaning time, temperature, mechanical action, and detergent concentration. The cleanability of the process line needs to be quantified by suitable measurement technologies before bench and pilot experiments can be directly applied in industry. There are un-tapped savings to be made by measuring the energy, water, chemicals and waste from CIP. Benchmarking of time, energy, water and chemicals used in one CIP regime revealed areas where CIP could be improved; the use of hot caustic was the biggest contributor to environmental impact and cost.

A summary of the literature revealed CIP is the ubiquitous method of removing unwanted fouling layers from process plant to maintain product safety and process efficiency. The classification of

cleaning problems into three types has enabled easy presentation and review of the most recent studies considering CIP parameters.

(iv)   For type 1 deposits, cleaning time seems to be related to Re. An increase in Re seems to decrease cleaning time. It was also seen that increasing the flow rate or wall shear stress and cleaning temperature to a mid range temperature (up to 50°C) decreases cleaning time.

(v)   For type 2 deposits, water rinsing parameters, temperature and wall shear stress, seemed to have a varied effects on removal. Removal behaviour seemed to be dependent on the microbial aging time on the surface. Using NaOH removed type 2 deposits in flowing systems. When considering one chemical concentration, flow and temperature seemed to have the biggest effect on removal at the start of cleaning, but it was clear that contact time was an important factor governing deposit removal.

(vi)   For type 3 deposits, an optimum NaOH concentration was found to occur in numerous studies, 0.5 wt %. However increasing wall shear stress and temperature were most beneficial to cleaning in this case.

The factors affecting the application of research in industry include cost, maintenance, product safety and product quality. The longevity of surface coatings and the traceability of enzymes out of a test system have not been fully demonstrated; as such industry cannot justify changing its current CIP operation. Cost benefit analysis of CIP is not done often; as a result the route of optimisation in unclear. Numerous methods at varied stages of commercialisation have been demonstrated capable of monitoring cleaning in the bulk and at the surface.

Chapter 3 demonstrated the feasibility of using yeast slurry to mimic both type A and type B fermenter deposits by varying the aging time. The cleaning rig can be used to study the removal of deposit film from a surface under different flow, temperature and chemical regimes and the behaviour quantified by U and deposit area measurements. The pilot plant system can be used to study bulk deposit removal under different flow, temperature and chemical regimes and the behaviour quantified by turbidity, conductivity, mass and visual observation.

7.2 Experimental findings

Experimental work can be summarised in three sections 7.2.1: Removal behaviour findings for yeast and caramel, 7.2.2: Measurement findings, 7.2.3: Industry recommendations and application.

7.2.1 Removal behaviour findings

(i) A type 1 soil: Yeast slurry removal mechanism (Type B)

The removal mechanism of yeast slurry, analogous to fermenter type B deposit, can be classified as Type 1 according to Fryer and Ateriadou (2009) when aged up to 5 hours in pipes, and on stainless steel coupons. At all flow velocities and temperatures tested yeast slurry was removed to give a visually clean surface. The visual cleaning times of the pipe and coupon also appear to be scale-able. Flow velocity has the greatest impact on removal behaviour and cleaning times. As the flow velocity was increased the cleaning time decreased. Similarly it took longer to remove the yeast slurry at the lowest flow velocity, 0.13 m s^{-1}.

Three distinct phases were identified during yeast slurry removal from coupons: (i) a lag phase, (ii) a removal phase, (iii) constant phase (no further removal or a clean surface). The lag and removal phases determine the cleaning time. Cleaning of this material was minimally affected by temperature. Consideration of the overall cleaning times revealed that as the flow velocity increased the effect of temperature became only marginally significant. The cleaning findings were supported by yeast slurry rheology, indicating increasing the oscillatory shear stress decreased viscosity. At higher flow rates the deposit is simply forced out of the pipe quicker. The viscosity of the yeast slurry is sufficiently low that no yeast film remains on the inner pipe surface when rinsed. Micromanipulation data suggested yeast slurry was adhesive, however at the minimum flow rate, 0.13 m s^{-1} the adhesive force was over come.

(ii) A type 2 soil: Fermenter deposit removal behaviour (Type A)

Removal of aged yeast slurry, analogous to fermenter type A deposit requires chemical action for complete removal. As such this deposit can be classified as a type 2 deposit. There are three characteristic phases for water and chemical rinsing, similar to type B deposit: (i) lag time, (ii) removal phase, (iii) constant phase (no further removal or clean surface). Rheology suggests that the deposit is shear thinning at all the test temperatures. Viscosity was seen to decrease with increasing shear rate. The addition of 2% Advantis 210 to industrial type A deposit reduced viscosity significantly compared to 0.2% Advantis and water (at low shear rates).

At constant low shear stress (0.4 Pa) the deposit became more elastic with increasing temperature suggesting it would be harder to move at higher temperatures without chemical treatment. Water rinsing did not reveal a clean surface. Generally speaking increasing the temperature decreased

lag time. An increase in flow velocity did not necessarily decrease the lag phase time. An increase in temperature up to 50°C seemed to minimise the removal phase up to 50°C. At 70°C the amount of deposit removed did not become constant. Most deposit was removed at 30 and 50°C. Flow velocity had no significant effect on the overall removal profiles except at 70°C where an increase in flow velocity did not remove deposit as quickly as the other flow velocities. Chemical rinsing did reveal a clean surface at all test temperatures and flow velocities. Rinsing at 70°C gave the quickest cleaning times at both NaOH concentrations and all flow velocities. The effect of chemical concentration was evident at low flow velocity. At higher flow velocity, 0.5 m s^{-1}, the effect of temperature became most significant.

(iii) A type 3 soil: Cooked caramel deposit removal behaviour

Viscosity measurement of caramel deposit revealed a semi solid material with elastic rather than viscous behaviour. An increase in oscillatory shear stress did not reduce the viscosity, chemical soaking did. An increase in temperature also reduced viscosity. Most of the caramel was removed by the pre-rinse in experiments. However the conditions of the pre-rinse did not have a significant effect on the amount of caramel removed from the pipe.

During detergent circulations, a visually clean surface was not achieved at temperatures less than 80°C in both pilot and lab scale experiments. An increase in concentration from 2.5 % Advantis to 5 % Advantis did remove more deposit at lower temperatures, 30, 50 and 70°C, however a visually clean surface was not achieved during 1 h of rinsing at 0.5 m s^{-1}. The cleaning temperature appears to be the most important factor in chemical rinsing. Temperature and chemical combinations may also be proportional. In this case as the temperature was increased

the amount of chemical required decreased. An increase in concentration is not desired in industry CIP because this increases CIP cost, increases H & S risk and environmental impact. Cleaning hotter at lower concentration is more desirable as latent heat from other processes in a plant, especially in a brewery, can be used to heat the CIP fluid. Also energy can be generated from renewable sources.

7.2.2 Measurement findings

Measurement of yeast removal from surfaces was not effectively measured using a heat flux sensor by U, or by offline automatic image analysis as in the work of Christian (2004) and Aziz (2008). This is because the aged yeast deposit changed colour during cleaning so automatic analysis was not possible. This also caused problems because the deposit and the surface could not be differentiated in grey scale. The series of images in each experiment was analysed manually as discussed in Chapter 3 Section 3.2.4. Automatic analysis could have worked for yeast slurry and caramel however was not used in this case because the images could be analysed quickly by the protocol set up for the aged yeast slurry.

Conductivity could not be used consistently to measure yeast or caramel removal in this case. This is because the volume of deposit relative to the volume of water used in cleaning was very small. Conductivity measurement may be valuable when cleaning meters of pipe or tanks with water. Measurement of yeast removal from 1 m pipe was trended well by turbidity and did indicate the cleaning time of the whole system accurately. The integration of turbidity during each cleaning phase also appeared to give an indication of mass of caramel removed in most cases. The frequency of measuring mass removed from the pipe should have been increased to

indicate at which point within the cleaning phase deposit was being removed. Lab scale findings revealed the deposit was removed in 'chunks'.

7.3 Industry recommendations

To obtain the best result from current CIP units, the online measurements used to determine cleaning should be

(i)   Working correctly.

(ii) Adequate for the task of measuring cleaning parameters.

Money has already been spent buying probes used in CIP and their installation in line. The integrity of the probe itself and the reliability of the data needs to be maintained regularly. This should already be included in the current work of engineers on plant. It is crucial to have reliable cleaning information because that is how we ensure our customers they are buying a quality product. More emphasis on efficient cleaning is required from site managers. Measurement of volume (flow rate), time, temperature, concentration should be made and control tolerances set. To ensure CIP is completed within the specification minimal measurements should be:

(i)   supply and return flow rate (and supply pressure for cleaning heads),

(ii) supply and return temperatures,

(iii) supply and return conductivity for water and chemical interfaces.

Turbidity has been shown in Chapters 4 and 6 to be a promising tool to measure deposit removal rather than ensuring CIP has gone according to plan. As such turbidity measurements could be used to optimise CIP. Based on such measurements in Chapter 4 the cleanliness of a pipe in each cleaning system (the cleaning rig and the pilot plant) could be determined effectively. From the cleaning data it was suggested that pipes and tanks with yeast slurry that has not been aged can be removed with water. A chemical or thermal sanitiser would need to be circulated through the tank and pipe work after the water rinse to ensure residual microbes are killed.

Cleaning of aged yeast slurry was achieved at lower temperatures and alkaline detergent concentrations than currently used at the brewery in vessels with yeast type deposits in. The wetting rate per m^2 achieved in the cleaning rig was larger than required in industry: $1.5 \ l \ min^{-1} \ m^{-2}$. This suggests the wetting rate per m^2 should be increased to achieve a clean surface in less time. This is achieved by using dynamic cleaning heads rather than spray balls. A pre-rinse of 50°C was shown to remove most aged yeast slurry and should be tried in industry. The industrial fermenter regime should be altered so that the chemical concentration and temperature is lower.

For heat induced deposits such as caramel, the cleaning temperature and concentration of detergent appeared inversely proportional. At 80°C a concentration of 1.25 % caustic would be required to give a visually clean surface in less than 1 h. Theoretically at 90°C, 0 % chemical would be required to clean the pipe and 9 % caustic would be required at 20°C. However there is no guarantee this would be true in practice.

7.4 Future work

The work suggested in this Section can be done within academia or within industry or collaboratively as in this work. The fermentation fouling and cleaning problems have been mapped out fairly well within this thesis, and are summarised in Figure 7.1. Fouling prevention methods discussed are within the red dashed box and cleaning solutions are within the blue dashed box. The input variables that can be controlled are:

(i)   The vessel design, typically vertical or horizontal and,

(ii) The quality i.e. yeast and beer type, which is either ale or lager typically.
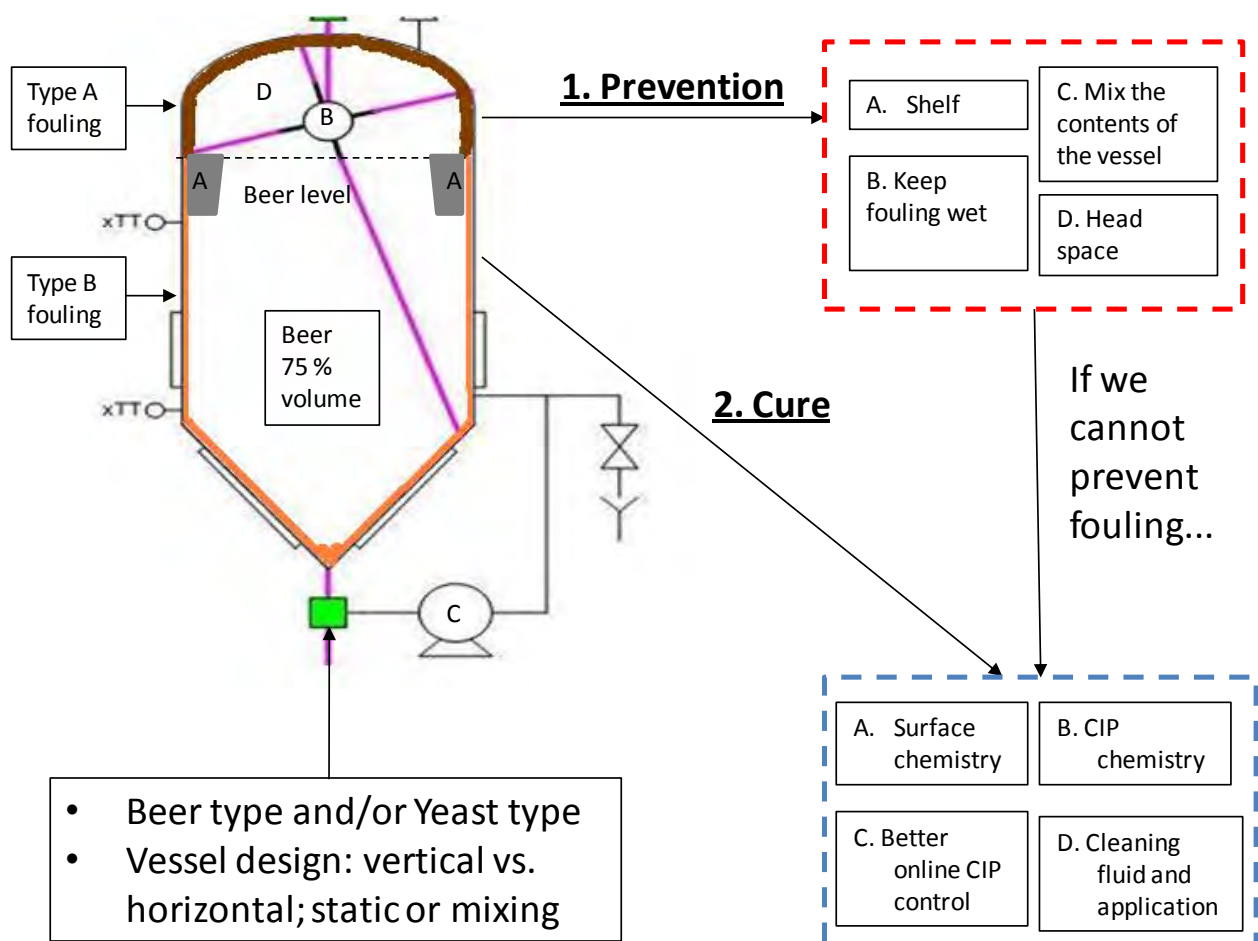
Figure 7.1: Map of the fouling and cleaning problem in cylindroconical fermenters.

The fouling prevention methods included in Figure 7.1 are:

A. Application of a shelf in the FV above the beer level to suppress the foam during fermentation.

B. Application of a mist layer (beer or water) during fermentation. A static/rotating spray ball technology in the down pipe above the cleaning head, exists within Alfa Laval and the Technical University of Denmark has offered its pilot fermenter for the trial.

C. IsoMix technology (Alfa Laval, UK) used to physically mix fermenters, which is currently done in Carlsberg Northampton achieving more consistent and quicker fermentations. Less fouling may occur as a result. The Isomix is used as the CIP head.

D. Modification of the headspace conditions: humidity, foam suppressor, aging time, temperature.

For a process to be sustainable determining what is a foulant is crucial in either preventing its occurrence and determining effective cleaning. As such research into determining what a deposit is should be conducted. In most cases, fouling still occurs. Therefore determining how to optimise the process from a scientific approach will be critical. Future work in the field of optimising cleaning should include:

(i)   Optimising tank cleaning with respect to soiling type and determining the impact pattern of cleaning heads.

(ii)   Determining the total cost of ownership of CIP. This is currently unknown. Determining carbonate levels in caustic that ensure effective CIP could reduce cleaning costs.

(iii)   The chemistry of deposit removal when fluid mechanical removal of a deposit does not work.

(iv)   Determining sanitiser efficacy and linking poor hygiene to specific problems with CIP process and design. This is difficult to do because measurements taken to determine if a process is clean do not measure in the 'worst to clean' point in the system.

(v)   Developing a cleaning index. For example, a heat exchanger with 'x' foulant will take 'x' pipe lengths to clean which will take 'x' minutes and costs £'x'. Deposits are likely to be cleaned a number of ways and providing numerous options to achieve a clean surface will enable industry to have more control over how and when to clean.

(vi)   Validation of online turbidity in CIP with particle count and or particle size measurements.

(vii)   The use of rheology and micromanipulation in predicting cleaning behaviour should also be further investigated. For example caramel studied here has many food components similar to brewer's wort however the viscosity of caramel is much greater than wort. If caramel was of similar viscosity to wort would the fouling and cleaning be similar?

The capability of online surface measurements must also be further investigated. Research into commercially available technologies revealed two viable possibilities: online area analysis and peltier elements.

For online area assessment the Vision System from Biokinetics should be investigated. It is an in-line sight glass (with fouled material), LED backlight array, camera and custom built control system and software for data analysis. The progress of cleaning by images taken every two

seconds is tracked in real time. A clean surface is the reference and the cleaning progress can be quantified as the deviation from the clean surface. An indication of the system is given in Figure 7.2.

Peltier elements use the Peltier effect: If a current flows in a circuit consisting of two different conductors then one junction is heated and one is cooled. This effect could be used to maintain the heat flux sensor used in the cleaning rig experiments at a consistent temperature. Also, the current required to maintain one surface at a given temperature could be an indicator of fouling and cleaning behaviour. Peltier elements are much cheaper and more robust than heat flux sensors and so more suitable to an industrial environment. Both techniques can be trialled in the cleaning rig and the pilot plant.
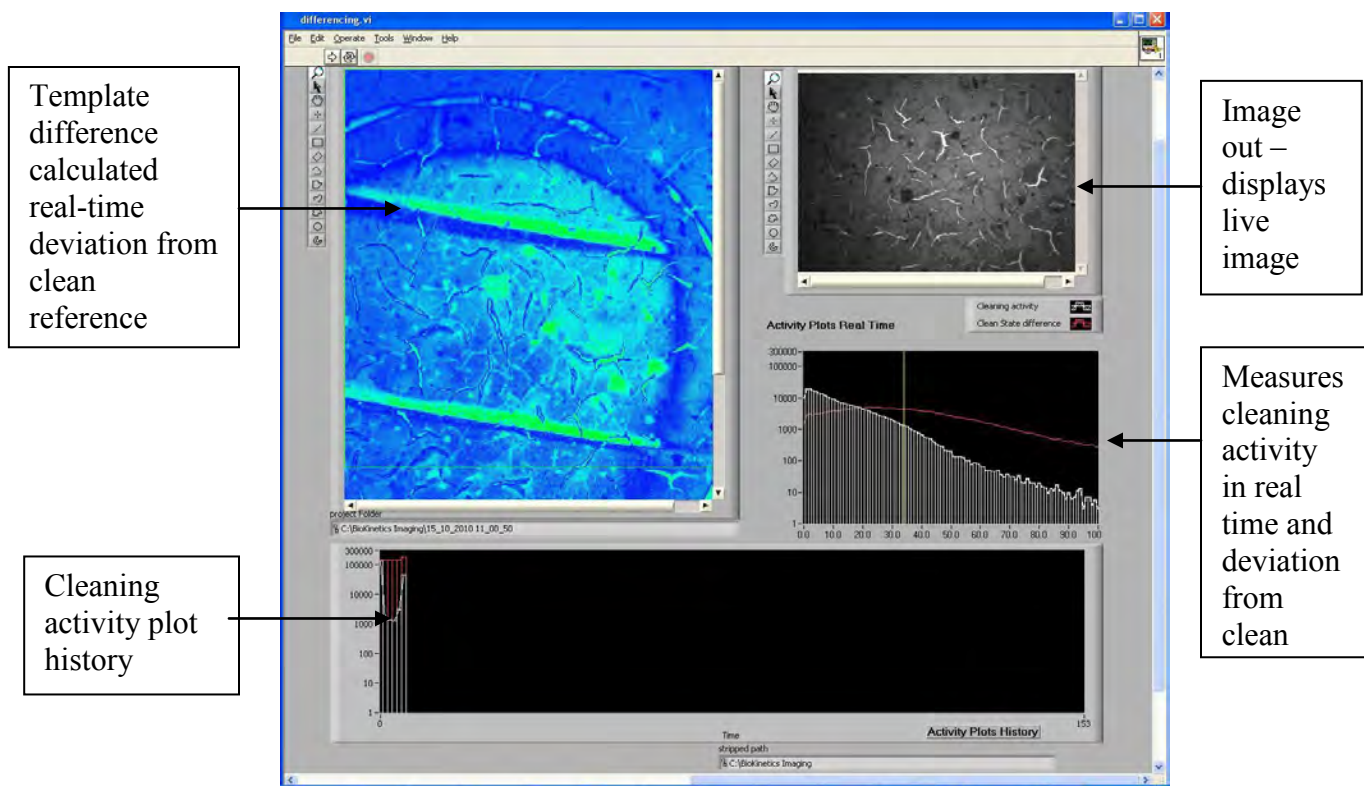
Figure 7.2: The Vision system (Biokinetics) indicating online measurements during cleaning of yeast from the glass surface.

REFERENCES

Allie, Z., Jacobs, E.P., Maartens, A., Swart, P., 2003, Enzymatic cleaning of ultrafiltration membranes fouled by abattoir effluent, Journal of Membrane Science 218: 107–116.

Akhtar, N., Bowen, J., Asteriadou, K., Zhang, Z., Fryer, P.J., 2010, Matching the nano- to the meso-scale: Measuring deposit–surface interactions with atomic force microscopy and micromanipulation, Food and Bioproducts Processing, 88: 341-348.

Akhtar, N., 2010, The fundamental interactions between deposits and surfaces at nanoscale using atomic force microscopy, School of Chemical Engineering, PhD Thesis, University of Birmingham.

Asteriadou, K., Hasting, A.P.M., Bird, M.R., Melrose, J., 2006, Computational fluid dynamics for the prediction of temperature profiles and hygienic design in the food industry, Food and Bioproducts Processing, 84 (C2): 157-163

Augustin, W., Fuchs, T., Föste, H., Schöler, M., Majschak, J., Scholl, S., 2010, Pulsed flow for enhanced cleaning in food processing, Food and Bioproducts Processing, 88: 384-391.

Aziz, N.S., 2008. Factors that affect cleaning process efficiency, School of Chemical Engineering, PhD Thesis, University of Birmingham.

Baier, R. E., 1980, Substrate influences on adhesion of microorganisms and their resultant new surface properties. In G. Bitton & K.C. Marshall (Eds.), Adsorption of microorganisms to surfaces (pp. 59−104). New York: John Wiley.

Balzer, D., Varwig, S., Weihrauch, M., 1995, Viscoelasticity of personal care products, Colloids and Surfaces A: Physicochemical and Engineering Aspects 99: 233-246.

Bayod, E., Willers, E.P., Tornberg, E., 2008, Rheological and structural characterization of tomato paste and its influence on the quality of ketchup, LWT Food Science and Technology 41: 1289–1300.

Bénézech, T., Lelièvre, C., Membré, J.M., Viet, A.F., Faille, C., 2002, A new test method for in-place cleanability of food processing equipment, Journal of Food Engineering 54: 7–15.

Benson, R.S., McCabe, D.J., 2004, From Good Manufacturing Practice to Good Manufacturing Performance, Pharmaceutical Engineering, 24: 26-34.

Bird M R., 1992, Cleaning of food process plant. PhD Thesis. University of Cambridge, UK.

Bird, M.R., Fryer, P.J, 1991, An experimental study of the cleaning of surfaces fouled by whey proteins. Transactions of the Institute of Chemical Engineers 69 13–21.

Bird, M.R., Bartlett, M., 2002, Measuring and modelling flux recovery during the chemical cleaning of MF membranes for the processing of whey protein concentrate, Journal of Food Engineering 53: 143–152.

Blanpain-Avet, P., Migdal, J.F., Bénézech, T., 2009, Chemical cleaning of a tubular ceramic microfiltration membrane fouled with a whey protein concentrate suspension. Characterization of hydraulic and chemical cleanliness, Journal of Membrane Science 337: 153–174.

Bode, K., Hooper, R.J., Augustin, W., Paterson, W.R., Wilson, D.I., Scholl, S., 2007. Pulsed flow cleaning of whey protein fouling layers. Heat Transfer Engineering 28, 202–209.

Boswell, C.D., Varley, J., Boon, L., Hewitt, C.J., Nienow, A.W., 2003, Studies on the impact of mixing in brewing fermentation, Trans IChemE, Part C, 81:33-39.

Bott, T. R., 1995, Fouling of heat exchangers. New York: Elsevier.

Bott, T.R., 1990, Fouling Notebook, Rugby, Institution of Chemical Engineers.

Bowen, W.R., Lovitt, R.W., Wright, C.J., 2001, Atomic Force Microscopy Study of the Adhesion of Saccharomyces cerevisiae, Journal of Colloid and Interface Science, 237: 54–61.

Bremer, P.J., Fillery, S., McQuillan, A.J., 2006, Laboratory scale Clean-In-Place (CIP) studies on the effectiveness of different caustic and acid wash steps on the removal of dairy biofilms, International Journal of Food Microbiology 106: 254 – 262.

Briggs, D.E., Boulton, C.A., Brookes, P.A., Stevens, R., 2004, Chapter 13 – 15, Woodhead Publishing, Cambridge, England.

Changani, S.D., Belmar-Beiny, M.T., Fryer, P.J., 1997, Engineering and Chemical Factors Associated with Fouling and Cleaning in Milk Processing, Experimental Thermal and Fluid Science, 14: 392 406.

Characklis, W.G., 1980, Biofilm development and destruction, Final report, EPRI CS-1554, project RP902-1, Electric power research institute , Palo Alto, CA.

Characklis, W.G., Marshall, K.C., 1990, Biofilms, John Wiley & Sons, USA.

Chen, M.J., Zhang, Z., Bott, T.R., 1998, Direct measurement of the adhesive strength of biofilms in pipes by micromanipulation, Biotechnology Techniques, 12: 875-880.

Chen, X.D., Li, D.X.Y., Lin, S.X.Q., N., Özkan 2004, On-line fouling/cleaning detection by measuring electric resistance—equipment development and application to milk fouling detection and chemical cleaning monitoring, Journal of Food Engineering 61: 181–189.

Chew, J.Y.M., Paterson, W.R., Wilson, D.I., 2004, Fluid dynamic gauging for measuring the strength of soft deposits, Journal of Food Engineering 65: 175–187.

Christian, G.K., Fryer, P.J., 2006, The effect of pulsing cleaning chemicals on the cleaning of whey protein deposits, Food and Bioproducts Processing, 84(C4): 320-328.

Christian, G.K., 2004. Cleaning of carbohydrate and dairy protein deposits, School of Chemical Engineering, PhD Thesis, University of Birmingham.

Christian, G.K., Changani, S.D., Fryer, P.J., 2002, The effect of adding minerals on fouling from whey protein concentrate. Development of a Model Fouling Fluid for a Plate Heat Exchanger, Trans IChemE, Part C, 80: 231-239.

Clauberg, B., Marcinak, M., 2009, Throwing light on photometry, Brewer & Distiller International, 5: 48-50.

Cluett, J.D., 2001, Cleanability of certain stainless steel surface finishes in the brewing process, Faculty of Mechanical Engineering, MPhil, Rand Afrikaans University.

Cole, P., Asteriadou, K., Robbins, P.T., Owen, E.G., Montague, G.A., Fryer, P.J., 2010, Comparison of cleaning of toothpaste from surfaces and pilot scale pipe work, Food and Bioproducts Processing 88: 392 – 400.

Cui, Z.F., Muralidhara, H.S., 2010, Membrane Technology: A Practical Guide to Membrane Technology and Applications in Food and Bioprocessing, Chapter 10, Elsevier Science, Oxford, UK.

Demilly, M., Bréchet, Y., Bruckert, F., Boulangé, L., 2006, Kinetics of yeast detachment from controlled stainless steel surfaces, Colloids and Surfaces B: Biointerfaces 51: 71–79.

Detry, J.G., Rouxhet, P.G., Boulange-Petermann, L., Deroanne, C., Sindic, M., 2007, Cleanability assessment of model solid surfaces with a radial-flow cell, Colloids and Surfaces A: Physicochem. Eng. Aspects 302: 540–548.

Dror-Ehre, A., Adin, A., Markovich, G., Mamane, H., 2010, Control of biofilm formation in water using molecularly capped silver nanoparticles, Water Research, 44: 2601 – 2609.

Epstein, N., 1983, Thinking about heat transfer fouling: a 5 x 5 matrix. Heat Transfer Engineering, 4: 43-56.

EHEDG 1992. A method for assessing the in-place cleanability of food processing equipment. Trends Food Sci. Tech. 3, 325–328.

Felgentraeger, W., Ricketts, N., 2003, Save energy and reduce operating costs, The Brewer International, 3: 22-23.

Fickak, A., Al-Raisi, A., Chen, W.D., 2011, Effect of whey protein concentration on the fouling and cleaning of a heat transfer surface, Journal of Food Engineering, 104: 323 – 331.

Fisher R.C., Rice, F.E., 1924, sweetened condensed milk II. A comparative study of methods for determining total solids, Journal of Dairy Science 7: 497 – 502.

Fornalik, M., 2008, Detecting biofouling in food processing systems, Photonics and Food, 58-61.

Fryer, P J., Robbins, P T., Cole, P A, Goode, K R., Zhang, Z., Asteriadou, K., 2011, Populating the cleaning map: can data for cleaning be relevant across different length scales? Procedia Food science, 1: 1761 – 1767.

Fryer, P.J., Asteriadou, K., 2009. A Prototype cleaning map: a classification of industrial cleaning processes. Trends in Food Science & Technology 20, 225–262.

Friis, A., Jensen, B.B.B., 2002, Prediction of hygiene in food processing equipment using flow modelling, Trans IChemE, C, 80:281-285.

Fryer, P.J., Christian, G.K., Liu, W., 2006, How hygiene happens: physics and chemistry of cleaning, International Journal of Dairy Technology 59: 76-84.

Gillham, C.R., Fryer, P.J., Hasting, A.P.M, Wilson, D.I., 2000, Enhanced cleaning of whey protein soils using pulsed flows, Journal of Food Engineering 46: 199-209.

Gillham, C.R., Fryer, P.J., Hasting, A.P.M., Wilson, D.I., et al., 1999, Cleaning-in-place of whey protein fouling deposits: Mechanisms Controlling Cleaning, Trans IChemE, 77: Part C 127 – 138.

Gillham C R., 1997 Enhanced cleaning of surfaces fouled by whey protein. PhD Thesis. University of Cambridge, UK.

Godfray, M., 2005, A system for reducing the occurrence of a biofilm in beer dispense systems, The Brewer & Distiller, 1: 30-32.

Goode, K.R, Asteriadou, K., Fryer, P.J., Picksley, M., Robbins, P.T., 2010, Characterising the cleaning mechanisms of yeast and the implications for Cleaning In Place (CIP), Food and Bioproducts Processing 88: 365-374.

Gordon, P.W., Brooker, A.D.M., Chew, Y.M.J., Wilson, I.W., York, D.W., 2010, Studies into the swelling of gelatine films using a scanning fluid dynamic gauge, Food and Bioproducts Processing, 88: 357-364.

Graßhoff, A., 2002, Enzymatic cleaning of milk pasteurisers, Trans IChemE, 80 (Part C): 247-252.

Graßhoff, A., 1997, Cleaning of heat treatment equipment. IDF Monograph, Fouling and cleaning in Heat Exchangers, International Dairy Federation, Brussels.

Güell, C., Czekaj, P., Davis, R.H., 1999, Microfiltration of protein mixtures and the effects of yeast on membrane fouling, Journal of Membrane Science, 155: 113-122.

Guillemot, G.,Vaca-Medina, G., Martin-Yken, H.,Vernhet, A., Schmitz, P., Mercier-Bonin, H., 2006.Shear-flow induced detachment of *Saccharomyces cerevisiae* from stainless steel: influence of yeast and solid surface properties. Colloids and Surfaces Part B: Biointerfaces 49: 126–135.

Guo, B., Song, S., Chacko, J., Ghalambor, A., 2005, Offshore pipelines, Elservier, Oxford, Chapter 16: Pigging Operations.

Henningsson, M., Regner, M., Östergren, K., Trägårdh, T., Dejmek, P., 2007, CFD simulation and ERT visualization of the displacement of yoghurt by water, on industrial scale, Journal of Food Engineering, 80: 166-175.

Hooper, R.J., Liu, W., Fryer, P.J., Paterson, W.R., Wilson, D.I., Zhang, Z., 2006, Comparative studies of fluid dynamic gauging and a micromanipulation probe for strength measurements, Food and Bioproducts Processing, 84(C4): 353–358.

Hughes, D., Field, R.W., 2006, Crossflow filtration of washed and unwashed yeast suspensions at constant shear under nominally sub-critical conditions, Journal of Membrane Science 280: 89–98.

Jackson, A.T. Low, W.M., 1982, Circulation Cleaning of a Plate Heat Exchanger Fouled by Tomato Juice: III The Effect of Fluid Flow rate on Cleaning Efficiency, Journal of Food Technology 17: 745-752

Jennings, W.G., Mckillop, A.A. and Luick, J.R. (1957), "Circulation Cleaning", Journal of Dairy Science, 40, 1471-1479.

Jensen, B.B.B., Stenby, M., Nielsen, D.F., 2007, Improving the cleaning effect by changing average velocity, Trends in Food Science & Technology 18: S52 - S63.

Jensen, B. B. B., & Friis, A., 2005, Predicting the cleanability of mix-proof valves by use of wall shear stress. Journal of Food Process Engineering, 28: 89-106.

Jensen, B. B. B., & Friis, A., 2004, Critical wall shear stress for the EHEDG test method. Chem. Eng. Process 43: 831–840.

Juszczak, L., Witczak, M., Fortuna, T., Banyś, A., 2004, Rheological properties of commercial mustards, Journal of Food Engineering 63: 209–217.

Klahre, J., Flemming, M., Flemming, H-C., 2000, Monitoring of biofouling in papermill process waters, Water Research, 34: 3657-3665.

Le Gentil, C., Sylla, Y., Faille, C., 2010, Bacterial re-contamination of surfaces of food processing lines during cleaning in place procedures, Journal of Food Engineering, 96: 37–42.

Lelieveld H.L.M., Mostert M.S., Holah J., 2005, Handbook of hygiene control in the food industry, EHEDG, 192 – 208. Woodhead publishing Limited, Cambridge.

Lelièvre, C., Antonini, G., Faille, C., Bénézech, T., 2002, Cleaning-in-place Modelling of Cleaning Kinetics of Pipes Soiled by Bacillus Spores Assuming a Process Combining Removal and Deposition, Trans IChemE, Vol 80: Part C 305-311.

Lewis, M.J., Young, T.W., 2002, Brewing, 2nd Ed, Kluwer Academic/Plenum Publishers, New York, USA.

Liu, W., Aziz, N.A., Zhang, Z., Fryer, P.J., 2007, Quantification of the cleaning of egg albumin deposits using micromanipulation and direct observation techniques, Journal of Food Engineering 78: 217–224.

Liu, W., Fryer, P.J., Zhang, Z., Zhao, Q., Liu, Y., 2006, Identification of cohesive and adhesive effects in the cleaning of food fouling deposits, Innovative Food Science and Emerging Technologies 7: 263–269.

Liu, W., Christian, G.K., Zhang, Z., Fryer, P.J., 2002, Development and use of a micromanipulation technique for measuring the force required to disrupt and remove fouling deposits, Trans IChemE, Part C, 80: 286-291.

Liu, M., Li, X., Lin, R., Nie, W., Zhang, N., Ling, N., 2004, Fouling prevention with fluidised particles in evaporation of traditional Chinese medicine extract, China Particuology, 2: 81-83.

Mercier-Bonin, M., Ouazzani, K., Schmitz, P., Lorthois, S., 2004, Study of bioadhesion on a flat plate with a yeast/glass model system, Journal of Colloid and Interface Science, 271: 342-350.

Mores, W.D., Davis, R.H., 2002, Yeast foulant removal by backpulses in crossflow microfiltration, Journal of Membrane Science, 208: 389-404.

Morison, K.R., Thorpe, R.J., 2002, Liquid distribution from cleaning-in-place sprayballs, Trans IChemE, Part C, 80: 270-275.

Mozes, M., Marchal, F., Hermesse, M.P., van Haecht, J.L., Reuliaux, L., Leonard, A.J., Rouxhet, P.G., 1987, Immobilization of microorganisms by adhesion: Interplay of electrostatic and nonelectrostatic interactions, Biotechnology and bioengineering, 30: 439.

O'Rourke, 2003, CIP – Cleaning In Place, The Brewer International, 3: 30-34.

Othman, A.M., Asteriadou, K., Robbins, P.T., Fryer, P.J., 2010. Cleaning of sweet condensed milk deposits on a stainless steel surface. In: Wilson, D.I., Chew, Y.M.J. (Eds.), Proceedings of the Fouling & Cleaning in Food Processing. 2010 Conference in Cambridge, Session V. Department of Chemical Engineering, Cambridge, pp. 174–182.

Parbhu, A., Hendy, S., Danne, M., 2006, Reducing milk protein adhesion rates. A Transient Surface Treatment of Stainless Steel, Food and Bioproducts Processing, 84(C4): 274–278.

Pereira, A., Mendes, J., Melo, L.F., 2009, Monitoring cleaning-in-place of shampoo films using nanovibration technology, Sensors and Actuators B: 376–382.

Pereira, A., Rosmaninho, R., Mendes, J., Melo, L.F, 2006, Monitoring deposit build-up using a novel mechatronic surface sensor (MSS), Food and Bioproducts Processing, 84(C4): 366–370.

Pereni, C.I., Zhao, Q., Liu, Y., Abel, E., 2006, Surface free energy effect on bacterial retention, Colloids and Surfaces B: Biointerfaces 48: 143–147.

Petrus H.B., Chen, H.L.V., Norazman, N., 2008, Enzymatic cleaning of ultrafiltration membranes fouled by protein mixture solutions, Journal of Membrane Science 325: 783–792.

Quarini, J., 2002, Ice-pigging to reduce and remove fouling and to achieve clean-in-place, Applied Thermal Engineering 22: 747–753.

Rao, M.A., 1999, Rheology of fluid and semisolid foods principles and applications, Aspen Publishers, USA.

Robbins, P.T., Elliott, B.L., Fryer, P.J., Belmar, M.T., Hasting, A.P.M., 1999, A comparison of milk and whey fouling in a pilot scale heat exchanger: Implications for modelling and mechanistic studies, Trans IChemE, Part C, 77: 97-106.

Rösch, P., Schmitt, M., Keifer, W., Popp, J., The identification of microorganisms by micro-Raman spectroscopy, Journal of molecular structure, 661-662: 363-369.

Sahu, K.C., Valluri, P., Spelt, P.D.M., Matar, O.K., 2007, Linear instability of pressure-driven channel flow of a Newtonian and a Herschel–Bulkley fluid, Physics of Fluids, 19: 122101.

Salo, S., Friis, A., Wirtanen, G., 2008, Cleaning validation of fermentation tanks, Food and Bioproducts Processing, 86: 204-210.

Salo, S., Johnson, S., Jensen, B.B.B., Storgårds, E., Friis, A., 2006, The mechanical effect of rinsing in cleaning of fermentation tank bottoms, In: Wilson, D.I., Chew, Y.M.J. (Eds.), Proceedings of the Fouling & Cleaning in Food Processing. 2006 Conference in Cambridge, Session II. Department of Chemical Engineering, Cambridge, pp. 162 – 171.

Schlüβer, H.J., 1976, Zur Kinetik von Reinigungsvorgängen an festen Oberächen, Brauwissenschaft, 29: 263 - 268.

Sharma, A., Garg, D., Gupta, J.P., 1982, Solidification fouling of paraffin wax from hydrocarbons. Letters in Heat and Mass Transfer, 9: 209-219.

Shorrock, C.J., Bird, M.R., 1998, Membrane cleaning: chemically enhanced removal of deposits formed during cell harvesting, Trans IChemE, 76 (Part C): 30-38.

Simões, M., Pereira, M O., Vieira, M J., 2005, Action of a cationic surfactant on the activity and removal of bacterial biofilms formed under different flow regimes, Water Research, 39: 478–486.

Stewart, J.C., Seiberling, 1996, D.A., Cleaning In Place, Chemical Engineering, 103: 72.

Storgårds, E., 2000, Process hygiene control in beer production and dispensing, Faculty of Agriculture and Forestry, PhD thesis, University of Helsinki.

Tamime, A.V., 2008. Cleaning-in-place: Dairy, Food and Beverage Operations, Society of Dairy Technology Series. Wiley-Blackwell, London.

Timperley, A.W., Boution, F., Bénézech, T., Carpentier, B., Curiel, G.J., Haugan, K., Hofman, J., et al., 2000, A method for the assessment of in-place cleanability of food processing equipment. EHEDG, 2nd Ed., 1–14. CCFRA Technology Ltd., Chipping, Campden, England.

Timperley D A and Smeulders C N M, 1988, Cleaning of dairy HTST plate heat exchangers: optimisation of the single-stage procedure. Journal of the Society of Dairy Technology 41 4–7.

Tse, K.L., Pritchard,A.M., Fryer, P.J., 2003, The rate and extent of fouling in a single-tube wort boiling system, Trans IChemE, Part C: 81: 13-22.

Tuladhar, T.R., Paterson, W.R., Wilson, D.I., 2002, Investigation of alkaline cleaning-in-place of whey protein deposits using dynamic gauging, TransI ChemE, Part C, 80: 199-214.

Tuladhar T R, 2001, Development of a novel sensor for cleaning studies. PhD Thesis. University of Cambridge, UK.

Van Asselt, A.J., Van Houwelingen, G.,Te Giffel, M.C., Monitoring system for improving cleaning efficiency of cleaning-in-place processes in dairy environments, Trans IChemE, Part C, 80: 276-280.

Van der Bruggen, B., Braeken, L., 2006 The challenge of zero discharge: from water balance to regeneration, Desalination, 188: 177-183.

Vinogradov, A.V., Winston,M., Rupp, C.J., Stoodley, P., 2004, Rheology of biofilms formed from the dental plaque pathogen *S. Mutans*, Biofilms 1: 49-56.

Whitehead, K.A., Verran, J., 2004, The effect of surface topography on the retention of microorganisms, Food and Bioproducts Processing, 84(C4): 253–259.

Whitehead, K.A., Rogers, D., Colligon, J., Wright, C., Verran, J., 2006,Use of the atomic force microscope to determine the effect of substratum surface topography on the ease of bacterial removal, Colloids and Surfaces B: Biointerfaces 51: 44–53.

Xiaokai, X., Chongfang, M., Yongchang, C., 2005, Investigation of the electromagnetic antifouling technology for scale prevention, Chem. Eng. Technol. 28: 1540-1545.

Yang, A., Martin, E.B., Montague, G.A., Fryer, P.J., 2008, Towards Improved Cleaning of FMCG Plants: a Model-based approach, Computer Aided Chemical Engineering 25: 1161-1166.

Zeimann, 2007, Fiesta Mexicana; under construction the largest brewery in the world, Brewing world, issue 4, p23.

Zhao, Q., Liu, Y., Wang, C., 2005a, Development and evaluation of electroless Ag-PTFE composite coatings with anti-microbial and anti-corrosion properties. Applied Surface Science 252: 1620–1627.

Zhao, Q., Liu, Y., Wang, C., Wang, S., Müller-Steinhagen, H., 2005b, Effect of surface free energy on the adhesion of biofouling and crystalline fouling, Chemical Engineering Science 60: 4858 – 4865.

Zhao, Q., Wang, S., Müller-Steinhagen, H., 2004, Tailored surface free energy of membrane diffusers to minimize microbial adhesion. Applied Surface Science, 230: 371−378.

APPENDIX

A.1 Benchmarking case study

To complete the benchmark of fermenter CIP cost and time, data had to be gathered from various sources. It was found that most of the required information was not measured or even estimated regularly. The information was acquired from theory and practice in the form required to calculate a cost. Criteria for data collection are listed in Table A.1. Installation of portable probes to collect data was done in many cases. Any additional work would be dependent on how readily available the equipment, probes and colleagues are. Energy (electricity and steam) and man hours were estimated from existing information; chemicals and water were measured by the re-installation of meters. Effluent cost was not quantified because the effluent is treated on site. The COD and total suspended solids content of brewery fermenter CIP effluent has been quoted by Van der Bruggen and Braeken (2006) as 2800 to 8700 mg l^{-1} and 760 to 2300 mg l^{-1} respectfully. Figures calculated and presented in the is thesis are accurate as of 2010.

A.2 CIP unit and cleaning stages

The CIP unit responsible for fermentation vessel (FV) cleaning is illustrated in Figure A.1. The unit comprised one fresh water tank, one recovered water tank (used for pre-rinsing), one diluted detergent tank and a day use drum of sanitiser. The detergent in the tank was heated by circulation through a heat exchanger loop to 65°C. The CIP operation included a pre rinse, detergent phase, intermediate rinse and final disinfection stage. The pre rinse used water recovered from the intermediate rinse of the previous clean. The first portion of the detergent phase was then put down the drain; the remainder was recovered. There was no final rinse because a sterile liquor flush was done prior to the next fermentation as part of production. The CIP set had four channels which in theory meant it could clean four unit operations at one time. However this was not the case because the volume of cleaning fluid required for some of the unit operations was more than a quarter of the CIP tank volume.

Table A.1: CIP resource and output information

Resource or output		Unit of measurement	Measured regularly	Estimated regularly	Method of Quantification	Work additional to plant operation
Water		m^3	no	no	Calculated from flow rates	Installation and use of portable flow meter
Chemicals	*Caustic Soda*	Tonne	no	no	Volume of neat caustic quantified form Volume of Caustic-Stabilon blend	Re-installation of flow totaliser, obtain concentrations and densities of chemicals
	Stabilon WT	L	no	no	Volume of Stabilon quantified from volume of Caustic-Stabilon blend	Re-installation of flow totaliser, obtain concentrations and densities of chemicals
	P3 Oxysan ZS	kg	no	yes	Visual observation of depleted volume	None
Energy	*Electricity*	kWh	no	yes	Multiplied pump KW ratings by hours of usage	Obtain pump power ratings and CIP stage times
	Steam	Tonne	no	yes	Estimated kJ and mass steam required to heat volume of detergent	Obtain CIP temperatures and stage times
Man power	*Equipment set up*	h	no	yes	Observed hours worked	None
	Equipment de-construction	h	no	yes	Observed hours worked	None
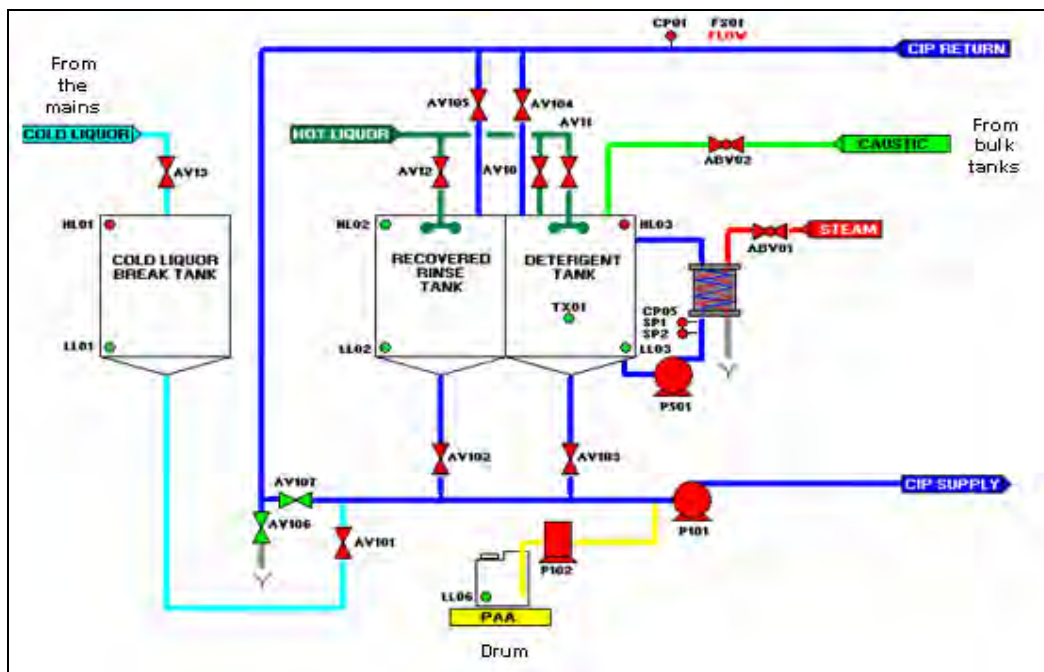
Figure A.1: Schematic of the CIP unit responsible for fermentation vessel cleaning. The CIP unit had four channels to stagger cleaning of four vessels or main pipe lines.

CIP stage times are given in Table A.2. The total average cleaning time was found to be 53 minutes. Including manual routing before and after CIP this would increase by 10 minutes per clean. The critical control points (CCPs) of the CIP operation included:

(i) Detergent strength and temperature during tank preparation and detergent re-circulation,

(ii) Return flow within 60 s during stage 1 and 9, and

(iii) Sanitiser dosing within the set time.

Table A.2: FV CIP stage times and kWh of each stage calculated from pump kW ratings.

CIP sequence	Time (s)	Time (h)	Pump rating (kW)	kWh
1. Fill the system	60	0.017	22.5	0.375
2. Pre-rinse	480	0.133	22.5	3.000
3. Pre-rinse scavenge	45	0.013	7.5	0.094
4. Pre-rinse purge	300	0.083	22.5	1.875
5. Detergent circulation	840	0.233	22.5	5.250
6. Detergent scavenge	45	0.013	7.5	0.094
7. Intermediate rinse	360	0.100	22.5	2.250
8. Intermediate rinse scavenge	45	0.013	7.5	0.094
9. Sanitizer fill	60	0.017	15	0.250
10. Sanitizer injection	54	0.015	0	0.000
11. Sanitizer circulation	780	0.217	22.5	4.875
12. Final rinse	0	0.000	0	0.000
13. Final scavenge	60	0.017	7.5	0.125
14. Final drain down	0	0.000	0	0.000
Total kWh per clean:				**18.3**
Total kWh per week:				**895.8**

Flow rates and temperatures recorded during one FV clean were measured at the CIP supply and return mains using a portable acoustic flow meter (Katronic, Leamington Spa, UK). The measured flow rates and velocities are listed in Table A.3. All CIP stages exceeded the minimum flow velocity of 1.5 m s^{-1}. CIP success was confirmed by visual inspection of the tank surface after CIP and by testing for the presence of the sanitiser PAA on the surface using a PAA test strip. The strip turned blue in the presence of a specific concentration of PAA. Rinse water and surface swab samples were tested for microbial contamination on site by Heineken UK standard protocol in the lab. CIP operations monitored for this study had 0 CFU in the rinse water and were positive for PAA at the end at the end of CIP.

Water, energy and chemical usage was monitored per clean and an annual cost quantified from site records. There were on average 49 FV cleans per week thus the average cleans per year was 2548. Four CIP tank recharges (emptying, re-filling and heating) were also carried out per week; 2 detergent tank recharges and 2 pre-rinse tank recharges.

Table A.3: Average flow rate from recorded flow rates and CIP times.

Cleaning Stage	Flow rate (l min^{-1})			Average flow velocity (m s^{-1})
	Average	*Maximum*	*Minimum*	
1st route fill	495	947	0	2.00
Pre rinse	392	643	375	1.59
Detergent rinse	400	711	0	1.62
Detergent circulation	419	717	393	1.70
Intermediate rinse	373	623	0	1.51
2nd route fill	341	520	0	1.38
Disinfectant circulation and rinse	426	569	390	1.73

A.3 CIP resource quantification

FV CIP resources and their cost are presented in Table A.4. Man hours were estimated by assuming £10 per hour rate. Yield loss was estimated as waste yeast proportion of the deposit observed that could have been sold to Marmite for £10 per tonne (A.2.7)

Table A.4: FV CIP resource costs and units

CIP resource	£	Per
caustic (47%)	286.01	tonne
additive	1.05	L
steam	14.00	tonne
Electricity	0.0607	kWh
RO water	0.13	m^3
sanitiser	2.15	kg

A.3.1 Water

During cleaning 8 minutes of water was used at an average flow rate of 392 L min^{-1} = 3136 L = 3.14 m^3. 6 minutes of intermediate rinse was recovered at 373 L min^{-1} = 2238 L = 2.24 m^3. Actually, 0.9 m^3 of fresh RO water was put down the drain every clean. Additionally 1.96 m^3 was put down the drain as part of the 2% detergent rinse = 2.86 m^3 per clean = **£947 pa.**

A.3.2 Detergent

During cleaning 5 minutes of 2% NaOH blend went to drain every clean. 5 minutes x 400 L min^{-1} = 2000 L of 2 % NaOH per clean. Using $c_1v_1 = c_2v_2$ to work out the volume of 47 % NaOH required, this gives $c_1v_1/c_2 = 85$ L = 0.085 m^3 per clean. Multiply by the density 1200 kg m^{-3} = 102 kg clean = 0.102 tonnes per clean = **£74 333 pa.**

A.3.3 Additive

The additive was quoted as 0.15% of the amount of 30% blended NaOH. During cleaning 320 L of 30% blended NaOH was added to the 2% tank per clean on average in a week of cleaning. 0.15 % of 320 L = 0.48 L per clean = **£1284 pa.**

A.3.4 Steam

During cleaning the refill volume was found to be 4.03 m^3 per clean and was heated from 19.4 to 73.7°C achieving a return temperature of 55°C over 590s. This is shown in Figure A.2 where:

(1) Establish a return flow rate (0-110s),

(2) Pre-rinse (110-590s) and scavenge (590-650s),

(3) Detergent rinse to drain to scavenge CO_2 (650-960s),

(4) Detergent circulation phase (960-1810s), sub route activity (1810-) scavenge (1890-1940s),

(5) Intermediate rinse (1940-2310s), sub route activity (2310-2550s) and scavenge (2550-2600s),

(6) Fill route to establish a return flow rate (2600-2720s), sanitiser dosing (2720-2780s) sanitiser circulation and scavenge to drain (2780-3620s).

From using Equation A.1 where $\dot{m}$ = 6.7 kg s^{-1}, C_p = 4.1 kJ kg^{-1}°C^{-1}, ΔT = 54.5, h_{fg} = 2075.7 kJ kg^{-1}, and assuming 80% heat exchanger efficiency; the steam required was found to be 0.825 kg s^{-1} = 49.5 kg min^{-1} = 248 kg steam in 5 minutes.

This equals 0.25 tonnes steam per clean = **£8918 pa.**

$$\dot{m}_s = \frac{\dot{m} \; c_p \; \Delta T}{h_{fg}}$$

[A.1]
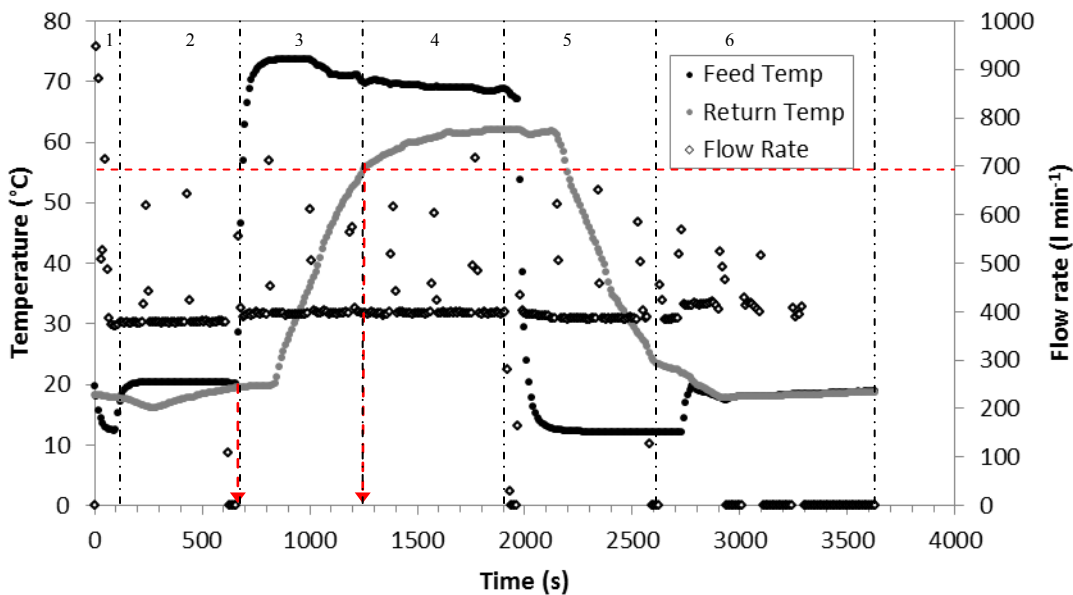
Figure A.2: Flow rate and temperature recorded using the acoustic flow meter during a FV clean.

A.3.5 Electricity

Electricity in kWh was quantified in Table A.2 = **£2830 pa**. A typical PC is rated at 0.075 kW and the monitor at 0.08 kW = 0.155 kW x 0.87 h = 0.13 kWh per clean = £21 pa. Adding the two annual costs gives **£2851 pa.**

A.2.6 Sanitiser

Sanitiser volume was read directly from the container and was on average 2.5 L per clean = **£13 696 pa.**

A.2.7 Yield loss estimation

The amount of fouling was found to be directly related to the surface area of the vessel taken up by the head space volume. The area fouled was found to range from 12.5 m^2 to 25.3 m^2 with a typical average thickness of 2 mm. Thus a volume of fouling of 0.025 – 0.0506 m^3 can be defined. 1 ml of fouling dried out by 65 %. This would equal 10.5 kg per clean = 0.0105 tonnes pa = **£268 pa**.

A.2.8 cost of CIP Tank recharges

There are 2 detergent tank recharges to 2% NaOH, 70°C every week. There are 2 water tank recharges every week. Both tanks hold 12000 L. Recharge pump is 22.5 kW.

Water: 12 m^3 x 2 = 24 m^3 per week for the water tank, 11.76 m^3 x 2 = 23.52 m^3 per week for the detergent tank = **£3.06 per week.**

Detergent: 24 m^3 of 2% NaOH every week. Using c_1v_1/c_2, v_2 = 1 m^3 47% NaOH per week x density 1200 kg m^{-3} = 1200 kg = 1.2 tonnes per week = **£343.21 per week.**

Additive*: using c_1v_1/c_2 and knowing 24000 L 2% detergent required, volume of 30% NaOH blend per week = 1600 L = 2.4 L additive per week = **£2.52 per week.**

Steam: each tank heating operation (12000 L) = 0.41 kg s^{-1} = 1476 kg h^{-1} = 1.478 tonnes x 2 = 3 tonnes per week = **£42 per week.**

Pumping: To reheat the detergent tank takes 1 h = 22.5 kWh per operation = 45 kWh per week = **£2.73 per week.**

Total cost of water tank dumping = £162 + £71 = **£233 pa.**

Total cost of caustic tank dumping = £159 + £17 847 + £131 + £2184 + £213 = **£20 534 pa.**

A.2.9 The total cost of FV CIP and MV CIP

The total usages and cost of FV CIP per clean and per annum is presented in Table A.4. Maturation vessel (MV) CIP is carried out by the same CIP regime as FV CIP. There were found to be on average 6 MV cleans per week = **£12 491 pa.**

Table A.4: Cost and amount of CIP resources per clean and per annum.

Resource	Unit cost	Unit	Per CIP		Per annum
			amount	cost	cost
caustic	286.01	tonne	0.102	29.17	74 325
additive	1.05	L	0.48	0.50	1 284
steam	14.00	tonne	0.25	3.50	8 918
pump	0.0607	kWh	18.43	1.12	2 850
water	0.13	m3	2.86	0.37	947
sanitiser	2.15	kg	2.5	5.38	13 696
waste yeast	10.00	tonne	0.0105	0.11	268
manual routing	10.00	h	0.17	1.70	4 332
Total costs:				**40.03**	**106 620**

A.2.10 The cost of cleaning YSTs

YST CIP was quantified as £27.35 per clean. The cost and amount of each resource is given in Table A.5. The YST CIP regime is given in Table A.6. 71 % of the cost was caustic, 16 % of the cost was sanitiser, 8 % of the cost was steam. Table A.4 assumptions are:

(i) Feed and circulation pumps 22.5 kW and scavenge pumps 7.5 kW as in FV/MV CIP.

(ii) Average flow rates the same as in FV/MV CIP.

(iii) Average of 6 cleans per week.

(iv) Heat from 15 to 70°C for detergent.

(v) 2 L sterilant used per clean.

Table A.5: Cost and amount of CIP resources used in YST CIP per clean and per annum

Resource	Unit cost	amount	Unit	Per CIP	Per annum
caustic	286.01	0.068	Tonne	19.45	6 068
additive	1.05	0.13	L	0.14	43
steam	14.00	0.16	Tonne	2.24	699
pump	0.0607	19.9	kWh	1.21	377
water	0.13	0.095	m3	0.01	4
sanitiser	2.15	2	Kg	4.30	1342
waste yeast	10.00	0	Tonne	0.00	0
manual routing	10.00	0	h	0.00	0
				27.35	**8 532**

Table A.6: Current YST CIP sequence (Tadcaster).

YST	Step Name	Time (s)
1	Initial drain lines	60
2	Prove route	100
3	Pre-rinse (to drain)	200
4	Scavenge (to drain)	100
5	Prime main with caustic	20
6	scavenge (to drain)	100
7	Water / Detergent interface	100
8	Caustic recirculation	1200
9	Scavenge (to detergent tank)	100
10	Prime main with RO water	20
11	Scavenge (to detergent tank)	100
12	Detergent / Water interface	100
13	Post detergent fresh water rinse	200
14	scavenge (to recovered rinse water tank)	100
15	Transfer water to product tank	40
16	Dose in sterilant	60
17	Sterilant recirculation	900
18	Scavenge (to drain)	180
19	Final drain lines	45
Total time (minutes)		**62**

B: SOP developed for the Cleaning Rig

All relevant risk assessments were done for the equipment and are filed in a cupboard next to the equipment. The cleaning rig was always drained and the test section disassembled at the end of each day because the rig was multi use. A blank coupon was used at the start of each day to ensure the sensors were recording and the test section did not leak.

(1)   Set up: Switch on the PC (open ZEAL Logger), conductivity meter (Ecolab), pump (Alfa Laval), tank heater and set the tank temperature. Fill the water and chemical tanks from the water mains supply and turn manual valves ($V_1 - V_7$) to the required position. Table B.1 gives details of the valve positions of each route. Reposition the base in the test section housing and screw in place using the screws and allen key.

(2)   Weigh fouled coupon, apply a thin layer of high vacuum grease (Dow Corning) to the un-fouled 2 mm rim of the coupon using a spatula and apply pressure to the back of the coupon to fix it into the base.

(3)   Apply a thin layer of heat sink (RS) to the copper stub containing the Microfoil heat flow sensor (MHFS). Place ice and water in the centre of the spring and around the cooling block in the plastic container and position the copper stub in the spring (illustrated in Figure 3.3). Move the container into position under the test section base so the copper stub is directly under the coupon. Lower the test section so the MHFS and coupon contact. The error estimated for U_c determined from the MHFS is given in Table B.2.

(4)   Position the camera stand (Hama, Germany) and camera (Canon, Japan) with timer (Canon, Japan)) over the test section. Manually focus the camera and set the timer to take pictures at the required rate throughout the experiment. Save the file in ZEAL logger at T_0, start the timer at a known time then start the pump.

(i) For yeast experiments the timer was started 5 s after logging and the pump 5 s after this. The images were taken every 1 s (type 1) or every 5 s (type 2).

(ii) For caramel experiments, the timer was started 10 s after logging and the pump started 10 s after this. Images were taken every 10 s.

(5) After the experiment is complete drain the test section and remove the coupon. Download the pictures from the camera CF card using the CF reader and start the process again from stage 2.

Table B.1: Manual valve positions for different cleaning rig operational routes.

Route	Flow through test section	Valve position							
		V1	*V2*	*V3*	*V4*	*V5*	*V6*	*V7*
Rinse	Yes	water/chemical tank	O	-	O	-	-	O
bypass rinse	No	water/chemical tank	-	O	-	O	-	O
Recirculation	Yes	water/chemical tank	O	-	O	-	O	-
bypass recirculation	No	water/chemical tank	-	O	-	O	O	-

Table B.2: Summary of error estimation for calculating U_c

Measurement technique	measurement principle	Accuracy	source	Actual reading	Maximum error	Minimum error
Temperature, T_{av}	Average of T4 and T5	± 1°C	Manufacturer	70	71	69
Temperature, T_4	reading on T4			66	67	65
Temperature, T_5	Reading on T5			68	69	67
Temperature, T_{c2}	reading on Tc2	± 1°C		58	59	57
Voltage output (V)	From MHFS	± 5%		0.0346	0.0363	0.0329
Heat flux, q (kW m^{-2})	See equation 3.4	± 0.003 kW m^{-2}		8.9638	8.9668	8.9608
Heat transfer coefficient, U (kW m^{-2} K^{-1})	see equation 3.5	± 0.03 %	from maximum & minimum error	0.8964	0.8967	0.8961

C.1: SOP for the pilot plant and file exporting to Excel

All relevant risk assessments were done for the equipment and are filed in a cupboard next to the equipment. User manuals for all probes and equipment contained in the pilot plant are filed in the same place.

C.2 Manual set up

Connect the pipe work together in the configuration required for the experiment. Pipe work is connected by way of 2" O ring and "" tri clamp (Alfa Laval). If using manual valves as part of the test section, move the manual valves in the open or closed position to ensure the cleaning loop is established for the experiment.

C.3 Start up procedure

C.3.1 The pilot plant

- Turn the power on at the mains and on the control panel (all valves should be green),
- Turn the compressed air power supply on at the mains and open the valve,
- Switch on the pump,
- Check that the main water valve is open to TK 21.

C.3.2 The laptop (Toshiba Satellite Pro)

- Connect to the control panel USB and Ethernet.
- Turn on (no password).
- Open OPUS (password **ZEAL**).

- Open MATLAB R2007b.

C.3.3 Using additional instruments

- Ensure instrument is in place in the li.ne. Connections made by 2" O ring and "" tri clamp.

- Switch on the instrument at the mains and ensure the instrument is reading.

- Download instrument data to the laptop at the required frequency. For the Kemtrak turbidity meter this is every 2 hours.

C.3.4 Tanks filling and concentration preparation.

Tank 21 refills automatically from the mains and has a high level probe to prevent over filling. Tank 22 and 23 and filled according to visual inspection. Normally to the level of the overflow pipe which gives an approximate volume of 380 L. No tanks have low level probes and so could run empty which would damage the pump. Depending on the flow rate, there is a set volume of water that can be used from each tank determined by visually timing draining times (Table C.1). Do not exceed these times when rinsing from the tank to the drain. The route functions are given in Table C.2.

The dosing kit hoses are connected in line to the outlet of tank 23 (see figure C.1). There are four chemical options: alkali, acid, booster and sanitiser (Ecolab). Each chemical type has an independent pump responsible for dosing in the chemical in line from a 20 L drum of chemical positioned within the skid. The correct pump pipe inlet is placed into the correct chemical drum. The amount of chemical dosed is input manually on the skid. The pump hoses are removed from the chemical drums after chemical dosing. Obtaining the required concentration via conductivity

measurement in presented in Chapter 3, Section 3.3.1. For chemical conductivity the probe sensitivity is reduced to the measuring range $0 - 200$ mS cm^{-1} marked as condition 4. Condition 1: $0 - 200$ µS, condition 2: $0 - 2$ mS cm^{-1} and condition 3: $0 - 20$ mS cm^{-1}.

For yeast rinsing experiments tank 21 was used. For caramel experiments tank 22 was filled with water by selecting route "8a" and heated to the required temperature using route "22-22". This tank was used as a pre-rinse tank. Tank 23 was also filled from tank 21 via route "4a" and heated to the required temperature by route "4b". Filling of one tank and heating of another could be done at the same time. Chemical was dosed in to the line while tank 23 was heating.

Table C.1: Length of experimental time available at 1, 1.5 and 2 m s^{-1} from tank 23 or 22.

Experiment flow rate (m^3/h)	Velocity (m s^{-1})	Tank 23 run time (s)
6.5	1	210
9.7	1.5	144
12.9	2	105

Table C.2: Pilot plant operational route functions.

Route	Description	Flow through the test section?
2	Water rinse from tk21 to the drain	yes
4a	Water from tk21 to tk23	no
4b	Circulation of tk23 for heating and making chemical up to concentration	no
4c	Chemical rinse from tk23 to the drain	yes
5a	Circulation of chemical from tk23	yes
8a	Water from tk21 to tk22	no
22-drain	Water rinse from tk22 to the drain	yes
22-22	Circulation of tk22 for heating	no

Table C.3: measurement technique estimation of error.

| Inline probes	Measurement principle	Measured	Accuracy	Source	Actual value	Max error	Min error
Flow transmitter (cleaning rig)	Electomagnetic method	$m^3 h^{-1}$	$0.01\ m^3 h^{-1}$	Alfa Laval	0.59	0.60	0.58
Promag 50L flow transmitter (pilot plant), F0	see above	$m^3 h^{-1}$	± 0.5%	Endress+ Hauser	10.97	11.02	10.91
Promag 50L flow transmitter (pilot plant), F1	see above	$m^3 h^{-1}$	± 0.5%	Endress+ Hauser	11.2	11.25	11.14
Conductivity LMIT08, C0	Induction method.	$\mu S\ cm^{-1}$	$\pm 1\ \mu S\ cm^{-1}$	Ecolab Engineering GmbH	119.95	120.95	118.95
Conductivity LMIT08, C1	see above	$\mu S\ cm^{-1}$	$\pm 1\ \mu S\ cm^{-1}$	Ecolab Engineering GmbH	121.02	122.02	120.02
Temperature LMIT08, T0	Resistance measurement with Pt 100 DIN using 3 wire connection method	°C	± 0.5°C	Ecolab Engineering GmbH	27.14	27.27	27.00
Temperature LMIT08, T1	see above	°C	± 0.5°C	(Ecolab Engineering GmbH	27.37	27.50	27.20
turbidity TC007	Attenuated and scattering light measured at 90°combined by nephelometric ratio algorithm ISO7027:1999(E)	FTU	± 1%	Kemtrak	0.0314	0.0317	0.0311
Turbidity TF16	Light scattered from particles (trace suspended solids, undissolved liquids or gas bubbles) in the medium is detected at an angle of 11°.	ppm	± 0.3 %	Optek	4.010	4.021	3.997
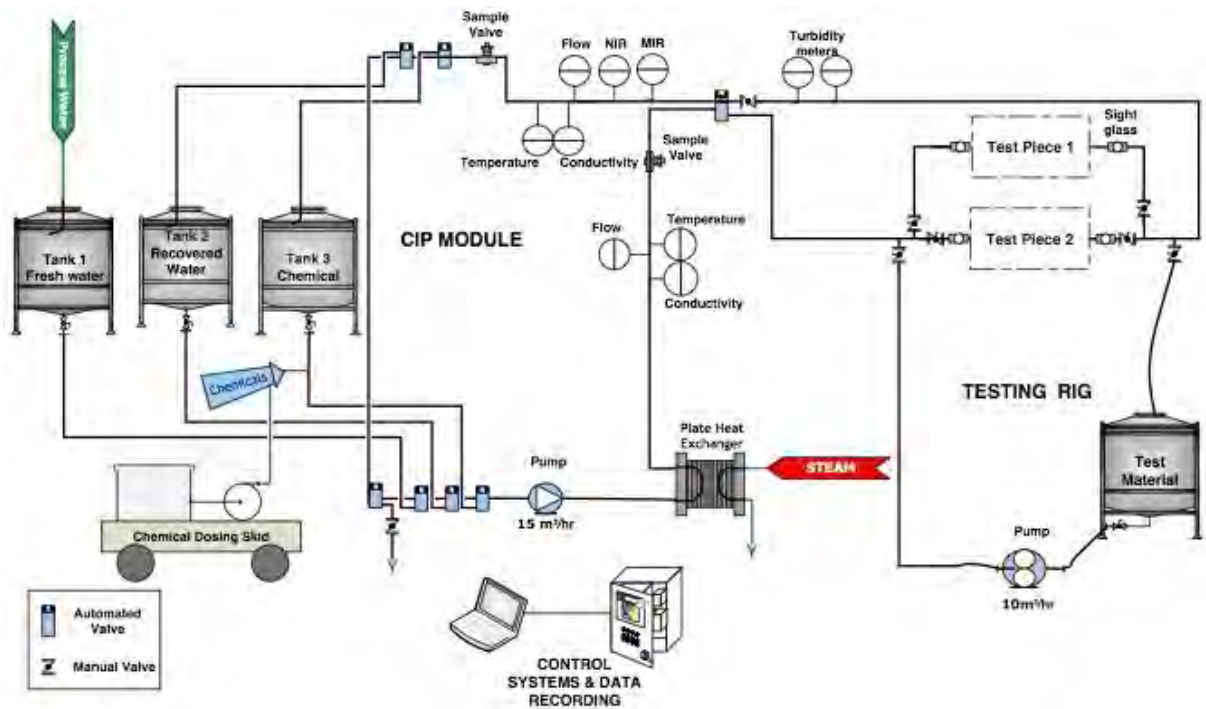
Figure C.1: Pilot plant P&ID. Tank 1, 2 and 3 are tank 21, 22 and 23.

C.4 Fouling

C.4.1 A pipe with yeast

Yeast slurry could be easily poured into a pipe and added into the test section. A closed manual valve was connected to the end of a 1 m pipe by way of a 2" O ring and tri clamp. The slurry was then poured from the bulk 20 L drum into a clean 5 L measuring jug. The slurry was then poured into the pipe until the pipe was full. The pipe was held at a slope as the yeast was added to avoid foaming. Another closed manual valve was connected to the top of the 1 m pipe and the pipe positioned in the line. This was a two person job.

C.4.2 A pipe with caramel

Caramel was cooked onto the wall of 0.5 m sections of pipe by way of the heated jacket system

presented in Chapter 3, Section 3.6.1. The deposit was semi-solid and did not need manual valve

connection to keep the deposit in place in the pipe. The section of pipe was simple placed in the

line by way of 2" O ring and tri clamp.

C.4.3 The whole test piece

- Place the steel pipe connecting to the test piece via the pump into the product.

- Move the manual valves to the correct position.

- Place the outlet of the plastic overflow pipe into an empty bucket.

- In Matlab type **soil(5)** and press enter; type **soil(0)** and be ready to press enter to

  stop the pumping (pumping does not have to be 5%)

C.5 Experiment procedure

- If doing a heated experiment open the steam valve a small amount initially (5-10°).

  Continue to open up to 45° and eventually 90° as the initial steam pressure entering

  the system reduces.

- Go to the directory **C\Matlab files\zeal_pilot**

- Type **run_zeal**

- Click **Run Experiment**

- Select the route number, temperature, and flow rate (m^3h^{-1}) and replace the word

  "data" with the required individual file name. Typical routes, tank filling operations,

  do not need a file name.

- When you are happy the set up is correct, click start experiment.

- When the time is up click the **STOP** button to stop the pump and end the experiment.

- After the experiment you have to drain the line into a bucket from the sample point

- Take swabs by opening the tri clamp at one end of the test piece

C.6 Saving and exporting data from Matlab files

- Save any additional instrument data on the laptop as required. For the Kemtrak turbidity meter this was done via usb connection and saved as an Excel .csv file.

- Open the directory: C:\temp\zeal_pilot and type exp_data in the command window. A prompt appears for the Matlab file name. Enter this file name as a .mat. A prompt appears for the Excel file name. Enter this file name as a .xls.

- All files are automatically kept in the temp file on the laptop hard drive. These files should be saved in an independent folder and on an external hard drive at the end of every working day.

C.7 Shut down procedure

- **IN AN EMERGENCY HIT THE RED BUTTON ON THE CONTROL PANEL. This automatically stops the pump.**

- Close the steam valve (if used).

- Close the main water valve to tank 21.

- Close Matlab and OPUS.

- Turn off control panel, mains to pilot plant and instruments, and air supply.

- Disconnect laptop from USB and Ethernet connections.

- Note: If the pilot plant is not in use for some days empty the tanks.

D: AR500 and AR1000 rheometer operation and file acquisition in Excel

Rheometer operation was done using the Rheology Advantage program. An example of the control page is illustrated in Figure D.1. At the start of each day the air supply to the rheometer was opened and the rheometer, water bath (kept at 20°C) and computer switched on. A selection of geometries is available for use on the equipment. The plate geometry was selected for use with yeast and cone geometry selected for use with caramels, discussed in Chapter 3, Section 3.4. The spindle protector was removed and the geometry screwed in to place. The geometry had to be mapped (calibrated) at the start of each day. This was an automatic prompt when the geometry was selected from the "geometry" drop down menu, highlighted in Figure D.1 by the dashed box 1.

The rheometer head with geometry attached was lowered to within approximately 1 cm from the stage plate (using dashed box 2, Figure D.1) and the gap zeroed (using dashed box 3, Figure D.1). The geometry was automatically backed away to a safe working distance after this procedure (using dashed box 4, Figure D.1). Every sample was carefully applied to the centre of the stage using a clean plastic spatula. The temperature was set by typing in the required box (Dashed box 5, Figure D.1).
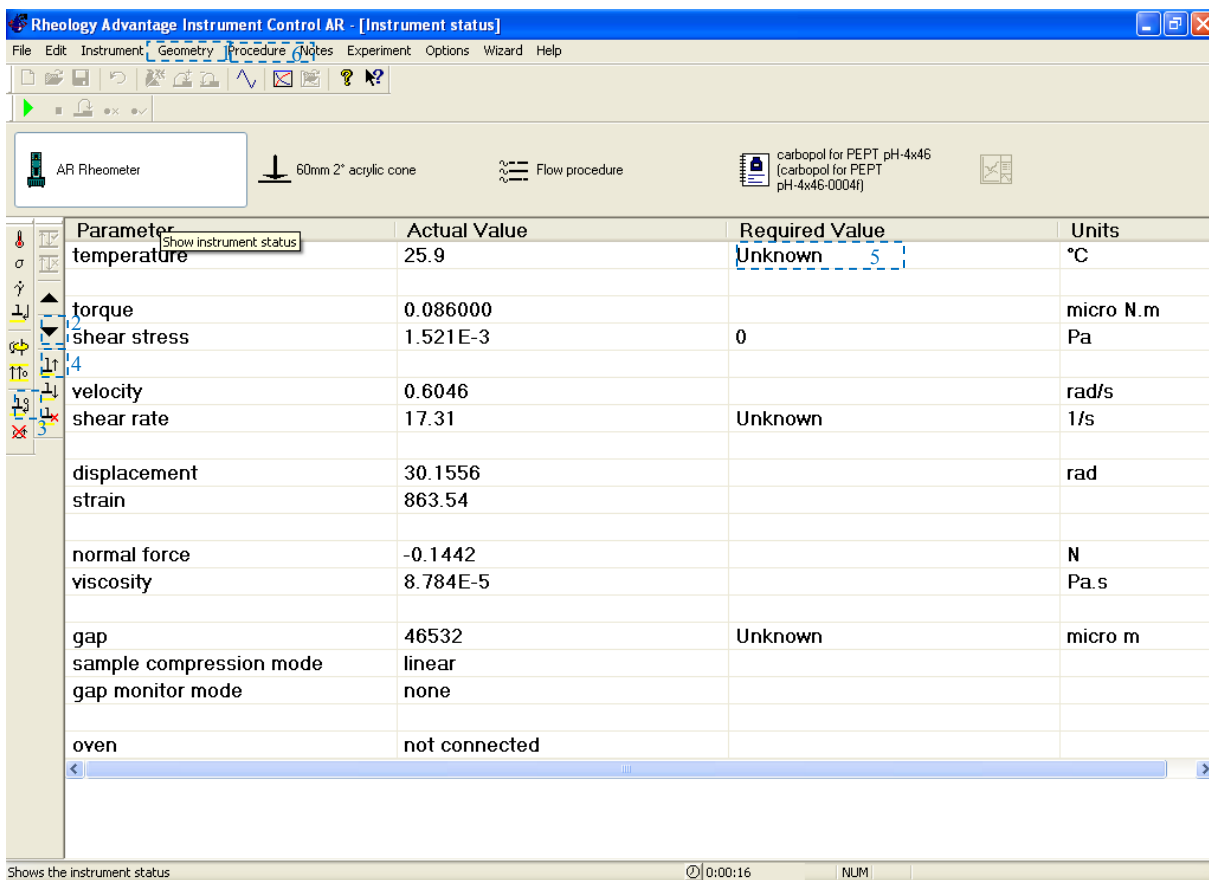
Figure D.1: Illustration of the control screen using the Rheology Advantage program. The Dashed boxes correspond to the details given in the text.

Depending on the test, the corresponding rheological procedure was selected from the drop down "procedure" menu (dashed box 6, Figure D.1). Flow or oscillation procedures used were selected from the menu. Figure D.2 illustrates the parameters that could be controlled for (a) a stress sweep and (b) a temperature ramp. An oscillatory stress from within the linear viscoelastic region of each deposit was used as the controlling variable in temperature ramps.
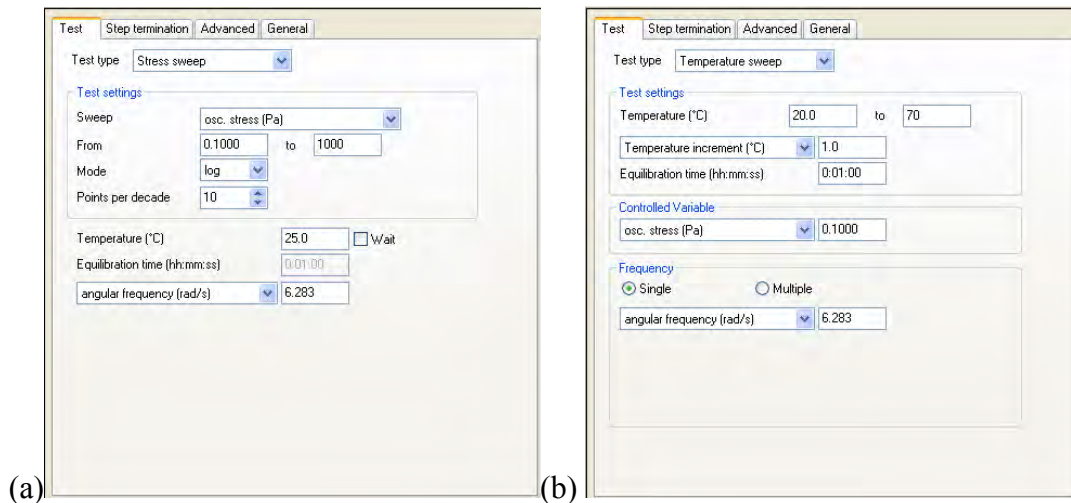
Figure D.2: illustration of (a) stress sweep and (b) temperature ramp procedure control boxes.

After each experiment the rheometer head and geometry were backed off to a gap of 10 cm (using dashed box 4, Figure D.1). Sample was carefully wiped from the stage and the plate using distilled water and a paper towel after each experiment. At the end of the day of use, the stage was also wiped with acetone and left to dry. RSL files were opened in the TA Data Analysis program to view the result. An example of industrial yeast slurry investigated in the shear range of $0 - 1000$ s^{-1} is illustrated in Figure D.3. The raw data was copied from the file into Excel and saved on an external hard drive.
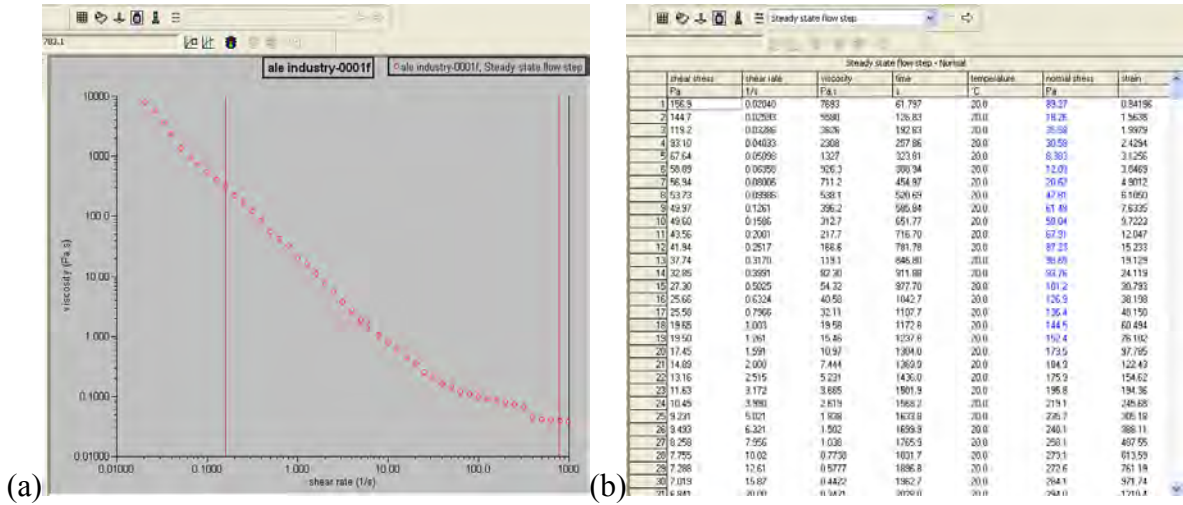
Figure D.3: illustration of (a) the graph of data and (b) the raw data in the TA Data Analysis program.